

UNIVERSIDAD COMPLUTENSE DE MADRID

FACULTAD DE CIENCIAS QUÍMICAS

Departamento de Bioquímica y Biología Molecular



TESIS DOCTORAL

**Inactivación y reactivación del surfactante pulmonar:
mecanismos moleculares e implicación en patologías
respiratorias**

MEMORIA PARA OPTAR AL GRADO DE DOCTOR

PRESENTADA POR

Elena López Rodríguez

Director

Jesús Pérez Gil

Madrid, 2013

Universidad Complutense de Madrid

Facultad de Ciencias Biológicas

Departamento de Bioquímica y Biología Molecular I



INACTIVACIÓN Y REACTIVACIÓN DEL SURFACTANTE PULMONAR: MECANISMOS MOLECULARES E IMPLICACIÓN EN PATOLOGÍAS RESPIRATORIAS

Tesis Doctoral

ELENA LOPEZ RODRIGUEZ

Director:

Dr.JESÚS PÉREZ GIL

MADRID, ESPAÑA 2012

Universidad Complutense de Madrid

Facultad de Ciencias Biológicas

Departamento de Bioquímica y Biología Molecular I



INACTIVATION AND REACTIVATION OF PULMONARY
SURFACTANT: MOLECULAR MECHANISMS AND
IMPLICATION IN RESPIRATORY PATHOLOGIES

Tesis Doctoral

ELENA LOPEZ RODRIGUEZ

Director:

Dr. JESÚS PÉREZ GIL

MADRID, ESPAÑA 2012

La presente Tesis doctoral ha sido realizada en el Departamento de Bioquímica y Biología Molecular I de la Universidad Complutense de Madrid, bajo la dirección del Dr. Jesús Pérez Gil.

Parte de los experimentos se llevaron a cabo en el centro de investigación BiomaGUNE (San Sebastian, España) en colaboración con el Dr. Ralf Richter y en el grupo de investigación Lungenfibrose en la Universidad Justus-Liebig Universität Giessen (Giessen, Alemania), bajo la dirección del Dr. Andreas Günther.

Esta Tesis se ha llevado a cabo gracias a la financiación de National Institutes of Health (2R01HL066410-05A3) y el Ministerio de Ciencia e Innovación (BES-2010-032336).



ABBREVIATIONS

| | |
|-----------|--|
| AECII | alveolar epithelial type II cell |
| ALI | acute lung injury |
| ARDS | acute respiratory distress syndrome |
| BAL | bronchoalveolar lavage |
| CBS | captive bubble surfactometer |
| Chol | cholesterol |
| CHOP | C/EBP-homologous protein |
| CRD | carbohydrate recognition domain |
| CRP | C-reactive protein |
| CRS | compliance of the respiratory system |
| DNA | deoxiribonucleic acid |
| DOPC/DOPE | dioleylphosphatidylcholine/dioleylphosphatidylethanolamine |
| DPPC/DPPE | dipalmitoylphosphatidylcholine/ dipalmitoylphosphatidylethanolamine |
| DYN | dynamic cycle |
| EDEM | ER degradation-enhancing mannosidase |
| ER | endoplasmic reticulum |
| GUV | giant unilamellar vesicle |
| HA | hyaluronic acid |
| IA | initial adsorption |
| ITO | indium-tin oxide |
| IPF | idiopathic pulmonary fibrosis |
| KO | knock-out |
| LA | large aggregate |
| LH | lung homogenate |
| LIS | lung injury score |
| LUV | large unilamellar vesicle |

| | |
|---------------|--|
| MAS | meconium aspiration syndrome |
| M β CD | methyl- β -cyclodextrine |
| MLV | multilamellar vesicle |
| mRNA | messenger ribonucleic acid |
| NRDS | neonatal respiratory distress syndrome |
| NS | native surfactant |
| OE | organic extraction |
| PBS | pulsating bubble surfactometer |
| PE | phosphatidylethanolamine |
| PEA | post-expansion adsorption |
| PEG | polyethyleneglycol |
| PG | phosphatidylglycerol |
| PI | phosphatidylinositol |
| PRISM | paediatric risk of mortality |
| QCM-D | quarz-crystal microbalance with dissipation |
| QSTAT | quasi-static cycle |
| RDS | respiratory distress syndrome |
| RT-PCR | reverse transcription- polymerase chain reaction |
| SA | small aggregates |
| SP-A, B, C, D | surfactant protein A, B, C, D |
| SM | sphingomyelin |
| TA | taurocholic acid |
| TTF-1 | thyroid transcription factor 1 |
| UPR | unfolded protein response |
| XBP | X-box binding protein |
| γ | surface tension |
| π | surface pressure |

| | |
|--|-----|
| ABSTRACT/RESUMEN | 11 |
| INTRODUCCION | 17 |
| - SURFACTANTE PULMONAR | 19 |
| - BIOLOGÍA DEL SURFACTANTE PULMONAR | 20 |
| - SURFACTANTE PULMONAR Y TENSIÓN SUPERFICIAL | 24 |
| - SURFACTANTE PULMONAR Y DEFENSA INNATA | 30 |
| - SURFACTANTE PULMONAR Y CLÍNICA | 32 |
| OBJECTIVES AND OUTLINE/OBJETIVOS | 40 |
| PART 1. FROM MOLECULES TO BIOPHYSICS | 46 |
| - CHAPTER 1: Meconium impairs pulmonary surfactant by a combined action of cholesterol and bile acids | 50 |
| o INTRODUCTION | 52 |
| o RESULTS | 53 |
| o DISCUSSION | 65 |
| - CHAPTER 2: Exposure to polymers reverses inhibition of pulmonary surfactant by serum, meconium or cholesterol in the captive bubble surfactometer | 68 |
| o INTRODUCTION | 70 |
| o RESULTS | 72 |
| o DISCUSSION | 80 |
| - CHAPTER 3: Structural and functional modification of pulmonary surfactant pre-activated by hyaluronic acid | 86 |
| o INTRODUCTION | 88 |
| o RESULTS | 90 |
| o DISCUSSION | 97 |
| GENERAL DISCUSSION PART 1 | 102 |
| PART 2. FROM BIOPHYSICS TO CLINICS | 106 |
| - CHAPTER 4: Biophysical characterization of surfactant from paediatric ARDS patients. Correlating biophysical and clinical parameters | 110 |
| o INTRODUCTION | 112 |
| o RESULTS | 114 |

| | |
|---|-----|
| Índice/Index | |
| ○ DISCUSSION | 120 |
| - CHAPTER 5: Molecular and biophysical characterization of a Napsin A knock-out mouse model with partial SP-B deficiency | 126 |
| ○ INTRODUCTION | 128 |
| ○ RESULTS | 130 |
| ○ DISCUSSION | 141 |
| | |
| GENERAL DISCUSSION PART 2 | 146 |
| | |
| CONCLUSIONS AND PERSPECTIVES / CONCLUSIONES Y PERSPECTIVAS | 150 |
| | |
| MATERIALS AND METHODS | 156 |
| | |
| LIST OF PUBLICATIONS | 176 |
| | |
| REFERENCES | 180 |

ABSTRACT

RESUMEN

ABSTRACT

Pulmonary surfactant inactivation occurs with many respiratory pathologies such as meconium aspiration syndrome (MAS), acute respiratory distress syndrome (ARDS) or idiopathic pulmonary fibrosis (IPF), resulting in abnormally high surface tension. Causes of inactivation of surfactant are different in origin and molecular mechanism. On the one hand, many inactivating agents reach the alveolar interface such as meconium, during MAS, or serum, due to leakage of fluid through the damaged epithelial barrier. On the other hand, deficiency in surfactant proteins may also influence the activity of surfactant, as in IPF. Studying molecular mechanisms of inactivation as well as optimizing new standardized methods allows the development of new surfactant preparations for clinical use in the treatment of respiratory pathologies. Addition of polymers such as hyaluronic acid (HA) to surfactant preparations results in an increase resistance to inactivation, independently of the inactivating mechanism. Entropic forces, such as osmotic pressure and depletion forces, act on surfactant in a non-reversible way resulting in a pre-activated surfactant preparation that shows enhanced resistance to inactivation. Moreover, the biophysical characterization of clinically relevant samples allow the combination of clinical and biophysical data that highlights the implication of surfactant inactivation in the development and outcome of the studied respiratory pathologies, such as ARDS. Significant correlation between high surface tension and clinical parameters such as $\text{PaO}_2/\text{FiO}_2$ (oxygenation index), CRS (compliance of the respiratory system), PRISM (paediatric mortality risk) and Murray score (lung injury severity), demonstrate the importance of surfactant inactivation in ARDS. Developing of inactivation-resistant surfactant preparations could be the key for the treatment of such pathologies. Finally the complete characterization of clinically relevant animal models allows the combination of molecular, cellular, biophysical and clinical data. Characterization of a Napsin A KO mouse model allows us to determine levels of protein not only in surfactant but also in lung tissue. Results from these mice seem to resemble type II cell injury that would result in development of fibrosis. This mouse model would be a tool for the study of fibrosis development and its treatment.

Combination of molecular, cellular, clinical and biophysical data is a powerful tool for understanding respiratory pathologies and developing effective treatments.

RESUMEN

La inactivación del surfactante pulmonar se encuentra asociada a muchas patologías respiratorias, como el síndrome de aspiración de meconio (MAS), síndrome del distrés respiratorio agudo (ARDS) o fibrosis pulmonar idiopática (IPF), que da lugar tensiones superficiales elevadas en la interfase alveolar. Las causas de la inactivación del surfactante son diferentes en origen y en su mecanismo molecular. Así, muchos agentes inactivadores llegan a los pulmones, como el meconio, durante el MAS, o suero debido al daño en la barrera epitelial. Por otro lado, deficiencias en las proteínas del surfactante también influye en la actividad del surfactante, como es el caso de IPF. El estudio de los mecanismos moleculares de la inactivación, así como la optimización de métodos permite el desarrollo de nuevas preparaciones de surfactante para su uso clínico en el tratamiento de patologías respiratorias. La adición de polímeros como el ácido hialurónico (HA) a las preparaciones de surfactante resulta en el aumento de la resistencia a la inactivación, de manera independiente del mecanismo de inactivación. Fuerzas entrópicas, como la presión osmótica y las fuerzas de exclusión (depletion forces), actúan en el surfactante de forma irreversible dando lugar a una preparación de surfactante pre-activada que muestra alta resistencia a inactivación. Además, la caracterización biofísica de muestras clínicamente relevantes permite la combinación de datos clínicos y biofísicos, que pone de manifiesto la implicación de la inactivación del surfactante pulmonar en el desarrollo y resultados de las patologías respiratorias estudiadas, como el ARDS. Correlaciones significantes entre la elevada tensión superficial y parámetros clínicos como $\text{PaO}_2/\text{FiO}_2$ (índice de oxigenación), CRS (distensibilidad del sistema respiratorio), PRISM (riesgo pediátrico de mortalidad) y el índice de Murray (severidad del daño pulmonar), demuestra la importancia de la inactivación del surfactante pulmonar en ARDS. Desarrollo de preparaciones de surfactante resistentes a la inactivación puede ser la clave para el tratamiento de estas patologías. Finalmente, la completa caracterización de modelos animales clínicamente relevantes permite la combinación de datos moleculares, celulares y biofísicos. La caracterización del modelo de ratones deficientes en napsina A permite determinar niveles de proteínas no solo en el surfactante sino también en el tejido pulmonar. Resultados de la caracterización de este modelo apuntan a la inducción de daño en neumocitos tipo II que podría dar lugar al desarrollo de fibrosis. Este modelo supondría una herramienta de estudio del desarrollo de tejido fibrótico y su tratamiento.

Combinación de datos moleculares, celulares, clínicos y biofísicos supone una buena herramienta para entender patologías respiratorias y desarrollar tratamientos eficientes.

Introducción

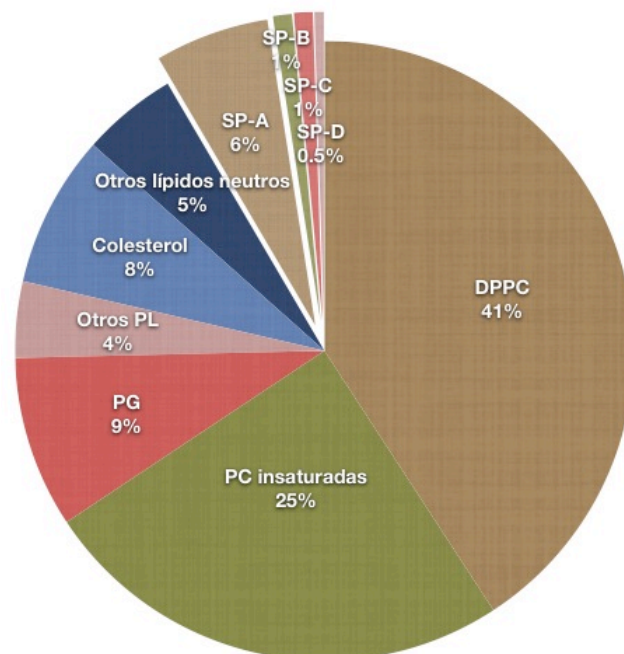
INTRODUCCIÓN

SURFACTANTE PULMONAR

El surfactante pulmonar es producido en los pulmones y tiene una función esencial en la respiración. Dispuesto en la interfase aire-líquido de los espacios alveolares tiene la principal función de reducir la tensión superficial de la fina capa de agua que recubre el epitelio pulmonar. De esta manera se reduce el trabajo necesario durante la inspiración y se evita el colapso alveolar durante la espiración. Además el surfactante supone la primera barrera a la entrada de patógenos, a través de una de las mayores superficies corporales expuestas al medio externo (Daniels and Orgeig 2003; Ochs et al. 2004; Pérez-Gil 2008). Se calcula que el pulmón humano tiene una superficie de unos 100m² con la función vital de llevar a cabo el intercambio gaseoso. Por esta razón, las patologías respiratorias son la causa de un 13.6% de las muertes al año en el mundo (World Health Organization, 2008).

El surfactante pulmonar es una mezcla de lípidos y proteínas, donde los lípidos suponen más del 90% en masa y 4 son las proteínas específicas del surfactante. Como se muestra en la figura 1, el principal componente del surfactante es un fosfolípido disaturado, la dipalmitoilfosfatidilcolina (DPPC), que llega a estar presente hasta en más de un 40%. La importancia de este fosfolípido reside en la saturación de sus dos cadenas de acilo, que permite una alta compactación de la molécula, siendo el principal responsable de la extrema reducción en tensión superficial que produce el surfactante. En proporción también importante se encuentran fosfatidilcolinas insaturadas, y el surfactante además cuenta con fosfatidilglicerol (PG) y otros fosfolípidos como fosfatidilinositol (PI), fosfatidiletanolamina (PE), y esfingomielina (SM) (Goerke 1998; Veldhuizen et al. 1998).

Figura 1: Composición del surfactante pulmonar que representa el porcentaje en masa de los diferentes componentes. Imagen modificada de Zuo et al 2008.



Igualmente importante para la función del surfactante pulmonar es la adecuada proporción de colesterol en sus membranas. Otros lípidos neutros, presentes en proporciones muy bajas, incluyen ésteres de colesterol, triglicéridos, diglicéridos y ácidos grasos libres (Günther et al. 1999b). La composición y proporción de lípidos en el surfactante varía entre especies y en diferentes condiciones ambientales, como puede ser la temperatura corporal (Lang et al. 2005). Pero también varía según las condiciones fisiológicas del animal, ya sean cambios en la velocidad del ciclo

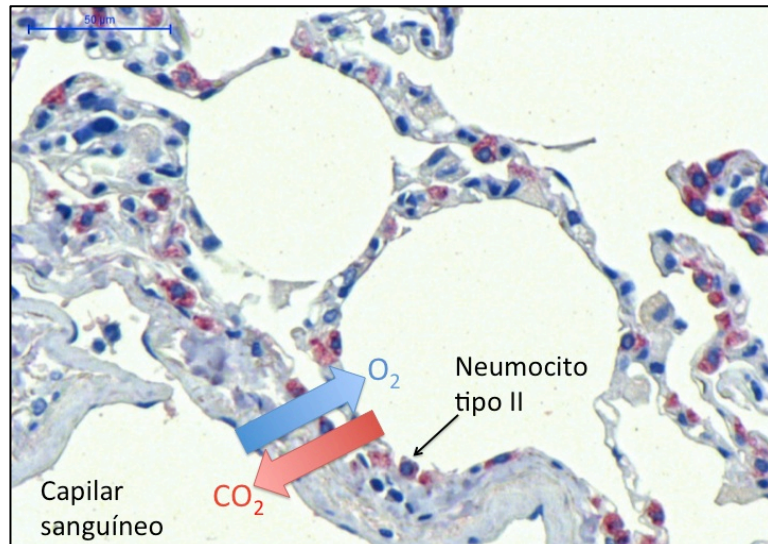
Introducción

respiratorio, como ocurre en animales que hibernan (Suri et al. 2012), o en condiciones patológicas, especialmente las relacionadas con daño pulmonar (Günther et al. 1999; Schmidt et al. 2001). Por otro lado, la composición proteica también es crítica para la correcta función del surfactante. La parte proteica del surfactante también está directamente relacionada con la función fisiológica del sistema. Así las proteínas SP-A y SP-D, que pertenecen a la familia de las colectinas, están directamente relacionadas con la defensa inmune innata del pulmón al reconocer y unirse a patógenos y contribuir a su eliminación (Johansson and Curstedt 1997; Orgeig et al. 2010). Las proteínas SP-B y SP-C son dos pequeñas proteínas hidrofóbicas que interactúan con los lípidos del surfactante y permiten, por un lado, la rápida adsorción interfacial de los fosfolípidos en la interfase aire-agua, y por otro la estabilidad mecánica de las películas de surfactante (Possmayer et al. 2010). Deficiencias en proteínas como la SP-A o la SP-C no son críticas en primera instancia, aunque los modelos animales deficientes en SP-A desarrollan infecciones pulmonares con mayor facilidad (Phelps et al. 2011), mientras que los deficientes en SP-C desarrollan enfermedades pulmonares crónicas (Nogee 2004). Sin embargo, la deficiencia en SP-B resulta letal a los pocos minutos tras el nacimiento, debido a la función esencial de la proteína SP-B en la reducción de la tensión superficial y la estabilización de una superficie alveolar abierta al intercambio gaseoso (Tokieda et al. 1997; Weaver and Beck 1999).

BIOLOGÍA DEL SURFACTANTE PULMONAR

Durante el desarrollo embrionario, el pulmón es el último órgano en desarrollarse y madurar, pues se estima que no es sino hasta la semana 35 de gestación cuando los pulmones están preparados para la respiración aérea y los neumocitos tipo II ya han madurado dando lugar a la síntesis de surfactante. El epitelio pulmonar está compuesto principalmente por dos tipos de células epiteliales, los neumocitos tipo I y II. Además, otros tipos de células se encuentran presentes en los pulmones, incluyendo células Clara que recubren los bronquios y bronquiolos, células endoteliales como las que componen los capilares sanguíneos que irrigan el pulmón y células basales, mesenquimales y fibroblastos, que componen el tejido conectivo o intersticial y ofrecen soporte estructural. Los neumocitos tipo I no son los mayoritarios en el epitelio alveolar pero recubren aproximadamente un 90% de la superficie alveolar. Su membrana basal suele estar en contacto con las células endoteliales de los vasos sanguíneos, de manera que a través de ellos se realiza el intercambio gaseoso desde los espacios alveolares hacia el interior de los capilares por donde circula la sangre. Los neumocitos tipo II son los encargados de sintetizar, secretar y reciclar el surfactante pulmonar (Yamano et al. 2001; Ban et al. 2007; Ravasio et al. 2010). Suponen el 60% de las células del epitelio alveolar. Tanto los lípidos del surfactante como la mayor parte de las proteínas, concretamente SP-A, SP-B y SP-C, son sintetizadas en estas células.

Figura 2: Micrografía modificada de alveolos pulmonares humanos. Tinción de neumocitos tipo mediante inmunohistoquímica anti-proSP-C (rosa).



Estos neumocitos tipo II son células ricas en retículo endoplásmico (RE), donde se sintetizan los lípidos y proteínas del surfactante (Herzog et al. 2008). Posteriormente, se produce el correcto ensamblaje de lípidos y proteínas en estructuras altamente compactadas, a partir de las cuales se secretan.

Los neumocitos tipo II poseen orgánulos especializados en el almacenamiento de los complejos lipoproteicos del surfactante pulmonar, como son los cuerpos lamelares (Weaver 1998). Éstos son secretados a la fina capa de agua del medio extracelular, donde el surfactante adopta una estructura altamente organizada en forma de red llamada mielina tubular (Nag et al. 1999). Por último son los fosfolípidos, ayudados por las proteínas hidrofóbicas, los que ocupan la interfase aire-agua alveolar. Una vez allí se piensa que se organiza una monocapa enriquecida en fosfolípidos, principalmente DPPC, conectada con multicapas que actúan de reservorio de material. Estas conexiones se piensa que son establecidas por medio de las proteínas hidrofóbicas que se encuentran íntimamente asociadas a los fosfolípidos (Keating et al. 2012).

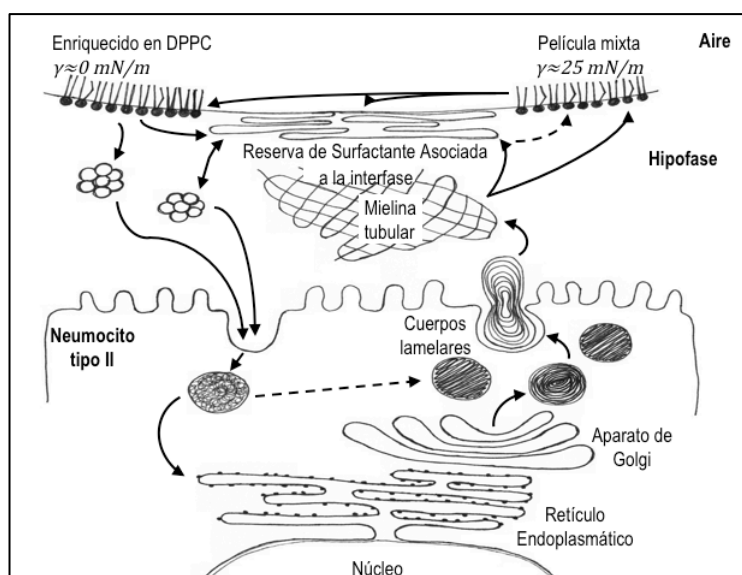


Figura 3: representación esquemática de la secreción y reciclaje del surfactante pulmonar por parte de los neumocitos tipo II. Imagen adaptada de Daniels y Orgeig 2003, Perez-Gil 2008 y Orgeig 2010.

Introducción

La síntesis y transporte de los lípidos de surfactante desde el retículo endoplásmico hasta los cuerpos lamelares no se conoce con exactitud. Considerando que el transporte por medio de vesículas parece jugar un papel importante en el procesamiento de las proteínas de surfactante, éste podría ser también relevante para el transporte de lípidos hasta los cuerpos lamelares. Las proteínas del surfactante, concretamente la SP-B y SP-C, son sintetizadas en el retículo endoplásmico, llegan a los cuerpos multivesiculares por medio del aparato de Golgi y pasan por otro compartimento endosomal intermedio antes de llegar a los cuerpos lamelares (Weaver 1998). Sin embargo, fosfolípidos específicos del surfactante como la DPPC no parece seguir la misma vía. La hipótesis más reciente plantea que DPPC y PG son transferidos directamente desde el RE hasta los cuerpos lamelares mediante un mecanismo sin vesículas. Esta hipótesis se apoya en la localización del transportador de lípidos ABCA3, que sólo se encuentra en la membrana más externa de los cuerpos lamelares (Takahashi et al. 2005). El transporte entre membranas independiente de vesículas debe estar relacionado con proteínas transportadoras de lípidos o con la difusión de lípidos entre membranas a través de los puntos de contacto entre las mismas. Este último mecanismo requiere de nuevo la participación de proteínas que sean capaces de establecer contactos transitorios entre membranas (Perez-Gil and Weaver 2010). Lo que sí queda establecido es la importancia del transportador de fosfolípidos ABCA3, ya que su ausencia resulta tan letal como la ausencia de la SP-B. ABCA3 pertenece a la familia de transportadores ABC, que unen e hidrolizan ATP acoplado al transporte transmembrana de diferentes moléculas como los lípidos. Se encuentra exclusivamente en neumocitos tipo II y además su expresión se encuentra aumentada justo antes del nacimiento, estando regulada por corticoides (Yamano et al. 2001; Yoshida et al. 2004; Ban et al. 2007)

Acoplada a la síntesis y ensamblaje de los lípidos del surfactante se encuentra el procesamiento de las proteínas hidrofóbicas. Tanto la SP-B como la SP-C son proteínas que se sintetizan como precursores de mucho mayor tamaño molecular que sufren diferentes cortes enzimáticos hasta resultar en los pequeños péptidos hidrofóbicos que se ensamblan en el surfactante.

Ambas proteínas siguen la misma vía de procesamiento endosomal desde el RE hasta los cuerpos lamelares, e incluso parecen compartir enzimas de procesamiento. Aunque no se ha podido establecer directamente, muchos resultados parecen apuntar a un mecanismo coordinado de procesamiento, maduración y secreción de ambas proteínas. Se ha descrito que la ausencia de SP-B causa deficiencias en la maduración y/o secreción de la SP-C, apuntando a un mecanismo conjunto de direccionamiento de ambas proteínas en el neumocito (Vorbroke et al. 1995). Además, los genes de ambas proteínas se encuentran bajo la regulación del mismo factor de transcripción, TTF-1 (del inglés, *thyroid transcription factor 1*). TTF-1 es un factor de transcripción nuclear, fosforilado, que se expresa en el epitelio pulmonar, y es esencial para la correcta diferenciación del pulmón durante su desarrollo. TTF-1 se une a numerosos elementos reguladores de la transcripción de genes como los de la secretoglobina A o los de las proteínas del surfactante (*sftpa*, *sftpb* y *sftpc*) (Zhou et al. 1996). La eliminación de TTF-1 resulta letal en modelos animales, y su hiper- o hipofosforilación permite el estudio de su implicación en el desarrollo de los pulmones y del surfactante pulmonar (deFelice et al. 2003).

En la siguiente figura se resumen los compartimentos intracelulares y las etapas proteolíticas conocidas hasta hoy en el procesamiento de las proteínas SP-B y SP-C (Nogee 1998; Brasch et al. 2002; ten Brinke et al. 2002; Brasch et al. 2003; Brasch 2004; Mulugeta and Beers 2006). Ambas proteínas son sintetizadas como precursores de gran tamaño molecular, flanqueadas por segmentos N- y C-terminales que probablemente protegen a las proteínas maduras, altamente hidrofóbicas, del ambiente polar del interior celular, asegurando su correcto plegamiento y evitando su agregación. Poco se conoce sobre la función o destino de los segmentos N- o C-terminales de ambos precursores, una vez liberados. Mientras forman parte del precursor algunos de estos dominio podrían tener una función chaperona. Así, el dominio C-terminal de la proSP-C, que posee un motivo estructural BRICHOS, cuya mutación provoca un fallo en el correcto plegamiento de la proteína (Mulugeta et al. 2007) podría relacionarse directamente con una función chaperona no solo hacia la SP-C madura, si no que una vez eliminado del precursor, podría facilitar el correcto plegamiento de otras proteínas. Por otro lado, se ha propuesto una posible función antibacteriana del segmento N-terminal de la proSP-B, que posee un dominio estructural de tipo saposina, que se asemeja a proteínas propiedades citolíticas y antibacterianas como amebaporos, granulicina y N-K lisina (Olmeda et al. ; Yang et al. 2010).

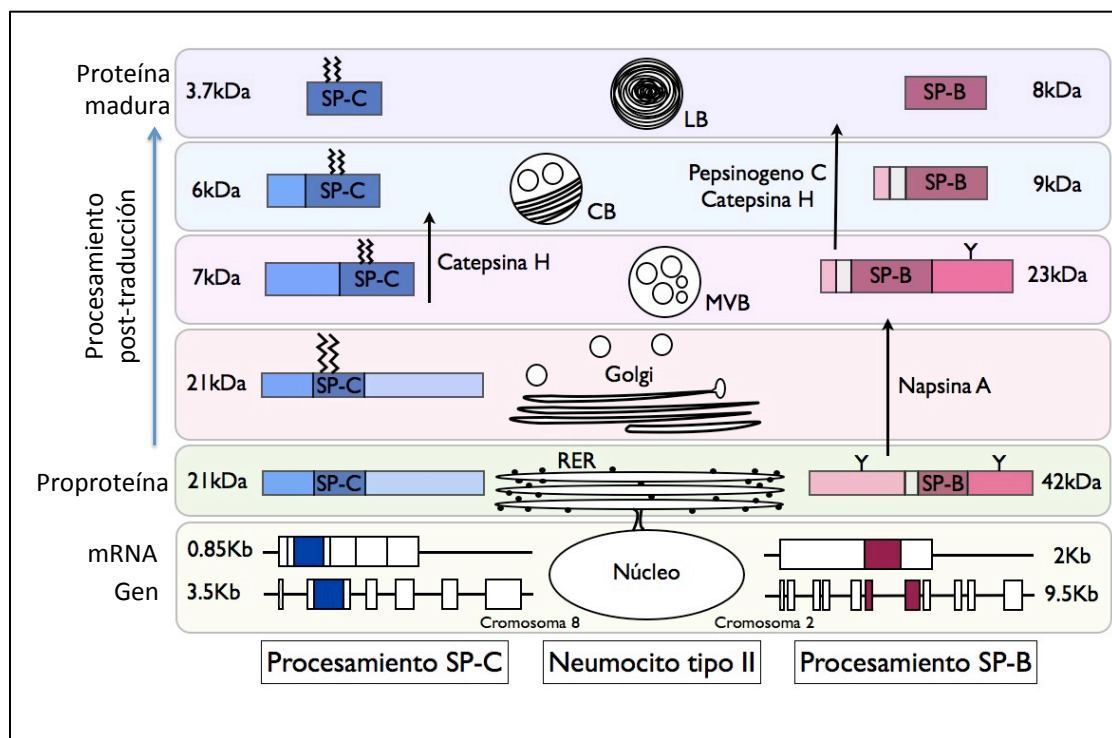


Figura 4: Ruta de procesamiento de las proteínas SP-B y SP-C en los neumocitos tipo II. Figura modificada a partir de Nogee 1998, Brasch et al 2002, ten Brinke et al 2002, Brasch et al 2004 y Mulugeta and Beers, 2006.

Por un lado, la SP-B es sintetizada como un precursor, proSP-B, de unos 40-42kDa de masa molecular (dependiendo del nivel de glicosilación). Un primer corte proteolítico llevado a cabo por la aspartil proteasa Napsina A parece eliminar gran

Introducción

parte del segmento amino terminal del precursor. El intermediario resultante, de unos 23-26kDa viaja a través del aparato de Golgi hasta los cuerpos multivesiculares. Desde allí, pasando por vesículas endosomales intermedias llega a los cuerpos lamelares como proteína madura. Durante este proceso, dos enzimas más parecen estar implicadas en la maduración final de la proteína, el pepsinógeno C (otra aspartil proteasa) y la catepsina H (una cisteín proteasa), encargadas de eliminar tanto los restos de segmento N-terminal como todo el segmento C-terminal (Guttentag et al. 2003). Por otro lado, la SP-C es sintetizada en el retículo endoplásmico como un precursor de 21kDa que es palmitoilado en el aparato de Golgi (ten Brinke et al 2002). Una enzima desconocida realiza el corte proteolítico del segmento C-terminal y más tarde, probablemente la Catepsina H elimina el segmento N-terminal, dando lugar a la proteína madura en los cuerpos lamelares (Brasch et al. 2002).

No sólo la deficiencia en las proteínas maduras da lugar a insuficiencia respiratoria, si no que la interrupción de cualquiera de los procesos proteolíticos antes descritos lleva no sólo a una parcial deficiencia en las proteínas maduras, sino también a la acumulación de precursores y formas mal plegadas de las proteínas. La acumulación de proteínas desplegadas en el retículo endoplásmico activa una respuesta denominada UPR (del inglés, *unfolded protein response*). Esto lleva a la activación en el retículo endoplásmico de vías de respuesta a estrés, que terminan con la activación de señales apoptóticas. Si esto ocurre dentro del contexto de los neumocitos tipo II el daño celular producido deriva en daño pulmonar, como se observa en el caso de la fibrosis pulmonar idiopática (IPF, del inglés *idiopathic pulmonary fibrosis*) (Günther et al. 2012)

SURFACTANTE PULMONAR Y TENSIÓN SUPERFICIAL

La tensión superficial (γ) de un líquido es la energía necesaria para aumentar su superficie por unidad de área y se expresa en unidades de energía por unidad de área o longitud (J/m^2 o mN/m). Esto quiere decir que γ cuantifica la energía necesaria para romper las fuerzas que tienden a minimizar el área expuesta a otro medio diferente al propio líquido. Esto se debe a las fuerzas de atracción entre las moléculas de líquido. En el interior de la fase líquida estas fuerzas se dan en todas las direcciones, anulándose, pero en la interfase con otro medio, estas fuerzas están descompensadas de manera que la fuerza neta está dirigida hacia las moléculas de líquido del interior y las adyacentes en la interfase. En el contexto del epitelio pulmonar, recubierto de una fina capa de agua, estas fuerzas juegan un papel esencial en la estabilidad estructural del pulmón e influyen notablemente en el proceso de la respiración. Si estas fuerzas no son minimizadas durante el vaciado de los pulmones en la espiración, los alveolos mas pequeños tenderían al colapso, ya que la fuerza asociada a la tensión superficial tiende a minimizar al área superficial de la capa acuosa, y en el caso de la interfase aire-líquido respiratoria, la superficie alveolar disponible al contacto con el aire (Hills 1999; Notter 2000).

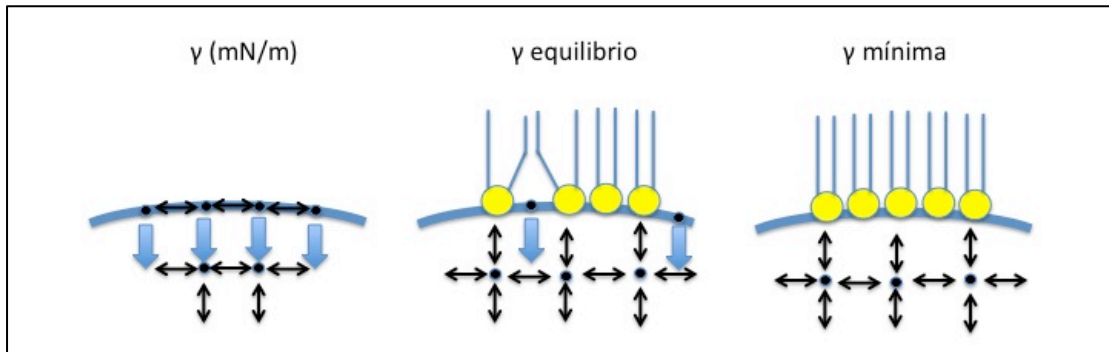


Figura 5: Representación esquemática de la tensión superficial del agua en ausencia y presencia de la película interfacial de fosfolípidos del surfactante. En ausencia de surfactante la fuerza neta tiende a la minimización del área expuesta al aire; en presencia de los fosfolípidos del surfactante, las moléculas de agua son excluidas de la interfase e interaccionan con las cabezas polares de los fosfolípidos. Cuando la interfase se satura de moléculas de fosfolípido se alcanza la tensión superficial de equilibrio. Si esa película interfacial se comprime lateralmente sin que se expulsen los fosfolípidos, puede eliminarse casi completamente la exposición de las moléculas de agua al aire, alcanzándose tensiones superficiales mínimas cercanas a 0mN/m.

La evolución ha desarrollado el surfactante pulmonar para minimizar estas fuerzas. El fundamento del surfactante pulmonar como agente tensioactivo reside en los fosfolípidos, que se colocan en la interfase aire-agua de manera que las moléculas de agua ahora pueden interaccionar con la cabeza polar del fosfolípido, minimizando así la descompensación neta de fuerzas. Además, las moléculas de fosfolípido que ocupan la interfase desplazan moléculas de agua de ésta hacia el interior del líquido. Cuando las moléculas de fosfolípido están establemente asociadas a la interfase se alcanza la tensión superficial de equilibrio (γ_{eq}), a partir de la cual la adición de más material no supone una mayor caída en la tensión sino que se establece un equilibrio molecular por el que las moléculas de fosfolípido se adsorben tanto como se desorben de la interfase. En el caso del agua, la tensión superficial típica es de unos 70mN/m y el surfactante pulmonar es capaz de reducir esta tensión hasta valores cercanos a lo 22-23mN/m de tensión superficial en equilibrio. Sin embargo, el área que ocupa la superficie interna pulmonar no es constante, pues la compresión y expansión producida durante los ciclos respiratorios de espiración e inspiración hace esta superficie dinámica y cambiante. Aunque fisiológicamente el pulmón tiene una capacidad total de unos 5-6L de aire, la distensión pulmonar es limitada y se calcula que el pulmón sólo es capaz de expandirse aproximadamente un 10% del total de su volumen en cada inspiración, y por lo tanto de comprimirse un 10% el total de su volumen en cada espiración (Hills 1999). Se calcula que el aire que entra y sale de los pulmones por ciclo es de unos 0.5L, y el resto hasta los 5-6L es aire que permanece en los pulmones y solo puede ser expulsado en caso de colapso total. Para evitar el colapso de los alveolos pulmonares, el surfactante es además capaz de reducir la tensión superficial alveolar a valores mínimos durante la compresión (espiración)

Introducción

debido a la capacidad de compactación de su especial composición lipídica, en especial relacionada con la presencia de la DPPC.

Los fosfolípidos son moléculas anfipáticas que poseen una región polar o hidrofílica y una región apolar o hidrofóbica. Este tipo de molécula adopta una disposición interfacial especial para minimizar la exposición de la región hidrofóbica a las moléculas de agua. Así, estas moléculas tienen preferencia energética a disponerse en la interfase, de manera que las regiones polares interactúan con el agua, y las regiones apolares con el aire. La región o cabeza polar de los fosfolípidos está compuesta por el grupo polar, el grupo fosfato y la molécula de glicerol, esterificada con dos ácidos grasos, que son los que componen la región hidrofóbica (ver figura 6). El grupo polar es el que caracteriza a cada tipo de fosfolípido, diferenciándose así fosfolípidos zwitteriónicos (con carga neta cero) como fosfatidilcolina y fosfatidiletanolamina, y fosfolípidos aniónicos (ya que poseen una carga neta negativa) como fosfatidilserina, fosfatidilglicerol y fosfatidilinositol.

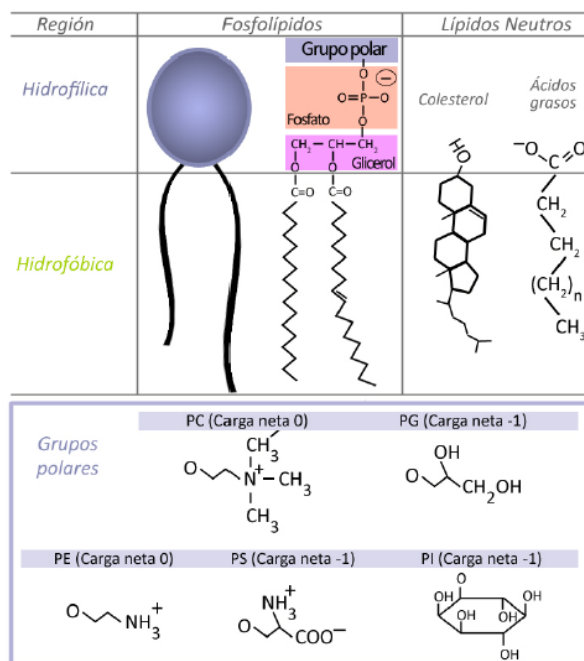


Figura 6: Representación esquemática de la estructura de los diferentes glicerofosfolípidos que pueden encontrarse en el surfactante

Los diferentes tipos de fosfolípidos que forman parte del surfactante ofrecen diferentes características; así por ejemplo, las proteínas hidrofóbicas de carácter catiónico podrían interactuar con los fosfolípidos aniónicos como PG. Por otro lado, la región hidrofóbica de los fosfolípidos está caracterizada por los ácidos grasos que esterifican el glicerol y se diferencian principalmente en la longitud de su cadena y el número y posición de las insaturaciones. El ácido palmítico es especialmente abundante en los fosfolípidos del surfactante, concretamente, en especies lipídicas disaturadas como es la DPPC. Las cadenas insaturadas suponen un impedimento estérico a la máxima compactación lateral de los lípidos, necesaria para reducir la tensión superficial a valores mínimos durante la compresión de la interfase alveolar. Por eso son las especies disaturadas las más importantes desde el punto de vista de la función biofísica del surfactante.

Sin embargo, la adsorción interfacial espontánea de los fosfolípidos es demasiado lenta y su desorción supone una pérdida continua de material de la interfase. Para optimizar estos procesos los complejos de surfactante contienen dos pequeñas proteínas hidrofóbicas que se encuentran siempre asociadas a los fosfolípidos y ayudan tanto a la rápida adsorción interfacial de los componentes más tensioactivos como a la conexión de la monocapa de la interfase con los complejos multicapa que actúan de reservorio en la subfase y permiten la rápida extensión de material a la interfase durante las etapas de expansión. La SP-B y la SP-C son junto con los fosfolípidos, los responsables de la actividad biofísica del surfactante.

La SP-B es una proteína constituida por una elevada proporción de aminoácidos hidrofóbicos (alrededor del 40%) y una estructura secundaria mayoritariamente en α -hélice (27-45%), con una masa molecular de 8.7kDa (Johansson and Curstedt 1997; Wüstneck et al. 2003; Wüstneck et al. 2005). Pertenece a la familia de proteínas tipo saposina que no solo tiene un alto contenido en aminoácidos hidrofóbicos sino también 6 cisteínas en posiciones altamente conservadas que establecen 3 puentes disulfuro intracatenarios (Olmeda et al.). Además, la SP-B posee una séptima cisteína que forma parte de un puente disulfuro intermolecular, formando un dímero covalente. La SP-B es una proteína catiónica, con carga neta positiva, lo que facilita su interacción con fosfolípidos aniónicos como PG. Se ha descrito que la SP-B se dispone de manera superficial, paralela a la membrana. Esto permite a la proteína establecer interacciones hidrofóbicas entre los segmentos helicoidales anfipáticos y la superficie de la membrana. Se ha determinado que alrededor de un 70% de la proteína adopta una disposición superficial, mientras el resto penetraría más o menos profundamente en la membrana, anclando la proteína (Vandenbussche et al. 1992). Esta disposición superficial parece ser esencial para el establecimiento de conexiones entre membranas (Baoukina and Tieleman 2011), por medio de la oligomerización supradimérica de la proteína (Olmeda 2011; Bernardino de la Serna et al. 2012). Además, se ha demostrado que la SP-B induce permeabilidad y agregación en membranas fosfolipídicas (Parra et al. 2011). Estos dos procesos son esenciales para la función biofísica del surfactante, que supone la aceleración del proceso de adsorción interfacial de los fosfolípidos. Mediante las conexiones entre membranas del surfactante, la SP-B favorece el refinamiento de la monocapa, durante la compresión, y la eficiente re-extensión del material desde el reservorio, durante la expansión. La proteína SP-B no sólo juega un papel esencial en la función biofísica del surfactante, sino que también puede facilitar la difusión de oxígeno a través de la capa de surfactante en la interfase respiratoria, probablemente gracias al establecimiento de contactos entre membranas y la formación de una red continua altamente conductiva para la molécula hidrofóbica de oxígeno (Olmeda et al. 2010).

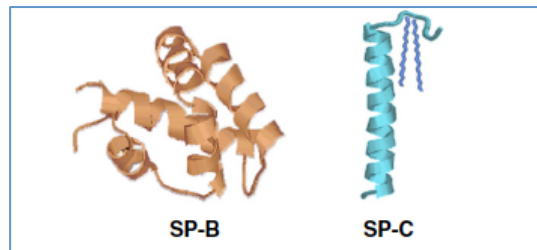


Figura 7: Modelo estructural del monómero de SP-B (Johansson and Curstedt 1997) y estructura resuelta de la SP-C en disolvente orgánico (Johansson et al. 1994).

La SP-C es otro pequeño péptido hidrofóbico de unos 3.7kDa, con una estructura secundaria principalmente helicoidal. Posee un pequeño segmento N-terminal catiónico y sin estructura secundaria determinada, que incluye los dos residuos de cisteín palmitoilados, mientras que la región C-terminal, rica en residuos alifáticos, preferentemente valina, forma una α -hélice altamente hidrofóbica. Esta hélice se dispone con una orientación transmembrana, con un ángulo de inclinación con respecto a la normal al plano de la membrana de unos 70° (Vandenbussche et al. 1992b). Los ácidos palmíticos parecen tener un papel esencial en el anclaje del segmento N-terminal a la membrana, de manera que proteínas recombinantes sin palmíticos son expulsadas de la interfase durante la compresión con mayor facilidad (Bi et al. 2002; Lukovic et al. 2012). El carácter catiónico de la SP-C le permite establecer interacciones preferentemente con los fosfolípidos aniónicos (Perez-Gil et al. 1995), aunque también se ha descrito un comportamiento especial en relación al colesterol. La SP-C parece tener un papel protector cuando existe un aumento de la cantidad de colesterol en las membranas de surfactante, y además la palmitoilación de la proteína parece ser clave para esta función (Gómez-Gil et al. 2009; Baumgart et al. 2010).

De esta manera ambas proteínas, SP-B y SP-C están directamente relacionadas con el papel biofísico del surfactante en el pulmón. Así, las propiedades biofísicas más importantes del surfactante pulmonar son:

- 1) Rápida adsorción interfacial hasta alcanzar la tensión superficial de equilibrio. Así el material llega rápidamente desde la subfase y se expande por la interfase formando la película interfacial de surfactante. Este proceso incluye la llegada y acumulación de material cerca de la interfase y la transferencia última de las moléculas tensioactivas a la interfase. Este proceso debe completarse en cuestión de segundos, para permitir, por ejemplo la eficiente apertura de los pulmones de un recién nacido, al enfrentarse a la respiración aérea por primera vez.
- 2) Compactación eficiente de la película interfacial durante la compresión, para reducir la tensión superficial a valores mínimos. Durante la espiración, la pequeña compresión que sufre el pulmón debe traducirse en una reducción de la superficie interfacial que solo es estabilizada mediante la disminución de la tensión superficial en los alveolos hasta valores mínimos. Para eso, el

material que ocupa la interfase debe compactarse al máximo y como se ha visto, solo los fosfolípidos disaturados como la DPPC son capaces de alcanzar el más alto grado de compactación debido al carácter saturado de sus cadenas de ácido graso. Así, se ha propuesto que la interfase se enriquece en DPPC durante la compresión, mediante la expulsión o “squeeze-out” de una parte importante de los fosfolípidos saturados y neutros al reservorio de material en las subcapas conectadas a la monocapa interfacial (Pérez-Gil and Keough 1998). Recientemente se ha descrito que este proceso podría verse facilitado por la formación de “poros de fusión/adsorción” que facilitarían la salida de fosfolípidos insaturados (Keating et al. 2012). Las proteínas hidrofóbicas del surfactante formarían probablemente parte de esos poros y de ahí su carácter esencial para que las películas del surfactante puedan alcanzar tensiones superficiales mínimas durante la compresión (Schürch et al. 2010; Bernardino de la Serna et al. 2012).

- 3) Eficiente re-extensión durante la expansión de las películas interfaciales previamente comprimidas, sin que la tensión superficial supere nunca los valores de la tensión superficial de equilibrio. Este es otro proceso de adsorción a partir de los reservorios de material interconectados con la interfase. De esta manera la transferencia de material desde los reservorios hasta la interfase es muy rápida y estaría directamente relacionada de nuevo con las proteínas SP-B y SP-C y su capacidad de conectar multicapas adyacentes a la monocapa de la interfase, quizá por los mismos “poros de fusión/adsorción” que se forman durante la compresión. Este proceso es importante durante la inspiración, ya que el mantenimiento de una tensión superficial menor que la tensión de equilibrio asegura la estabilidad de la interfase alveolar y del pulmón.

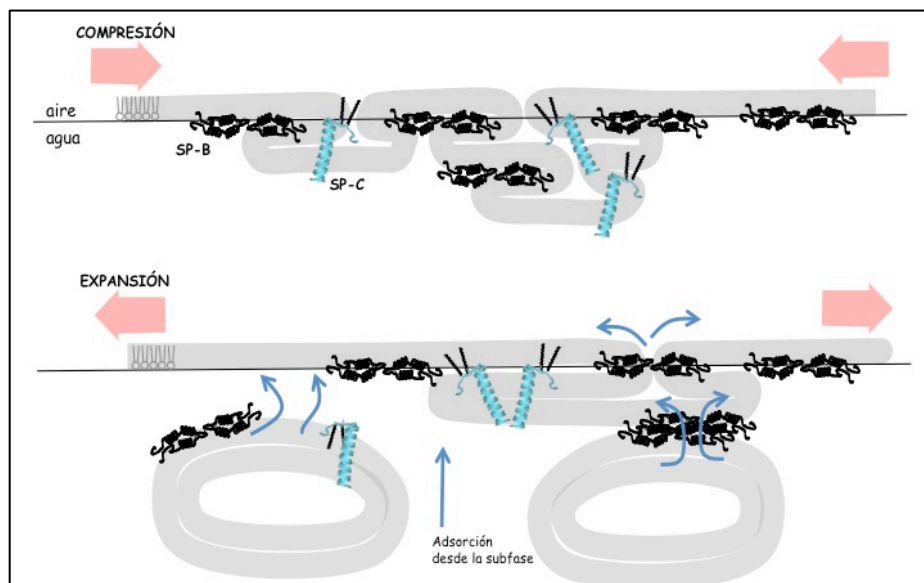


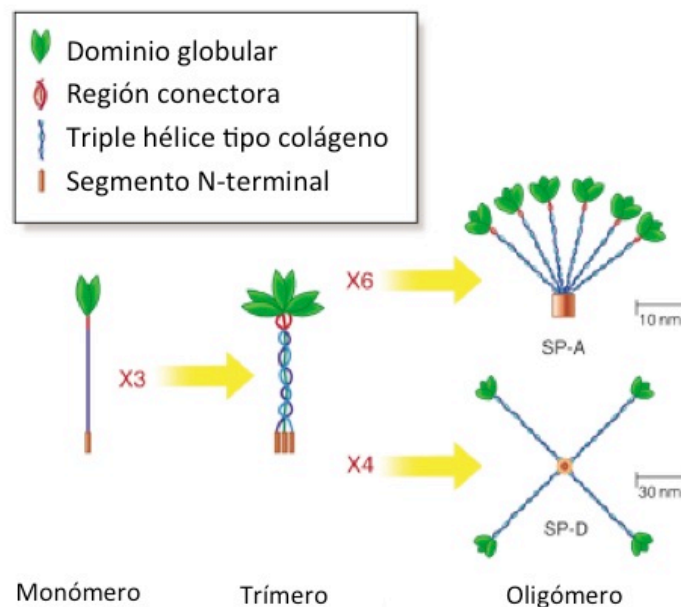
Figura 8: Esquema de la disposición de las proteínas SP-B y SP-C en los complejos de surfactante pulmonar (tomado de Perez-Gil and Weaver 2010). Esquema superior: monocapa y reservorio de surfactante conectado por las proteínas SP-B y SP-C incluyendo la exclusión de material de la interfase facilitada por ambas

Introducción

proteínas durante la compresión. Esquema inferior: re-extensión de material en la interfase y adsorción de nuevo material durante la expansión, facilitada por la interconexión entre membranas que realizan la SP-B y C.

SURFACTANTE PULMONAR Y DEFENSA INNATA

En el pulmón, los principales componentes de la defensa innata incluyen el sistema de aclaramiento muco-ciliar de las vías nasales y vías respiratorias altas, la acción de células fagocíticas como los macrófagos alveolares y las actividades de una serie de proteínas de defensa entre las que se encuentran las proteínas específicas del surfactante A y D. La acción integrada de todos estos elementos tiene como principal función la eliminación de posibles patógenos y la regulación la respuesta inflamatoria. La SP-A y la SP-D son miembros de la familia de las colectinas que reconocen, unen y facilitan la eliminación de patógenos del pulmón (Ruano et al. 2000). Son las encargadas de reconocer y opsonizar microorganismos presentándoseles a las células del sistema inmune, como son los macrófagos, para ayudar a su eliminación (Wright 2003). Sin embargo también se ha descrito una actividad antimicrobiana directa de estas proteínas (Wu et al. 2003) en ausencia de células efectoras. La SP-A y la SP-D unen un amplio rango de microorganismos, incluyendo virus, bacterias, hongos y extractos de ácaros. La SP-A une preferentemente la forma rugosa del lipopolisacarido de las membranas de las bacterias Gram-negativas, mientras que la SP-D se une también a peptidoglicano y ácido lipoteicoico (Kingma and Whitsett 2006).



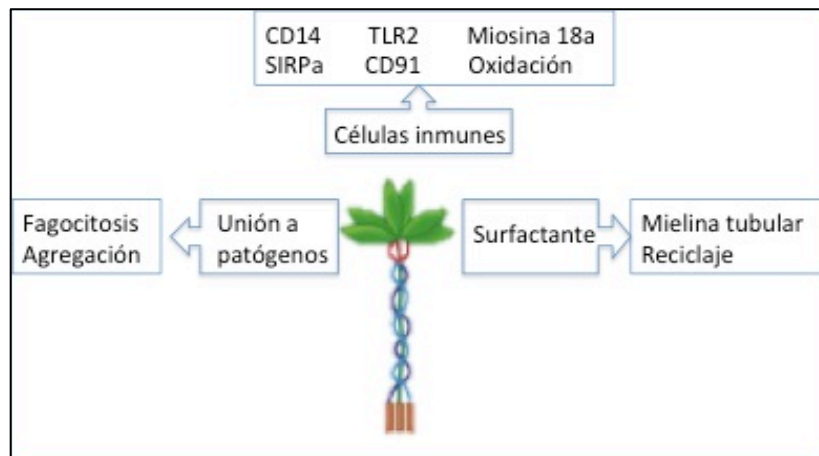


Figura 9 : Esquema representativo de la estructura (arriba) de las proteínas SP-A y SP-D y funciones de la SP-A (abajo). Ambas proteínas poseen motivos estructurales comunes: una región amino terminal rica en cisteínas que establecen puentes disulfuro intercatenarios; un dominio tipo colágeno que forma una triple hélice superenrollada entre tres monómeros; una región conectora helicoidal con organización tipo “coiled-coil”; y por último un dominio globular de reconocimiento de carbohidratos (tomada de Wright 2003). Por otro lado las principales funciones de estas proteínas incluyen: unión a patógenos, provocando agregación y fagocitosis de los mismos; activación de las células inmunes, mediante su unión a varios receptores de células como los macrófagos alveolares; y por último su implicación en la organización estructural del surfactante pulmonar, contribuyendo a la formación de la mielina tubular y al reciclaje de los complejos lipoproteicos (modificada de Wright 2003 y Kingma and Whitsett 2006).

La estructura de estas proteínas está directamente relacionada con la función que cumplen en el pulmón. Así, poseen un dominio globular de reconocimiento de carbohidratos (CRD, del inglés *carbohydrate recognition domain*), a través de la cual se unen a los patógenos y además, la SP-A es capaz de unirse a DPPC también por este dominio. La unión de la SP-A a fosfolípidos mediante el dominio CRD parece jugar un papel importante en la formación de la mielina tubular, una red de membranas característica del surfactante cuyo papel se desconoce (Sano and Kuroki 2005). También se ha sugerido que la unión a fosfolípidos facilita su reciclaje por parte de los neumocitos tipo II, aunque trabajos recientes apuntan al papel esencial de la SP-D en la homeostasis del surfactante (Wert et al. 2000). Los dominios colágeno y conector juegan un papel crucial en la estabilización de los oligómeros de la proteína. Y por último, el dominio N-terminal, también crítico para la estabilización del oligómero, parece ser también importante para el establecimiento de interacciones con los lípidos y la formación de mielina tubular (Palaniyar et al. 2002).

SURFACTANTE PULMONAR Y CLÍNICA

La estabilidad alveolar que aporta la reducción en tensión superficial se puede explicar por la ley de Laplace. De acuerdo con la ley de Laplace, la presión que se produce en la superficie de un líquido que recubre el interior de una esfera y que tiende al cierre de la cavidad es directamente proporcional a la tensión superficial del líquido e inversamente proporcional al radio de la esfera. Es decir, cuanto más pequeña es la esfera y más elevada es la tensión superficial, mayor es la presión que tiende al cierre de la cavidad esférica. De esta manera dos alveolos de diferentes tamaños interconectados deben alcanzar tensiones superficiales diferentes durante la compresión para compensar la diferencia de presión entre ellos, evitando el vaciado de los alveolos mas pequeños en los más grandes y el colapso progresivo del pulmón (Figura 10) (Notter 2000; Parmigiani and Solari 2003).

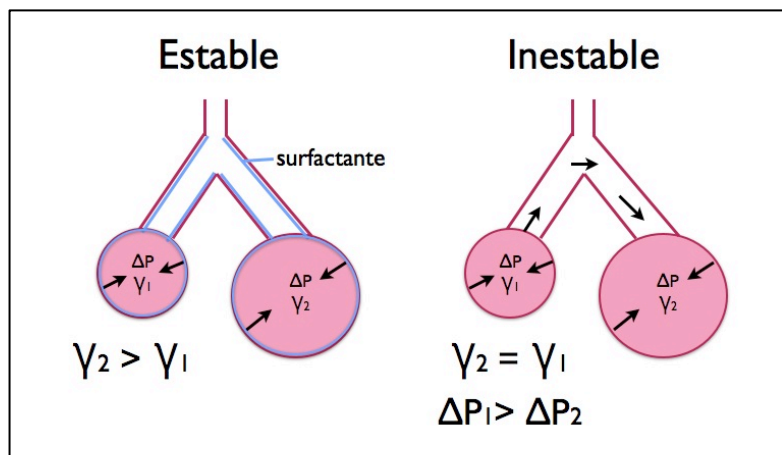


Figura 10: Esquema de fuerzas que intervienen en la estabilidad de los alveolos. y representa la tensión superficial, mientras P es la presión del aire en los alveolos. Modificado de Hills 1999.

Por lo tanto, y como se ha explicado anteriormente, la reducción de la tensión superficial juega un papel crucial en la estabilidad del pulmón. Es la presencia de surfactante lo que proporciona el control sobre la tensión superficial alveolar, de manera que deficiencias en la función del surfactante se traducen en deficiencias respiratorias implicadas en numerosos síndromes y enfermedades respiratorias.

La ausencia de surfactante pulmonar al nacer da lugar a lo que se conoce como síndrome del distrés respiratorio neonatal (NRDS, del inglés *neonatal respiratory distress syndrome*). El descubrimiento de la causa de esta patología respiratoria puso de relevancia la importancia de una adecuada actividad del surfactante pulmonar en la estabilidad del pulmón (Creuwels et al. 1997; Whitsett and Weaver 2002; Willson et al. 2005). Y no fue hasta la introducción de la terapia de suplementación con un surfactante pulmonar exógeno, cuando la mortalidad de neonatos prematuros disminuyó un 80%. Actualmente, el surfactante se aplica de manera profiláctica en los neonatos con una edad gestacional inferior a las 35 semanas, lo que ha permitido

disminuir la mortalidad en neonatos prematuros de hasta solo 25 semanas (Rushing and Ment 2004).

Numerosas patologías respiratorias se asocian con la inactivación del surfactante pulmonar, aunque en muchas de éstas no está claro si esta inactivación forma parte de las causas primarias o es una consecuencia que se traduce en incremento de la tensión superficial y un agravamiento de la patología. Así por ejemplo, en síndromes complejos como son el síndrome del distrés respiratorio agudo en adultos (ARDS, del inglés *acute respiratory distress syndrome*) o el síndrome de aspiración de meconio en neonatos (MAS, del inglés *meconium aspiration syndrome*), la llegada de líquido a los pulmones supone no sólo la activación de procesos de inflamación sino también la inactivación del surfactante pulmonar por ciertos agentes que normalmente no están en el pulmón. Por otro lado, patologías en las que se altera la composición del surfactante tanto en lo que se refiere a los componentes lipídicos como proteicos, ello da lugar a una alteración intrínseca de la actividad del surfactante sin necesidad de agente inactivadores externos. Por ejemplo, la deficiencia en proteínas del surfactante debido a la mutaciones en los genes que las codifican supone otra fuente de desarrollo de patologías respiratorias. No solo las deficiencias genéticas en las proteínas del surfactante causan disfunción del surfactante; la interrupción de los diferentes pasos implicados en la maduración proteolítica de estas proteínas lleva no solo a deficiencias en las mismas, sino también a la acumulación de precursores en el interior de las células, lo que como ya se ha descrito, puede causar daño celular.

La inactivación de la función del surfactante pulmonar por cualquier agente externo tiene como consecuencia el incremento de la tensión superficial alveolar. Esto desemboca en el colapso parcial de los alveolos, o atelectasis, y por lo tanto en una reducción notable de la superficie disponible para realizar el intercambio gaseoso, con la consecuente hipoxemia. La inactivación del surfactante pulmonar se produce fundamentalmente cuando existe un trasvase de suero desde los capilares sanguíneos que irrigan el pulmón hacia los espacios alveolares, como ocurre en el ARDS o cuando el neonato ha inspirado meconio dentro del útero, como en el caso del MAS. La entrada de componentes sanguíneos o de meconio en los pulmones supone, en primer lugar, la dilución del surfactante en el volumen de líquido que se libera indebidamente, y en segundo lugar, la llegada de moléculas que puedan interferir con la actividad del surfactante.

Dos son los principales mecanismos de inactivación del surfactante pulmonar descritos a nivel molecular (Taeusch et al. 2005; Gunasekara et al. 2008; Zuo et al. 2008; Fernsler and Zasadzinski 2009). Por un lado, en condiciones patológicas el surfactante puede encontrarse con otras moléculas que poseen acción tensioactiva, de manera que se establece una competencia por alcanzar la interfase. Por ejemplo, la albúmina, una de las proteínas más abundantes en suero, tiene propiedades tensioactivas siendo capaz de reducir la tensión superficial hasta valores de equilibrio de unos 45-50mN/m (Stenger et al. 2009b). En el caso de la albúmina, como en el de los detergentes, si se comprime la interfase no disminuye la tensión superficial, sino que se establece un equilibrio en el que las moléculas de albúmina entran y salen de la interfase manteniendo la tensión superficial de equilibrio durante la compresión. En condiciones normales, el surfactante es capaz de llegar a la interfase en pocos segundos, pero si esta interfase se encuentra ya ocupada por

Introducción

otras moléculas, el surfactante encuentra una barrera estérica que puede no ser capaz de atravesar (Zasadzinski et al. 2005; Stenger and Zasadzinski 2007; Zasadzinski et al. 2010). Así, en presencia de suero o albúmina, la adsorción interfacial del surfactante se ve alterada y no se alcanzan valores de tensión superficial suficientemente bajos.

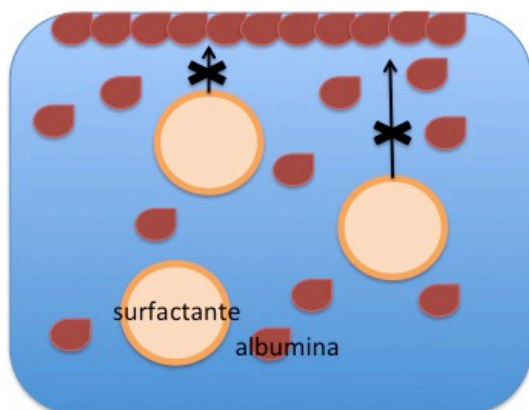


Figura 11 : Inhibición de la acción del surfactante por competición de los complejos de surfactante pulmonar con las proteínas tensioactivas procedentes del suero para alcanzar la interfase. Modificado de Zuo et al., 2008.

Por otra parte, se ha determinado que en condiciones patológicas, el surfactante incorpora otros componentes del suero a parte de las proteínas, como un exceso de colesterol o ácidos grasos libres. La exposición a meconio da lugar a la incorporación de moléculas que pueden perturbar las propiedades biofísicas de las membranas del surfactante como el colesterol o las sales biliares. El colesterol es una de las moléculas más estudiadas en relación a su efecto en la función del surfactante pulmonar (Bernardino de la Serna et al. 2004; Markart et al. 2007; Gunasekara et al. 2008; Bernardino de la Serna et al. 2009). El contenido en colesterol de los complejos de surfactante parece estar determinado por numerosos factores, como puede ser la dieta o la temperatura corporal, y pequeños cambios en la proporción de colesterol están implicados en la modificación de la actividad del surfactante. Esto se debe a la capacidad del colesterol de modular las propiedades biofísicas y la organización y distribución de fases en membranas en general y en las membranas y películas interfaciales del surfactante en particular. La tendencia general es que el colesterol fluidifica los lípidos en fase gel ($L\beta$, donde las cadenas de acilo de los fosfolípidos están altamente compactadas, en una configuración *trans*, resultando en una fase altamente ordenada donde los lípidos casi inmóviles no poseen prácticamente difusión lateral ni rotacional), mientras que tiene un efecto condensante en los lípidos de la fase líquido-cristalina o desordenada ($L\alpha$, donde las cadenas de acilo se encuentran poco compactadas de manera que los fosfolípidos pueden experimentar movimientos rotacionales y traslacionales y numerosas transiciones *trans-gauche* en sus cadenas de acilo). La adición de colesterol genera así una nueva fase conocida como fase líquido-ordenada (L_o), con propiedades intermedias a las de las fases libres de colesterol. Así los lípidos en la fase L_o tienen una organización similar a la de la fase gel pero una mayor movilidad lateral y rotacional (Veldhuizen et al. 1998; Pérez-Gil 2001; Cruz and Perez-Gil 2007; Casals and Cañadas 2012). La cantidad de colesterol que contiene el surfactante, parece ser característico de cada especie y puede estar optimizada para permitir una eficiente segregación de fases de cada mezcla lipídica en las condiciones fisiológicas particulares, por ejemplo según la temperatura corporal de cada organismo. Si la

proporción de colesterol en las membranas de surfactante se modifica excesivamente se produce la disfunción del mismo.

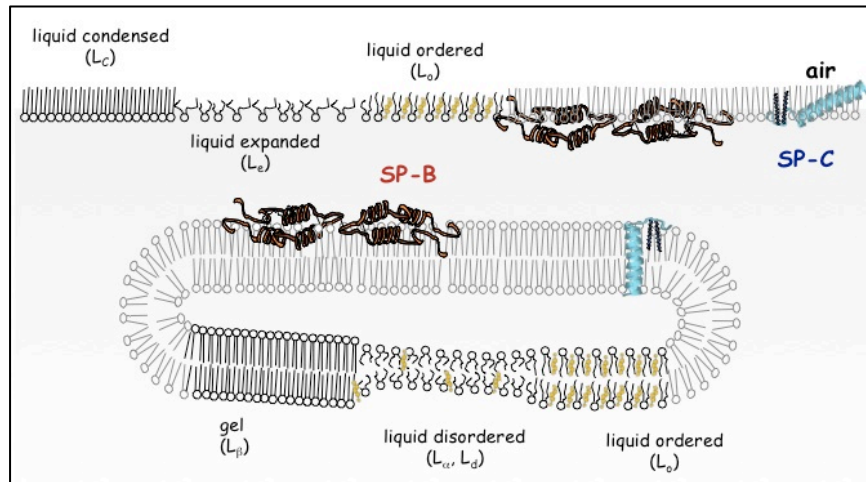


Figura 12: Organización y empaquetamiento de los lípidos en las diferentes fases del surfactante en membranas y monocapas interfaciales. Existen fases de alta compactación lipídica donde no existen movimientos laterales de los lípidos ni rotacionales o traslacionales de las cadenas de acilo como la fase gel (L_{β}) en membranas o líquido condensada (L_c) en monocapas. Por otro lado, pueden existir fases de baja compactación, donde los lípidos tienen además una gran movilidad lateral y amplios movimientos traslacionales y rotacionales de sus cadenas de acilo, como son las fases líquido-cristalina (L_{α}) o líquido-desordenada (L_d) en membranas, o las fases líquido-expandido L_e en monocapas. La fase líquido-ordenado (L_o), tanto en membranas como en monocapas, se genera en presencia de colesterol y posee propiedades intermedias (tomada de Perez-Gil 2008).

La perturbación de la estructura de las fases en las membranas del surfactante pulmonar altera su actividad biofísica. Se ha descrito que excesiva fluidificación de las membranas y películas de surfactante por la inserción de un exceso de colesterol provoca el colapso temprano de éstas, de manera que no se alcanzan los valores mínimos de tensión superficial necesarios para asegurar la estabilidad pulmonar. En este caso no existe ninguna barrera estérica a la adsorción interfacial del surfactante pero el comportamiento de las películas formadas durante su compresión y expansión es anómalo.

No solo el colesterol es capaz de interferir en la actividad biofísica del surfactante, sino que otras moléculas pueden también modificar de las propiedades de las membranas y películas interfaciales, como pueden ser los ácidos grasos libres o proteínas como la CRP (del inglés *C-reactive protein*) (McEachren and Keough 1995; Markart et al. 2007; Sáenz et al. 2010). Además, la modificación de la composición lipídica como resultado de la modificación del metabolismo de síntesis, reciclaje y movilización de los diferentes lípidos, tiene consecuencias en la segregación de fases y en el correcto funcionamiento del surfactante. Así en ARDS e IPF se observan

Introducción

alteraciones de la composición lipídica del surfactante de pacientes, que debe contribuir a la inactivación del surfactante en estas patologías (Günther et al. 1996; Günther et al. 1999; Schmidt et al. 2001).

En muchas patologías pulmonares, la disfunción del surfactante pulmonar conlleva el incremento de la tensión superficial en lo alveolos, lo que contribuye notablemente al agravamiento de la patología. Aunque estas patologías son muy complejas y no se puede considerar que la inactivación del surfactante sea una causa directa de las mismas, sí puede suponer una de las principales causas de que finalmente se pueda producir un fallo respiratorio. En la siguiente tabla se incluye un resumen de la posible implicación de la inactivación de surfactante en el desarrollo de las patologías respiratorias que se consideran en esta Tesis.

| Patología respiratoria | Agente inactivador | Mecanismo molecular de inactivación | Resultado clínico |
|------------------------|----------------------|--|--|
| MAS | Meconio (colesterol) | Modificación de las propiedades biofísicas de las membranas y películas interfaciales. ↑Tensión superficial durante la compresión y expansión. | Atelectasis (colapso parcial alveolar) |
| ARDS | Suero (proteínas) | Competencia por la interfase. Adsorción interfacial reducida → ↑Tensión superficial | Disminución de la distensibilidad pulmonar (compliance) |
| IPF | | Alteración de la composición lipídica y proteica del surfactante. ↑Tensión superficial + daño en neumocitos tipo II | Disminución de la distensibilidad pulmonar (compliance) + Desarrollo de tejido fibrótico |

Tabla 1: Patologías respiratorias en cuyo origen y desarrollo se propone una contribución significativa de la inactivación del surfactante. (Gross et al. 2006; Gunasekara et al. 2008; Zuo et al. 2008; Fernsler and Zasadzinski 2009; Stenger et al. 2009; Zasadzinski et al. 2010; Günther et al. 2012).

El meconio constituye las primeras deposiciones de los neonatos y debe ser excretado tras las 24-48 primeras horas de vida. Sin embargo, cuando existe estrés durante el parto o en caso de asfixia intrauterina el meconio puede ser expulsado, mezclándose con el líquido amniótico con el riesgo de llegar a las vías aéreas del bebé. La presencia de meconio en el líquido amniótico se da en el 12-15% de los partos, mientras que el síndrome de aspiración de meconio ocurre en el 5-10% de estos casos. Aproximadamente un 4% de los casos de MAS no sobrevive representando el 2% de la mortalidad neonatal en los hospitales (Lim and Arulkumaran 2008; van Ierland and de Beaufort 2009). El meconio es una mezcla compleja de compuestos resultantes del crecimiento y metabolismo fetal. Así, por ejemplo, contiene colesterol, sales biliares, proteínas, fosfolipasas y ácidos grasos libres. Como se ha descrito anteriormente, muchos de estos compuestos pueden mezclarse con el surfactante y alterar sus propiedades y actividad biofísica. Este síndrome es muy complejo y tiene muchos síntomas. Clínicamente se caracteriza por presentar obstrucción de las vías aéreas, neumonitis, hipertensión pulmonar,

acidosis e hipoxemia (Nkadi et al. 2009), lo que se traduce en un déficit severo de oxigenación, reducción de la distensibilidad pulmonar, taquipnea y dispnea. El tratamiento mediante suplementación con surfactante pulmonar exógeno no funciona, probablemente debido a la inactivación del surfactante exógeno por el mismo mecanismo que da lugar a la inactivación del endógeno (El Shahed et al. 2007).

Por otro lado, el síndrome de distrés respiratorio agudo (ARDS) se produce en niños y adultos y supone un fallo respiratorio como consecuencia de daño pulmonar por numerosas causas. Este síndrome está caracterizado por un proceso de inflamación severo que causa daño alveolar difuso y resulta en hipoxemia severa y disminución de la distensibilidad pulmonar (Dushianthan et al. 2011). La incidencia del ARDS se estima en EEUU de alrededor de 58/100000 personas por año (Rubenfeld et al. 2005) y en Europa de 4.2-13.5/100000 personas por año (Lühr et al. 1999). La mortalidad asociada al ARDS es de 36-44% (Phua et al. 2009) ya que los pacientes sufren frecuentemente un fallo sistémico, siendo éste la principal causa de mortalidad de los pacientes de ARDS junto con sepsis, más que por fallo respiratorio (Montgomery et al. 1985). El ARDS se caracteriza por estar asociado a un proceso inflamatorio descontrolado que conlleva daño alveolar y vascular en el pulmón. Durante la fase aguda inicial se incrementa la permeabilidad vascular lo que da lugar a extravasación de suero y proteínas plasmáticas a los espacios aéreos alveolares. Las proteínas tensioactivas contenidas en el suero, como se ha explicado anteriormente, compiten con el surfactante pulmonar por ocupar la interfase, comprometiendo la adsorción interfacial de éste y reduciendo su actividad biofísica. Además, el daño producido por estos elementos en los neumocitos tipo I contribuye al edema pulmonar y la rotura de la barrera epitelial. La fase aguda es seguida de una fase de proliferación de tejido fibrótico y remodelación pulmonar que lleva a hipertensión pulmonar e hipoxemia (Ware and Matthay 2000). Como uno de los factores que contribuyen al desarrollo de esta patología es el aumento de la tensión superficial provocado por la inactivación del surfactante pulmonar, se ha propuesto como tratamiento la terapia de suplementación con surfactante. Varios ensayos clínicos han demostrado que esta terapia resulta beneficiosa en la mejora de algunos parámetros clínicos, aunque no ha demostrado aumentar la supervivencia de los pacientes (Gregory et al. 1997; Spragg et al. 1999; Wiswell et al. 1999). Se piensa que la principal causa del limitado resultado de la terapia de suplementación es, al igual que en el caso del MAS, la inactivación del surfactante exógeno, por los mismos mecanismos que lleva a la inactivación del endógeno. La optimización de nuevos surfactantes pulmonares de uso clínico, con resistencia mejorada a la inactivación, es probablemente necesario en el desarrollo de nuevas estrategias terapéuticas para el tratamiento de estas patologías (Spragg 2002).

Por último, la fibrosis pulmonar idiopática (IPF) no se asocia con un factor externo inactivador del surfactante pulmonar, sino que la modificación de la propia composición del surfactante puede ser la principal causante. La IPF es relativamente poco común, 1.6-1.7/100000 personas por año y una media de supervivencia de 2-5 años (Coultas et al. 1994; Günther et al. 2012). Afecta predominantemente a personas de más de 67 años, y es más común entre varones y fumadores. El surfactante procedente de pacientes de IPF muestra una reducida capacidad de alcanzar tensiones superficiales mínimas. Se ha descrito que la elevada tensión

Introducción

superficial produce daño crónico en el epitelio pulmonar y en los neumocitos tipo II, lo que se traduce en una alteración de la composición lipídica y proteica del surfactante. Por un lado, el surfactante de pacientes de IPF muestra una reducción en el contenido de SP-B y SP-C, que como se ha explicado, son esenciales para la función biofísica. Por otro, se observa una reducción de la proporción de PG, junto con un incremento en PI y SM (Günther et al. 1999; Günther et al. 1999b). Estos cambios en composición comprometen la actividad del surfactante. El daño producido en los neumocitos tipo II conlleva respuestas de estrés en el retículo endoplásmico, daño lisosomal y daño en el DNA. Todo ello desemboca en la activación de procesos apoptóticos en estas células esenciales para el mantenimiento de la estabilidad pulmonar, en la secreción de agentes profibróticos al espacio alveolar. Estos compuestos activan la proliferación de células mesenquimales y promueven el desarrollo de tejido fibrótico. La terapia utilizada actualmente en pacientes con IPF se basa en interferir en el proceso fibrótico, y promover la regeneración de neumocitos tipo II. Además, se ha propuesto el uso de terapias de suplementación con surfactante pulmonar para evitar el daño celular debido a la elevada tensión superficial.

OBJECTIVES

OBJETIVOS

Objectives/Objetivos

OBJECTIVES

The main objective of this thesis is to describe molecular processes associated with surfactant inactivation, both *in vitro* and *in vivo*. From molecular description of inactivating processes to the biophysical signatures of surfactant impairment. From biophysical characterization of *in vivo* models to correlation with clinical parameters and disease outcome. Specific objectives are the following:

The first part is focused in the description of molecular processes with relevant biophysical implications in surfactant dysfunction. *In vitro* characterization of surfactant inactivation includes molecular studies of surfactant inactivation by meconium, development of a protocol for studying surfactant inactivation in captive bubble surfactometry in a standard and detailed way, and production of a highly inactivation-resistant surfactant preparation pre-treated with hyaluronic acid.

1.- Molecular description of meconium-induced inactivation of surfactant. Identification of inactivating agents in meconium and its mechanism of action in surfactant membranes, necessary to understand surfactant inactivation during meconium aspiration syndrome (MAS).

2.- Optimization of captive bubble surfactometer protocols for the study of surfactant inactivation by different inactivating substances. Different agents, such as serum, meconium and cholesterol, were studied using a novel standardized and detailed protocol, which also allows assessing the addition to surfactant of substances such as hyaluronic acid, looking for an enhanced resistance to inactivation.

3.- Description of entropic forces that hyaluronic acid (HA) is promoting in surfactant membranes to elucidate the molecular mechanism by which HA increases surfactant resistance to inactivation. Proposal of a highly inactivation-resistant surfactant preparation by pre-treatment with HA.

The second part of this Thesis is focused on the biophysical study of clinically relevant samples. This part includes the biophysical description of surfactant function from control and patients with acute respiratory distress syndrome (ARDS) and a complete molecular, cellular, histological and biophysical characterization of a Napsin A KO mouse model, looking for an animal model of idiopathic pulmonary fibrosis (IPF). It will include the study of the implication of surfactant dysfunction in both pathologies that show an increased alveolar surface tension.

4.- Biophysical characterization of surfactant from ARDS paediatric patients. Correlation of clinical parameters, such as lung compliance and arterial oxygenation as indicators of lung performance, and PRISM and Murray's score as indicators of clinical outcome for these patients, with biophysical data for highlighting the importance of surfactant function in the development of this syndrome.

5.- Description of a Napsin A KO mouse as potential model for IPF. Study of surfactant protein B and C content in BAL and lung tissue, quantification of and localization of protein accumulation in type II cells and development of ER stress, resembling early stages of IPF conditions. Study of aspartyl proteases and proposal of a secondary alternative pathway for SP-B processing.

Objectives/Objetivos

OBJETIVOS

El principal objetivo de esta Tesis es describir procesos moleculares asociados con la inactivación de surfactante pulmonar, tanto *in vitro* como *in vivo*. Desde la descripción molecular de los procesos de inactivación hasta la caracterización de las propiedades biofísicas de un surfactante dañado. Desde la descripción biofísica de modelos *in vivo* hasta su correlación con parámetros clínicos y con el desenlace de la patología. Los objetivos específicos se enumeran a continuación:

La primera parte se centra en la descripción molecular de procesos con implicaciones biofísicas relevantes en la disfunción del surfactante pulmonar. Se aborda una caracterización *in vitro* de la inactivación de surfactante que incluye: estudio de los procesos moleculares de la inactivación por meconio; desarrollo de un nuevo protocolo para estudiar la inactivación de surfactante pulmonar en el surfactómetro de burbuja cautiva de manera estandarizada y detallada; y la propuesta de una preparación de surfactante que muestra una alta resistencia a inactivación, mediante su pre-tratamiento con ácido hialurónico.

1.- Descripción molecular de la inactivación de surfactante inducida por meconio. Identificación de agentes inactivantes en el meconio y su mecanismo de acción sobre membranas de surfactante, que lleva como resultado la desactivación de surfactante durante el síndrome de aspiración de meconio.

2.- Optimización de un protocolo en el surfactómetro de burbuja cautiva para el estudio de la inactivación de surfactante por diferentes sustancias. Diferentes agentes inactivadores, como el suero, meconio o colesterol, son estudiados con un protocolo estandarizado que permite la adición de sustancias al surfactante, como el ácido hialurónico, en búsqueda de un incremento en su resistencia a la inactivación.

3.- Descripción de las fuerzas entrópicas que ejerce el ácido hialurónico (HA) sobre las membranas y complejos del surfactante para dilucidar el mecanismo molecular por el cual el HA incrementa la resistencia a inactivación del surfactante. También se propone una preparación de surfactante con alta resistencia a inactivación, tras su pre-tratamiento con ácido hialurónico.

La segunda parte esta centrada en el estudio biofísico de muestras con relevancia clínica. Esta parte incluye la descripción de la actividad biofísica de surfactante procedente de controles y pacientes pediátricos del síndrome de distrés respiratorio agudo, y una caracterización completa molecular, celular, histológica y biofísica de un modelo KO para Napsina A en ratón, en búsqueda de un modelo para fibrosis pulmonar idiopática. Estudio de la implicación de la disfunción del surfactante pulmonar en ambas patologías que muestran una elevada tensión superficial alveolar.

4.- Caracterización de la función biofísica de surfactante procedente de pacientes con síndrome de distrés respiratorio agudo. Correlación de parámetros clínicos, como distensión pulmonar y oxigenación arterial, como indicadores de la función pulmonar, y PRISM junto con Murray's score, indicadores del desarrollo del daño pulmonar y del desenlace de la patología, con datos biofísicos para subrayar la importancia de la función del surfactante en el desarrollo de este síndrome.

Objectives/Objetivos

5.- Descripción de un modelo KO para Napsina A en ratón como potencial modelo de fibrosis pulmonar idiopática. Estudio del contenido en proteínas SP-B y SP-C del surfactante en lavado broncoalveolar y tejido pulmonar, cuantificación y localización de la acumulación de proteína en neumocitos tipos II y desarrollo de estrés en el retículo endoplásmico, simulando las condiciones iniciales del desarrollo de fibrosis pulmonar. Estudio de aspartil-proteasas y propuesta de una ruta alternativa de procesamiento de la SP-B.

FROM MOLECULES TO BIOPHYSICS

FROM MOLECULES TO BIOPHYSICS

This first part of the Thesis is focused on describing molecular processes and biophysical implications that take place when surfactant is under critical conditions, as may occur in different respiratory distresses. Understanding the basics of these pathophysiological processes is very important to improve the treatments. Improving treatments include the optimization of surfactant preparations with higher resistance to inactivation. Through this part we describe the molecular mechanisms of surfactant inactivation, we develop a model for studying surfactant inactivation and reactivation by polymers in CBS, and propose the optimization of inactivation-resistant surfactants by the pre-activation with hyaluronan.

In the first chapter we describe the molecular mechanism of inactivation of surfactant by meconium. Even though meconium aspiration syndrome is nowadays a respiratory disease of minor importance, still in the USA it causes around 20.000 deaths per year. The inactivating mechanisms of surfactant have been already studied, but meconium inactivation of surfactant was not clearly understood. Therapeutic treatment of babies with MAS consists on the application of exogenous (clinical) surfactant as it is done in RDS. The supplementation with exogenous surfactant of neonates suffering or at risk of RDS is a success that allows babies to open their lungs and start breathing, but it has been disappointing on the treatment of MAS. The main reason why application of surfactant is not working when meconium is present in the lung is due to the fact that exogenous surfactant is inactivated as the endogenous one. In the second chapter we describe the optimization of a methodology to study surfactant inactivation in simple models that we could later apply on complex and more clinically relevant samples, as for example samples from ARDS patients described in the second part of this Thesis. Optimizing the protocol for studying surfactant inactivation starts with understanding the molecular mechanisms and physiologically relevant conditions of the inactivation. According to the mechanism of inactivation that has been described so far, the inactivation of surfactant should be very different in the case of serum (or surface-active proteins) and meconium/cholesterol (or membrane-perturbing molecules). Thus each mechanism requires a different approach and a different methodology to be studied. To simulate physiological conditions of alveolar oedema, serum without any dilution is applied into the bubble, as it would happen in an alveolus full of fluid as a consequence of alteration of the permeability of the alveolar-capillary barrier. On the other hand, premixing of surfactant with meconium or cholesterol, would allow these membrane-perturbing molecules to exhibit their inactivating action. Once the model has been set to study inactivation, it has been applied to study the addition of different substances to surfactant in order to determine its beneficial effect on restoring surfactant activity. In the third chapter we analyse thoroughly the molecular mechanism by which polymers such as HA are able to reactivate surfactant under inactivating conditions. Physical and entropic forces may have a role to play on the effect of HA in surfactant. Deeply understanding the mechanism of reactivation may help to optimize new surfactant-HA preparations. Finally in this chapter we proposed the development of a pre-activated surfactant that is more resistant to inactivation and could be a good therapeutic option.

**MECONIUM IMPAIRS PULMONARY SURFACTANT BY A COMBINED ACTION OF
CHOLESTEROL AND BILE ACIDS**

Elena Lopez-Rodriguez, Mercedes Echaide, Antonio Cruz, H. William Taeusch and
Jesus Perez-Gil

Biophysical Journal (2011) 100 (3): 646-655

This work has been done in collaboration with MD H. William Taeusch (General Hospital of San Francisco, University California San Francisco)



MECONIUM IMPAIRS PULMONARY SURFACTANT BY A COMBINED ACTION OF CHOLESTEROL AND BILE ACIDS

INTRODUCTION

Pulmonary surfactant is a complex mixture of lipids and proteins lining the alveolar air-water interface. By lowering the surface tension at the respiratory interface, pulmonary surfactant stabilizes the respiratory surfaces against physical forces tending to collapse the air spaces (Been and Zimmermann 2007; Nkadi et al. 2009). Surfactant and the respiratory system is one of the latest systems to be developed during embryonic gestation and surfactant maturation does not occur until the 35th week of gestation. Pre-mature babies with less than 35 weeks of gestation may suffer from respiratory distress syndrome (RDS), due to the lack in surfactant (Creuwels et al. 1997; Willson et al. 2005). Lack or alteration of surfactant is associated with severe respiratory pathologies in neonates and adults, such as respiratory distress syndrome (RDS), acute respiratory distress (ARDS), pulmonary hemorrhage, meconium aspiration syndrome (MAS) or genetic disorders of surfactant (Rubin et al. 1996; Been and Zimmermann 2007; Nkadi et al. 2009). Surfactant replacement is commonly and successfully used for the therapeutic treatment of RDS, but it is failing in the treatment of MAS (El Shahed et al. 2007). The working hypothesis is that the presence of meconium into the alveolar spaces is inactivating surfactant, both the endogenous, from the baby, and the exogenous, clinical surfactant applied as therapy.

Meconium is supposed to be excreted during the first 24-48h hours of life, but when there is stress during delivery or intrauterine asphyxia, the baby can release meconium into the amniotic fluid and then, there is a high risk of aspiration leading meconium into the airways. Staining of the amniotic fluid with meconium occurs in 12-15% of deliveries, and MAS in 5-10% of the meconium staining cases. Only a 4% of the cases do not survive, but MAS represents the 2% of neonatal deaths in hospitals. Even though nowadays the percentage of meconium aspiration syndrome is not very high, it is still the cause of about 20.000 deaths per year in USA (Lim and Arulkumaran 2008; van Ierland and de Beaufort 2009). In contrast to RDS, the longer the pregnancy (post-mature babies) the higher risk has the baby to suffer from MAS.

Meconium aspiration causes many effects and is a complex syndrome. Clinically, MAS courses with airway obstruction, pneumonitis, pulmonary hypertension, ventilation/perfusion mismatch, acidosis and hypoxemia (Nkadi et al. 2009). Clinical symptoms of MAS include severe oxygenation deficit, hyperexpansion, decreased lung compliance, increase airway resistance, tachypnea (increase breathing rate to eliminate increased CO₂ levels (hypercapnia)) and dyspnea (shortness of breath).

There is also an underlying inactivation of surfactant that contributes to the main symptoms of MAS. The presence of meconium on the air-water interface may lead to dilution of surfactant and inactivation, but also to inflammation and release of inflammatory mediators, many of them inactivating surfactant. Inactivation of surfactant may lead to increased surface tension and alveolar collapse or atelectasis (partial collapse of the alveoli). Hypoxia is one of the symptoms of MAS, as there is a reduced entrance of air and thus impaired gas exchange. All together, within the

context of a newborn baby, who should open his lungs for the first time and successfully breathing to survive, imposes a severe complication in this syndrome. Also it has been observed that babies suffering from MAS have higher risk to develop asthma when they get to childhood. At least two different mechanisms have been proposed for surfactant inactivation after lung injuries causing respiratory distress (Gunasekara et al. 2008; Zuo et al. 2008). A first model involves blood proteins, inflammation proteins and other surface-active substances, which compete with surfactant complexes for reaching the interface (Fernsler and Zasadzinski 2009). A second model hypothesizes that surfactant dysfunction results from the intrinsic impairment of surfactant complexes by small amphiphilic molecules such as free fatty acids, cholesterol, lysolipids, bile acids and/or diacylglycerol. These substances, in part coming from the degradation of surfactant itself by inflammatory phospholipases, insert into the surfactant complexes rendering it dysfunctional (Iwanicki et al. 2010).

Meconium is a complex mixture that accumulates in the fetal gut during gestation. It contains proteins, sterols, bile salts and inorganic molecules. The main sterol is cholesterol and bile salts include cholic acid, taurocholic acid and glycocholic acid (Tollofsrud et al. 2002; Righetti et al. 2003; Lindenskov et al. 2005). All of these components are inactivating agents of surfactant function. These compounds maybe inserted into surfactant membranes, perturbing its structure and phase segregation, essential for surfactant proper function. Therefore, the mixing of meconium with surfactant at the alveolar spaces may result on surfactant inactivation (Park et al. 1996).

The objective of this chapter is to thoroughly study the molecular mechanism of the inactivation of surfactant by meconium. On the one hand, identifying the main inactivating agents present in meconium and its mechanism of action on surfactant complexes. And on the other hand, characterizing the biophysical implication of the presence of these inactivating molecules, studying the functional and structural properties of surfactant that get modified in the presence of meconium. Better understanding of the molecular mechanism by which surfactant is inactivated during respiratory distress is important not only to deeply understand the pathophysiology but also to improve treatments.

RESULTS

We first studied meconium-induced inhibition of natural surfactant purified from animal lungs, before trying to elucidate the molecular mechanism undergoing this inhibition.

Interfacial Adsorption. Native surfactant adsorbs in a few seconds from the subphase into the interface, rapidly reaching equilibrium surface pressures (π_{eq}) of about 45mN/m (figure 1.1A). Increasing concentrations of meconium produce a progressive reduction of interfacial adsorption, which keeps being fast at first instance, but reaches progressively lower equilibrium pressures at longer term. A similar dose-dependent effect had already been observed by Park (1996) after

exposure of Surfactant-TA to meconium. The insert in figure 1A plots the maximum pressure reached during the time of the experiment vs. the concentration of meconium into the subphase. The lowest meconium concentrations tested already produce a substantial decrease in the adsorption of surfactant.

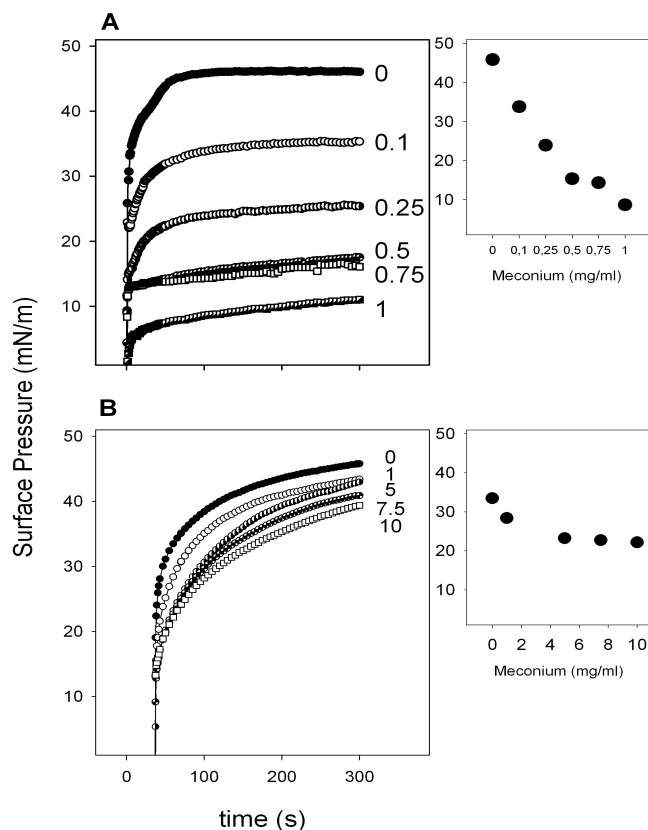


Figure 1.1. Interfacial adsorption of native surfactant exposed to different concentrations of meconium.

A) Interfacial adsorption of surfactant upon injection into the subphase of a Wilhelmy balance containing the indicated concentrations of meconium (mg/ml); insert) surface pressure reached by the absorbed material at 100 seconds after injection vs. the concentration of meconium. B) Interfacial adsorption of surfactant preincubated with the indicated concentrations of meconium once spread directly at the air-water interface of a surface balance; insert) surface pressure reached by the spread material 100 seconds after spreading vs. the concentration of meconium.

Adsorption of surfactant complexes from the subphase involves two processes: movement of surfactant particles through the bulk aqueous phase to reach sub-surface compartments and transfer of surface active molecules from surface attached structures into the interface. To discriminate the effect of meconium in these two processes, we analyzed the effect of meconium exposure on the ability of surfactant to adsorb and spread after direct deposition at the interface. Figure 1.1B compares spreading kinetics of native surfactant onto a meconium-free subphase and onto subphases containing increasing concentrations of meconium. Exposure to progressively higher meconium concentrations also reduces the ability of surfactant

to spread and adsorb at the interface, but to a much lesser extent than observed when injecting the surfactant sample into the bulk subphase.

Compression Isotherms. Figure 1.2A compares the compression isotherms obtained from films formed by interfacial spreading of native surfactant or from native surfactant pre-treated with meconium (10mg/ml). Typical isotherms from native surfactant show increasing surface pressure as a function of area reduction from a variable lift-off molecular area –the area at which surface pressure starts to rise- up to reaching a plateau at around 45mN/m. Differences in apparent molecular areas of the surfactant isotherms are due to minor, uncontrollable, differences from sample to sample in the efficiency of transfer of spread surfactant into the interface. Compression beyond the plateau causes a sharp increase in pressure up to reach a collapse pressure of 70mN/m. The isotherm from meconium pre-treated surfactant differs. At low surface pressures, the isotherm exhibits an expansion to larger areas, meaning that the material transferred into the interface occupies a larger space than that taken by surfactant mixtures without meconium. However, meconium-treated surfactant requires a greater degree of compression to reach and maintain high surface pressures compared with meconium-free surfactant. These data are consistent with meconium constituents inserting into surfactant and expanding the isotherm at low compression. This material from meconium may well have low collapse pressures and hence is desorbed from the interface at high pressures. The data also suggest that at high compression rates, desorption of meconium products may also remove some of the surfactant phospholipids. Results in Figure 1.2B, obtained either from meconium-free or meconium treated surfactant films, show that the expansion isotherm of meconium pre-treated surfactant yields lower area/pressures, likely as a consequence of the irreversible loss of part of the material (surfactant + meconium) during compression. Figure 1.2C shows the compression isotherm of pure meconium, spread at the air-liquid interface. The collapse pressure of meconium film is 25mN/m, indicating that most of its components are squeezed-out from the interface at pressures above that threshold. Interestingly, meconium isotherms exhibit segments with clearly distinct slopes, which may indicate the coexistence of components with different interfacial stability.

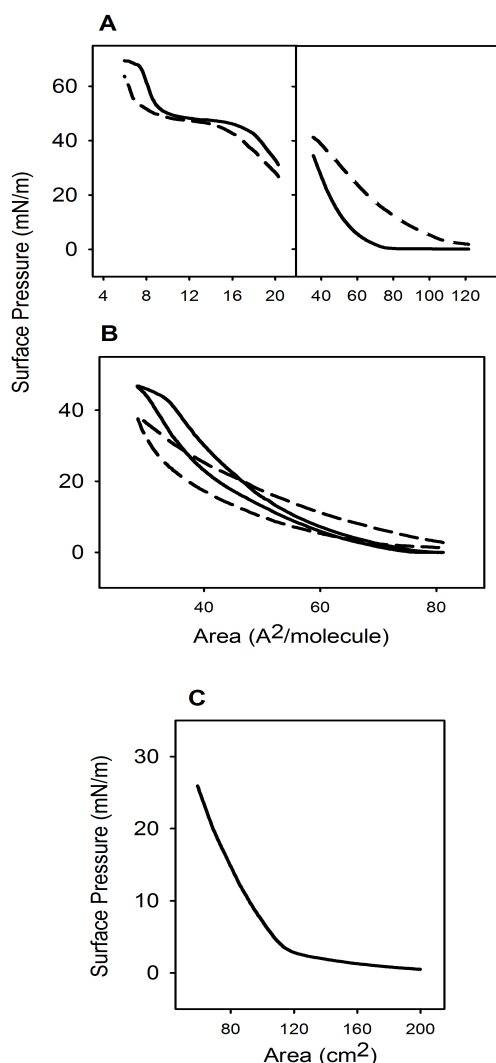


Figure 1.2 Compression isotherms of surfactant and meconium.

A) Low-pressure (right panel) and high-pressure (left panel) segments of the compression isotherm of films formed by native pulmonary surfactant without (solid line) or with (short dashed line) pre-exposure to meconium, once spread at the air-water interface. B) Full compression-expansion cycling isotherms of films formed by meconium-free (solid line) or meconium-treated (dashed line) surfactant. C) Compression isotherm of a film formed by spreading of meconium at the air-water interface.

Captive Bubble Surfactometry (CBS). This technique better simulates the compression-expansion cycling that occurs at the breathing interface (Schoel et al. 1994; Schürch et al. 1998; Gunasekara et al. 2008). Figure 1.3A compares interfacial adsorption kinetics of native surfactant and surfactant pre-exposed to meconium, as assessed after deposition at the interface of the captive air bubble in the CBS. NS adsorbs to form a stable surface film with a minimum equilibrium surface tension of about 23mN/m within the first second after deposition. Pre-treated surfactant adsorbs initially almost as fast as non-treated surfactant, but to a higher equilibrium tension of 25 mN/m. However, re-adsorption of excess material upon expansion of the bubble (see right panel in figure 1.3A) occurs identically in meconium-treated and non-treated surfactant.

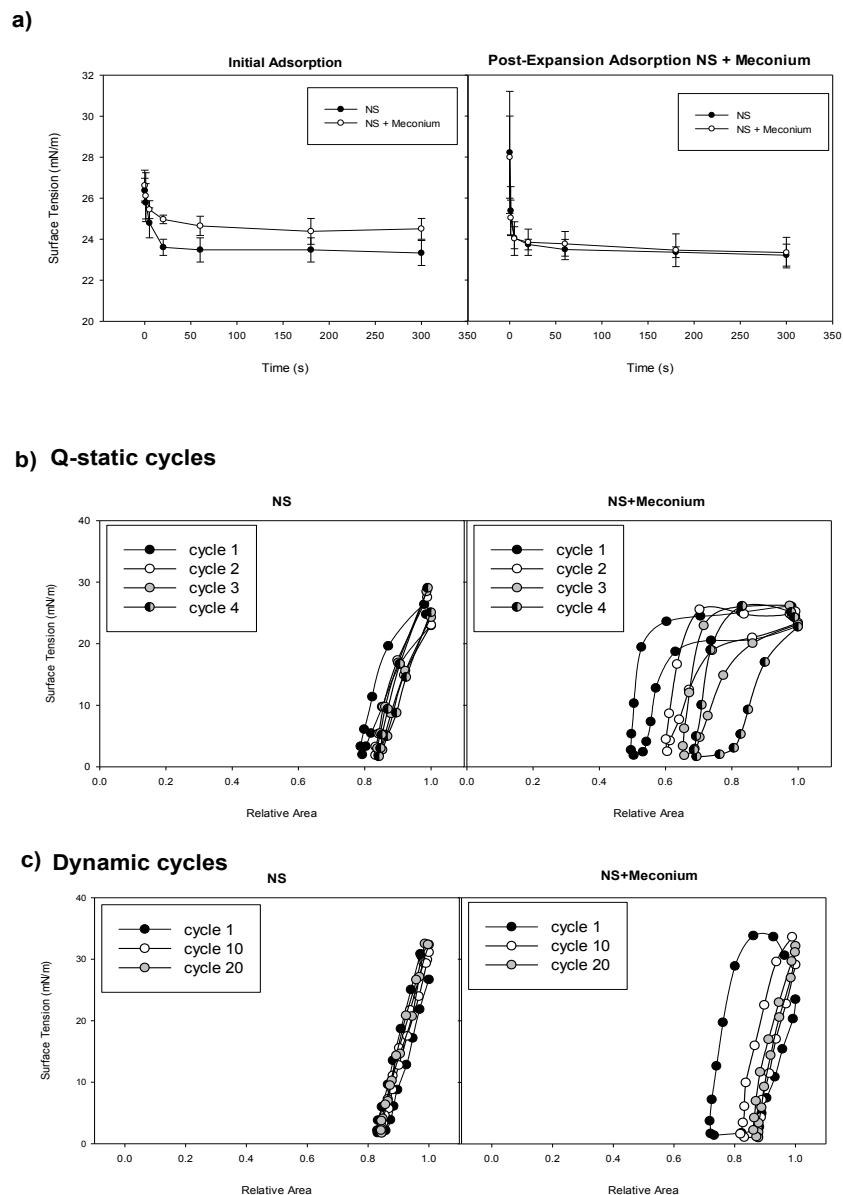


Figure 1.3. Effect of meconium on the surface activity of surfactant as evaluated in a Captive Bubble Surfactometer.

A) Initial and Post-Expansion adsorption of native surfactant in the absence (closed circles) or in the presence (open circles) of 10 mg/ml meconium (representing 1.6% Chol w/w) B) Quasi-static (Q-static, upper panels) and dynamic (lower panels) compression-expansion isotherms of surfactant films formed in the absence (left panels) or in the presence (right panels) of meconium; plotted are isotherms obtained from cycle 1 (black), 2 (white), 3 (grey) and 4 (half black) for the quasi-static and 1 (black), 10 (white) and 20 (grey) for the dynamic cycling.

Cycling isotherms obtained from native surfactant films show practically no compression/expansion hysteresis along the successive quasi-static or dynamic cycles (Figure 1.3B). Only the first quasi-static cycle exhibits a marginal hysteresis,

which is lost in the subsequent cycles, likely as a consequence of an equilibration/reorganization of the film during compression. Native surfactant isotherms reach surface tensions ≤ 2 mN/m with less than 20% compression (see summary of data from CBS obtained with meconium-free and meconium-treated surfactant in Table 1.1).

| Q-stat 4 | | | |
|----------------|---------------------|---------------------|-------------------------------|
| Sample | γ min (mN/m) | γ max (mN/m) | Relative Area (γ min) |
| NS | 1.7 ± 0.3 | 27.7 ± 1.4 | 0.8 ± 0.1 |
| NS+Meconium | 11.1 ± 9.4 | 25.9 ± 0.3 | 0.6 ± 0.2 |
| NS+TA+Chol | 5.1 ± 4.8 | 26.2 ± 0.9 | 0.5 ± 0.2 |
| NS+Cholesterol | 4.9 ± 3.2 | $25,4 \pm 0.7$ | 0.6 ± 0.1 |
| Dyn 20 | | | |
| NS | 1.7 ± 0.3 | 32.5 ± 1.4 | 0.8 ± 0.1 |
| NS+Meconium | 1.4 ± 0.3 | 32.1 ± 0.8 | 0.8 ± 0.1 |
| NS+TA+Chol | 1.2 ± 0.8 | 31.3 ± 2.4 | 0.8 ± 0.1 |
| NS+Cholesterol | 1.7 ± 0.4 | 31.2 ± 2.1 | 0.8 ± 0.1 |

Table 1.1: Effect of meconium on the surface behavior of pulmonary surfactant as assessed in a captive bubble surfactometer under quasi-static and dynamic conditions. NS: native surfactant; Q-stat 4: parameters obtained at the 4th quasi-static compression-expansion cycle; Dyn20: parameters obtained at the 20th dynamic cycle.

In contrast, isotherms of meconium-treated surfactant films exhibit a considerable hysteresis. Under quasi-static conditions, both compression and expansion isotherms show marked plateaus at the equilibrium pressure, which are progressively reduced in the subsequent cycles. These plateaus practically disappear upon dynamic cycling, likely due to completion of film depuration, i.e. once rapid cycling to the highest pressures promotes the squeeze-out and the subsequent desorption of the components inserted from meconium into the surfactant films. However, complete refining of the isotherms requires much larger compression ratios (in the order of 50%) than required by meconium-free surfactant. Meconium addition does not increase the maximum surface tensions, reached upon expansion, again confirming that meconium does not impair the re-spreading potential of surfactant that is already associated with the interface.

Structure of the surface film. Evidence suggests that meconium incorporates constituent molecules into surfactant films and that meconium-treated surfactant films require compression-driven depuration before becoming competent to reach the lowest tensions. This finding may indicate that meconium also affects the structure of surfactant films and hence their biophysical behavior. Under epifluorescence microscopy, the lateral structure of native surfactant films subjected to compression, exhibits features that have been well characterized (Discher et al. 1996; Nag et al. 1998) (Figure 1.4A).

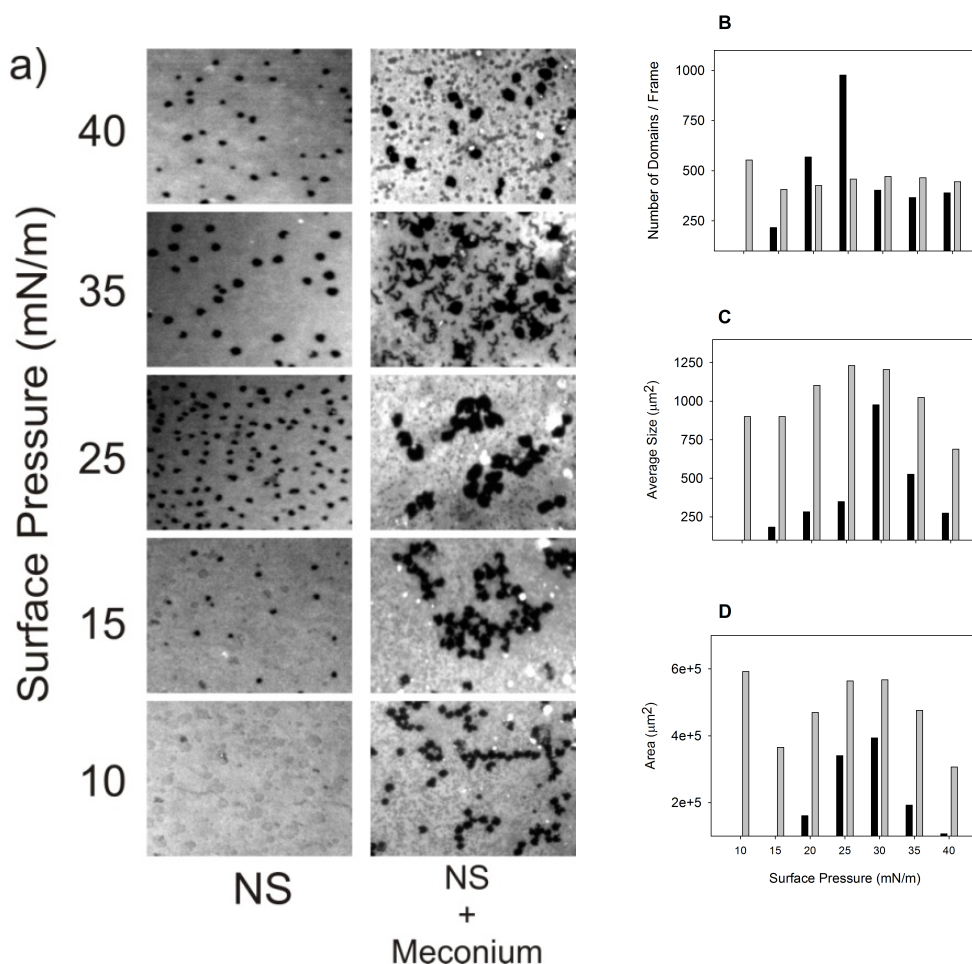


Figure 1.4 Effect of meconium on the structure of surfactant films. A) Epifluorescence microscopy images from interfacial films of native surfactant containing a trace of the fluorescent probe BODIPY-PC, in the absence (left pictures) or in the presence (right pictures) of meconium, obtained upon transfer to glass at the indicated surface pressures. Graphs on the right correspond to the quantitative analysis of the density of condensed domains (B), their average size (C) and the total area occupied by the condensed phase (D) vs. the surface pressure, for meconium-free (black bars) and meconium-treated (grey bars) surfactant films.

No apparent segregation of dark condensed domains is observed at low pressures, below 10mN/m, at least under the resolution of the optical microscope. At higher pressures there is a progressive segregation of small, condensed domains, which grow with compression to reach maximum size at around 30mN/m and then decrease upon higher compression (see quantitation of pressure-driven changes of

domain morphologies in Figure 1.4 B-D). Dark condensed domains always showed a rounded shape and were homogeneously distributed, as dispersed in the fluorescent, presumably liquid-disordered, film matrix. In contrast, morphology of films from meconium-treated surfactant was different. Overall, meconium surfactant mixtures showed higher proportions of condensed-like phase at any pressure. This could be related with a condensing effect caused by the components inserted into surfactant by meconium. Also in contrast to natural surfactant films, condensed domains showed a strong tendency to aggregate in meconium-exposed layers, producing a relatively heterogeneous morphology in these films. Segregation of large clusters of condensed phase from large areas devoted of condensed domains could be an important source of instability for the films as a whole, particularly at the most compressed states. Meconium-treated films also showed the presence of numerous bright spots, which were not present in films from non-treated surfactant. These spots likely correspond to material that has been already squeezed-out from the interface during compression due to its low interfacial stability.

Biochemical analysis of meconium. Table 1.2 summarizes the amounts of total protein, phospholipids, cholesterol and bile acids in meconium preparation tested here. Still, most of meconium weight seems to consist of non-determined components, possibly salts, heme by-products, and others. Particularly remarkable is the presence of a substantial amount of cholesterol and bile acids, which may perturb the structure and function of surfactant. We have therefore compared the effect of meconium with that of the exposure of surfactant to cholesterol and taurocholic acid (Chol/TA). TA was used because it is one of the most abundant human bile acids (Gross et al. 2006).

| Component | Mass (mg/mg meconium) |
|---------------|-----------------------|
| Proteins | 0.015 |
| Phospholipids | 0.013 |
| Cholesterol | 0.040 |
| Bile Acids | 0.005 |

Table 1.2: Compositional analysis of meconium. Mass (mg) of each component in a mg of dried meconium

Accumulation of surfactant at the interface. A method recently developed allows evaluation of the amount of surfactant material reaching and accumulating at the interface (Ravasio et al. 2008). We therefore tested whether meconium and Chol/TA produced similar alteration in the ability of surfactant to form surface films. Figure 1.5A shows how native surfactant rapidly reaches the interface and stably remains associated with it, while its exposure to increasing concentrations of meconium produces a progressive reduction in the amount of surfactant associated with the interface. A similar inhibiting effect was observed when native surfactant was exposed to a suspension prepared from a chloroform/methanol extract of meconium (see Figure 1.5A, middle panel), indicating that the inhibiting compounds

are extractable by organic solvents. The lower panel in Figure 5a shows how the inhibition profile of surfactant by meconium or its organic extract can be fully mimicked by exposure of surfactant to a mixture Chol/TA containing quantities of cholesterol comparable to those found in meconium. Figure 1.5B illustrates that the concentration dependence of surfactant inhibition by meconium is matched by meconium organic extract or the Chol/TA mixture when comparing relative fluorescence as a function of the amount of cholesterol, particularly at long term, when the maximal amount of surface-associated material is reached. The larger differences observed at short times likely highlight the different kinetics of inhibition once surfactant is exposed to the three substances. Meconium could be the slowest inhibiting substance due to its complexity.

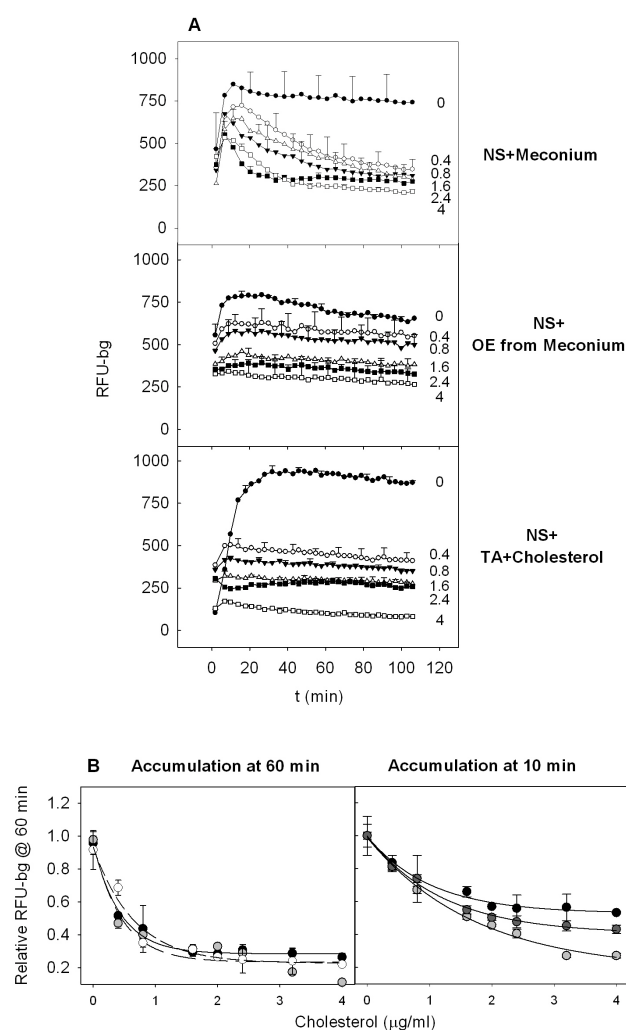


Figure 1.5. Effect of meconium on the interfacial accumulation of surfactant.

A) Accumulation of material into the interface upon adsorption of fluorescently-labelled native surfactant in the presence of the indicated concentrations of meconium (top), of the organic extract (OE) from meconium (centre) or of a mixture of taurocholic acid (TA) and cholesterol (bottom), all of them expressed as $\mu\text{g/ml}$ of cholesterol added. B) Accumulation of labeled surfactant into the interface as a function of the amount of meconium (black), meconium organic extract (white) or TA + cholesterol (grey), 60 min (right panel) after and 10 min (left panel) after

injection into the subphase. Lines are mere guides to eye, illustrating the similar trends of the three types of samples.

Mimicking of meconium inhibition by cholesterol mobilizing complexes. Figure 1.6 shows that exposure of surfactant to Chol/TA has similar inhibiting effects as meconium. Perturbation of surfactant by Chol/TA mixtures reduces only slightly the initial adsorption rate of surfactant with no effect in adsorption post-expansion. Compression-expansion isotherms of Chol/TA-treated surfactant were however substantially affected, in a manner entirely comparable to the effect of meconium (compare Figure 1.6 with Figure 1.3). Much larger compression ratios were required for surfactant to reach the minimal tensions if pre-exposed to Chol/TA, particularly during the quasi-static regime. The hysteresis of the isotherms was progressively reduced during the subsequent compression-expansion cycles presumably as a result of the progressive depuration of spurious (i.e. bile acid, cholesterol) components. Exposure to Chol/TA combinations did not increase the maximal surface tension, as occurred upon exposure to meconium. In some experiments, we pre-incubated surfactant with dried cholesterol films, prepared by evaporation of organic solutions of cholesterol and, in contrast to the effect of Chol/TA mixtures, we did not detect significant effects on surfactant surface activity, probably because there was no proper incorporation of cholesterol into surfactant membranes. This suggests a potential role of bile acids as cholesterol mobilizing agents to facilitate transference of cholesterol into surfactant complexes and so to mediate inhibition. Figure 1.6 shows how the exposure of surfactant to the combination of cholesterol with another well-known steroid-mobilizing agent, methyl- β -cyclodextrin, produces perturbations on surfactant surface activity that are practically indistinguishable from those induced by meconium or Chol/TA complexes.

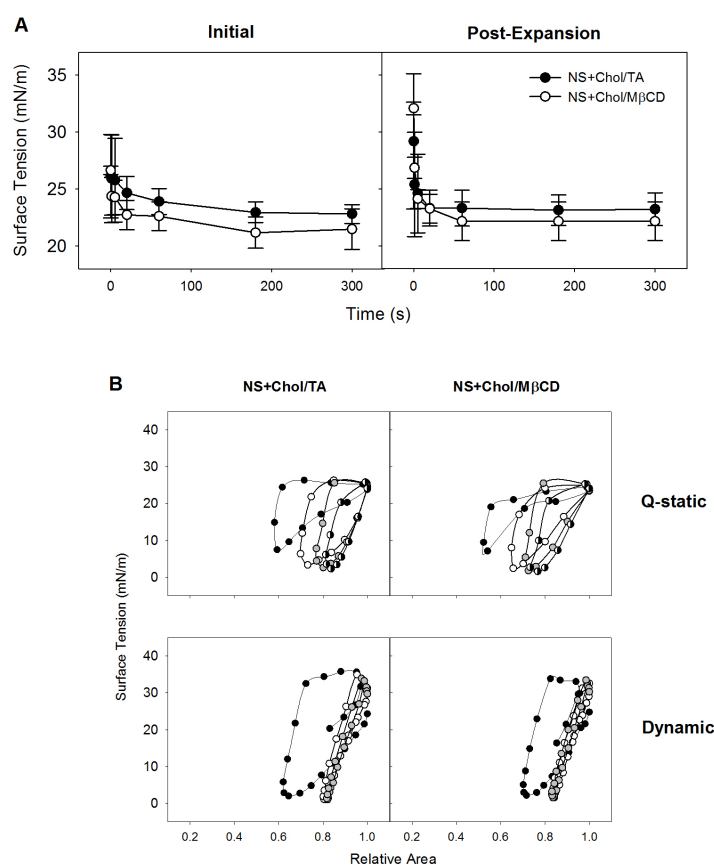


Figure 1.6. Effect of cholesterol-mobilizing complexes on the surface activity of surfactant as evaluated in a Captive Bubble Surfactometer.

A) Initial and Post-Expansion adsorption of native surfactant in the presence of a mixture of TA and cholesterol (1.6% Cholesterol w/w) (open circles) or in the presence of complexes of cholesterol and M β CD (closed circles) representing a final proportion of cholesterol of 1.6% w/w (cholesterol/phospholipid). B) Quasi-static (Q-static, upper panels) and dynamic (lower panels) compression-expansion isotherms of surfactant films formed in the presence of Chol/TA (left panels) or Chol/M β CD (right panels) complexes; plotted are isotherms obtained from cycle 1 (black), 2 (white), 3 (grey) and 4 (half black) for the quasi-static and 1 (black), 10 (white) and 20 (grey) for the dynamic cycling.

Thermotropic profiles of surfactant membranes. Laurdan is a fluorescent probe widely used to study membrane structure, as it is sensitive to the level of hydration of the headgroup region of phospholipid bilayers, which depends on lipid packing and membrane phase (Parasassi et al. 1994). The thermotropic profile of the fluorescence of a Laurdan trace incorporated into native surfactant membranes provides information on the effect of temperature on surfactant membrane structure. Figure 1.7A shows that native surfactant membranes manifest a broad transition from ordered, relatively dehydrated and highly packed states at low temperatures to more disordered and loosely packed configurations at high temperatures, with a melting temperature (calculated as the temperature at which Laurdan GP is halfway from that of ordered to that of disordered membranes) of approximately 35°C. Fluorescence of Laurdan inserted into surfactant membranes treated with meconium indicates that these membranes have become more hydrated/disordered at low temperatures and more ordered/dehydrated at high temperatures than the membranes that were not exposed to meconium. A practically identical broadening of the thermotropic transition of surfactant membranes was observed upon exposure of surfactant to the Chol/TA mixture. On the other hand, if only taurocholic acid was used as surfactant perturbing compound, the thermotropic profile of surfactant membranes was only affected at low temperatures, where the bile acid seems to produce an apparent disordering effect over the surfactant membrane ordered states.

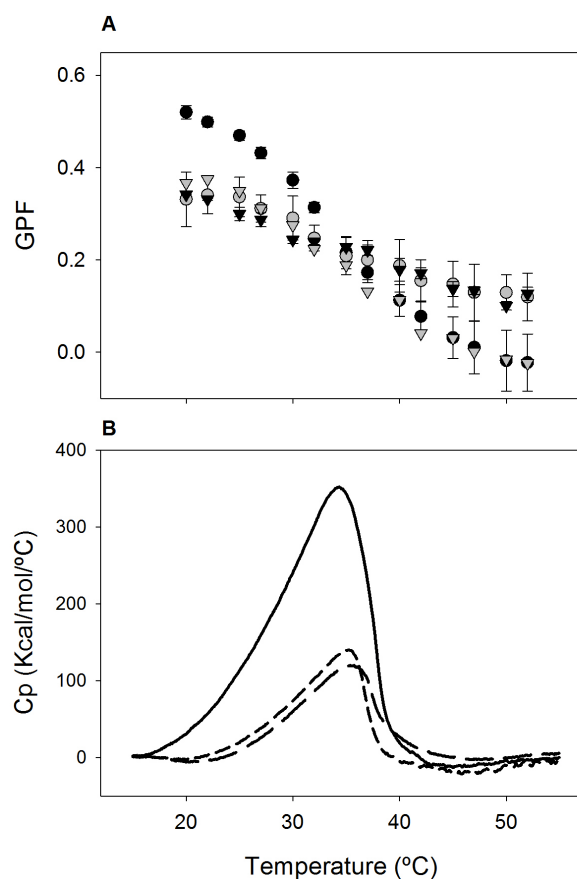


Figure 1.7. Effect of meconium on the thermotropic properties of surfactant membranes.

A) Thermotropic profiles of generalized polarization fluorescence (GPF) obtained from the fluorescence spectra of Laurdan-labelled native surfactant (black dot) or surfactant pre-exposed to meconium (grey dot), TA + cholesterol (black triangle) or TA alone (grey triangle). B) DSC thermograms from native surfactant (solid line) or surfactant pre-exposed to meconium (long dashed line) or TA + cholesterol (short dashed line).

To confirm the nature of the perturbations introduced by meconium components into surfactant membranes, we obtained and compared differential scanning calorimetry thermograms of native surfactant and surfactant treated with meconium or the Chol/TA mixture. Native surfactant shows a complex and broad calorimetric peak between 15 and 40°C with a T_m of approximately 35°C (Figure 7B) as it has been reported before (Bernardino de la Serna et al. 2009). The thermogram obtained from surfactant exposed to meconium exhibits also a similarly broaden thermotropic peak, but with a substantially reduced associated enthalpy (calculated as the area under the peak, see summary of calorimetric parameters in Table 1.3). The thermotropic behavior of surfactant membranes treated with the Chol/TA mixture reproduces that of meconium-treated surfactant, including a similar reduction of the enthalpy of the ordered-disordered membrane transition. The reduction in enthalpy caused by the combined action of cholesterol and the bile acid therefore parallels the decrease in the amplitude of the thermotropic transition as reported by Laurdan.

| Sample | T_m (°C) | Enthalpy (kcal/mol) | $T_{1/2}$ (°C) |
|-------------|------------|---------------------|----------------|
| NS | 35.7±2.4 | 2.46±0.30 | 9.87±0.33 |
| NS+Meconium | 35.4±0.4 | 1.48±0.39 | 9.47±1.48 |
| NS+TA+Chol | 35.7±2.1 | 1.38±0.31 | 9.30±1.88 |

Table 1.3: Effect of exposure to meconium or to a mixture of bile acids and cholesterol on the thermotropic transition of native surfactant membranes as evaluated by DSC. Data are expressed as averages \pm standard deviations (n=3)

DISCUSSION

In the past, inhibition by meconium had been found with clinical surfactants such as Curosurf (Gross et al. 2006), Surfactant-TA (Park et al. 1996; Bae et al. 1998; Oh and Bae 2000), or others (Herting et al. 2001), but no data were available on the inhibition of natural pulmonary surfactant by meconium, a process actually occurring with MAS. The data presented here support that the inhibitory action of meconium is mediated by a direct incorporation of meconium components into surfactant membranes and films and their subsequent perturbation. The nature of the perturbations observed are compatible with cholesterol being an important inhibitory element that alters the properties of surfactant membranes and films in defined and recognizable ways.

The inhibitory action of the presence of excess cholesterol in surfactant complexes has been widely reported and largely studied. The early finding that cholesterol was deleterious for surfactant function, at least as assessed *in vitro*, led to the removal of cholesterol from most of the surfactant preparations currently used for the treatment of respiratory pathologies (Blanco and Pérez-Gil 2007). Recent studies have also reported that excess of cholesterol could be also a pathogenic factor in ARDS (Markart et al. 2007). How much cholesterol is essential as a constituent of pulmonary surfactant is under much discussion in recent reports, as a minimal amount of cholesterol is required for natural pulmonary surfactant membranes to adopt their characteristic lateral structure (Bernardino de la Serna et al. 2004) and proper dynamics (Bernardino de la Serna et al. 2009). Therefore the amount of cholesterol in surfactant must be carefully regulated to maintain the proportions that optimize surfactant performance while excessive cholesterol has deleterious consequences (Gunasekara et al. 2008). Moreover, regulation of the amount of cholesterol in surfactant may be a physiological adaptive response to certain environmental changes (Orgeig and Daniels 2001). The nature of the possible processes and structures that are involved in cholesterol mobilization in and out of surfactant structures, under physiological conditions, are as yet not known.

Our findings indicate that the effect of cholesterol contained in meconium as an inhibitor of surfactant, could be mediated by the bile acids in this material. Cholesterol alone failed to reproduce the effects caused by meconium on surfactant performance and structure. The low solubility of cholesterol in aqueous medium may prevent extensive transfer into surfactant complexes. Therefore bile acids may act to enable insertion of cholesterol into surfactant membranes resulting in surfactant dysfunction as occurs if surfactant is exposed to complexes of methyl- β -cyclodextrine and cholesterol. Inhibition by meconium could therefore constitute a particular case of inhibition by excess cholesterol facilitated by the presence of bile salts as cholesterol-mobilizing agent. Facilitated transfer of cholesterol into surfactant complexes could be also a significant contribution in other pathological alterations of surfactant such as in the increase of neutral lipids associated with

surfactant inhibition that is found in patients with ARDS (Markart et al. 2007). The increase of cholesterol in surfactant as a consequence of serum leakage into airspaces could be dependent on the cholesterol-mobilizing properties of lipoproteins. The notion of the effect of cholesterol-mobilizing agents on structure and activity of pulmonary surfactant is also behind the idea proposed by Amrein's group that cyclodextrine could be used as an additive in therapeutic surfactants, where it could aid to deplete the excess of cholesterol from endogenous inhibited surfactant (Gunasekara et al. 2010). Our results suggest that incorporation of cholesterol-mobilizing agents such as cyclodextrine into exogenous surfactants might even have the opposite, negative, effect and promote further inhibition if more extensive mobilization of cholesterol occurs.

An effective surfactant must optimize three main properties: rapid interfacial adsorption, very low surface tension upon film compression, and efficient film replenishment upon expansion (Serrano and Pérez-Gil 2006; Zuo et al. 2008). Meconium alters these three properties, impairing surfactant performance. It reduces substantially accumulation of surfactant at the interface, preventing the ultimate transfer of surface active molecules into the interface. Perhaps some of the elements incorporated by meconium into surfactant complexes are directly altering the molecular structures responsible for their attachment to the interface. Meconium itself has a relatively low interfacial collapse pressure, suggesting that it desorbs easily from the interface. Perhaps the accumulation of meconium components into surfactant membranes may also lead to a facilitated desorption, which reduces the amounts of surfactant accumulated at the interface. The adsorption kinetics of meconium-treated surfactant supports this interpretation, as they exhibit significant concentration- and time-dependent desorptive-segments (see Figure 5).

The detergent properties of bile acids may be responsible for facilitated desorption of surfactant complexes from the interface. The effects of bile acids as a single inhibitory component had been previously studied with a clinical surfactant, Curosurf (Gross et al. 2006). This study identified some similarities between taurocholic acid and meconium, but in the present study, taurocholic acid by itself did not reproduce all the effects observed after exposure of surfactant to meconium. The alteration of the structure of surfactant membranes and films, as a consequence of the exposure to meconium, could explain the altered ability of meconium-treated surfactant to reach very low surface tensions upon compression. Bile acid-promoted incorporation of cholesterol, and perhaps other lipids with limited surface activity, into surfactant could be at the same time responsible of the partial fluidization of the condensed states of membranes and films, of the alteration of the in-plane lateral organization of surfactant layers and of the requirement of much larger compression to deplete surface films before reaching the lowest tensions with little hysteresis. Our experiments in the CBS indicate that during compression-expansion cycling, surface films may lose deleterious components of meconium, but this could be dependent on the total amount of deleterious material incorporated. It is particularly intriguing that addition of meconium increases the fraction of surface films occupied by apparently condensed domains as observed by epifluorescence microscopy, especially considering that meconium seems to fluidize/decrease

packing in surfactant membranes. We speculate that incorporation of cholesterol, and perhaps bile salts, into the condensed domains would increase their fractional area while decreasing their internal molecular packing. This would also explain the reduction of melting enthalpy of surfactant membranes that had been exposed to meconium. An altered composition of condensed surfactant domains could be also responsible for their abnormal propensity to cluster, which, in turn, could have consequences on the lack of stability of meconium contaminated films.

The nature of the inhibitory mechanisms of meconium revealed here suggests strategies to improve the surfactant treatment of several lung diseases. In the case of meconium aspiration pneumonia, the use of surfactant preparations free of cholesterol would appear logical based on our *in vitro* results. A cholesterol-free preparation might resist meconium inhibition to a greater degree than a cholesterol-containing surfactant. However, a complete lack of cholesterol may adversely affect the beneficial effects offered by physiological amounts of cholesterol. Supplementing clinical surfactants with antagonists of bile acids is an alternative approach. Ursodeoxycholic acid, for instance, is a hydrophilic bile acid which has been proposed as a membrane-protective agent useful in the treatment of cholestasis (Zhou et al. 2009). Similar strategies may be useful in ARDS wherein increased amounts of cholesterol have been found with surfactant obtained from these patients (Markart et al. 2007). Targeting of surfactant inhibitors by adding specific inhibitor antagonists to therapeutic surfactants may improve clinical responses in patients with surfactant dysfunction who heretofore have not responded well to conventional surfactant therapy.

**EXPOSURE TO POLYMERS REVERSES INHIBITION OF PULMONARY SURFACTANT BY
SERUM, MECONIUM OR CHOLESTEROL IN THE CAPTIVE BUBBLE SURFACTOMETER**

Elena Lopez-Rodriguez, Olga Lucia Ospina, Mercedes Echaide, H. William Taeusch
and Jesus Perez-Gil

Biophysical Journal (2012) 103:1-9

This work has been done in collaboration with MD H. William Taeusch (General Hospital of San Francisco, University California San Francisco)



EXPOSURE TO POLYMERS REVERSES INHIBITION OF PULMONARY SURFACTANT BY SERUM, MECONIUM OR CHOLESTEROL IN THE CAPTIVE BUBBLE SURFACTOMETER

INTRODUCTION

Three main functions determine the activity of surfactant preparations and the impact of inhibition. First, surfactant must adsorb quickly (in a few seconds) to reduce interfacial surface tension. Secondly, surfactant must be efficiently re-absorbed to the air-subphase interface (as occurs during inspiration in alveoli), and finally surfactant must form rigid films on compression of the surface (as occurs during expiration), which exhibit low surface tension. Inhibition of surfactant may impair adsorption (e.g., as with serum) (Taeusch et al. 2005; Zasadzinski et al. 2005; Zuo et al. 2008), or by perturbation of the composition and structure of surfactant films (e.g. by cholesterol or bile salts) (Gunasekara et al. 2008; Vockeroth et al. 2010; Lopez-Rodriguez et al. 2011), which prevents attainment of maximally compressed states.

Understanding the molecular mechanism of inactivation of surfactant by a variety of clinically relevant substances is essential for developing new improved therapeutic applications. Simulating pathological conditions, supposedly occurring *in vivo*, which could be relevant to reveal the molecular mechanism of surfactant impairment this chapter describes the optimization of a new protocol in Captive Bubble Surfactometry to standardize the study of surfactant inactivation *in vitro*.

The surface behavior of pulmonary surfactant and the mechanisms by which it is altered by different inhibitory substances have been analyzed using different approaches, including Langmuir surface balances (Wüstneck et al. 2005), the pulsating bubble surfactometer (PBS) (Hall et al. 1992; Holm et al. 1999; Lu et al. 2005), axisymmetric drop shape analysis in conjunction with constrained sessile drop (ADSA-CSD) surfactometry (Saad et al. 2009), or the captive bubble surfactometer (Schürch et al. 1989; Schoel et al. 1994; Schürch et al. 1998; Zuo et al. 2008). Limitations of these methods prevent study of inhibition under (patho) physiologically relevant conditions that include temperature and humidity, high concentrations of both surfactant and inhibitory substances, and alveolar geometry.

Captive Bubble Surfactometry is a technique in which surface tension can be monitored from the shape and size of an air bubble sealed into a chamber filled with an aqueous subphase. The bubble interface is intended to simulate the air-water interface of an alveolus. The use during the last two decades of the Captive Bubble Surfactometer (CBS) has allowed us to simulate *in vitro* the conditions of a “healthy” alveolus. In the present study, we have developed the methodology for simulating the conditions of a “pathological” alveolus, at least with respect to the presence of surfactant-inactivating substances.

Surfactant inactivation is associated with a variety of respiratory diseases that affect many people in the world each year. In the previous chapter we have described MAS as one example of a respiratory syndrome affecting neonates and where surfactant is inactivated by meconium. Another important respiratory syndrome, affecting adults and infants, is ARDS (Acute Respiratory Distress Syndrome). ARDS is a very complex pathology with a variety of aetiologies that lead to an inflamed state of the

lung and to the leakage of fluid into the alveolar air spaces, as a result of the alteration of the permeability of the capillary-epithelium barrier. This leaked fluid, mainly serum, is the responsible for the impairment of surfactant biophysical properties. As discussed in chapter 1 for the treatment of MAS, the supplementation with an exogenous clinical surfactant for the treatment of ARDS has rendered disappointing results in the treatment of ARDS patients. Again, the hypothesis is that the inactivation of surfactant, both the endogenous and the clinical one, prevents a more favourable outcome. As meconium is the responsible of inactivating surfactant in MAS, serum leaked into the alveolar spaces is the responsible for diluting and inactivating surfactant in ARDS inflamed lungs. However, the molecular mechanism of surfactant inactivation by these two substances is very different.

For a variety of reasons, inhibition has been difficult to study in the CBS (Gunasekara et al. 2008). In the present study, we have modified the method of application of the sample to simulate competition between serum proteins and surfactant complexes for the interface (Taeusch et al. 2005; Zasadzinski et al. 2005; Zuo et al. 2008; Nag et al. 2010). Traditionally, serum has been introduced into the subphase in which the bubble is formed. We have applied undiluted serum onto the surface of the bubble thus allowing serum proteins to form a concentrated film at the interface prior to the application of surfactant. Surface tension of serum at the interface falls to $\approx 50\text{mN/m}$ (Stenger et al. 2009). Although the actual concentration of serum leaked into an injured lung is difficult to establish, testing a layer at high concentrations of serum mimics the most potentially harmful conditions. Surfactant is then applied near the surface of the bubble, instead of directly onto the surface of the bubble as it has been done in the past. Therefore surfactant finds a steric barrier to adsorption, as would happen in vivo after surfactant is freshly secreted by pneumocytes, and must traverse a serum layer in an injured and edematous alveolus to adsorb at the interface. Similarly exogenous surfactant introduced via the trachea, as therapy, must also find its way to the alveolar interface through the leaky, inflamed interior of the lung. Thus, surfactant inactivation by serum imposes a competition for the interface between surfactant complexes and surface active proteins. In contrast, as previously described in chapter 1, meconium inactivation consists in the impairment of surfactant structure itself by the insertion of molecules like cholesterol into surfactant complexes. To study meconium/cholesterol inhibition we premixed and incubated each with surfactant in order to allow these inhibitors to incorporate into surfactant complexes, as the main inhibitory mechanism for both agents is disruption of surfactant structure (Gunasekara et al. 2008; Zuo et al. 2008). In a lung full of serum or meconium, surfactant may suffer dilution. So we also studied various surfactant concentrations. For inhibition experiments, we use critical conditions, that is to say, low concentrations of surfactant, which are still functional but susceptible to inhibition. The concentration of surfactant in the subphase of healthy alveoli is estimated at approximately 30-100mg/ml. However, during inflammation, reduced production by damaged epithelia, an accelerated catabolism by lipases and proteases, and dilution by edema, all contribute to a substantial decrease of surfactant concentrations.

Traditionally, surfactant activity is assessed at high concentrations of phospholipids (commonly 25mg/ml or even 72mg/ml), as the concentration of surfactant in a healthy alveolus can reach up to 100mg/ml. Lowering surfactant concentration down

to 10mg/ml brings surfactant to critical conditions, where it is still functional but more susceptible to inhibition by different agents.

Optimization of the CBS protocol allowed us not only to study potentially pathogenic conditions, but also to test, in a systematic and standard way, different chemical or natural compounds, that would be useful as additives in clinical surfactant. This opens the possibility to look for agents promoting increased activity and resistance to inactivation, with the aim of improving potential therapeutic surfactant preparations for the future treatment of pathologies like MAS or ARDS. In addition, optimizing the study of surfactant samples into the CBS, as well as the identification of defined biophysical signature of surfactant impairment, also rise up the possibility to study clinically relevant samples. Comparing the behaviour of surfactant from patients with different pathologies with the behaviour of surfactant from inactivation models developed in this chapter could provide a better understanding of the mechanism behind the pathology regarding the implication of surfactant.

Addition of polymers such as hyaluronic acid or dextran has proven to restore surfactant function in the presence of some inactivating agents under particular experimental conditions. In the modified CBS protocol, both polymers (anionic hyaluronic acid and non-ionic dextran) are able to restore surfactant activity *in vitro* in the presence of different inactivating agents.

RESULTS

In order to study changes in biophysical properties when inhibitory agents are added to NS, we modified the usual CBS protocol in three ways: First we tested relatively low concentrations of surfactant, 10mg/ml phospholipid, applying the sample without contacting with the surface bubble (see images in Figure 2.1a). Second, we injected undiluted serum near the surface of the bubble. As a consequence of the high density of the sucrose-containing subphase, the undiluted serum forms a layer of concentrated material surrounding the bubble. This can be observed when serum is doped with a trace of fluorescently-labeled albumin (see image in Figure 2.1b).

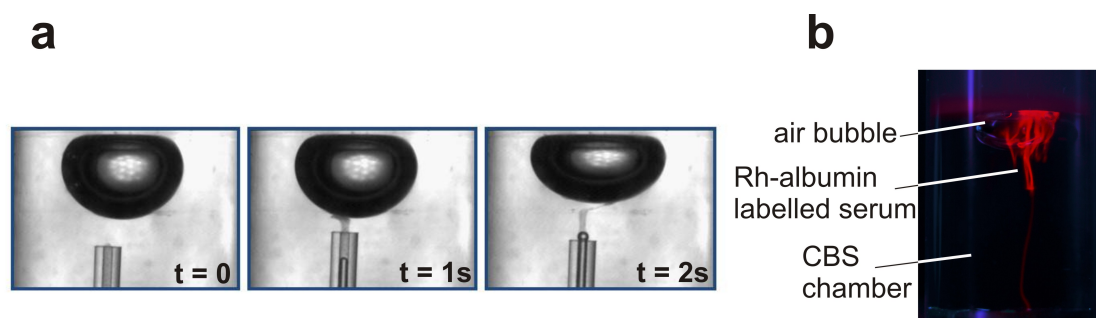


Figure 2.1: CBS model to test surfactant inhibition by serum. a) Sequential images of a surfactant sample immediately before ($t=0$) and at the different times after injection underneath an air bubble at the CBS. b) Fluorescence image of a serum sample doped with a trace of rhodamine-labelled albumin, injected underneath the bubble at the CBS.

Figure 2.2 illustrates how injection of surfactant in the absence of serum, at such a low phospholipid concentration as 10mg/ml, decreased surface tension to 22.1 ± 1.2 mN/m after 5 min of initial adsorption and 22.9 ± 1.1 mN/m after expanding the bubble for 5 minutes. In the initial adsorption graph we can see how surfactant is able to reach the interface in a few seconds (as described by Schürch et al., 1998). Figure 2 also shows how serum (2 μ l) applied near the surface of the bubble decreases surface tension to 45.4 ± 2.4 mN/m after 5 min of initial adsorption and to 49.5 ± 2.3 mN/m after 5 min the expansion of the bubble, likely coming from serum proteins adsorbed at the interface (Zasadzinski et al. 2005). When we applied NS (10mg/ml) underneath the pre-formed serum film, without touching the bubble surface, no adsorption of NS occurred as surface tension remained 39.8 ± 3.3 mN/m, significantly higher than that reached by NS in absence of serum. After expansion, the minimal surface tension after 5 min also remained unchanged 43.9 ± 1.5 mN/m (Figure 2.2).

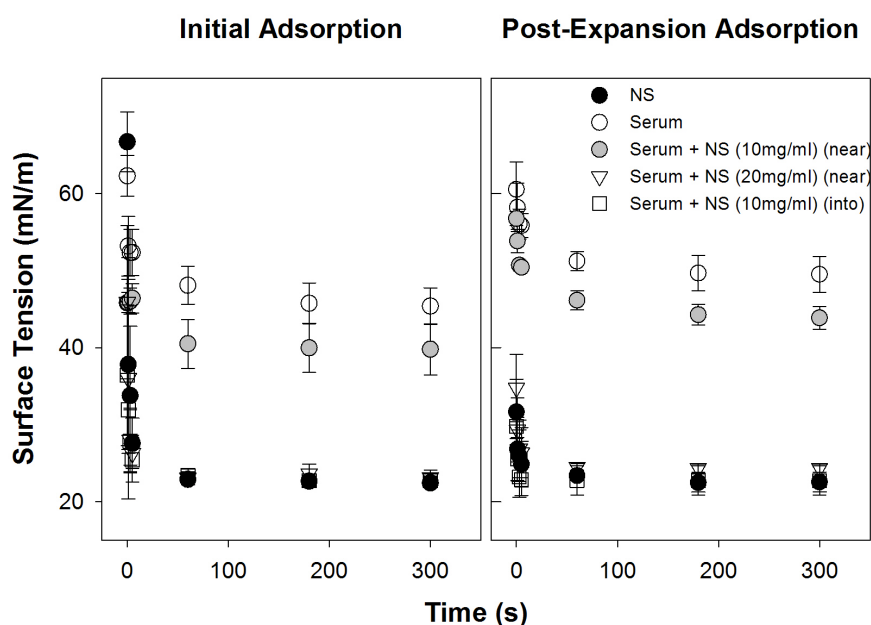


Figure 2.2 Interfacial adsorption of native surfactant in the absence or presence of serum. Initial (left panel) and post-expansion (right panel) adsorption kinetics of surfactant (NS) (black dots), serum alone (white dots), NS 10mg/ml applied underneath (near) the bubble surface coated with a preformed serum layer (grey dots), NS 20mg/ml applied underneath (near) the bubble surface coated with serum (triangles), and NS 10mg/ml (into) applied directly into the bubble coated with serum (squares), all at 37°C. Data are means \pm standard deviation after averaging data from three experiments.

Figure 2.2 also shows that a concentration of surfactant of 20mg/ml is not inhibited by serum. In other experiments, surfactant at 10mg/ml was applied directly into the

bubble surface, thus breaking through the serum protein layer, resulting in equilibrium surface tensions similar to non-inhibited surfactant.

Figure 2.3 summarizes compression-expansion isotherms of surfactant films formed in the absence or presence of serum. In the absence of serum, NS exhibits well-characterized behavior, with the first quasi-static cycle showing greater hysteresis than the subsequent cycles. Thus at the end of the fourth quasi-static cycle surface tension is $1.6 \pm 0.6 \text{ mN/m}$ after area compression of about 20% (see Table 2.1).

| QSTAT 4 | | | |
|------------------------------|---------------------|--------------------|---|
| Sample | γ min (mN/m) | γ max(mN/m) | Relative Area ^(γ_{min}) |
| NS | $1,57 \pm 0,61$ | $27,33 \pm 1,85$ | $0,76 \pm 0,03$ |
| Serum | $37,86 \pm 2,37$ | $52,42 \pm 2,49$ | $0,52 \pm 0,04$ |
| Serum + NS 10mg/ml (near) | $21,68 \pm 1,58$ | $36,97 \pm 9,56$ | $0,47 \pm 0,01$ |
| Serum + NS 20mg/ml (near) | $13,66 \pm 10,85$ | $27,16 \pm 3,27$ | $0,59 \pm 0,20$ |
| Serum + NS 10mg/ml (into) | $19,01 \pm 1,05$ | $25,98 \pm 0,47$ | $0,47 \pm 0,05$ |

| DYN 20 | | | |
|------------------------------|---------------------|--------------------|---|
| Sample | γ min (mN/m) | γ max(mN/m) | Relative Area ^(γ_{min}) |
| NS | $1,85 \pm 0,72$ | $32,08 \pm 3,62$ | $0,83 \pm 0,02$ |
| Serum | $37,36 \pm 3,08$ | $54,00 \pm 3,02$ | $0,54 \pm 0,03$ |
| Serum + NS 10mg/ml (near) | $17,05 \pm 6,02$ | $51,72 \pm 3,47$ | $0,52 \pm 0,02$ |
| Serum + NS 20mg/ml (near) | $1,84 \pm 0,57$ | $28,13 \pm 1,15$ | $0,84 \pm 0,01$ |
| Serum + NS 10mg/ml (into) | $2,07 \pm 0,45$ | $31,05 \pm 2,56$ | $0,84 \pm 0,01$ |

Table 2.1: Effect of surfactant concentration and the mode of application. Parameters for the 4th quasi-static and the 20th compression-expansion cycle of surfactant (NS), serum alone (Serum), NS 10mg/ml applied underneath (near) the bubble surface coated with a preformed serum layer, NS 20mg/ml applied underneath (near) the bubble surface coated with serum, and NS 10mg/ml (into) applied directly into the bubble coated with serum. Data are average \pm standard deviation, n=3

Reorganization of material during Q-static compression is something we were not able to study at high surfactant concentrations, 25mg/ml or 72mg/ml (Schoel et al. 1994; Schürch et al. 1998). Dynamic cycles show normal function of surfactant in the absence of serum, with very low surface tension ($1.8 \pm 0.7 \text{ mN/m}$) with less than a 20% area reduction. In Figure 2.3, the surface tension of a pure serum layer under Q-static and dynamic conditions is never lower than $37.8 \pm 2.4 \text{ mN/m}$. NS (10 mg/mL) applied just below the surface of the bubble, underneath a pre-formed serum layer, was not able to lower surface tension below $21.7 \pm 1.6 \text{ mN/m}$ (Q-static) or

17.1±6.0mN/m (dynamic cycle), even after as much as a 50% reduction of surface area. These values were always significantly higher than the surface tension reached by NS applied in the same conditions in the absence of serum. When we doubled the concentration of surfactant, the film was still not able to reduce surface tension below 20 mN/m under slow quasi-static compression-expansion cycling. However, if cycled at fast dynamic rate (20 cycles/min), films made by concentrated surfactant reduced tension below 10 mN/m already in the first compression and reached minimal tensions below 5 mN/m with very little compression in all the subsequent cycles. This means that surfactant at concentrations ≥ 20 mg/mL is only partly inhibited by full serum when rapid compression-expansion is imposed. We therefore selected to use 10 mg/ml as the appropriate surfactant concentration to study full inhibition in the following experiments.

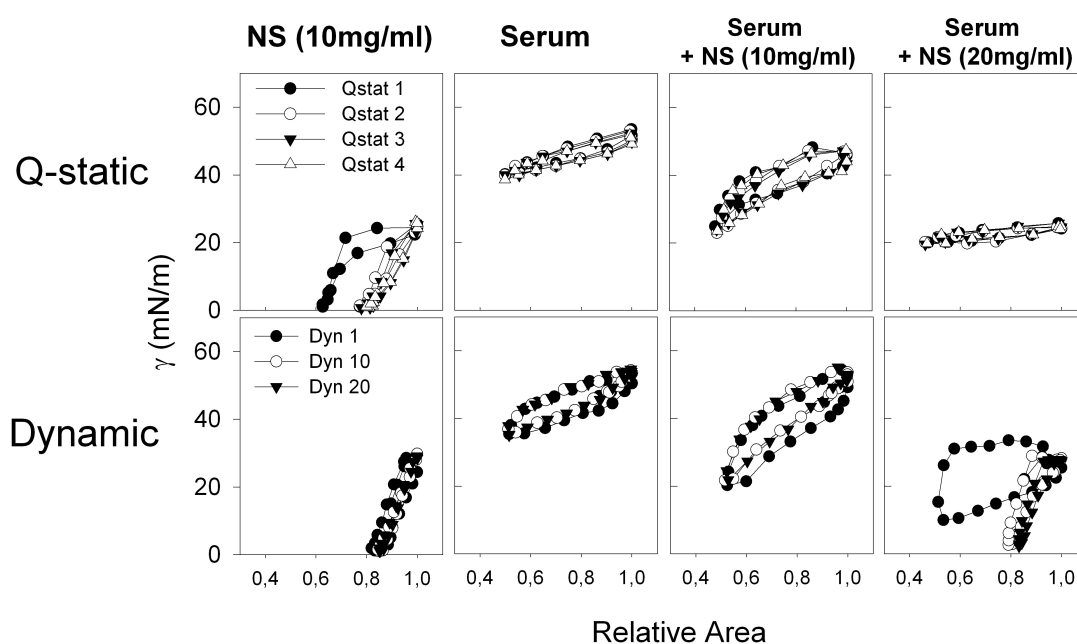


Figure 2.3: Compression-expansion isotherms of native surfactant films in the absence or presence of serum. Q-static (upper panels) and dynamic (lower panels) compression/expansion isotherms from surfactant films formed upon injection of native surfactant (NS) at 10 or 20 mg/mL phospholipid, in the absence or in the presence of a preformed serum layer. A representative experiment is shown here after repeating three independent experiments with each sample.

Figures 2.4-2.6 show a summary of the inhibitory effect of serum, meconium or cholesterol on the surface behavior of surfactant and the prevention of this inhibition by pre-exposure of surfactant to polymers such as hyaluronic acid (negatively charged) or dextran (non-charged).

Panel a of Figure 2.4 illustrates how the presence of a pre-formed serum layer at the bubble surface does not allow surfactant to reach the interface, as the surface tension reached upon surfactant injection is not lower than 40mN/m. Application of surfactant pre-mixed with either of the polymers (HA 0.25% w/v or dextran 0.5% w/v) restores the ability of surfactant to reach the interface and lower surface tension to 22-23mN/m. Addition of the polymers by themselves does not affect interfacial adsorption of NS, as surfactant pre-mixed with polymers had surface tensions that were not significantly different from the tensions reached by NS alone. The polymers tested do not possess surface activity by themselves either, because the introduction of the polymers alone in the subphase does not produce apparent changes in the surface tension of the saline solution, either in the CBS or as tested in Langmuir troughs (see chapter 3). To test inhibition of adsorption by meconium or cholesterol, we pre-mixed each with NS, before applying the mixture near the surface of the bubble. Figure 2.4 (panel b) also illustrates that the equilibrium surface tension reached upon adsorption, either initially or after bubble expansion of meconium- or cholesterol-pretreated surfactant, was not different from that of NS alone. It can be noticed that the surface tension reached upon 5 min of expansion of the bubble coated with NS pre-mixed with meconium is apparently higher, but with a rather large error as a consequence of high heterogeneity in the behavior of replicas, likely associated with the intrinsic complexity and heterogeneity of meconium.

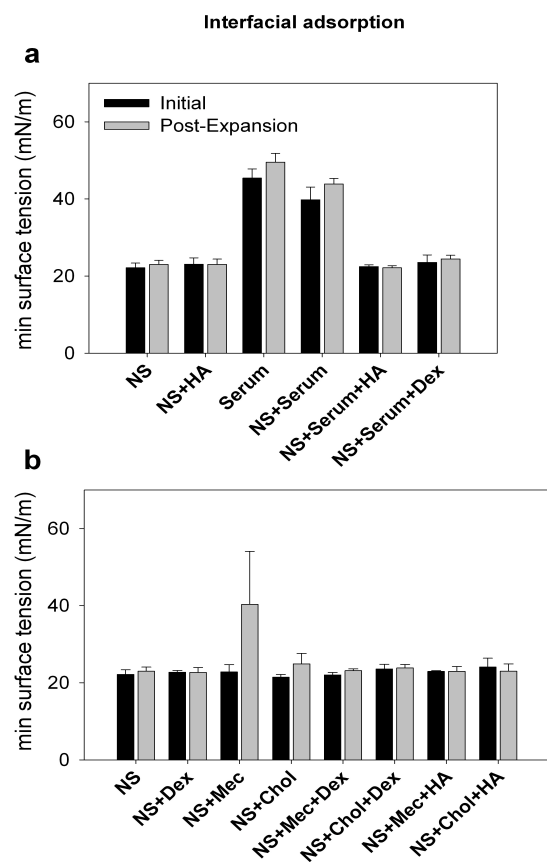


Figure 2.4: Interfacial adsorption of native surfactant in the absence or presence of inhibitors and polymers. (Panel *a*) minimal surface tension upon 5 minutes of initial (black bars) or post-expansion (grey bars) adsorption of a native surfactant sample combined or not with the indicated polymers, injected under a clean or a serum-coated bubble. (Panel *b*) minimal surface tension upon initial or post-expansion adsorption of surfactant in the absence or presence of meconium, cholesterol, and/or polymers. Data are means \pm standard deviation after averaging three independent experiments from each sample.

Figure 2.5 summarizes quasi static cycling of NS in the absence or in the presence of serum, meconium or cholesterol, with or without pre-mixing with dextran or HA.

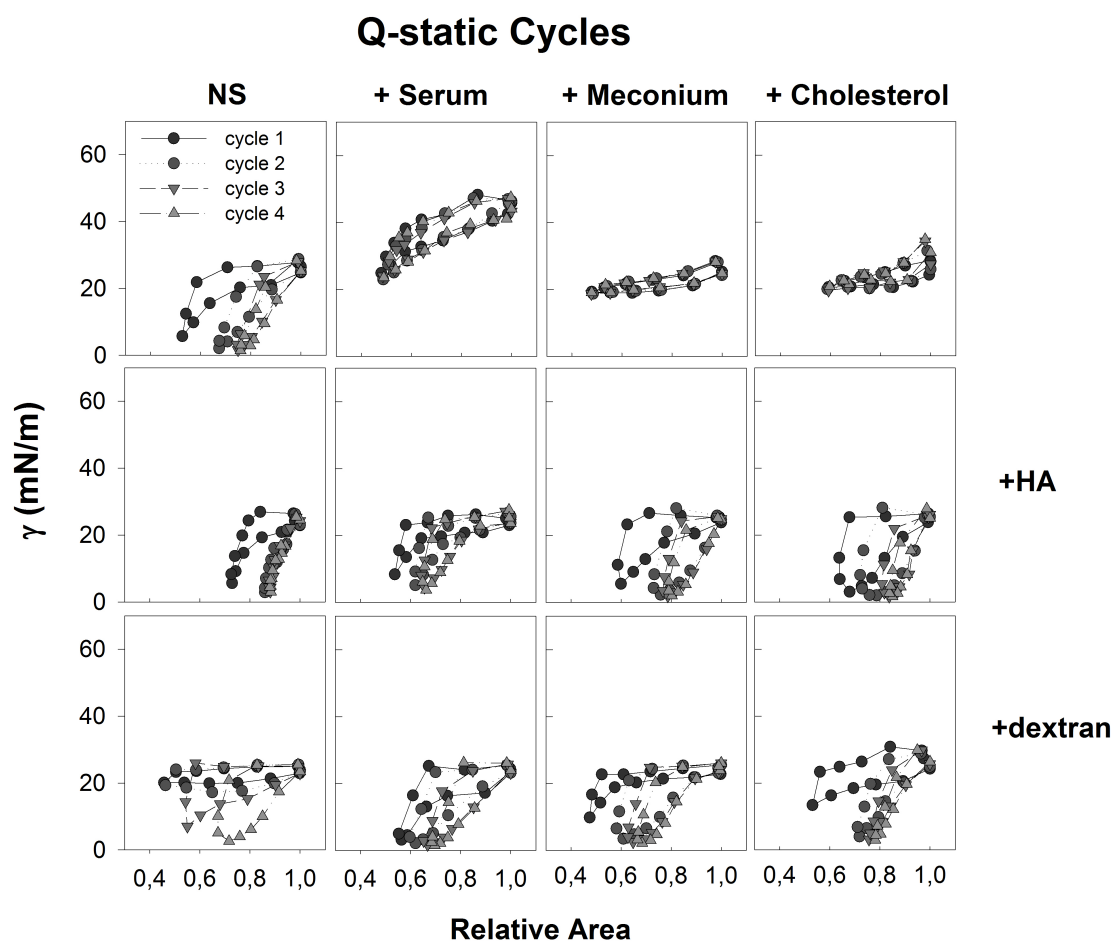


Figure 2.5: Quasi-static compression-expansion isotherms of surfactant in the absence or presence of inhibitors and polymers. Quasi-static compression-expansion cycling isotherms for surfactant injected under the bubble at the CBS, in the absence or in the presence of serum, meconium or cholesterol, combined or not with HA (0.25%) or dextran (0.5%). A representative experiment is shown in each panel, after three repetitions from each sample.

Q-static cycling of NS in the presence of a serum film (2 μ l, 100 mg/ml total protein) was highly defective, with surface tension decaying only to 37.9 ± 2.4 mN/m after about 50% of area compression (see also Table 2.2).

| QSTAT 4 | | | |
|--------------|---------------------|--------------------|---|
| Sample | γ min (mN/m) | γ max(mN/m) | Relative Area ^(γ_{\min}) |
| NS | 1.6 ± 0.6 | 27.3 ± 1.8 | 0.8 ± 0.1 |
| NS+HA | 2.3 ± 0.9 | 26.1 ± 1.1 | 0.6 ± 0.2 |
| Serum | 37.9 ± 2.4 | 52.4 ± 2.5 | 0.5 ± 0.1 |
| Serum + NS | 21.7 ± 1.6 | 36.9 ± 9.6 | 0.5 ± 0.1 |
| Serum+NS+HA | 2.6 ± 0.7 | 26.3 ± 1.4 | 0.8 ± 0.1 |
| Serum+NS+Dex | 12.8 ± 9.9 | 26.3 ± 0.3 | 0.5 ± 0.1 |

| DYN 20 | | | |
|--------------|---------------------|--------------------|---|
| Sample | γ min (mN/m) | γ max(mN/m) | Relative Area ^(γmin) |
| NS | 1.8±0.7 | 32.1±3.6 | 0.8±0.1 |
| NS+HA | 2.2±1.1 | 31.7±1.9 | 0.8±0.1 |
| Serum | 37.4±3.1 | 54.1±3.1 | 0.5±0.1 |
| Serum+NS | 17.1±6.1 | 51.7±3.5 | 0.5±0.1 |
| Serum+NS+HA | 2.5±1.1 | 29.6±0.9 | 0.9±0.1 |
| Serum+NS+Dex | 1.9±0.5 | 33.2±2.9 | 0.8±0.1 |

Table 2.2: Effect of serum and polymers on pulmonary surfactant surface activity. Data are average \pm standard deviation, n=3.

Addition of 4% (w/w) cholesterol to NS, either as taking part of meconium or solubilized by M β CD, produced a similar deleterious effect on the behavior of NS complexes, which required an area compression of 50% to reach surface tension of only around 20mN/m (19.6±0.8mN/m for meconium- and 20.2±0.6mN/m for cholesterol- M β CD -treated surfactant; see table 2.3).

| QSTAT 4 | | | |
|----------------|---------------------|--------------------|---|
| Sample | γ min (mN/m) | γ max(mN/m) | Relative Area ^(γmin) |
| NS | 1.6±0.6 | 27.3±1.8 | 0.8±0.1 |
| NS+Dex | 2.1±1.1 | 26.7±2.1 | 0.6±0.1 |
| NS+Meconium | 19.6±0.8 | 37.5±9.1 | 0.5±0.1 |
| NS+Cholesterol | 20.2±0.62 | 29.2±4.9 | 0.5±0.1 |
| NS+Mec+Dex | 6.9±7.9 | 25.3±0.5 | 0.5±0.1 |
| NS+Chol+Dex | 2.9±0.9 | 28.2±1.4 | 0.7±0.1 |
| NS+Mec+HA | 7.9±10.5 | 25.4±0.8 | 0.6±0.2 |
| NS+Chol+HA | 1.5±0.1 | 26.1±1.7 | 0.8±0.1 |

| DYN 20 | | | |
|----------------|---------------------|--------------------|---|
| Sample | γ min (mN/m) | γ max(mN/m) | Relative Area ^(γmin) |
| NS | 1.8±0.7 | 32.1±3.6 | 0.8±0.1 |
| NS+Dex | 1.7±0.6 | 39.9±11.3 | 0.7±0.2 |
| NS+Meconium | 18.3±3.7 | 45.4±5.9 | 0.5±0.1 |
| NS+Cholesterol | 7.2±4.1 | 37.9±4.2 | 0.7±0.1 |
| NS+Mec+Dex | 1.3±0.1 | 30.9±1.4 | 0.8±0.1 |
| NS+Chol+Dex | 1.9±0.8 | 31.9±0.9 | 0.8±0.1 |
| NS+Mec+HA | 1.9±0.5 | 31.3±0.9 | 0.8±0.1 |
| NS+Chol+HA | 1.5±0.6 | 29.3±2.6 | 0.9±0.1 |

Table 2.3: Surfactant inhibition by meconium or cholesterol in the absence or presence of polymers. Data are average \pm standard deviation, n=3.

The inhibitory effect of the exposure of surfactant to cholesterol-loaded M β CD is clearly due to the increase in the proportion of cholesterol produced in surfactant membranes, from 3 to around 6% with respect to phospholipid (see above), because exposure of surfactant to cholesterol-free cyclodextrine does not produce any effect on its Q-static or dynamic compression-expansion isotherms (see Figure 2.6).

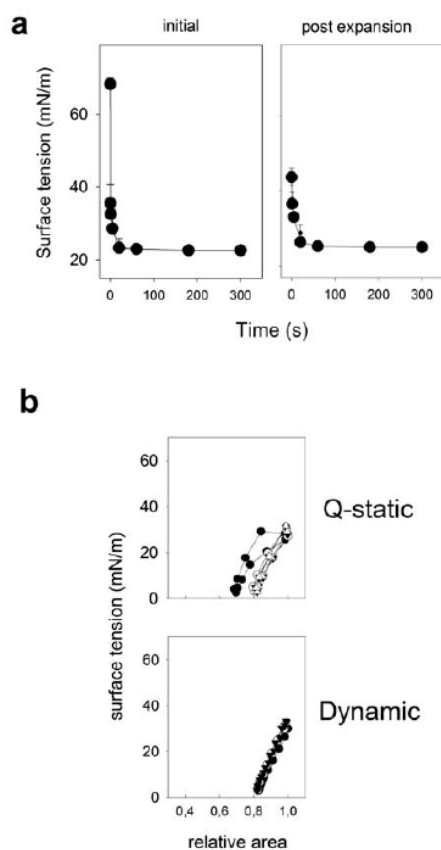


Figure 2.6: Surface behavior of NS membranes upon exposure to cholesterol-free M β CD.

a) Interfacial initial and post-expansion adsorption of native surfactant pre-exposed to 10 mg/mL of M β CD, as assessed in the CBS at 37°C. Data are means \pm standard deviation after averaging data from three experiments. b) Compression-expansion isotherms of films formed by M β CD pre-exposed NS under Q-static (upper panel) or dynamic (lower panel) cycling. Presented are the 1st (closed circle), 2nd (open circles), 3rd (closed triangles) and 4th (open triangles) compression-expansion Q-static cycles, and the 1st (closed circles), 10th (open circles) and 20th (triangles) dynamic cycles.

Addition of dextran or HA totally restored the behavior of NS films during Q-static compression-expansion cycling, which finally reached very low tensions with only \sim 20% area compression even in the presence of serum, meconium or cholesterol. Finally, Figure 2.6 confirmed the differences in behavior under quasi-physiological dynamic cycling between inhibited and polymer-restored surfactant samples. Presence of a serum film resulted in NS reaching minimal surface tension under dynamic cycling of 17.0 ± 6.0 mN/m, with an area reduction of 50%. Addition of 4% cholesterol (w/w) contained in 10 mg/ml of meconium resulted in minimal surface tension of 18.3 ± 3.7 mN/m (area compression 50%) and 4% cholesterol solubilized by M β CD allowed NS to reach 7.2 ± 4.0 mN/m (area compression 30%).

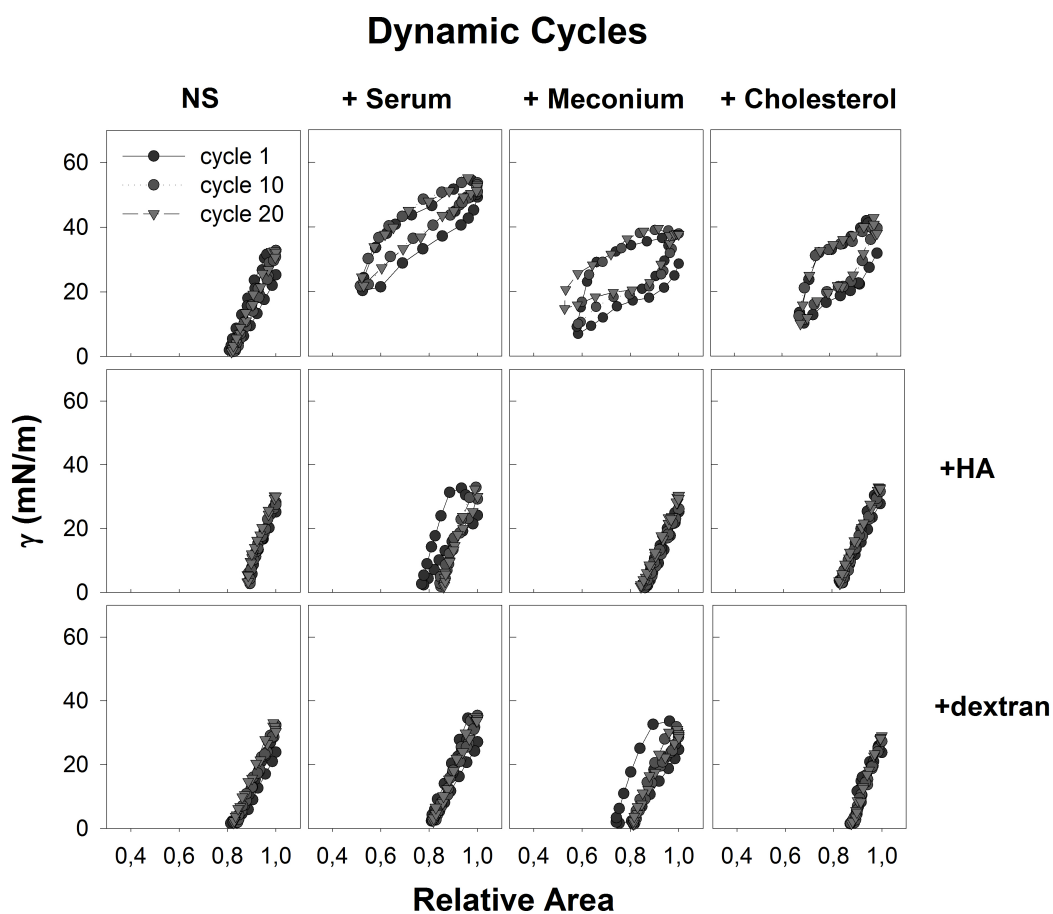


Figure 2.7: Dynamic compression-expansion isotherms of surfactant in the absence or presence of inhibitors and polymers. Dynamic compression-expansion cycling isotherms for surfactant injected under the bubble at the CBS, in the absence or in the presence of serum, meconium or cholesterol, combined or not with HA (0.25%) or dextran (0.5%). A representative experiment is shown in each panel, after three repetitions from each sample.

In spite of the presence of any of the inhibitory agents, the exposure of NS to either HA or dextran prevented the inhibitory effects observed under dynamic cycling, resulting in NS films that were completely functional, with parameters that were similar than exhibited in the absence of inhibitors. The films were able to reach the lowest surface tensions, statistically indistinguishable from those reached in the absence of inhibitors, with practically no hysteresis, needing approximately only 20% of area compression.

DISCUSSION

This study has established a revised protocol using the CBS to study inhibition of surfactant by several substances relevant to human lung injury. Further, we have documented the remarkable ability of ionic (HA) and nonionic (dextran) polymers to reverse not only serum inhibition of surfactant, but also inhibition by meconium or cholesterol that inhibit surface activity by mechanisms that differ from serum.

Study of the mechanisms of inhibition of surfactant action using the CBS (Gunasekara et al. 2008), has had more or less success. We have introduced two main modifications of the current technique that allow us to observe reproducible surfactant inhibition: i) using a decreased concentration of surfactant, and ii) a novel way to challenge surfactant with the inhibitory agent. Use of critical concentrations of surfactant, in which surfactant is completely functional but susceptible to inhibition, allows us to study not only inhibition but also to observe subtle differences between Q-static cycles and the process of reorganization of material during step-wise low speed compression-expansion. The presence in the alveoli of a reduced concentration of endogenous (secreted) and exogenous (administered therapeutically) surfactant is probably inherent to an injured lung due to i) the larger volumes of fluid lining the epithelium due to edema, ii) a reduced production of endogenous surfactant by the damaged epithelium and iii) an accelerated catabolism of both endogenous and exogenous surfactant by liberated lipases and proteases. We think that the use in our inhibition studies of undiluted serum (protein concentration 100mg/mL) also simulates *in vivo* conditions (Stenger and Zasadzinski 2007). This technique better reproduces the situation occurring *in vivo*, with relatively concentrated serum leaked into alveoli –as a consequence of an injured epithelium- into which endogenous surfactant is secreted unlike previous inhibition models wherein serum inhibition was usually tested at much lower concentrations and higher surfactant concentrations. Our setup would mimic at less extent the processes by which serum leaked at an uncertain concentration could disrupt and alter a previously formed and already working interfacial surfactant layer. Still, our method may also allow evaluating inhibitory susceptibilities and resistances of clinical surfactant under conditions similar to what an exogenous surfactant may encounter when delivered into the context of an injured and inflamed lung.

Clearly, the ability of surfactant to reach the interface in the presence of inhibitors depends on surfactant concentration. NS is highly surface active in very low concentrations (10 mg/mL) and is resistant to inhibition at phospholipid concentrations ≥ 20 mg/mL. *In vivo*, after lung injury, relative concentrations of serum and other inflammatory inhibitors and surfactant are difficult to ascertain and vary over the course of the disease. Lung injury and concomitant edema is associated not only with leakage of serum, lipoproteins, cholesterol and other inhibitory agents into alveoli but also produces an effective dilution of the surfactant, which could be further reduced by an impairment in synthesis/secretion of new surfactant due to epithelium damage.

Our data suggest that a decrease in concentrations of surfactant below a certain threshold could allow the study of inhibition. Therefore one therapeutic strategy is to overcome inhibition associated with lung injury by introduction of exogenous

surfactant. However, previous work has demonstrated that current clinical surfactants are substantially more susceptible to inhibition than NS (Taeusch et al. 2005). The optimized CBS model developed may be a useful tool to gain deeper insight into the molecular mechanisms of surfactant inactivation, and to test improved clinical surfactants for resistance to inhibition.

Our model confirms that serum forms an interfacial barrier comprised of serum proteins that impedes proper adsorption of surfactant. This explains why minimal tensions achieved by diluted surfactant are not much lower than surface tensions produced by pure serum layers. Surfactant fails to reach an interface that is previously occupied by a concentrated layer of surface-active serum proteins. Our results show that a brief disruption of the serum layer caused by the mere injection of surfactant at the bubble surface can be enough to give surfactant the opportunity to compete with serum components for adsorption into a newly opened interface, thereby displacing serum proteins to reach an (uninhibited) low tension. The concept of competitive adsorption of serum and surfactant has been developed in the inhibition models proposed by Zasadzinski group (Zasadzinski et al. 2005; Fernsler and Zasadzinski 2009; Zasadzinski et al. 2010). We show here that the mere mechanical disruption of the inhibitory layer can also be a crucial contribution to overcome surfactant inactivation provided that surfactant is active enough to compete efficiently with the less surface active but much more concentrated serum components.

The addition of non-ionic or anionic polymers such as dextran or HA can improve substantially the resistance of surfactant to inactivation. This activity of polymers had been extensively documented (Lu et al. 1999; Lu et al. 2005; Taeusch et al. 2005; Taeusch et al. 2008; Lu et al. 2011), but not under the restrictive conditions imposed in our assay. The action of polymers has been explained by models that invoke polymer-created depletion forces that push the large surfactant complexes against the interface, thereby overcoming the steric and electrostatic barrier imposed by serum layers (Taeusch et al. 2005; Zasadzinski et al. 2005; Zuo et al. 2008). Still, it is difficult to envision how depletion forces can propel surfactant, injected far –in molecular terms– below the interface, to cross the concentrated layer of serum to reach the interface where surface-active species are finally transferred. The polymers in our experiments are restricted to the small volume of injected surfactant. After injection of surfactant/polymer combinations, the polymers are likely homogeneously distributed and diluted into the thin layer of fluid constituting the subphase, without a particular accumulation at the interface, because injection of equivalent amounts of polymer alone does not produce apparent effects on surface tension. These conditions are different from previously published work as the polymers in our experiments are not previously present in the subphase where in principle they could be diluted to concentrations much lower than those required to promote depletion forces shortly after injection of the surfactant/polymer mixtures. The ability provided by the polymers tested for surfactant to successfully cross the serum layer and adsorb at the interface is remarkable. Preliminary experiments using a quartz-microbalance model (Wolny et al. 2010) discarded the interaction of HA with surfactant complexes (see chapter 3), indicating that the effect of the polymers to promote interfacial adsorption against the serum layer is not due to the formation of polymer/surfactant complexes with particularly

favourable surface properties. It remains to be determined whether the establishment of interactions between negatively charged polymers like HA and cationic protein components in serum could play a role in counteracting serum-promoted surfactant inhibition. However, this possibility does not seem likely because i) a non-ionic polymer like dextran seem to produce qualitatively similar effects, and ii) the total amount of polymer introduced in the surfactant/polymer combinations of our experiments is orders of magnitude smaller than the amount of serum proteins in the surface layer. The conditions of our experiments may mirror the introduction of therapeutic surfactant into edematous alveoli that are replete with inflammatory inhibitors after acute lung injuries, and provide a proof of concept of the utility of certain polymers as useful additives in therapeutic surfactants.

One would not have predicted that addition of polymers to surfactant mixtures would have a similar beneficial effect after inhibition by meconium or cholesterol, which act by mechanisms that differ from true competitive adsorption by serum proteins (Leonenko et al. 2007; Gunasekara et al. 2008; Lopez-Rodriguez et al. 2011). These agents, meconium and cholesterol, do not cause strong inhibition of interfacial adsorption of surfactant, but rather a substantial modification of its compression-expansion properties. This can be explained by insertion of excess of cholesterol into surfactant membranes and films, and a concomitant reduction of their compressibility, as it has been discussed in the chapter 1 of this Thesis. Cholesterol, solubilized either by bile salts (as in meconium) or by M β CD, is transferred into surfactant films rendering them dysfunctional during Q-static and dynamic cycles. It seems that altered films experiment early collapse and do not lower down surface tension as a result of the incorporation of 4% w/w cholesterol. Even though this is a relatively small amount of cholesterol (Gunasekara et al. 2010) it seems that in a soluble state (in complexes with bile salts or M β CD) cholesterol has a particularly notable deleterious effect.

Exposure to the polymers counteracts the perturbation of rheological properties of surfactant caused by incorporation of excess cholesterol. It is conceivable that a potential depletion force-originated compaction of membrane structures, with creation of extensive membrane-membrane interactions, promotes a highly cohesive multilayered structure that compensates for a loss of rigidity caused by an excess of cholesterol-promoted fluidification. We have shown that exposure to polymers such as dextran or HA do in fact create compaction of surfactant structures and generation of membrane-based networks by different surfactant preparations (Lu et al. 2009). We cannot fully discard the possibility that HA would also interact with surfactant membranes and/or films providing a surplus of mechanical stability compensating the likely higher deformability of cholesterol-enriched phases. The reversal or prevention of surfactant inhibition by polymers has been extensively documented both *in vitro* (Taeusch et al. 1999; Tashiro et al. 2000; Lu et al. 2005b; Stenger and Zasadzinski 2007; Taeusch et al. 2008) and *in vivo* (Campbell et al. 2002; Dehority et al. 2005; Lu et al. 2005b; Calkovska et al. 2008). The new approach described here demonstrates that certain polymers help NS overcome not only the inactivating effect of serum, but also that of meconium and cholesterol. Thus, the reversion mechanism is general for NS and not specific for inhibitory agents that we tested. We are not aware of previous data showing that polymers not only promote interfacial adsorption but also restore compressibility of surfactant films during

compression-expansion cycling in the presence of inhibitors. Further studies are required to analyze in more detail the ways in which polymers may structure and organize surfactant membranes and films, particularly when surfactant has been pathologically-altered. We speculate that exposure to polymers like dextran or HA may induce an “activation” of surfactant by modifying its structure so that it is much more resistant to different types of inhibition and has better surface properties in terms of both better interfacial adsorption and improved rheological properties to sustain high pressures without collapsing. If this is the case, addition or treatment with polymers may produce new clinical surfactants for lung injuries for which there is as yet not good therapy.

**STRUCTURAL AND FUNCTIONAL MODIFICATION OF PULMONARY SURFACTANT
PRE-ACTIVATED BY HYALURONIC ACID**

Elena Lopez-Rodriguez, Antonio Cruz, Ralf Richter, H.William Taeusch and Jesus
Perez-Gil

Article in preparation

This work has been done in collaboration with MD H. William Taeusch (General Hospital of San Francisco, University California San Francisco)



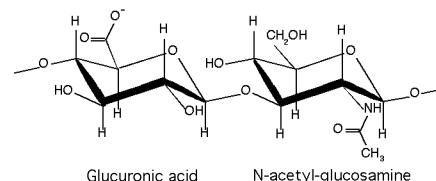
and PhD Ralf Richter (CICBiomaGUNE)



STRUCTURAL AND FUNCTIONAL MODIFICATION OF PULMONARY SURFACTANT PRE-ACTIVATED BY HYALURONAN

INTRODUCTION

Hyaluronic acid (HA) is a naturally occurring linear polysaccharide with repeating disaccharide units of glucuronic acid and N-acetylglucosamine, linked via alternating β 1-4 and β 1-3 glycosidic bonds, present in tissues as cartilage, synovial fluid and also in lungs. It is known that HA is present in the aqueous layer lining the respiratory epithelium because type II pneumocytes secrete it (Sahu 1980; Bray 2001). The size of HA molecules vary among specific tissues. Normal synovial fluid has HA of an average of 7,000kD (Fraser et al. 1997).



In cartilage and lung, it has 2,000 (Holmes et al. 1988) and 220kD (Nettelbladt et al. 1989), respectively. A unique characteristic of HA, which relates to its variable functions, is its hydration capability. HA exist in solution in a flexible coiled configuration, which is well hydrated and contains approximately 1000-fold more water than polymer (Bray 2001; Turino and Cantor 2003). The volume of solution that is controlled by HA molecule is determined by the molecular weight of the HA. In addition to the large contribution that the negative charged carboxyl groups of HA make to the expansion of the coil and thus the volume of water it enfolds, the model of HA of Heatley and Scott (1988) suggests that water molecules are hydrogen-bonded to the HA chain with some regularity (Bray 2001). Thus, the concentration of HA in tissue can determine its water content. This relationship has been demonstrated for normal animal lungs, where reductions in lung HA induced by hyaluronidase have been correlated with reductions in the extravascular lung water volume (Bhattacharya et al. 1989). This correlation has also been demonstrated in experimental alveolitis. HA is also involved in several other functions, such as tissue repair and protection against infections and the activity of proteolytic granulocyte enzymes (Souza-Fernandes et al. 2006).

The HA molecules behave in solution as highly hydrated random coils, which start to entangle at concentrations of about 1mg/ml, forming a meshwork. This is stabilized by chain-chain interactions through hydrophobic patches (Laurent et al. 1996). The ability to self-aggregate make HA an ideal molecule to organize a network in the aqueous subphase as it is known to do in the vitreous humor of the eye and cartilage (Bray 2001).

A polymer network offers a high resistance to the bulk flow of solvent. Thus, HA and other polymers prevents excessive fluid fluxes through tissue compartments. Furthermore, the osmotic pressure of HA solution is non-ideal and increases exponentially with the concentration (Comper and Laurent 1978). This exponential relationship makes HA and other polysaccharides excellent osmotic pressure buffering substances, as moderate changes in concentration lead to marked changes in osmotic pressure. Flow resistance together with osmotic buffering makes hyaluronan and ideal regulator of the water homeostasis in the body (Laurent et al. 1996).

The phenomenon of steric exclusion of other molecules is another attribute of the molecular meshwork of HA. At the normal HA content of synovial fluid, about 15% of the total water volume is unavailable to albumin, so that its true concentration in the remainder solution is in fact higher. The degree of exclusion increases with molecular size and explains in part why the largest plasma proteins are reduced in extravascular fluid to an even greater degree than albumin (Fraser et al. 1996).

As seen in chapter 2, the addition of polymers such as hyaluronic acid (HA) restores the biophysical activity of surfactant in the presence of different inactivating agents. Others have also showed this effect in animal models. But still the mechanism by which surfactant is reactivated by polymers has been only explained by models involving depletion forces (Taeusch et al. 1999; Taeusch et al. 1999; Taeusch et al. 2005; Zasadzinski et al. 2005; Taeusch et al. 2008; Zuo et al. 2008). In this chapter we try to identify and clarify the entropic forces that HA meshwork may assert into surfactant complexes.

It has been previously shown that addition of polymers such as hyaluronic acid (HA), dextran or polyethylene glycol (PEG) enhance the activity of surfactant in vitro as well as in vivo (Taeusch et al. 2005). It has been previously proposed that the mechanism by which HA enhances surfactant adsorption through an albumin steric barrier would be explained by depletion forces. This entropic driven force pushes surfactant complexes toward each other, causing aggregation of surfactant complexes and towards the interface, enhancing its adsorption (Zasadzinski et al. 2010). However, these entropic forces do not explain why the addition of polymers to surfactant restores its activity when membrane-perturbing agents, such as cholesterol, are the inactivating agents. Thus, something else more than simple depletion forces may be acting on surfactant membranes.

Recent work has shown that hydrogen bonds form along the axis of the HA molecule. These create a twist on the chain, impart stiffness and generate hydrophobic patches that permit association with other HA chains, despite their negative charge. This stiffness of the HA polymer promotes an extended random coiled configuration and ensure that their long chains occupy enormous molecular domains. These begin to overlap and form an entangled meshwork at levels of around 1mg/ml, which may be stabilized by chain-chain interactions (Fraser et al. 1997). This concentration depends on great extent on the persistence length, a parameter defining polymer elasticity. This persistence length is ten times greater for HA than for other polymers such as PEG, and that would be the reason why the overlap concentration of HA is normally ten times lower than that of other polymers (Desmedt et al. 1993; Fam et al. 2007; Rubinstein and Colby 2008; Fam et al. 2009).

A final goal of the present study is to integrate the molecular and biophysical data to develop a surfactant preparation with improved resistance to inactivation. The basic knowledge on the molecular mechanisms of the inactivation of surfactant and the counter effect of polymers, should allow us to propose an enhanced surfactant preparation for potential therapeutic treatment of ARDS and MAS. As described in chapter 1, surfactant supplementation therapy in case of MAS does not have a positive effect as the exogenous surfactant is inactivated in the same way the endogenous surfactant is. In ARDS, a clinical trial has also demonstrated a partial

inactivation of exogenous surfactant (Spragg et al. 2011). Therefore enhancing surfactant resistance to inactivation may open the possibility of designing more efficient treatments for respiratory pathologies such as MAS and ARDS.

We propose that the formation of a meshwork through the entanglement effect at a critical concentration (overlap concentration) of HA may lead to entropic forces, as osmotic and depletion forces, that would act on surfactant complexes independently of the inactivating agent. These physical forces may produce some changes in structure and composition that contribute to the resistance of surfactant to inhibition, not only by serum proteins, but also by membrane-disturbing substances such as cholesterol or meconium. However, *in vivo* application of surfactant together with HA has several disadvantages, being the most important one the higher viscosity of surfactant-HA preparations that impose difficulties on the application and homogeneous distribution of surfactant-HA preparation in animal models. Also it has been shown that introduction of high polymer concentrations into the airways may create fluid imbalance and altered clearance of liquid from the air-spaces (Matar et al. 2002; Gaver et al. 2005; Blanco and Pérez-Gil 2007). We propose that alteration created by polymers like HA on surfactant structure may be, at least in part, irreversible, leading to a sort of pre-activation of surfactant that may persist once HA is removed. We have characterized structure and biophysical behavior of this pre-activated surfactant for activity in the presence or absence of inhibitory agents on CBS and we have analyzed the potential utility of this higher resistance to inactivation.

RESULTS

For assessing the question whether there is interaction between surfactant complexes and HA chains we have used a hyaluronan-grafted membrane system in quartz crystal microbalance with dissipation (QCM-D) described by Wolny et al. (2010). The lack of interaction between surfactant and HA is a requirement for depletion forces to act, as volume exclusion may occur between molecules. But the real occurrence of this interaction was never studied. With hyaluronan-grafted membranes we can directly study whether stable interaction between molecules are really established. In figure 3.1 a representative experiment is illustrated, where surfactant in form of MLVs (multilamellar vesicles) is applied on the top of the hyaluronan-grafted membrane. For the formation of the grafted membranes, first vesicles of a mixture of DOPC and biotinylated PE are applied. We can follow the deposition of the vesicles as fast drop of frequency and increase in dissipation, due to the increased mass attached to the surface of the sensor. Vesicles collapse and break down liberating their aqueous content, this loss in mass is seen as an increase in frequency at the same time dissipation decreases to its original position till the supported lipid bilayer is stably at the surface of the sensor. Supported lipid bilayers show almost no dissipation due to its rigid properties. Latter, the addition of neutravidin (NAv) will decrease further the frequency, as this protein is binding to biotin from the PE. Biotinylated HA is then applied, with the consequent decrease in frequency, due to the new mass attached to the surface, and increase in dissipation, due to the high stiffness of HA chains. Any molecule attaching to HA will show an

increment on frequency. But the application of surfactant show no changes in frequency nor in dissipation. Thus we can conclude that there is not apparent interaction between surfactant complexes and hyaluronan.

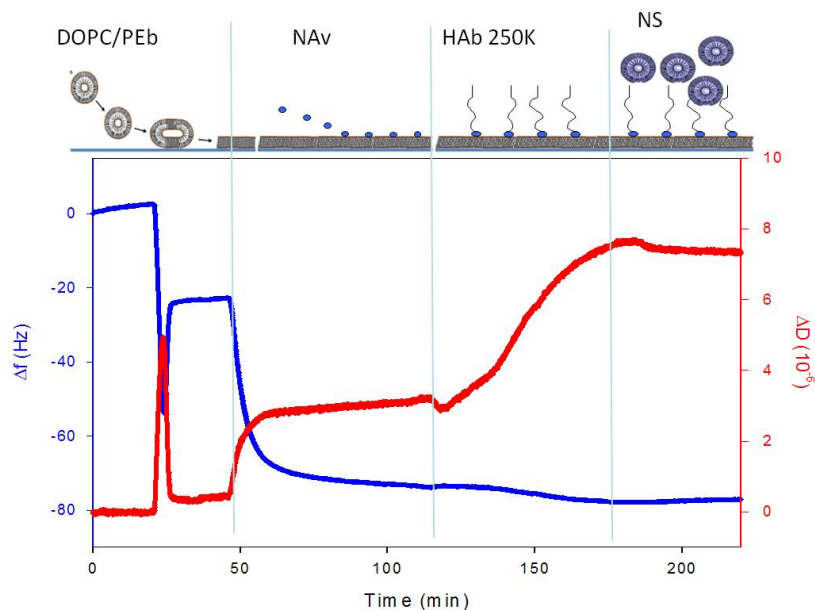


Figure 3.1: Hyaluronan-grafted membranes for studying surfactant interaction with HA in QCM-D. Panel A: scheme of the procedure of the experiment correlated with the result in the plot in panel B. Panel B: changes in frequency (blue line) and dissipation (red line) within the time of the experiment.

It has been previously shown that interfacial adsorption of surfactant is enhanced in the presence of HA (Taeusch et al. 2005). Figure 3.2 shows that the application of NS together with HA on the surface of a Langmuir trough results in an enhanced adsorption and transfer of material to the interface, with a high efficiency that reproduces transfer of material when it is directly deposited at the air-water interface as an extract in organic solvents (OE). It seems that HA induces 100% efficiency in the transfer of material into the interface. It should be noticed that the addition of HA to surfactant does not displace the isotherm over the one from OE, meaning that HA is not occupying space at the interface. Most probably HA is completely diluted away into the subphase at the application time, confirming that no interaction would previously exist between surfactant complexes and hyaluronan. It seems that instead of interaction between the two materials, repulsion or exclusion forces could be acting, which would fit with the processes described by depletion forces theory, already proposed by Zasadzinski et al. (2005).

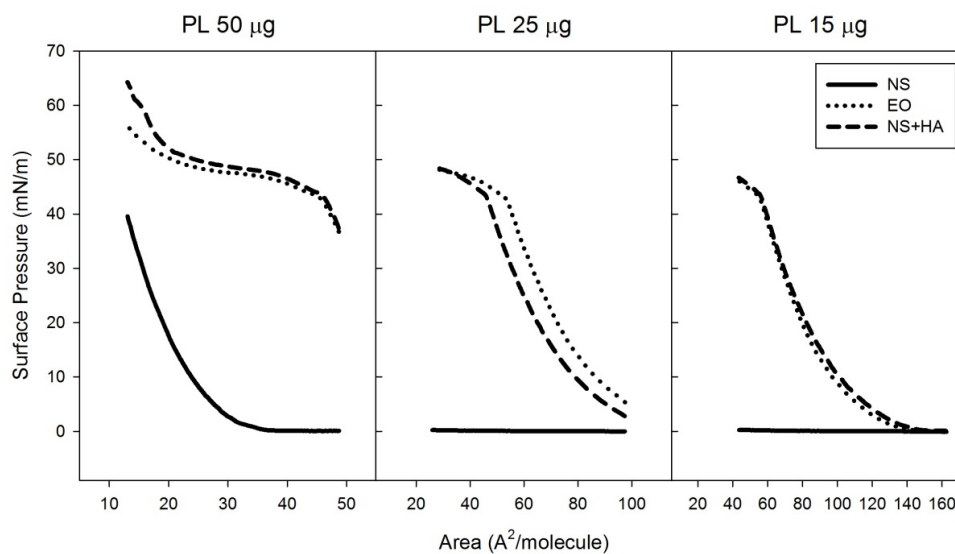


Figure 3.2: Compression isotherms of native surfactant in a Langmuir balance, in the presence or absence of HA. Compared are isotherms of native surfactant (NS) (solid line), extracted surfactant in organic solvents (OE) (dotted line) and native surfactant together with HA (NS+HA) (dashed line). Three different quantities of phospholipids were applied in three different experiments (15, 25 and 50 μg of total phospholipids in surfactant).

Analysis of surfactant membranes converted into GUVs (Giant Unilamellar Vesicles) as model of surfactant bilayers allows the study of certain membrane properties such as the lateral structure of lipid phases, and how this is modified by the addition of hyaluronic acid to the bulk phase. As it is shown in figure 3.3, GUVs of native surfactant show an average size of about $12\mu\text{m}$ and a more or less homogeneous segregation of rounded domains of presumably fluid liquid-disordered phase from a matrix of DPPC- and cholesterol-enriched liquid-ordered phases. When HA is present in the bulk solution at a final concentration of 2.5mg/ml then both domain distribution and GUVs size change. We found a heterogeneous domain distribution, with less number of domains and different sizes, aggregated-like domains, and also the average size of the GUVs decreases to $8\mu\text{m}$.

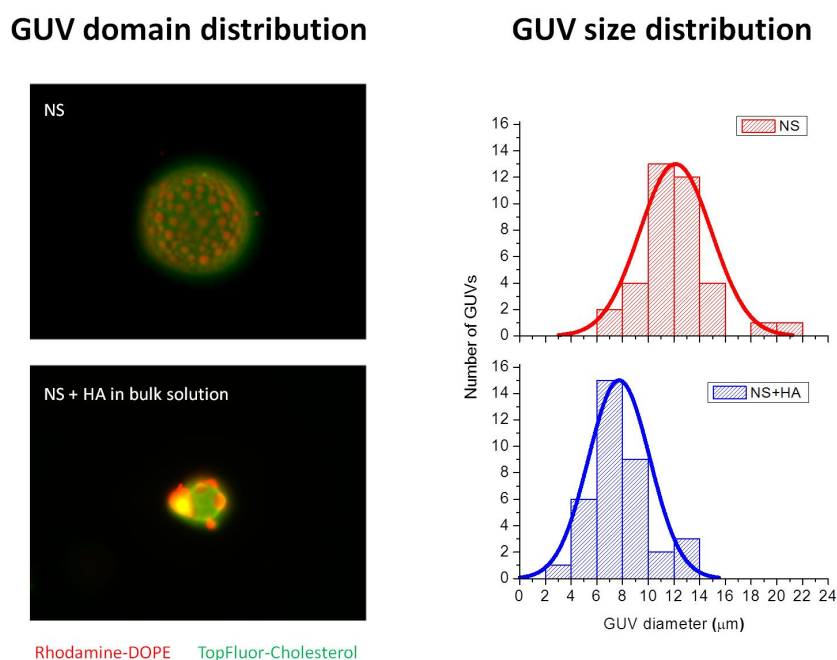


Figure 3.3: domain distribution and size in GUVs of surfactant labeled with rhodamine-DOPE (red) and TopFluor-Cholesterol (green). Panel A: on the top, example of a GUV from native surfactant, and on the bottom, example of a GUV from native surfactant in a bulk phase containing HA (2.5mg/ml). Panel B: size distribution of vesicles by quantification of the diameter of GUVs from surfactant in the absence (top) and presence (bottom) on HA in the bulk phase. (n=70 vesicles per group).

It seems that the HA-promoted decrease in size of surfactant GUVs may change the distribution of segregated domains and lead to the segregation of some phospholipid components, out of from the GUVs.

To study whether HA may promote real segregation of some specific phospholipid species and thus a refining of the composition of surfactant membranes, we have included Rhodamine probes, one attached to a saturated phospholipid (DPPE) and other attached to an unsaturated phospholipid species (DOPE). To fractionate segregated domains and small vesicles, potentially segregated from large membranes and complexes upon exposure to HA, we have centrifuged the sample and resuspend only the pellet, where most of the larger aggregates are deposited, eliminating small vesicles and HA in the supernatant. As it can be observed in figure 3.4, the pre-exposition of Rho-DPPE labeled surfactant to different concentrations of HA does not cause any change on the fluorescence intensity of the probe, indicating that there is no change on the amount of saturated labeled phospholipids of the pelleted large surfactant complexes after HA exposure. In contrast, the pre-exposition of Rho-DOPE labeled surfactant to HA causes a substantial loss of the fluorescence of the probe, when the membranes are pre-exposed to concentrations of HA above 1mg/ml. As this labeled surfactant was centrifuged to remove HA, small

protrusions of unsaturated lipids were likely segregated out from the large aggregates and MLVs of surfactant and were lost together with the HA in the supernatant. This HA-driven refining of the composition would then be non-reversible which may have a positive impact on surfactant surface activity and resistance to inactivation. The effect of different HA concentrations suggest that there is a critical concentration for HA to produce compositional refining of unsaturated phospholipids. This concentration, around 1mg/ml, is the overlapping concentration above which HA forms a meshwork.

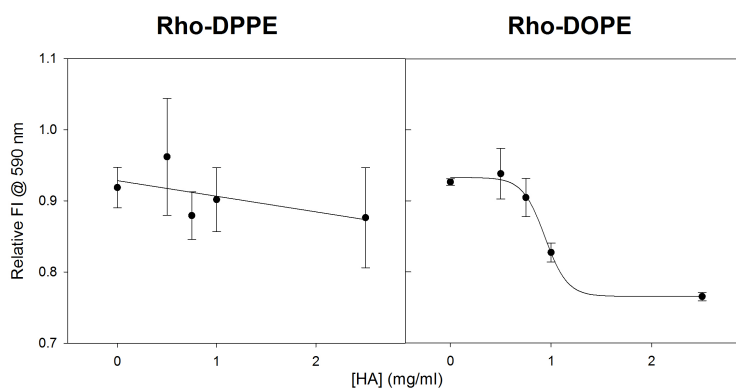


Figure 3.4: Fluorescence intensity of Rhodamine-DOPE and Rhodamine-DPPE in surfactant complexes after exposure to different concentrations of HA. Decay of the fluorescence probes Rhodamine-DOPE (left

panel) or Rhodamine-DPPE (right panel) in surfactant membranes pelleted by centrifugation after pre-exposure to increasing concentrations of HA.

Moreover measuring cholesterol content after exposure to HA resulted in a decrease in cholesterol on surfactant complexes when high concentrations of HA are present in the bulk phase (figure 3.5). Confirming that the formation of a meshwork above 1mg/ml of HA produces a refining on the composition.

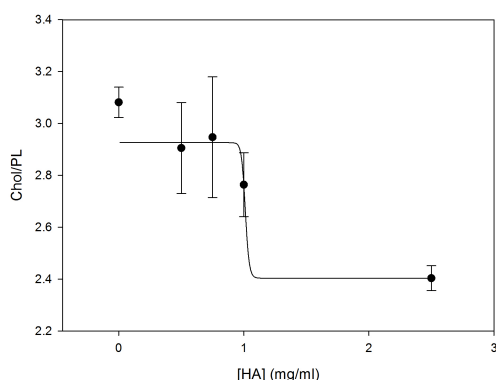


Figure 3.5: Cholesterol content intensity in surfactant complexes after exposure to different concentrations of HA. Decay of cholesterol proportion in surfactant membranes pelleted by centrifugation after pre-exposure to increasing concentrations of HA.

As previously shown by Lu et al., (2009) exposure to HA induces aggregation of surfactant preparations. As seen in figure 3.6, surfactant LUVs aggregate when HA is present in the subphase at a concentration higher than 1mg/ml. Again, the effect of HA on aggregation is appreciable only above the overlapping concentration, suggesting that the meshwork of HA may be directly responsible for the aggregation of surfactant complexes. This agree with the formation of a continuous surfactant free space observed by Lu et al., (2009), where the HA meshwork could be placed.

HA meshwork would then exclude surfactant from this space, inducing aggregation and possible compaction of surfactant in the HA free space.

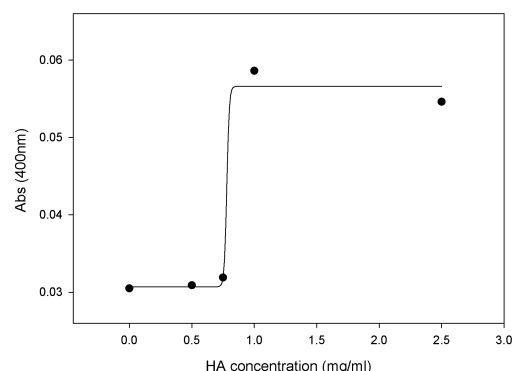


Figure 3.6: Aggregation of surfactant MLVs by HA. Absorbance at 400nm after 20 minutes of exposure to different concentrations of HA (mg/ml). Data are fitted to a sigmoidal curve.

If the structural and compositional changes induced by HA are non-reversible, removal of HA may still maintain the pre-activated state of surfactant, with a potentially better surface activity and higher resistant to inactivation. So we tested pre-activated surfactant by exposure to different HA concentrations on a Langmuir balance. Figure 3.7 shows that pre-exposure to HA at concentrations higher than 1mg/ml results in a significantly enhanced surfactant adsorption, even after removal of HA from the preparation. Thus it seems that depletion forces may act previously in the bulk solution, rather than at the interface. The meshwork nature and physical properties of HA together with the formation of HA may play an important role on the pre-activation of surfactant.

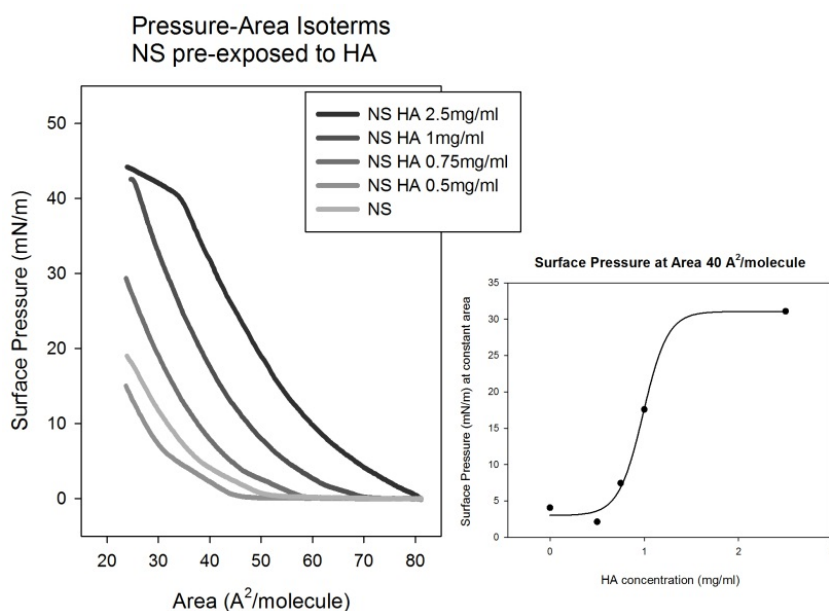


Figure 3.7: Compression isotherms of films formed by NS pre-exposed to HA. Left panel: compression isotherms of surfactant pre-activated upon exposure to increasing concentrations of HA, later removed by centrifugation. Right panel: surface pressure reached at a defined area (40Å²/molecule) in films formed by

equivalent amounts of surfactant, as a function of the concentration of HA at which surfactant was pre-exposed.

We have tested pre-activated surfactant against serum inhibition in the modified protocol on CBS, described in chapter 2. Figure 3.8 shows how serum inactivates surfactant as previously described, while pre-activated surfactant (HA-free preparation) is able to adsorb into an interface saturated of serum proteins. Pre-activated surfactant also shows a similar behavior to surfactant mixed with HA, concerning the restoring of the activity of surfactant even in the presence of a serum film. Pre-activated surfactant shows a normal decrease of surface tension not only during adsorption (both initial and post-expansion) but also during compression-expansion cycling (both step-wise slow Qstatic and continuous and fast dynamic regimes) leading to a full surfactant activity.

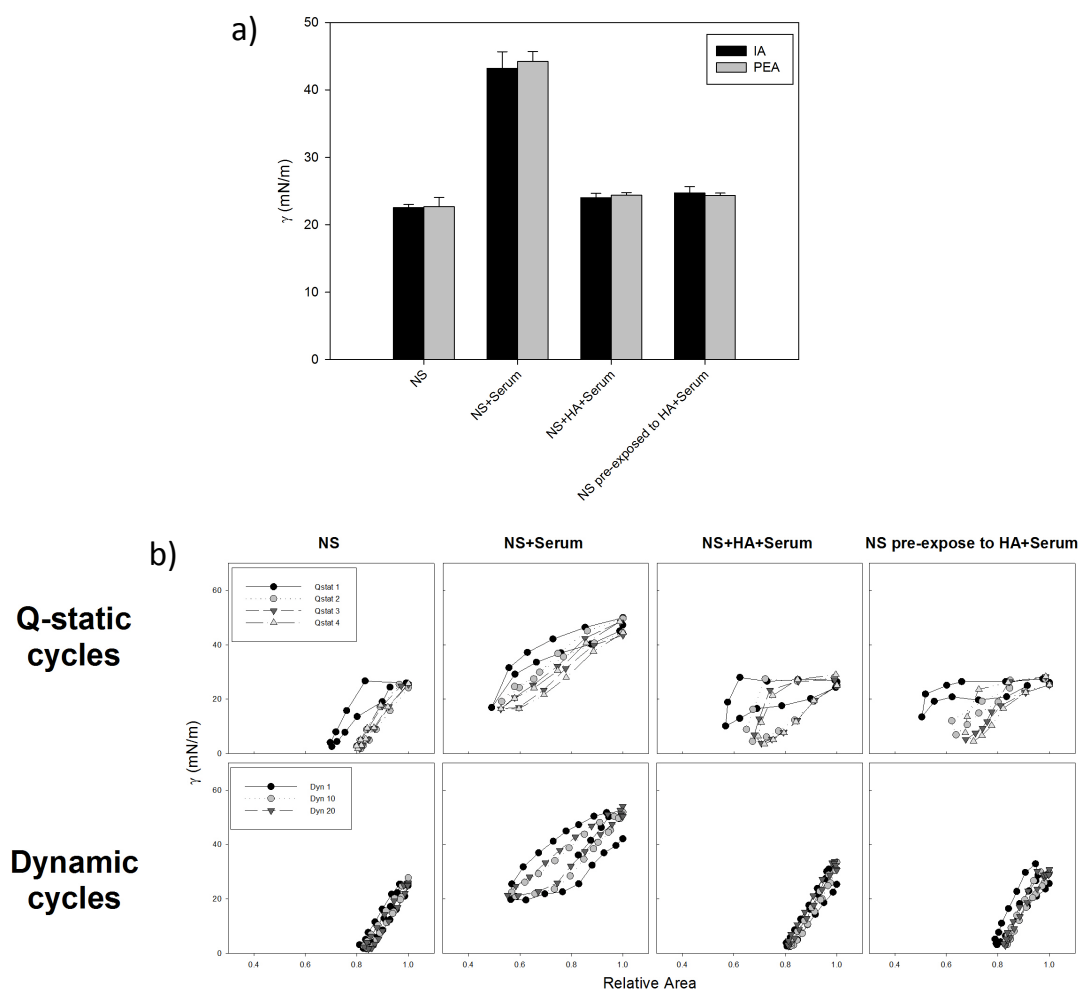


Figure 3.8: Captive bubble surfactometry of native surfactant with or without HA in the presence of serum. Panel A: surface tension after 5 minutes of initial (black bar) and post-expansion (grey bar) adsorption of native surfactant (NS) in the absence or presence of serum and native surfactant pre-exposed to or combined with HA (2.5mg/ml). Panel B: Qstatic (Top) and dynamic (Bottom) cycles.

DISCUSSION

Increasing resistance to inactivation of surfactant may lead to new surfactant preparations as part of improved therapeutic strategies for treatment of ARDS and MAS, where therapies of supplementation with exogenous surfactant are not working because the exogenous surfactant is getting inactivated the same way the endogenous surfactant is.

The effect of HA to reverse or prevent inactivation of surfactant has been explained so far by depletion or exclusion forces induced by HA on surfactant complexes. These physical forces have been proposed as able to push surfactant structures towards each other (aggregating surfactant complexes) and towards the interface even overcoming a steric barrier, such as the one formed by serum proteins when they occupy the interface. The displacement of serum proteins by surfactant complexes with the aid of HA would permit recovering surfactant activity at the interface (Taeusch et al. 2005; Zasadzinski et al. 2005). However, this theory does not entirely describe the processes undergoing surfactant reactivation. Specially, it is difficult to figure out how depletion forces could also promote the reactivation of surfactant impaired by different mechanism of inactivation such as the membrane-perturbing effect of molecules such as cholesterol. We propose that the effect of HA on reactivating surfactant should be mediated by reorganization of surfactant structure promoted by the integration of different entropic contributions exerted by HA, which ends in a pre-activated form of surfactant with better surface activity and the potential to overcome inactivation.

We have reported a lack of interaction between surfactant complexes and hyaluronan molecules, which supports the existence of exclusion or depletion forces induced by HA on surfactant structures. Theoretically, depletion forces act between two hard, non-interacting spheres (Taeusch et al. 2005; Zasadzinski et al. 2005), such in our system, surfactant and HA should be two non-interacting components. We observed the absence of interaction between surfactant and HA by QCM-D, where neither a decrease in frequency nor an increase in dissipation was observed when surfactant MLVs were exposed to a HA-grafted membrane. In the same direction compression isotherms in a Langmuir surface balance showed that HA is not occupying space at the interface, so it is effectively diluted away in the subphase.

As previously described by others (Lu et al. 2005b; Stenger and Zasadzinski 2007; Taeusch et al. 2008; Stenger et al. 2009b; Zasadzinski et al. 2010; Lu et al. 2011) the presence of HA enhances surfactant adsorption, that in our experiments can account for up to 100% of transfer of material to the interface, since the compression isotherm of a film of surfactant adsorbed in the presence of HA almost completely resembles that of a film formed by directly spreading of extracted surfactant in organic solvent. One could in principle assume that this adsorption is due to HA-promoted exclusion or depletion forces pushing surfactant towards the interface, as it has been previously proposed. We have observed aggregation of surfactant in the presence of HA, which would also fit into the depletion/exclusion theory. Exclusion forces also describes the exclusion of certain volume of solvent from other molecules (Laurent et al. 1996), increasing its local concentration as it may happen

when HA has an aggregating effect on surfactant. It is well known that surfactant concentration rather than total mass plays a key role on surfactant activity.

On the other hand, the effect of HA in the structure of surfactant membranes as observed in the GUVs experiment results, would agree with the results reported by Zasadzinski et al (2010), where they described that PEG may not enter the aqueous spaces between bilayers. The generation of a colloid osmotic pressure by the polymer between outside and inside of the vesicles would promote a flow of water to be expelled. The observed HA-promoted decrease in size of the GUVs may indicate that the difference in concentration of HA between inside and outside the vesicle is creating an osmotic pressure that may force water to get out of the vesicle. It has already been described that HA osmotic activity is non-ideal and increases exponentially with concentration (Fraser et al. 1997), mainly due to the polyelectrolyte nature of HA.

When cells are exposed to a hypertonic solution, water from inside the cell flows rapidly to the outer solution and cells would shrink and die. In the same way, the movement of water outside the vesicle, induced by the osmotic pressure of the outer polymers, may lead to the shrink or collapse of the vesicle, which may be further promoted by depletion forces. Under these osmotic stresses, regions of the membrane particularly dynamic, or prone to adopt a high curvature such as domains enriched in unsaturated species, could be expelled out of the vesicle, reducing the surface of the bilayer and thus, the volume. HA-promoted selective exclusion of unsaturated phospholipids has been confirmed by the loss of fluorescently labelled unsaturated PE added to surfactant MLVs. Selective exclusion of some components of surfactant may play a key role in restoring the activity of surfactant when a membrane-perturbing molecule is inactivating surfactant, something that can not be explained by the mere action of depletion forces.

Therefore it seems that there is a non-reversible HA-driven refining of the surfactant composition, similar to the one that supposedly happens during compression-expansion cycling of interfacial surfactant films, known as squeeze-out (Pérez-Gil and Keough 1998; Keating et al. 2012). The fact that these phenomena can only be observed above a threshold HA concentration (above the overlap concentration, approximately 1mg/ml) leads us to the conclusion that is the meshwork of HA the one responsible for the effect on surfactant. Thus, the osmotic pressure promoted HA would be responsible for the refining of surfactant aided by depletion forces originated by the large volumes of solution taken by the HA meshwork, once it reaches concentrations above the entanglement threshold.

As seen in by the increase of the absorbance at 400nm, surfactant LUVs become aggregated when HA is present in the bulk phase, again at concentrations above 1mg/ml. Therefore the aggregation of surfactant can be also correlated with the exclusion forces promoted by the meshwork of HA. Thus it seems that the physico-chemical properties of the meshwork are governing the entropic forces (exclusion/depletion forces and osmotic stress) asserted into the surfactant complexes when HA is present in the bulk phase. It remains to be elucidated whether HA-promoted transformation of surfactant complexes go beyond a mere compositional depuration, but also implies any type of phase transition favoured by

the particular composition of surfactant. It has been proposed that inverted H_{II} phase promotes interfacial surfactant adsorption (Perkins et al. 1996), and hydrophobic surfactant proteins favour highly curved lipid organizations such as cubic and H_{II} phases (Chavarha et al. 2010; Possmayer et al. 2010). Certain lipid systems enriched in PE and cholesterol under limited hydration conditions particularly adopts these non-lamellar phases. It is therefore conceivable that local dehydration promoted by HA may induce in surfactant membranes structural transitions toward non-lamellar phases especially at the local environments where surfactant proteins are distributed. Those lipid-protein assemblies could be responsible for the higher ability of pre-activated surfactant to transfer material to the interface. The fact that non-lamellar lipid organization could mimic the structure of possible transient states during fusion of membranes with the interfacial film would support this hypothesis. Complementary experiments applying X-ray scattering or phosphorous NMR to HA-pre-activated surfactant samples should provide important information to confirm the implication of possible non-lamellar phases in the ability of polymers like HA to promote surface activity.

As conclusion, we have clearly shown that a concentration of HA near to 1mg/ml is needed for the polymer to induce the structural reorganizations associated with the activation of surfactant, which correlates with the conditions required for the HA molecule to entangle and form a meshwork. This special configuration that HA adopts spontaneously would then be the responsible of the entropic contribution that HA asserts into surfactant in the bulk phase, both exclusion forces and osmotic pressure.

Moreover, it has been previously described that the addition of HA increases the viscosity of surfactant preparations (Lu et al. 2009), thus imposing a barrier to the *in vivo* application of HA-surfactant mixtures. Interestingly the viscosity of hyaluronan solutions above the entanglement point increases rapidly and exponentially with concentration, and elasticity of the system increases with increasing molecular weight (Laurent et al. 1996). This may be an insuperable problem, as viscous solutions may not spread properly once introduced into alveolar air spaces, making difficult for surfactant to reach the distal alveoli. Our results show that elimination of HA meshwork from the mixture does not revert the effect of the polymer enhancing surfactant adsorption into the interface. This means that although entropic forces may act on the bulk phase, once HA is eliminated surfactant aggregation and refining could be maintained bringing surfactant to a sort of “pre-activated” state. That would mean that HA might not have to be present within the surfactant preparations for their potential *in vivo* use. This would eliminate the viscosity problem and would permit production of highly active surfactant preparations for therapeutic application under challenging conditions such as those existing in an injured lung.

Finally we have shown that HA pre-activated surfactant is able to cross the steric barrier imposed by a serum film adsorbed at the interface of an air bubble in the captive bubble surfactometer, confirming the enhanced resistance to inactivation of the pre-activated surfactant. Pre-activation of surfactant with HA not only gives surfactant the ability to cross those inactivating steric barriers, but also restores

surfactant activity during compression-expansion cycling, resulting in a complete functional surfactant even in the presence of a inactivating amount of serum.

For further development of inactivation resistant surfactants still requires assessing the capability of this pre-activated surfactant *in vivo*, looking for a better outcome of the respiratory pathologies compared with common clinical surfactants currently in use.

GENERAL DISCUSSION PART 1

GENERAL DISCUSSION PART 1

We studied surfactant inactivation as one of the common causes of respiratory distress. Surfactant inactivation *in vivo* is mainly caused by the infiltration of substances into the lung. Two different mechanisms of inactivation have already been described (Zuo et al. 2008). On the one hand, surfactant inactivation by surface-active components, such as albumin in serum, leads to competition for the interface. Membrane-perturbing substances such as cholesterol and meconium may reach the air-water interface in pathological conditions. It has been already described that in ARDS, serum infiltration into the lungs also carried increasing amounts of cholesterol, and in MAS meconium is aspirated by the baby together with the amniotic fluid. Thus these substances can be mixed with surfactant membranes, rendering them non-functional.

Traditionally cholesterol inhibition has been studied by adding cholesterol in organic solvent into extracted surfactant, also in organic solvents. It has been described that at least 20% of cholesterol (w/w, phospholipid/cholesterol) is needed to observe dysfunction of surfactant phospholipids (Gunasekara et al. 2005; Leonenko et al. 2007; Zuo et al. 2008; Vockeroth et al. 2010). However, cholesterol in organic solvent is not physiologically relevant, as cholesterol in the organism is solubilized in water. Bile salts are detergents derived from the cholesterol metabolism, in fact transformation of cholesterol to bile salts in the gallbladder is a mechanism of the body to eliminate excess of cholesterol, as the enzymes regulating bile acids synthesis is up-regulated by cholesterol. The main function of bile acids is to solubilize dietary fat, so it forms micelles that can solubilize lipids and cholesterol. Mixing bile acids and cholesterol seems to provide a more physiologically relevant model to study cholesterol inactivation of surfactant. This could be the reason why we only need 4% cholesterol (w/w) to observe a significant lost in surfactant activity. Moreover, we observed changes in surfactant phospholipid domain shape and size in the presence of meconium, at such a low concentration of cholesterol solubilized by bile salts. Most probably, the harmful potential of the soluble cholesterol resides in the ability of inserting into surfactant membranes changing the domain coexistence. When cholesterol and surfactant are mixed together in organic solvent, reconstitution processes may lead to a homogeneous distribution of cholesterol or exclusion to phases where the perturbation effect is minimized. In water solution cholesterol most probably would insert into disordered phases changing them to liquid-disordered or ordered phases with different properties and decreased compressibility. In addition, cholesterol coupled with methyl- β -cyclodextrine (M β CD) is another novel way to insert cholesterol into surfactant membranes, as it has traditionally been made for cell membranes. So far, M β CD has been used in the surfactant field to take out the excess of cholesterol from surfactant membranes (Gunasekara et al. 2010), confirming though the possible reactivating effect of cyclodextrine., but never to insert it. We have checked that the use of cholesterol solubilized with M β CD provides a standard technique to study inactivation of surfactant under more physiologically relevant conditions.

Many people has already tried to develop a methodology to study in a systematically manner stable inactivation of surfactant by many different substances. We propose the optimization of the CBS protocol according to the inactivating mechanism of

each of the most physiologically relevant inactivating agents. In this way, we let surfactant compete with serum (following the surface-active competition for the interface inactivation mechanism) and allow the incorporation of cholesterol from meconium (following the mechanism of membrane-perturbing molecules). Our new methodology provides us with a powerful technique to systematically study surfactant inactivation of different samples and surfactant preparations. Moreover, this protocol opens the possibility to study the inactivation susceptibility of different surfactant preparations such as different commercially available surfactants. But also, we can study in a standardized way the addition of substances to enhance surfactant resistance to inactivation, as the addition of polymers.

Finally we have shown that addition of HA to surfactant leads to structural, compositional and functional changes, explained through the effect of entropic forces. Traditionally, reactivation of surfactant has been explained by depletion forces when surfactant should compete for the interface with surface active proteins. But this mechanism does not entirely explain reactivation process in the presence of cholesterol or membrane perturbing molecules. Changes in osmotic forces due to the presence of HA in the bulk phase would complete the understanding of the reactivation mechanism. Changes in osmotic pressure seem to be responsible of the change in composition of surfactant resulting in enrichment in saturated phospholipid species. This refining of the composition is comparable to that occurring during compression of the interfacial film, termed squeeze-out (Pérez-Gil and Keough 1998; Keating et al. 2012). This compression-driven squeeze out results in the segregation of unsaturated phospholipid species out of the interfacial monolayer. The addition of HA to the bulk phase seems to resemble the segregation of unsaturated phospholipid species out of the surfactant bilayers and complexes, in a process of HA-driven squeeze out. It has also been proposed that changes in osmotic pressure would drive surfactant complexes to a higher packing states (Chavarha et al. 2010) that could be more resistant to inactivation. Whether surfactant treated with HA has a different structure, rather than lamellar, has still to be determined. We have also confirmed that the presence of HA is not essential for reactivation of surfactant, thus changes in structure and composition seem to be non-reversible, avoiding the increment on viscosity due to the presence of polymer. We proposed an incubation step as potential production step of clinical surfactants that may lead to a more resistant clinical surfactant that may not fail on the treatment of pathologies such as MAS and ARDS. Whether clinical surfactants may undergo the same changes in structure and composition should still be determined, taking into account that these surfactant preparations come from organic extracted surfactants with different structural and compositional properties. Further studies should confirm the potential use of the pre-activation of surfactant in animal model of lung injury that simulates the pathological conditions of ARDS or MAS.

FROM BIOPHYSICS TO CLINICS

FROM BIOPHYSICS TO CLINICS

The main objective of the second part of this Thesis is to study the biophysical properties of surfactant from clinically relevant samples. We have already described the molecular basis and developed *in vitro* models to study biophysical effect of inactivation of surfactant by several agents. In this chapter we want to characterize and describe the biophysical behaviour of surfactant inactivated *in vivo*, meaning surfactant coming from patients or animal models with respiratory dysfunctions potentially affecting pulmonary surfactant performance. The analysis of samples from patients allows highlighting the importance of surfactant function in the development and outcome of respiratory pathologies like ARDS. Samples from patients are of high interest but very limited in number and amount and optimization of protocols is required in order to carry out a complete biophysical study. On the other hand, samples from animal models should allow carry out a complete molecular, cellular and biophysical study. Thus we can also study the implication of surfactant function in the development of lung diseases such as IPF.

Both IPF and ARDS are pathologies where high surface tension, due to surfactant dysfunction, seems to play an important role in their development and outcome. In ARDS high surface tension may lead to alveolar collapse resulting in lower pulmonary compliance, while in IPF it has been described that high surface tension may lead to type II cell injury.

In chapter 4 we have analysed the function of surfactant from paediatric ARDS patients and controls. For the first time, this study has analysed the behaviour of individual samples in a captive bubble surfactometer. Following the CBS protocol developed in chapter 2 and optimizing the isolation of surfactant from limiting samples, we have been able to study each patient and control individually. The availability of clinical data from each patient has allowed us to correlate surfactant dysfunction with physiological parameters such as lung compliance and oxygenation index, and clinical indexes like Murray's score and PRISM, typical scores for ARDS outcome. Thus, a direct correlation of biophysical and clinical parameters has been pursued in order to highlight the implication of surfactant function in ARDS.

In the last chapter of this Thesis, we describe a Napsin A knock-out mouse model. Animal models allow the detailed study of molecular and cellular processes in parallel to the characterization of the biophysical properties of surfactant. The main aim of studying this animal model was to describe its potential use as a model for IPF. The observation that IPF patients have a reduced amount of Napsin A, lead us to the hypothesis that a KO model for this enzyme could in principle resemble IPF conditions. Napsin A is a key enzyme in the pathway of SP-B processing, and IPF patients show deficiency in SP-B, which is essential for surfactant function. Surfactant dysfunction leads to high surface tension at the alveolar surface that, together with intracellular accumulation of precursors forms of SP-B, would produce type II cell injury, resulting in activation of fibrotic tissue formation. Studying the protein composition of surfactant and type II cells, together with lung morphology and the biophysical function of surfactant, we should be able to get a deep insight into the development of fibrotic processes and IPF outcome.

**BIOPHYSICAL CHARACTERIZATION OF SURFACTANT FROM PAEDIATRIC ARDS
PATIENTS. CORRELATING BIOPHYSICAL AND CLINICAL PARAMETERS**

This work has been done in collaboration with MD Daniele de Luca (University Hospital “A.Gemelli”, Catholic University of the Sacred Heart)



BIOPHYSICAL CHARACTERIZATION OF SURFACTANT FROM PAEDIATRIC ARDS PATIENTS. CORRELATING BIOPHYSICAL AND CLINICAL PARAMETERS

INTRODUCTION

Acute respiratory distress syndrome (ARDS) is a life threatening respiratory failure due to lung injury from a variety of sources. It was first described by Ashbaugh et al in 1967. ARDS and ALI (milder form of acute lung injury) are a spectrum of lung diseases characterised by a severe inflammatory process causing diffuse alveolar damage and resulting in ventilation perfusion mismatch, severe hypoxemia and poor lung compliance (Dushianthan et al. 2011). The estimated incidence of ARDS in the USA (by 2005) is around 58/100000 person years (Rubenfeld et al. 2005) and in Europe the range varies from 4.2-13.5/100000 person years (Webster et al. 1988; Luhr et al. 1999). Mortality for ARDS is between 36-44% (Phua et al. 2009). Patients with ARDS frequently have multi-organ failure, and the majority of patients die of sepsis syndrome with multi-organ failure rather than respiratory failure (Montgomery et al. 1985). The different potential causes leading to ARDS are summarized in the next table.

| Direct lung injury | Indirect lung injury |
|---|--|
| Common Causes | Common Causes |
| Pneumonia | Sepsis |
| Aspiration of gastric contents | Severe trauma with shock and multiple transfusions |
| Less common causes | Less common causes |
| Pulmonary contusion | Cardiopulmonary bypass |
| Fat emboli | Drug overdose |
| Near drowning | Acute pancreatitis |
| Inhalational injury | Transfusion of blood products |
| Reperfusion pulmonary oedema after transplantation or pulmonary embolectomy | |

(Dushianthan et al. 2011)

ARDS is characterised by an overwhelming inflammatory process leading to alveolar and vascular injury in the lung. During the initial acute phase there is alveolar flooding with protein-rich fluid due to increased vascular permeability. Alveolar injury of type I cells contributes to the pulmonary oedema and the breakdown of this epithelial barrier (Dushianthan et al. 2011). The acute phase is followed by a fibroproliferative phase with fibrosis, neovascularisation and later resolution (Gattinoni et al. 1994). Vascular injury and remodelling may lead to pulmonary arterial hypertension, which may compromise right ventricular function, exacerbating hypoxemia and leading to a poor clinical outcome (Ware and Matthay 2000).

The treatment of ARDS involves general supportive measures, necessary for all critically ill patients, combined with focused ventilator strategies and appropriate treatment of underlying conditions. In addition, intrabronchial surfactant administration was shown to be beneficial in different ARDS models. Impaired surfactant function may therefore play a role in the development of gas exchange abnormalities in clinical ARDS (Markart et al. 2007). So far, clinical trials involving surfactant supplementation in ARDS have shown that exogenous surfactants, especially synthetic ones (Exosurf, Surfaxin, Venticute) do not show any improvement in the clinical outcome (Anzueto et al. 1996; Walmrath et al. 1996; Wiswell et al. 1999). However, natural surfactants (Curosurf, Alveofact, Survanta and Infasurf), from animal source, have shown to improve some of the clinical parameters (Gregory et al. 1997; Willson et al. 2005). Therefore, improving resistance to inactivation of natural surfactants (as seen in chapter 3 of this Thesis) may be a potential therapeutic strategy for the future (Taeusch 2000).

ARDS has been previously related to surfactant dysfunction (Taeusch 2000; Dushianthan et al. 2011). Leakage of plasma proteins into the alveolar air spaces because of impaired function of the air-blood barrier is a very early event in the pathogenesis of ARDS and may substantially contribute to surfactant alteration and dysfunction in ARDS (Günther et al. 2001).

Following Laplace's law ($\Delta P=2\gamma/R$, where P is the pressure, γ is the surface tension and R is the radius) two interconnected alveoli of different radius with the same surface tension cannot coexist at a given pressure. The pressure in the smaller alveolus would tend to collapse into the larger one. By decreasing surface tension at variable extent as a function of the size of the alveoli surfactant plays a major role in the stability of the lung (Parmigiani and Solari 2003). Concomitantly, loss of surface activity leading to an increased alveolar surface tension is assumed to cause alveolar instability and atelectasis. Therefore an increase in surface tension should result in a marked decrease of lung compliance (Günther et al., 2001).

It has been previously proposed that the molecular mechanism by which surfactant is inactivated during ARDS is multifactorial and mainly relies on the fluid leaked into the alveolar spaces. On the one hand it has been commonly described that leaked serum proteins form a protein steric barrier at the interface, so that surfactant cannot reach the interface and lower down surface tension. Particularly, surface-active proteins such as albumin may occupy the alveolar air spaces, displacing surfactant from the interface (Taeusch et al. 2005; Zasadzinski et al. 2005). On the other hand, inflammatory proteins such as C-reactive protein (CRP) and other soluble proteins, may have a direct effect on inactivating surfactant function. It has already been shown that CRP is able to bind PC and reduce surfactant adsorption into the air-water interface (Li et al. 1989; McEachren and Keough 1995; Casals et al. 1998). It was recently described that the deleterious effect of CRP on surfactant function includes fluidification of surfactant membranes (Sáenz et al. 2010). In addition, other proteins such as fibrinogen or fibrin monomers may also interact with surfactant. It has already been demonstrated that polymerizing fibrin leads to a loss of surfactant phospholipids (Günther et al. 1999c) and specific proteins (Günther et al. 1995). Moreover, it has also been observed an increase amount of phospholipases, especially PLA2, in BAL from ARDS patients (De Luca et al. 2008; De

Luca et al. 2009). Lipolytic activity may lead to increasing amounts of lysophospholipids (specially lyso-PC), and an increasing the amount of free fatty acids, therefore resulting in an altered surfactant composition that may cause a further impairment in surfactant function.

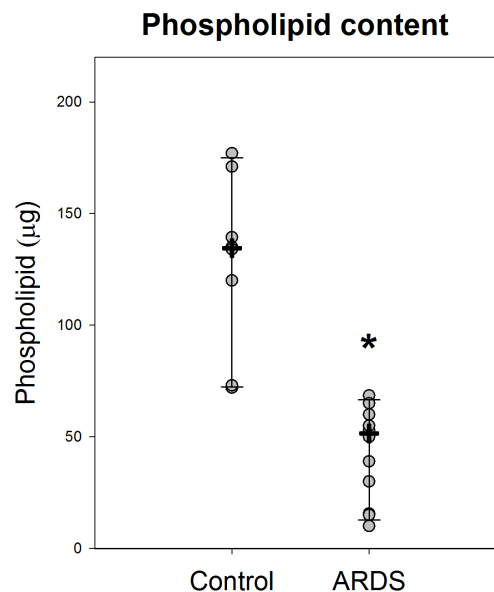
The occurrence of altered surfactant composition associated with ARDS has already been studied. Changes in both phospholipids (Hallman et al. 1982; Pison et al. 1989; Gregory et al. 1991; Günther et al. 1996) as well as in proteins (Pison et al. 1989; Gregory et al. 1991; Günther et al. 1996; Greene et al. 1999) were observed. In general it has been reported that ARDS progress courses with a decrease in DPPC and PC content, together with PG, while PI, PE and SM were increased in ARDS patients. In addition a marked reduction of surfactant proteins SP-A, SP-B and SP-C have been detected. On the other hand ARDS patients show a decrease proportion the most surface active aggregates (LA) in surfactant, while at the same time this LA fraction contains an increased amount of neutral lipids. In addition, increased amounts of cholesterol in surfactant from ARDS patients have also been observed (Markart et al. 2007). Changes in cholesterol content of surfactant cause severe surfactant dysfunction, but the mechanism regulating cholesterol content in surfactant is still not well known. It has been proposed that the membrane perturbing effects of cholesterol in surfactant membranes are the origin of cholesterol promoted surfactant inactivation, as seen in the chapter 1 of this Thesis (Gunasekara et al. 2010; Lopez-Rodriguez et al. 2011).

The aim of the work described in the present chapter is to biophysically characterize surfactant samples from ARDS paediatric patients. For this purpose we have optimized protocols for studying individual samples in captive bubble surfactometer. In addition we have correlated interfacial behaviour of surfactant with clinical parameters and outcome of each ARDS patients. Individual clinical data were available from these patients, and we have chosen oxygenation index and compliance as representative of lung function, as well as the Murray's score and PRISM, as representative for clinical outcome of the syndrome, to correlate with surfactant function. This combined analysis highlights the importance of surfactant activity in the development and outcome of ARDS.

RESULTS

For a complete biophysical study we should first analyse the phospholipid content in the isolated surfactant samples from the same BAL volume. Figure 4.1 illustrates that samples from ARDS group contains significantly less phospholipids than samples from the control group. Apart of the potential dilution of surfactant that could be expected due to the leakage of fluid in to the injured alveolar air spaces of ARDS patients, the reduction of total phospholipid content may also indicate reduced secretion, increased catabolism and clearance or both.

Figure 4.1: Phospholipid total content in pelleted BAL from patients and controls. Total mass (μg) of phospholipids in pelleted BAL from each sample (grey circles). Medians are represented as black cross and the upper and lower hinges are the 5th and 95th percentiles of the group as T-bars. *statistically significant T-test ($p < 0.001$)



As some of the ARDS samples had less than $50\mu\text{g}$ of total phospholipids, we were not able to study all of them in the CBS. CBS experiments were all carried out at the same surfactant phospholipid concentration (10mg/ml), thus only samples with more than $50\mu\text{g}$ were used. ARDS samples could also be divided into two different types of ARDS whether ARDS is originated directly in the lung (caused by pneumonia, bronchiolitis or thoracic trauma) or not, indirect (systemic sepsis, flu or other causes). Most of the ARDS direct causes did not have enough material for CBS studies.

Figure 4.2 shows an example of the most relevant results we can obtain from CBS experiments. No differences were observed in initial adsorption (IA) of ARDS direct or indirect and control samples but the kinetics of adsorption during post-expansion (PEA) reveal that minimal surface tension reached by surfactant from ARDS patients are significantly higher surface tension than that reached by surfactant from control samples (see figure 4.3). Quasi-static and dynamic cycling show the same behaviour in control and ARDS samples. Compression-expansion of the samples shows that none of the samples, either from ARDS or control patients, are able to reach surface tension lower than approx. 20mN/m , although ARDS samples do not even reach minimal surface tension under 30mN/m . In addition all the samples may need more than 50% of area reduction to reach minimum surface tension.

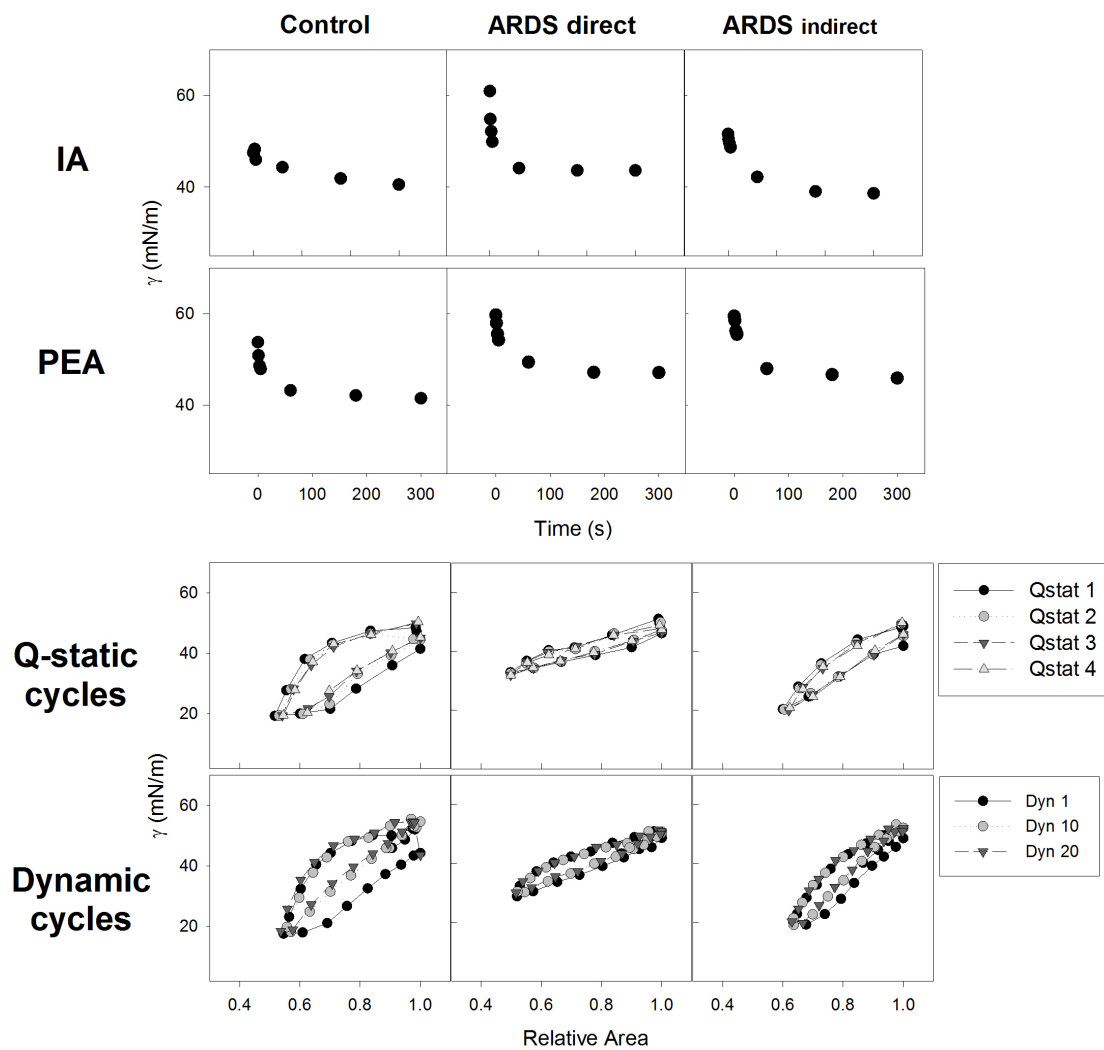


Figure 4.2: Captive bubble surfactometry of surfactant samples from ARDS and control patients. Top: example of initial (IA) and post-expansion (PEA) adsorption kinetics for an ARDS direct and indirect and a control sample. Bottom: example of q-static and dynamic cycles for surfactant from one control and one ARDS direct and indirect patient (C).

A summary of all the data from CBS experiments is shown in figures 4.3 to 4.5. Each dot in the different plots results from the average of three CBS experiments of each sample. As seen in figure 4.3 (left panel) minimal surface tension reached after 5 minutes of initial adsorption (IA) do not show significant differences between control and ARDS samples. Surprisingly, equilibrium surface tension reached by both control and ARDS samples after IA resulted higher than expected (over 40mN/m). Similarly, minimal surface tension after 5 minutes of PEA reaches relatively very high equilibrium surface tension (over 40mN/m). Surface tension reached by samples from ARDS group was significantly higher than that reached by samples from the control group.

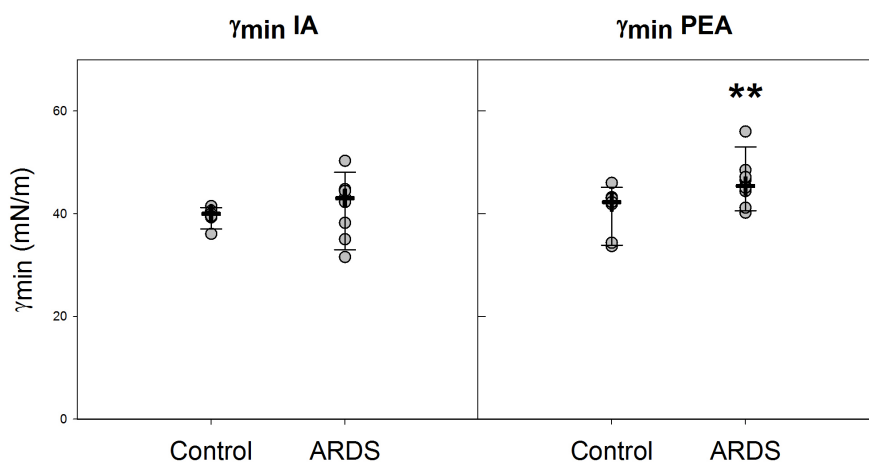


Figure 4.3: Minimum surface tension reached after 5 minutes of initial adsorption (left panel) or 5 minutes of post-expansion adsorption (right panel). Averaged surface tension from each patient sample is represented as a grey circle. Medians are represented as black cross and the upper and lower hinges are the 5th and 95th percentiles of the group as T-bars. **statistically significant T-test ($p < 0.05$).

Figure 4.4 shows a summary of the most important parameters defining quasi-static compression-expansion isotherms of films formed by samples from control and ARDS patients. We have analysed minimal and maximal surface tension as well as the proportion of area compression to reach minimum surface tension. Results show that during compression-expansion cycling the minimum surface tension reached by the sample from control patients is around 20 mN/m, while the median of minimal surface tension reached by samples from ARDS group is significantly higher. No differences were found in the maximum surface tension or in the reduction of area required to reach minimal tension.

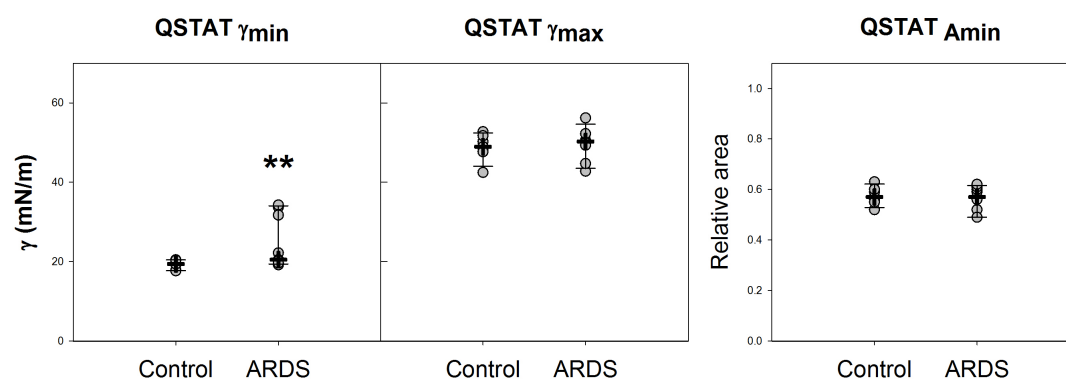


Figure 4.4: Quasi-static cycling of surfactant from control and ARDS patients. Minimum surface tension (left panel), maximum surface tension (middle panel) and relative area compression required to reach minimal surface tension (right panel) after 4 q-static compression-expansion cycles. Averaged values from each patient sample are represented as grey circles. Medians are represented as black cross and

the upper and lower hinges are the 5th and 95th percentiles of the group as T-bars. **statistically significant Rank Sum Test ($p < 0.05$).

Similarly, parameters defining dynamic cycles (at physiologically relevant compression-expansion rates, 20 cycles/min) show no differences between groups in maximum surface tension and relative area compression. Again, minimum surface tension reached by samples from ARDS group was significantly higher than that reached by control samples.

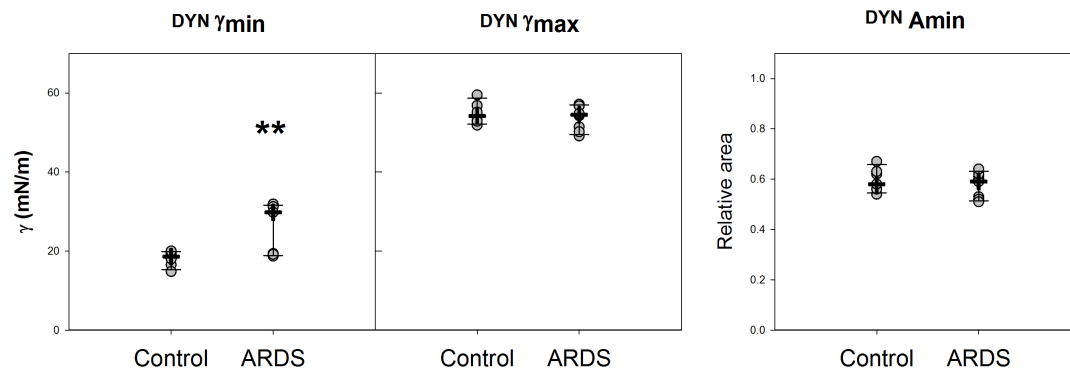


Figure 4.5: Dynamic cycling of surfactant from control and ARDS patients. Minimum surface tension (left panel), maximum surface tension (middle panel) and relative area compression required to reach minimal surface tension (right panel) after 20 dynamic cycles. Averaged values from each patient sample are represented as grey circles. Medians are represented as black cross and the upper and lower hinges are the 5th and 95th percentiles of the group as T-bars. **statistically significant Rank Sum Test ($p < 0.05$).

So far, biophysical results themselves suggest that, as expected, surface tension produced by surfactant from ARDS patients is higher than the value reached by surfactant from control patients. On the other hand, whole set of clinical data was available for each of the patients whose surfactant was analysed in CBS. Then we have tried to correlate biophysical parameter defining surfactant performance with clinical parameters and outcome. Figure 4.6, shows for instance that there is a significant correlation between minimum surface tension and some clinical parameters, that depends on the proper performance of the lung function. In addition, even though correlations were made with the whole set of data, we could distinguish three different group of patients characterized by their clinical data and surface tension of their surfactant.

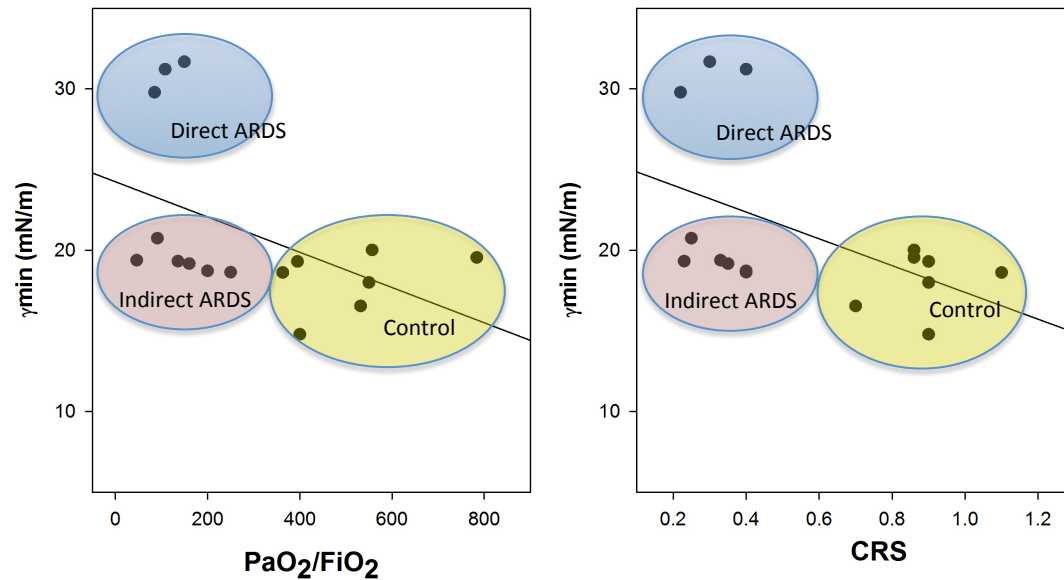


Figure 4.6: Correlation of minimum surface tension after 20 dynamic cycles with clinical parameters. Left panel: correlation of tension with PaO_2/FiO_2 (spearman correlation coefficient = -0.506 , $p < 0.05$). Right panel: correlation of tension with compliance of the respiratory system (CRS) (spearman correlation coefficient = -0.605 , $p < 0.05$). Patients are grouped in direct ARDS (blue), indirect ARDS (pink) and control (yellow).

On the one hand PaO_2/FiO_2 values represent the oxygenation index that corresponds to ratio of partial pressure of arterial O_2 with respect the fraction of inspired O_2 as measured bedside in the patient. Normal values of PaO_2/FiO_2 are considered between 300-500. Values lower than 200 are considered as indicative of ARDS. On the other hand CRS is the compliance of the respiratory system, expressed as the compliance of the lung (pressure applied to a volume of air to inflate the lung) per kilo body weight of the patient. Normal values of CRS are between 0.9 and 1ml/cmH₂O/kg. Both parameters depend greatly on the proper performance of the lung. Efficiently compressing and re-expanding the lung during the breathing cycle would lead to normal compliance values and therefore a proper gas exchange, resulting in normal arterial oxygenation. Both parameters show a negative correlation with minimal surface tension produced by surfactant, demonstrating that reduced values of PaO_2/FiO_2 and CRS correlate with higher surface tension in ARDS patients.

Further analysis of clinical scores with respect to surface tension highlight the importance of surfactant function in the development and outcome of the pathology. Murray score and PRISM were then correlated to minimal surface tension values reached by each respective patient. Murray score or Lung Injury Score (LIS) is designed to characterize the presence and extent of pulmonary damage. This score has been used in fact for the diagnosis of ARDS, when the score is higher than 2.5. Figure 4.7 shows that there is a positive significant correlation between minimal surface tension and the extent of lung damage. In the same direction, PRISM

(Paediatric Risk of Mortality) and surface tension show also a positive significant correlation, meaning that there is a significantly higher mortality risk when the minimal surface tension reached by surfactant is higher.

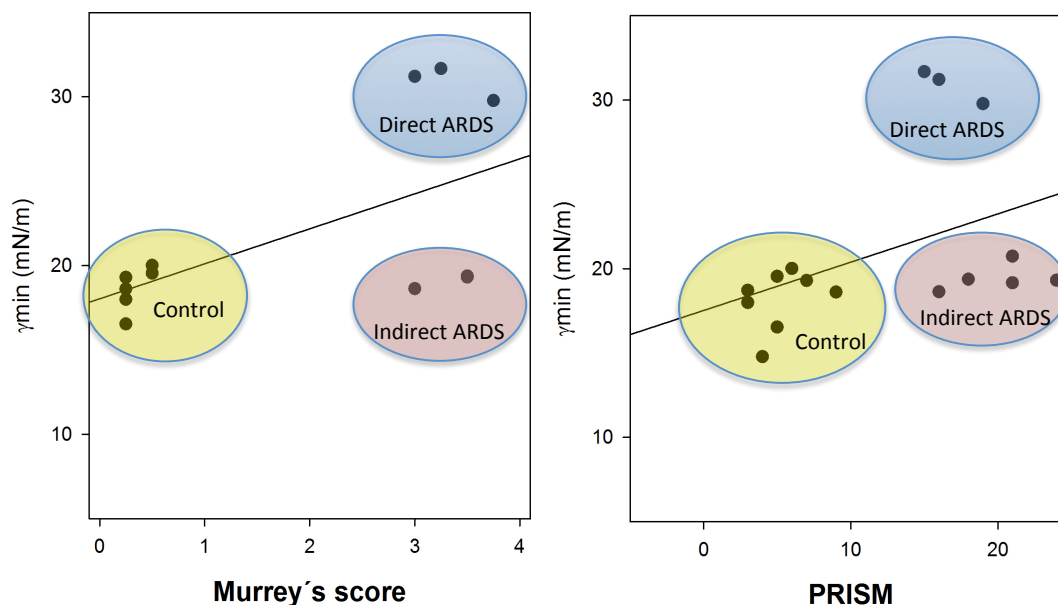


Figure 4.7: Correlation of minimum surface tension after 20 dynamic cycles with clinical outcome. Left panel: correlation of minimal tension with Murrey's score (spearman correlation coefficient = 0.605, $p < 0.05$). Right panel: correlation of tension with PRISM (spearman correlation coefficient = 0.499, $p < 0.05$). Patients are grouped in direct ARDS (blue), indirect ARDS (pink) and control (yellow).

DISCUSSION

In this study we have analysed the functional properties of surfactant from ARDS and control patients. Particularly we have accomplished the study of surfactant from individual paediatric patients in a captive bubble surfactometer (CBS), something that to our knowledge was never done before. Samples have been characterized as isolated from bronchoalveolar lavage (BAL) without being subjected to organic extraction, as common practice when clinical surfactant samples have been studied before (Lewis et al. 1990; Veldhuizen et al. 1995). The aim of such procedure is to isolate the hydrophobic fraction of the BAL, including surfactant phospholipids together with SP-B and SP-C, and so eliminating soluble components. This procedure would in our opinion not only perturb the structure of the native surfactant samples as obtained from the samples but also potentially remove the most polar components either favourable (SP-A) or unfavourable (inhibitors) to surfactant function. Therefore, we decided not to perform organic and so estimating the functional properties of full surfactant complexes as they were acting at the alveolar spaces of the different patients. We have centrifuged BAL at 100.000xg, which renders total surfactant including large (LA) and small (SA) aggregates. In many studies a centrifugation at 48000xg is preferred to collect preferentially the LA

fraction of surfactant, with the highest surface activity, eliminating the less surface active fraction of (SA) in the supernatant (Gregory et al. 1991; Günther et al. 1999b). We chose to collect both LA and SA by centrifuging at higher speed, because the conversion from LA to SA has been reported to be impaired in ARDS patients (Günther et al. 1999b; Günther et al. 2001), and the reduced fraction of LA may have an important impact in surface activity. Total phospholipid content in samples was, as expected, lower in surfactant from ARDS patients than in control samples. It has already been described that surfactant in ARDS suffers dilution as a consequence of the leakage of fluid into the alveolar air spaces (Günther et al. 1999b; Schmidt et al. 2001). Furthermore, reduced amounts of surfactant in alveolar spaces of injured lungs have been related to a reduced synthesis and secretion by the damaged epithelium and an exacerbated catabolism by lipases and proteases liberated to the airspaces (Leaver and Evans 2007). In our protocol, however, all the CBS experiments were carried out at the same phospholipid concentration, and so differences between samples may rely on quality and composition of surfactant rather than in concentration.

Surfactant performance was then analysed in a captive bubble surfactometer, where we can analyse surfactant activity in terms of adsorption into the interface and efficient packing and re-extension of the interfacial material during dynamic compression-expansion of the surface (Schürch et al. 1989; Schoel et al. 1994; Schürch et al. 1998). Firstly, a significant reduced amount of surfactant phospholipids may lead to higher equilibrium surface tension *in vivo*. An interfacial film reaches the minimal equilibrium surface tension when there are enough surfactant molecules to completely occupy the interface, compensating in this way the attractive force of the water molecules at the interface. In the CBS experiments, we observed that the minimum surface tension reached by surfactant from ARDS patients is higher than the tension reached by surfactant from control patients. As explained above, these experiments compare samples at identical phospholipid concentration, indicating that the difference in adsorption is due to an impaired capacity of surfactant from ARDS patients to transfer enough surface active molecules in to the interface.

Surprisingly, control samples did not reach equilibrium surface tension near 23mN/m, value that has been described as the equilibrium surface tension of a good surfactant. We hypothesize that such a relatively high minimal surface tension may be due to the limited concentration of surfactant assessed. The physiological concentrations of surfactant in the airways has been estimated in the order of 100mg/ml phospholipid and we have reported that optimal CBS tests can be carried out injecting surfactant at 25mg/ml (Schürch et al. 2010; Blanco et al. 2012). Functional tests of surfactant at 10mg/ml are close to limiting conditions and therefore, very sensitive to the functional capacities of the material (see chapter 3). Samples from control patients, as detailed in the Materials and Methods section, come from patients that were intubated and mechanically ventilated for reasons different from lung injury or respiratory failure, most of them being paediatric patients that underwent general anaesthesia for surgery. It has already been described that mechanical ventilation impairs surfactant activity, in many cases as a consequence of alteration in altering surfactant composition (Vockeroth et al. 2010). It has already been reported that mechanical ventilation results in an increased

proportion of cholesterol within surfactant membranes. The fluidifying effect of cholesterol may be the main responsible for the impairment of surfactant function. And as shown in Dan Vockeroth et al., (2009), surfactant obtained from animal models subjected to mechanical ventilation produces increased equilibrium surface tension. Even though surfactant availability from these control patients did not allow to carry out a compositional study, we can hypothesize that higher equilibrium surface tension of surfactant from ventilated patients might be due at least in part to changes in the optimal surfactant composition due to mechanical ventilation. Although such altered surfactant could be still functional in the patients, it may already show signs of partial inactivation under the limiting conditions imposed by our test. Whether mechanical ventilation imposes a pathological effect contributing to ARDS or other pathologies should still be determined.

Interestingly, differences in adsorption between ARDS and control patients showed somehow amplified under the enlarged in post-expansion adsorption (PEA) regime. PEA kinetics evaluate to what extent the efficient re-organization of interfacial material in an expanding surface results in a drop in surface tension to the equilibrium. Even though we cannot infer any mechanistic origin for the alteration in the interfacial adsorption (IA), PEA seems to indicate a deficient activity of surfactant from ARDS patients as a consequence of inactivation, possibly due to an altered composition. In addition, early collapse of the films during compression-expansion of the interface also supports the hypothesis of a deteriorated surfactant composition. Higher minimum surface tension even after an area compression of more than 50 %, seems to indicate failure in properly re-organizing the material in a cycling interface. It has already been described that ARDS causes significant changes in surfactant composition, including an increase in the proportion of unsaturated phospholipids and neutral lipids that clearly alters surfactant biophysical activity (Markart et al. 2007). Whether the mechanism for inactivation is due to changes in phospholipid profile and/or protein profile, to membrane-perturbing effects due to cholesterol or CRP, to an altered conversion from LA to SA or to a combination of all these contribution needs to be clarified. In comparison with chapter 2, it seems that inactivation of surfactant in ARDS is a multifactorial process with impaired adsorption, as in serum inactivation, and early collapse of the film during compression, as in cholesterol inactivation. Although alteration on the composition of surfactant may also contribute to inactivation.

The occurrence of abnormally high surface tension *in vivo* has been widely described as a pathogenic factor, not only in ARDS but also in other lung diseases. Instability of lungs leads to reduced compliance but also triggers injury at the pulmonary epithelium. Surfactant would therefore play a key role to sustain a proper function and morphology in a healthy lung. Captive bubble surfactometry was developed to simulate the dynamic of the air-water interface at the alveolus by means of the compression and expansion of an air bubble. Specially, dynamic cycles were set at a ratio of 20 compression-expansion cycles/min to resemble normal breathing rate in humans. CBS allows then following surface tension not only during adsorption processes, but also during compression-expansion dynamics. The study of surfactant from patients in the CBS provides then information about the surface tension each of the materials are able to reach in an air-water interface subjected to dynamics that

simulate breathing constrains. Apart from BAL samples, Daniele De Luca MD kindly allowed us to analyse clinical data obtained bedside from each of the patients.

Statistically significant correlations were obtained between parameters defining the functional properties of surfactant from patients and different clinical parameters that are frequently used in clinics as indicators of proper lung performance. Firstly, the index of arterial oxygenation ($\text{PaO}_2/\text{FiO}_2$) is a measure of gas-exchange efficiency. This is the ratio of partial pressure of arterial O_2 to the fraction of inspired O_2 . Therefore it is the ratio of inspired oxygen through the lungs that reaches the blood torrent. Normal values for this index are between 300-500, and values lower than 200 indicate severe hypoxemia and it is used in clinics to diagnose ARDS. In ARDS, impaired oxygenation is the result of pulmonary shunt. Pulmonary shunt is a condition that results when the alveoli of the lung are perfused with blood as normal, but ventilation fails to supply oxygen to the perfused region. A pulmonary shunt often occurs when alveoli are filled with fluid, causing parts of the lung to be unventilated although they are still perfused. Moreover, atelectasis or partial alveolar collapse contributes notably to this condition. Surfactant plays a key role in maintaining alveoli open and thus a negative correlation is expected between surface tension and oxygenation index. Our data confirms that increased surface tension in ARDS patients correlate with lower $\text{PaO}_2/\text{FiO}_2$ ratio. On the other hand collapsed alveoli may impose a physical barrier to distend the lung. Pulmonary compliance is a measure of the ability of the lung to distend and increase volume in response to air pressure without disruption. Compliance or distensibility of the lung is increased in conditions such as emphysema in which the lung distends more readily and is decreased in fibrotic conditions and ARDS in which the lung distend with difficulty. In agreement with this, higher surface tension in ARDS patients correlates with reduced compliance. Even though increased surface tension is not the only symptom in ARDS, considering that inflammation of the epithelium should also play an important role, it seems that there is a direct relation between lung performance and surfactant function. Moreover, we can distinguish three groups of samples matching with patient groups: control, direct ARDS and indirect ARDS. Every group is characterized by a value in clinical parameter and surface tension. Control group has normal values for clinical parameters and relatively low surface tension, indirect ARDS group has abnormally low values for clinical parameters such as $\text{PaO}_2/\text{FiO}_2$ and CRS with the same surface tension as control group, and finally direct ARDS group shows also low values for clinical parameters with abnormally high surface tension.

In addition, we wanted to explore the correlation between abnormally high surface tension and the clinical outcome of ARDS. Again, we are not trying to explain ARDS only in terms of surfactant function, but to highlight the importance of the contribution of altered surface tension and an impaired biophysical behaviour of surfactant to lung pathologies. Murray's score or lung injury score (LIS) was designed to characterize the presence and extent of lung injury. It has been used to diagnose ARDS, when values are under 2.5. A positive correlation of this score with surface tension agrees with the already described contribution of high surface tension to lung injury. And finally we have also analysed PRISM (Paediatric risk of mortality). This score was designed to calculate the mortality rate in the paediatric intensive care unit and is measured during the first 24h after admission in intensive care unit.

Again, a positive correlation between PRISM and elevated surface tension may indicate that surfactant inactivation may also be contributing to the fatal outcome of ARDS. In the same direction we can match the three groups of data with groups of patients according to the origin of ARDS. It seems that clinical data identifies two groups, control and ARDS, and it is the surface tension the one that can differentiate between direct and indirect ARDS groups.

In conclusion, impairment of surfactant in ARDS leads to high surface tension that contributes to the development and outcome of ARDS. This work highlights the importance of lung surfactant function in ARDS, especially in direct ARDS originated directly in the lung, concerning the use of surfactant supplementary therapy in ARDS patients as treatment for counteracting increased surface tension in addition to standard treatment.

**MOLECULAR AND BIOPHYSICAL CHARACTERIZATION OF A NAPSIN A KNOCK-OUT
MOUSE MODEL WITH PARTIAL SP-B DEFICIENCY**

**This work has been done in collaboration with MD Andreas Günther
(Universitätsklinikum Giessen und Marburg, Justus-Liebig-Universität Giessen)**



MOLECULAR AND BIOPHYSICAL CHARACTERIZATION OF A NAPSIN A KNOCK-OUT MOUSE MODEL WITH PARTIAL SP-B DEFICIENCY

INTRODUCTION

In the previous chapter we have analysed samples from ARDS patients that show impairment in lung function and also in the biophysical activity of surfactant. We could conclude that abnormally high values of surface tension could play an important role in the outcome of this pathology. However, the characterization of these samples was quite limited due to the limiting quantity of BAL. With the study of animal models, the availability of samples should allow to carry out a deep molecular and cellular study, which combined with the characterization of surfactant function, should permit a complete analysis of the connection between molecular and cellular profiles and physiological outcomes.

Idiopathic pulmonary fibrosis (IPF), sarcoidosis and pulmonary hypertension are interstitial lung diseases with a common factor. All of them show an increase in alveolar surface tension that may play a role in the development of the diseased lung. Lung surfactant from IPF patients show increased surface tension (Günther et al. 1999). It has already been described that increased surface tension in IPF patients may lead to chronic damage in type II cells. The combination of ER stress, lysosomal stress and mitochondrial and DNA damage may lead to apoptosis of type II cells (Günther et al. 2012). On the other hand, it has already been described that injured type II cells release a number of pro-fibrotic compounds that may activate mesenchymal cells, and promoting development of fibrotic tissue. But there are a number of different hypotheses for explaining the molecular and cellular basis of fibrosis. IPF patients also show alteration of surfactant composition, not only regarding the protein content, such as decreasing amounts of SP-B and SP-C in BAL, but also changes in the lipid profile, with a decrease in PG concomitant with an increase in PI and SM (Günther et al. 1999).

The aim of this chapter is to characterize in detail a Napsin A KO mouse model. The working hypothesis is built on the observation that sporadic IPF patients show a decrease amount of Napsin A in their lung tissue (Korfei et al. 2007). Absence of Napsin A would result in SP-B deficiency, as Napsin A is an aspartyl protease responsible of the processing of SP-B from its precursors (Hirano et al. 2000; Brasch et al. 2003; Dejmek et al. 2007). As SP-B is an essential protein for lung surfactant function, an impairment in surfactant function would be expected, also resembling SP-B deficiency related syndromes. Thus the Napsin A KO mouse model may have a clinical relevance in the study of the pathogenic and progress of fibrotic process and its treatment.

IPF is relatively uncommon, with a prevalence estimated at 1.6-1.7 individuals per 100.000 population and a median survival of 2-5 years (Coulas et al. 1994; Günther et al. 1999). It is a disease predominately of the elderly, with a mean age onset of 67 years. It is slightly more common in males and in those with a history of smoking. Various environmental stimuli have been suggested as risk factors for developing IPF, including cigarette smoking, antidepressants, chronic aspiration, metal and wood dusts and infectious agents, including Epstein Barr virus.

Originally, it was thought that IPF was mainly due to a chronic inflammatory disease, occurring in response to an unknown stimulus, and if left untreated, led to progressive lung injury and ultimately fibrosis (Selman et al. 2001; Noble and Homer 2005). For this reason, anti-inflammatory therapy, using oral corticosteroids and cytotoxic agents was first proposed. However, it is now increasingly evident that inflammation does not play a pivotal role in IPF, which explains why these therapies have been ineffective. Therefore targeting the anti-fibrotic pathway is the alternative strategy followed today (Dempsey et al. 2006). In addition, as injury in type II cells is an early and consistent finding in IPF, approaches to regenerate and repair epithelium have also been proposed (Selman et al. 2004). The parallel use of surfactant supplementary therapy has also been proposed (Raghu et al. 1999; Meyer and Zimmerman 2002) to counteract the increase in surface tension and contribute to reduce the lung working load.

Deficiencies in SP-B protein are lethal as described in babies with modifications in the SP-B gen (Nogee et al. 1994). These infants show symptoms of RDS (respiratory distress syndrome), as they lack on a functional surfactant (Pryhuber 1998; Williams et al. 1999). Also SP-B knock-out mice die of severe RDS, typically within minutes of birth (Clark et al. 1995; Tokieda et al. 1997). Even partial SP-B deficiency perturbs lung function (Ikegami et al. 2005; Nessler et al. 2005). Not only genetic modifications of the SP-B gene causes SP-B deficiency; interrupting the SP-B processing pathway may lead also to SP-B deficiency and impairment in lung function. As for example in sporadic IPF, where deficiency in SP-B has been observed in bronchoalveolar lavage (BAL) from patients as well as accumulation of unprocessed SP-B in the lung tissue (Korfei et al. 2007; Korfei et al. 2008).

SP-B processing has been studied in detail and localised in alveolar type II cells. Precursors of SP-B can be also found in Clara cells. Synthesis of proSP-B starts in the endoplasmic reticulum and continues in the Golgi, multivesicular bodies and lamellar bodies (LB), considered as the intracellular reservoir of surfactant. Surfactant packing, including the sorting out and assembling of SP-B and SP-C are the major function of LB. It has been previously described that the proteolytic maturation of these proteins involves the activity of enzymes, that are also found in lysosomes and whose activity depends greatly on the pH of the media. Very acidic pH (around 3-5) is necessary for the correct cleavage and processing of SP-B and SP-C. Several enzymes have been proposed to be involved in the processing and maturation of SP-B, although the complete pathway is not entirely known. It has been described that the aspartyl protease Napsin A (found in alveolar epithelial type II cells and Clara cells) is the main responsible of the processing of SP-B, cleaving the 40-42kDa precursor to the 25kDa proSP-B intermediate (Hirano et al. 2000; Brasch et al. 2003; Dejmeek et al. 2007). In latter cleaving steps, Pepsinogen C and Cathepsin H may play an important role in the processing of the 25kDa precursor into a 9kDa proSP-B intermediate and also in the ultimate cleavage of this into the mature form of SP-B (8kDa) (Brasch et al., 2004, Ueno et al., 2004, Gerson et al 2008) (Brasch 2004; Ueno et al. 2004; Gerson et al. 2008). Pepsinogen C is another aspartyl protease found mainly in type II cells and Cathepsin H is a cysteine protease involved not only in the processing of SP-B but also in the processing of SP-C (Brasch et al. 2002).

As Napsin A seems to play an essential role in the processing of SP-B, studying mice models that lack on this enzyme could be an important tool for simulating SP-B deficiency and for studying the processing of SP-B, its assembly in surfactant complexes, and its associated pathologies. Napsin A KO mice (TF2924, Lexicon Pharmaceuticals Inc.), which present a deletion of 7 out of 9 exons in the *napsa* gene, were generated to test this hypothesis. The aim of this work is to characterize this mice model. Molecular and biophysical characterization should describe this mice model in detail, as well as its potential for the study of SP-B processing pathways and its physiopathological consequences.

RESULTS

Napsin A KO mice do not apparently show impairment of the lung function and they breathe and live normally. The characterization of the lung morphology and structure (figure 5.1) does not show significant differences between WT and KO mice. Tissue staining with TTF-1 antibody (thyroid transcription factor 1, essential for lung development) shows similar structure of the lung with no fibroblast development. Moreover, AECII morphology is similar in both cases, indicating that elimination of the Napsin A gene does not affect the structure and morphology of the cells in the lung.

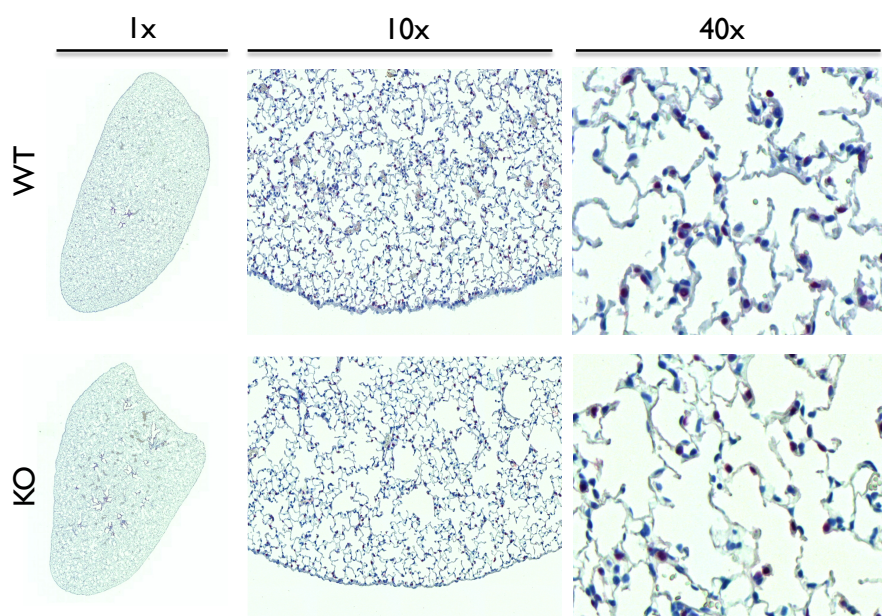


Figure 5.1: Characterization of lung morphology and structure in WT and KO mice. Representative immunochemistry (using TTF-1 antibody) of WT (top) and KO (bottom) lung tissues. Three different magnifications (1, 10 and 40x) are compared to observe general structure and morphology of AECII (red stain).

As Napsin A is an enzyme involved in the processing of SP-B, we have first analysed the SP-B content in bronchoalveolar lavage (BAL) and lung homogenate (LH). Figure

5.2 illustrates that there is a partial deficiency of SP-B in BAL from Napsin A KO mice compared with WT animals as analysed by western-blot. Quantification of the bands estimates a decrease in SP-B content of about 50% in BAL of the genetically modified animals.

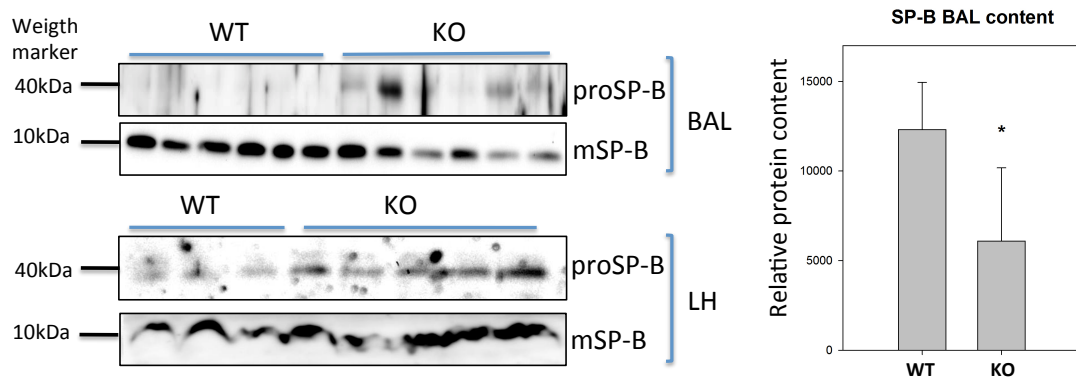


Figure 5.2: SP-B content in WT and KO mice. Example of immunoblots (left) and quantitative immunoblot analysis (right) of proSP-B and mature SP-B (mSP-B) in lung tissue (LH) and bronchoalveolar lavage (BAL) of WT and KO mice. Shapiro Wilk Test * $p < 0.001$.

It is quite surprising that even though Napsin A is completely absent in KO mice, SP-B is still processed, it is not a complete and efficient processing as there is a 50% deficiency, still this reduced amount of SP-B seems to be enough for surfactant to be functional and for the mice to breath normally and survive. On the other hand we have also analysed the proSP-B content in BAL and LH. ProSP-B is a large soluble protein that is not normally secreted, so it should not appear in the BAL. Figure 5.2 reveals the presence of some proSP-B in the BAL of the KO mice and it seems that there is accumulation of the 40kDa form of proSP-B in the tissue (LH). The accumulation of precursor forms of SP-B in the lung tissue is consistent with a deficient processing of SP-B, resulting in a partial deficiency of the mature protein in the BAL.

Immunohistochemistry of lung tissue from WT and KO mice (figure 5.3) shows the localisation of mSP-B in type II cells (pink staining) in both WT and KO samples. On the other hand, analysis by immunohistochemistry of the localisation of proSP-B reveals that the precursor accumulates in type II cells and also in Clara cells (bronchiolar cells) as it would be expected. In both, WT and KO animals, proSP-B shows a similar distribution.

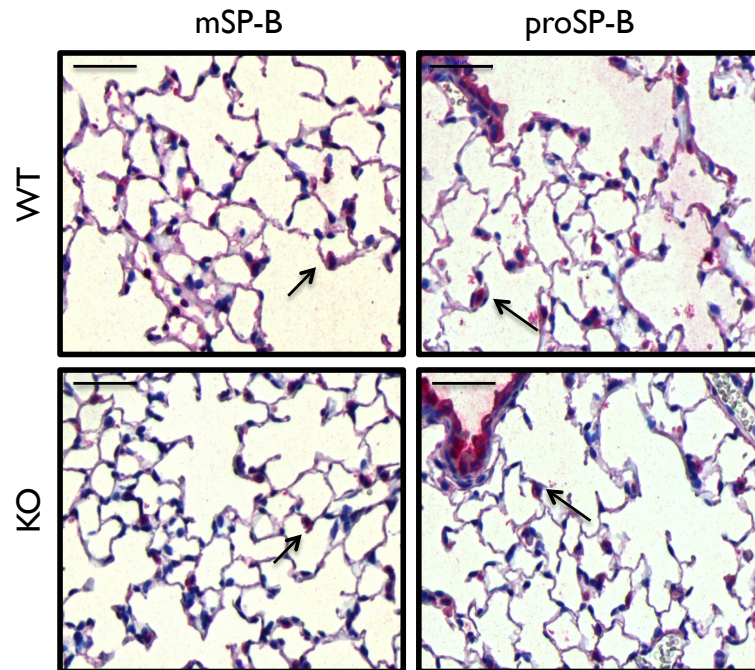


Figure 5.3: Localisation of SP-B and proSP-B in WT and KO lung tissue. Representative immunohistochemistry for mature SP-B and proSP-B. Left panels: mSP-B stain (red stain) in AECII (arrows indicate examples of AECII) in WT (top) and KO (bottom) lung tissues. Right panels: proSP-B stain (red stain) in AECII (arrows indicate examples of AECII) and Clara cells (at the left top corner of each image) in WT (top) and KO (bottom) lung tissues. Photomicrographs were taken with x40 magnification (bar = 50 μ m).

Interestingly, the absence of Napsin A does not result in a complete deficiency of the mature form of SP-B, suggesting that there should be an alternative pathway of processing of ProSP-B precursor. We have analysed the potential participation of possible enzyme candidates with similar proteolytic activities. These candidates include aspartyl proteases associated with lung cells, and therefore we focused our search on Pepsinogen C, Cathepsin D and Cathepsin E. Running a pBLAST (NCBI), using as query sequence that of Napsin A, we have found that there is a substantial similarity between the amino acid sequence of all these proteases, ranging 49-63% identity, as shown in table 5.1.

| Subject sequence | Max Score | Total Score | Query Coverage | Max identity | Positives |
|------------------|-----------|-------------|----------------|--------------|-----------|
| Cathepsin E | 332 | 332 | 88% | 47% | 63% |
| Cathepsin D | 368 | 368 | 89% | 47% | 63% |
| Pepsinogen C | 266 | 266 | 94% | 39% | 55% |

Table 5.1: pBLAST result for similarity and homology between different lung aspartyl proteases. Comparison between sequences was done using NCBI services (<http://blast.ncbi.nlm.nih.gov/Blast.cgi>).

Complementary sequence alignment shows that particular patches of similarity (dark blue) are located in regions of the sequences involving the active sites (aspartic residue, D) of all these proteases (figure 5.4).

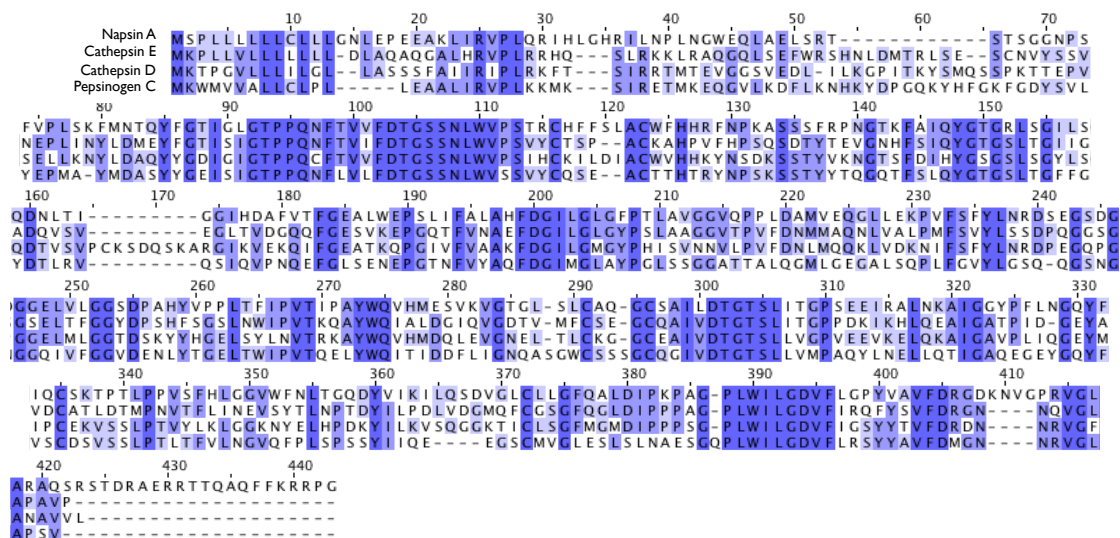


Figure 5.4: protein sequence alignment of aspartyl proteases found in lung cells. Compared are the sequences of Napsin A, Pepsinogen C, Cathepsin D and Cathepsin E, as aligned by ClustalW (<http://www.ebi.ac.uk/Tools/msa/clustalw2/>). Color coding indicates levels of similarity, being the darker blue total identity between the four proteases and lighter colors identity between two or three of the proteases.

Sequence similarity between the proteases did not allow us to study them at the protein level, as for example Napsin A antibody used gave positive results in KO mice samples in both western-blot and immunohistochemistry, as it is also recognizing other proteases. but we have studied their gene expression using semiquantitative RT-PCR in LH mRNA. Figure 5.5 summarizes the comparison of gene expression at the mRNA level of different proteins in WT and KO mice.

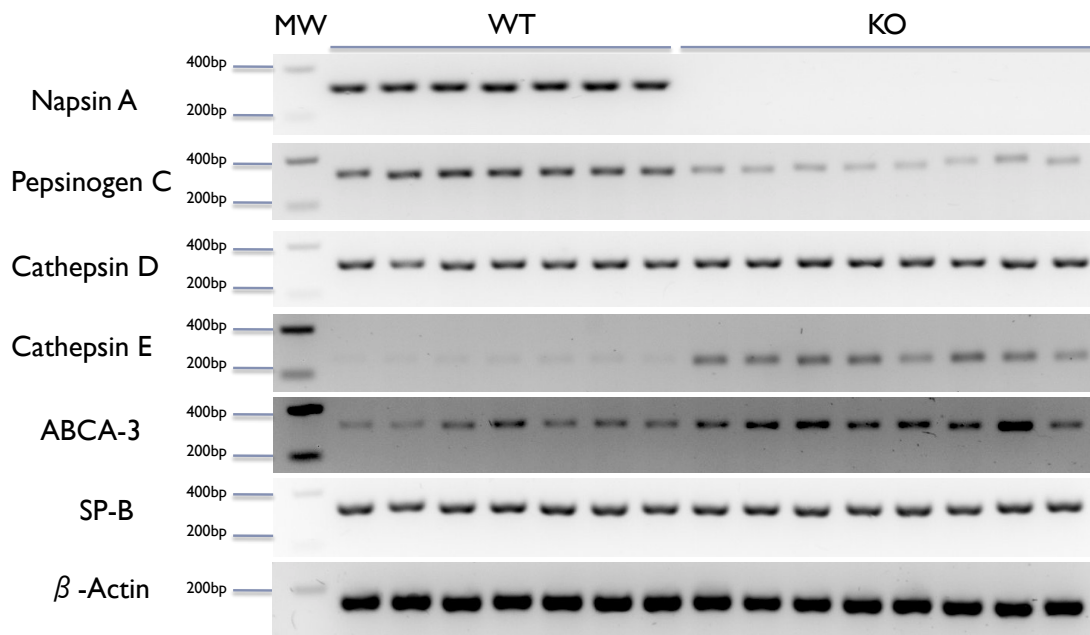


Figure 5.5: Semiquantitative RT-PCR analysis of mRNA in lung tissue. Gene expression of different aspartyl proteases (Napsin A; Pepsinogen C; Cathepsin D and Cathepsin E) a lipid transporter, ABCA3, involved in surfactant biogenesis; and two loading controls, SP-B and β -actin.

Analysis of gene expression confirms that Napsin A is completely absent and interestingly, Pepsinogen C is substantially downregulated in the KO mice. In contrast, the expression of the genes of Cathepsin D and E is up-regulated, particularly that of Cathepsin E. It could therefore be possible that these two enzymes may be responsible for the alternative SP-B processing in the absence of Napsin A. Quantification of the amplified DNA signal in agarose gels allows the estimation and quantitative comparison of the level of expression of the different genes as a consequence of the KO and WT condition (figure 5.6). The semiquantitative analysis confirms that the level of expression of Pepsinogen C gene is 3-4 times lower than in WT mice. In contrast, lung tissue from KO mice exhibit around a 20% higher expression of Cathepsin D and 5 times more expression of Cathepsin E than WT animals. Surprisingly the expression of the gene for the phospholipid transporter ABCA3, involved in phospholipid import into LB and SP-B sorting out (Ban et al. 2007), also shows up-regulation to 2-3 higher expression levels than those observed in WT animals.

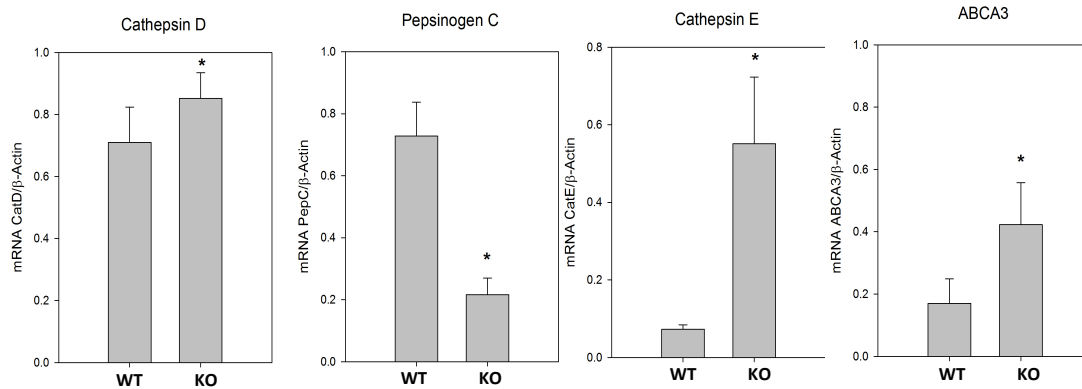


Figure 5.6: Quantitation of expression levels of genes of aspartyl proteases and ABCA3 as determined by RT-PCR. Densitometric ratios of the respective band related to β -actin band for Pepsinogen C (PepC), Cathepsin D (CatD), Cathepsin E (CatE) and ABCA3 in WT and KO tissue. Shapiro Wilk test * $p < 0.001$, *** $p < 0.05$.

On the other hand we have also analysed the SP-C content in BAL and LH of Napsin A KO and WT mice (figure 5.7). BAL from KO mice contains a reduced amount of SP-C, about 65% less than the amount of SP-C present in WT animals. This reduction of SP-C in BAL was accompanied of a clear accumulation of SP-C in the tissue (LH). Thus it seems that SP-C is properly processed in the lung of Napsin A KO mice but there is significant impairment in the sorting out of the protein, which is not properly incorporated into surfactant complexes. Moreover we can also observe a further accumulation of SP-C precursors in the tissue of KO mice. Figure 5.7 shows clear increased amounts of the 21 and 16 kDa proSP-C intermediates in LH western-blot from KO mice. These precursors were not found in BAL. These data suggest that the Napsin A defective processing machinery is also causing a SP-C sorting out impairment which is causing an abnormal accumulation of SP-C and its precursors.

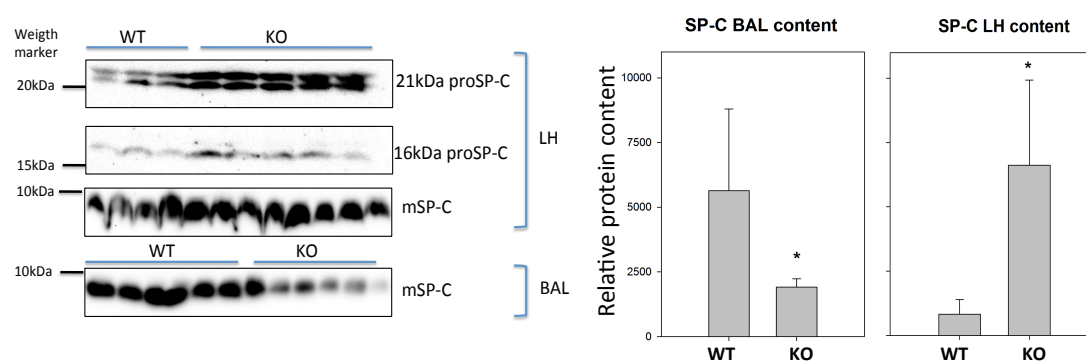


Figure 5.7: SP-C content in WT and KO mice. Example of immunoblots (left) and quantitative immunoblot analysis (right) of tissue (LH) and bronchoalveolar lavage (BAL) of WT and KO mice. Shapiro Wilk test * $p < 0.001$.

In addition, we wanted to investigate whether Napsin A is directly involved in the processing of SP-C. Figure 5.8 shows that there is accumulation of an aberrant form of SP-C, rather than the mature form, as analysed with a different antibody. It seems that the absence of Napsin A results in an intracellular accumulation of an aberrant form of an apparent size of 11-12kDa. Therefore the lack on SP-C in BAL seems to be more related with a deficient maturation of the protein rather than with the sorting out. Whether the impairment on SP-C maturation is the consequence of the SP-B deficiency or the Napsin A lack has still to be determined, as others has observed this phenotype in SP-B deficiency models.

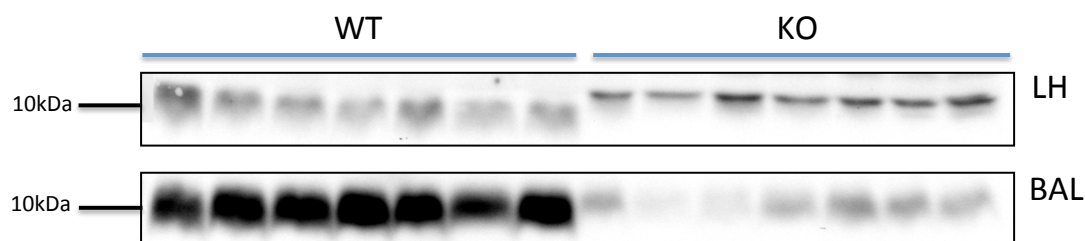


Figure 5.8: SP-C content in WT and KO mice. Example of immunoblots of tissue (LH) and bronchoalveolar lavage (BAL) of WT and KO mice using a proSP-C antibody from Chemicon in the LH antiSP-C form SevenHills in BAL.

Immunohistochemistry data also supports these results (figure 5.8). Even though immunohistochemistry is not a quantitative technique, intensity differences on the staining of SP-C and proSP-C between WT and KO slides seem to follow the same pattern we have observed in western-blot. More intense staining of the proteins in the KO lung tissue confirms accumulation of SP-C and its precursors in AECII.

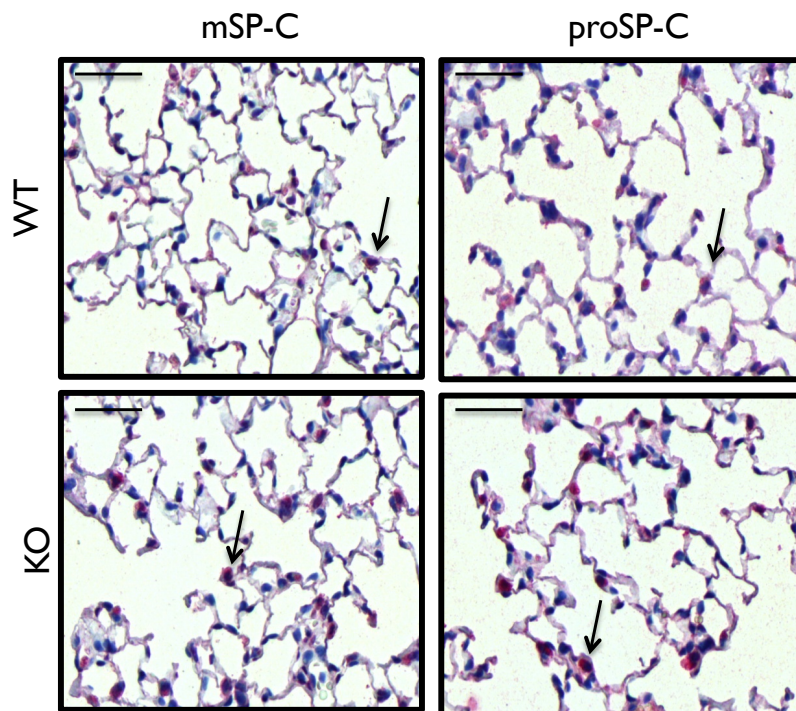


Figure 5.9: Localisation of SP-C and proSP-C in WT and KO lung tissue. Representative immunohistochemistry for mature SP-C (mSP-C) and proSP-C. Left panels: mSP-C stain (red stain) in AECII (arrows indicate examples of AECII) of WT (top) and KO (bottom) lung tissues. Right panels: proSP-C stain (red stain) in AECII (arrows indicate examples of AECII) of WT (top) and KO (bottom) lung tissues. Photomicrographs taken with x40 magnification (bar = 50 μ m).

Intracellular accumulation of proteins, specially small and hydrophobic proteins, may cause some changes in the cell, as for example ER (endoplasmic reticulum) stress. For testing the hypothesis that the accumulation of mSP-C inside the cells could be generating ER stress, we analysed the potential co-localisation of an ER stress marker and mSP-C in the lung tissue of WT and KO mice by immunohistochemistry. We have determined that the ER stress marker XBP-1 (X-box protein-1) is completely absent from WT sections, while it is clearly stained in KO mice tissues (figure 5.9). XBP-1 and mSP-C co-localise inside AECII.

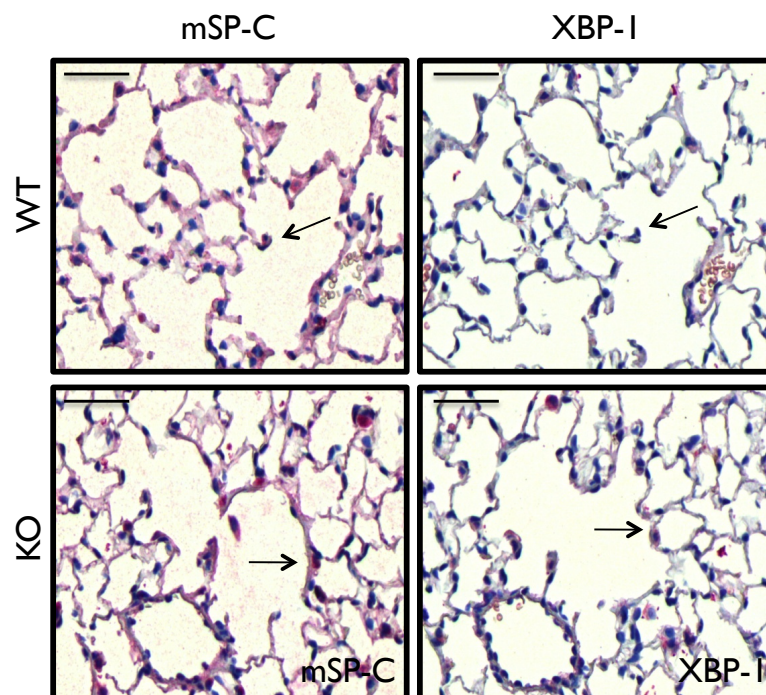


Figure 5.10: Localisation of SP-C and XBP-1 in WT and KO lung tissue. Representative immunohistochemistry micrographs of tissue sections labelled with antibodies against mature SP-C and XBP-1. Left panels: mSP-C stain (red stain) in AECII (arrows indicate examples of AECII) in WT (top) and KO (bottom) lung tissues. Right panels: XBP-1 stain (red stain) in AECII (arrows indicate examples of AECII) in WT (top) and KO (bottom) lung tissues. Photomicrographs were taken with x40 magnification (bar = 50 μ m).

To confirm that accumulation of surfactant proteins and their precursors causes the up-regulation of ER stress markers we have analysed the expression of genes related with ER stress in the lung of WT and KO mice. We have thus checked the expression of XBP-1 and EDEM, two ER stress markers, and CHOP, apoptosis marker, by a semiquantitative RT-PCR. Figures 5.10 and 5.11 show that the lung of Napsin A KO mice exhibits a clear up-regulation of XBP-1, as determined by immunohistochemistry, while CHOP undergoes a slight up-regulation. There is no differential expression of EDEM.

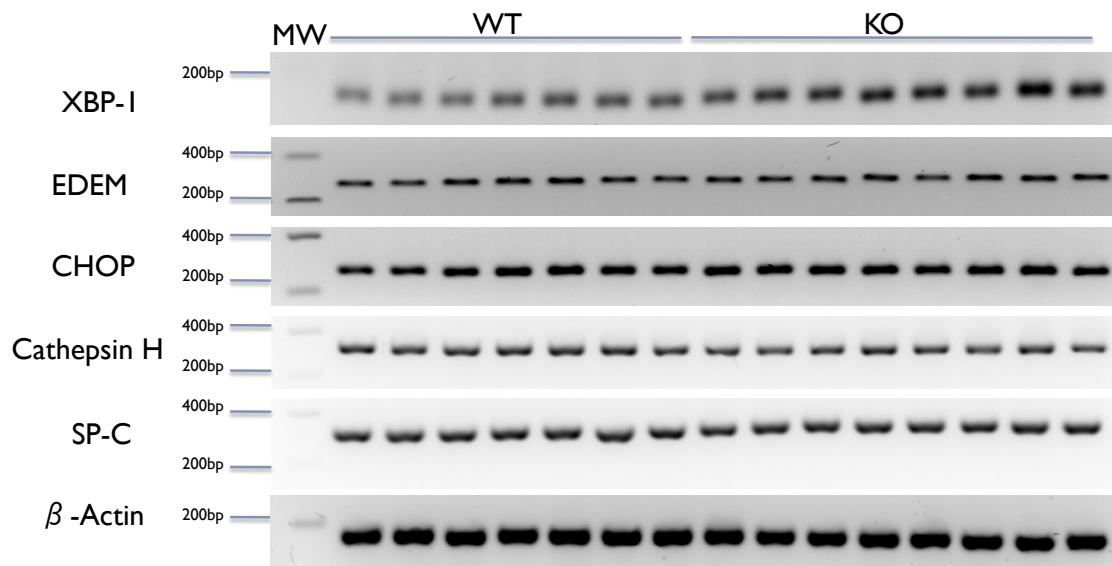


Figure 5.11: RT-PCR analysis of ER stress markers and CHOP in mice lung tissue from WT and KO. Levels of mRNA from two ER stress markers (XBP-1 and EDEM) and CHOP, Cathepsin H (cystein proteases), SP-C and B-Actin as loading controls were analysed.

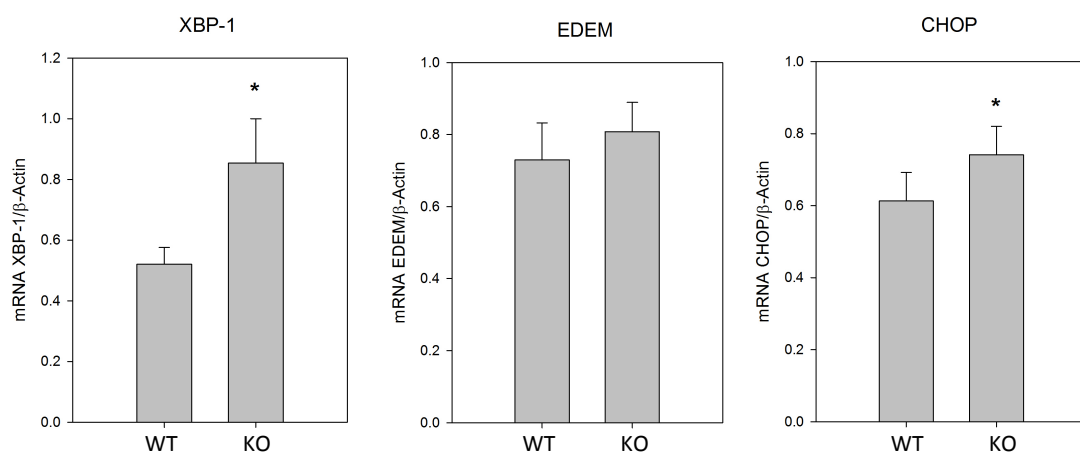


Figure 5.12: Quantitation of the expression levels of ER stress markers and CHOP. Densitometric ratios of the respective band related to β -actin band for XBP-1, EDEM and CHOP in WT and KO tissue. Shapiro Wilk test * $p < 0.001$, ** $p < 0.01$.

The analysis illustrated in Figure 5.10 confirms that SP-C deficiency detected in BAL is not the consequence of a down-regulation of the enzymes responsible of the processing of this protein. Cathepsin H (cysteine protease), directly involved in the processing of SP-C, is expressed at levels similar to WT in the lung of KO mice. The levels of expression of the SP-C gene seem also comparable in KO and WT mice, confirming that SP-C deficiency is caused by impairment on the sorting of the protein out to the alveolar air spaces. All these results lead to the conclusion that Napsin A

deficiency originates an altered protein profile of hydrophobic proteins in pulmonary surfactant, characterized by the significant reduction of the proportion of SP-B and SP-C. We have then analysed whether alteration of the expression profile is accompanied or not with changes in the level of phospholipids in the alveolar spaces and in the biophysical properties of surfactant.

The analysis of phospholipid content reveals a significant increase in total amount of phospholipids in BAL of KO samples with respect to WT mice (figure 5.12).

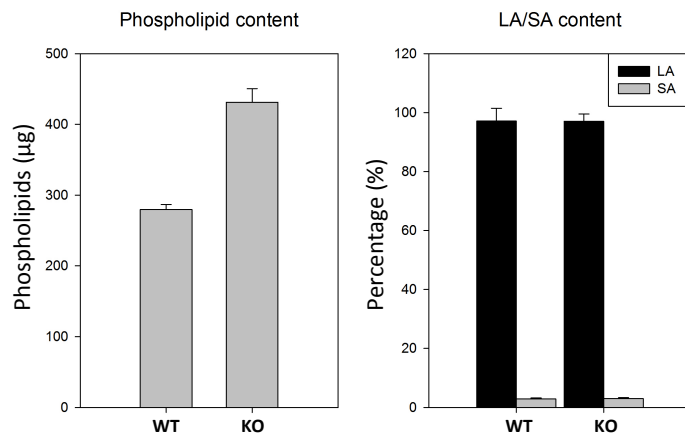


Figure 5.12: phospholipid content in WT and KO mice BAL. Total phospholipid content (left) and percentage of phospholipid in large (black) and small (grey) aggregates (right) in BAL from WT and KO mice.

Surprisingly, KO mice seems to produce and liberate to the alveolar spaces more phospholipids than WT animals, while maintaining a similar LA/SA ratio. Enhanced production of phospholipids could be a compensatory mechanism in KO mice and which could be connected with the up-regulation of ABCA3 in these mice.

Preliminary biophysical data does not reflect the difference in surfactant composition between WT and KO mice, as the minimal surface tension reached upon adsorption of the two materials was not significantly different. Also both WT and KO surfactant reach low enough surface tension (< 5mN/m) during compression-expansion cycling (figure 5.13).

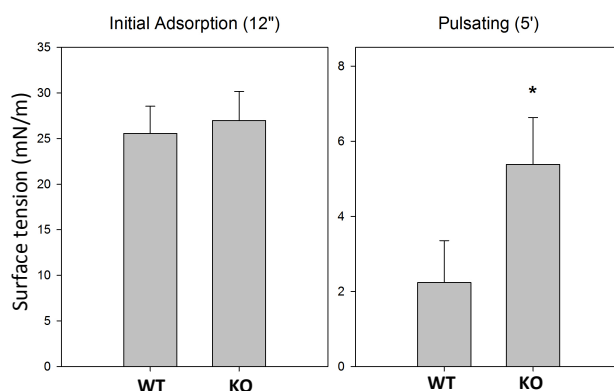
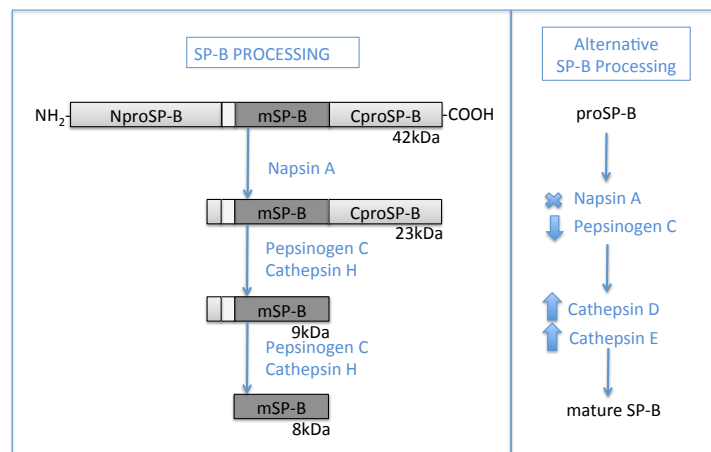


Figure 5.13: Surface activity of surfactant from WT and KO mice. Surface tension reached upon 12 seconds of initial adsorption (left) and after 5 minutes of compression-expansion of the bubble (right) into a Pulsating Bubble Surfactometer. Shapiro Wilk test * $p < 0.001$.

DISCUSSION

Surfactant protein B is essential for pulmonary surfactant function, and therefore for breathing and live. SP-B deficiency is lethal (Tokieda et al. 1997; Weaver and Beck 1999) and this deficiency could be caused by genetic mutation of the corresponding gene or by impairment of any of the processes required to facilitate maturation and trafficking of the protein. It has been reported that one of the main enzymes responsible for the processing of SP-B is Napsin A (Woischnik et al. 2008), involved in the cleavage of the intermediate forms of 40 and 25kDa. However, the elimination of 7 out of 9 exons of the Napsin A gen results only in a partial deficiency of SP-B, as shown by our results. Thus, SP-B is still getting processed even in the total absence of Napsin A. This leads us to hypothesize that compensatory mechanisms likely activate alternative processing pathways for SP-B. Other enzymes, most probably other aspartyl proteases present in type II cells (AECII), must be responsible for maturation of SP-B from its precursors in the absence of Napsin A. It has already been reported that Pepsinogen C (aspartyl protease found in type II cells) is directly involved in the processing of SP-B during pneumocyte differentiation (Foster et al. 2004). Another two aspartyl proteases have been found in lung cells. On the one hand, Cathepsin D is expressed in type II cells (Saftig et al. 1995) and on the other hand, Cathepsin E has been described to be found in Clara cells (Cook et al. 2001). Therefore, we proposed that these three proteases could be good candidates for alternative processing of SP-B. We found that these four enzymes share about 39-47% similarity of their sequences, but most importantly, that they exhibit full sequence identity in segments containing the catalytic groups (aspartate residues) at the active site. Thus Pepsinogen C, Cathepsin D and Cathepsin E seem to be potential alternative to Napsin A in the processing of SP-B. A critical condition on SP-B processing is the optimal pH at which aspartyl proteases should be active. Napsin A has an optimum pH of around 4.7 (Schauer-Vukasinovic et al. 2000), as all lysosomal proteases. It has been previously described that Pepsinogen C has an optimum pH of around 3.2 (Szecsi 1992), Cathepsin D of about 3.5 (Barrett 1970) and Cathepsin E of around 4 (Yasuda et al. 1999). Therefore all of them seem to fulfil the requirements to be candidates for SP-B processing in multivesicular bodies and LBs, the organelles where processing of SP-B is coupled to surfactant assembly. The analysis of the gene expression of these lung aspartyl proteases revealed that the complete absence of Napsin A entails down-regulation of Pepsinogen C gene expression. Pepsinogen C has been proposed to act after cleavage by Napsin A in the processing pathway so far elucidated for SP-B (Brasch 2004; Ueno et al. 2004; Gerson et al. 2008). It seems therefore that both enzymes belong to the same branch of the pathway which could explain why changes in the expression of one of them interferes with the expression of the other one. Thus, with the Napsin A/Pepsinogen C pathway down-regulated, Cathepsins may be the available alternative. As shown in the results, expression of Cathepsin D and E is in fact up-regulated, especially Cathepsin E in the Napsin A KO model. Thus we propose a Cathepsin alternative pathway for the processing of SP-B, which we have summarized in the following scheme.



However, so far, Cathepsin E has only been detected in Clara cells (Cook et al. 2001). Clara cells express proSP-B, but it is not known whether they process it completely to yield mature SP-B. For a proper packing and assembly of and operative surfactant, SP-B must be present into the lamellar bodies (intracellular reservoir of surfactant) in AECII. Whether the overexpression of Cathepsin E is due to the activation of the expression of the enzyme within AECII or Clara cells should be determined in the future, in order to understand the complete alternative processing pathway. Another important enzyme involved in processing of not only SP-B but also SP-C, is Cathepsin H. This cysteine protease has been reported to act in the last steps of the processing of SP-B and SP-C (Brasch et al. 2002; Guttentag et al. 2003; Ueno et al. 2004). Gene expression analysis of this protease reveals that it is normally expressed in KO compared to WT mice. Thus, the steps where Cathepsin H participates at the processing pathway are probably not altered in the KO mice model, but earlier stages when the aspartyl proteases may act. Although activation of the alternative processing the partial deficiency of SP-B reveals that the Cathepsin pathway is not 100% efficient, which may lead to accumulation of unprocessed SP-B, still it could produce enough SP-B for surfactant to be functional and for the mice to survive.

In addition, we have analysed SP-C content in the BAL and lung tissue of Napsin A KO mice. Surprisingly, SP-C partial deficiency seems to be stronger than that of SP-B. Even though Napsin A has not been related to SP-C processing, KO mice show an important SP-C deficiency. Our results reveal that SP-C content in BAL is decreased, while SP-C content in lung tissue is markedly increased. We discovered that an aberrant form of SP-C is accumulating inside type II cell instead of the mature form. Thus we can conclude that SP-C partial deficiency is due to a processing impairment, resulting from the lack on Napsin A or the SP-B deficiency. It was already reported that SP-B deficiencies entails an associated SP-C deficiency in surfactant or BAL (Vorbroker et al. 1995; Weaver and Beck 1999). And SP-B deficient models also show accumulation of an aberrant form of SP-C of around 11-12kDa (Vorbroker et al. 1995; Tokieda et al. 1997). Our results provide additional piece of information linking the maturation of SP-B with the processing of SP-C. Thus a concerted mechanism

seems to exist to ensure that both proteins are assembled and secreted together into alveolar air spaces.

It is interesting that activation of alternative maturation pathways may restore production of mature SP-B in a Napsin A deficient mice but at the cost of losing a proper coupling with the assembly of SP-C in surfactant complexes. We hypothesized that alternative processing by Cathepsins may take place at different time or location than those required to also ensure proper targeting of mature SP-C, something efficiently achieved by Napsin A.

The accumulation of SP-C and its precursors in AECII leads to an ER stress response. We have observed XBP-1 co-localisation with mSP-C in AECII, but ER stress response may be the result of the accumulation not only of SP-C but also of all the unprocessed intermediates in the incomplete pathway to SP-B and SP-C. The observed up-regulation of the expression of Cathepsin D could be not only involved in the alternative processing of SP-B, but it has also been described as molecular marker of lysosomal stress (Mahavadi et al. 2010). Finally up-regulation of CHOP may be related to activation of apoptotic processes in lung tissue from KO mice (Korfei et al. 2008). ER stress, lysosomal stress and apoptosis have been described as potential promoters of fibrosis development in lung tissue (Günther et al. 2012).

Partial deficiency of SP-B and SP-C, accumulation of precursors and activation of ER stress in AECII resembles the phenotype exhibited by IPF patients (Korfei et al. 2007; Lawson et al. 2008; Günther et al. 2012) which also show a decreased amount of Napsin A. Mice studied here did not show fibrotic tissue, but the oldest mice analysed were 6 months old and as a progressive process, it may take longer for fibroblast foci to develop. Nevertheless, it is conceivable that Napsin A KO mice would be particularly predisposed to suffer sporadic IPF or be more sensible to induction of IPF, constituting a new model for studying fibrotic processes and treatments.

IPF constitutes one of the chronic interstitial lung injuries, together with sarcoidosis and hypertension, and other lung injury as ARDS, where abnormally high surface tension may play an important role. Considering the partial deficiency on SP-B and SP-C deficiency, the specific surfactant proteins involved in surfactant adsorption into the interface, and in ensuring proper compression-expansion dynamics of the surface active films during breathing cycling, it is important to analyse whether the altered protein complement in surfactant from these Napsin A-deficient IPF-sensitive animals gives rise to impaired interfacial activity, which could contribute an additional pathogenic factor. Interestingly, we found an increased amount of total phospholipids in BAL from KO mice, while maintaining LA/SA ratio constant. This is probably part of compensatory mechanisms, trying to counter act the SP-B deficiency. In the same line could contribute the up-regulation of the expression of ABCA3, a crucial lipid transporter involved in phospholipid trafficking into lamellar bodies and the processing and sorting out of SP-B (Ban et al. 2007). Preliminary biophysical analysis on a Pulsating Bubble Surfactometer showed no important differences in interfacial adsorption capabilities of surfactant from WT and KO mice into the bubble air-water interface. The slight but significant difference found in minimal surface tension reached upon compression-expansion of the bubble

interface seems to indicate that although functional, surfactant from KO mice might be more sensitive to inactivation processes such as those that could be triggered during occasional lung inflammation and injury.

GENERAL DISCUSSION PART 2

GENERAL DISCUSSION PART 2

We have complemented the study of clinically relevant samples and animal models with biophysical data approaching biophysics to clinics. Integrating molecular, cellular, biophysical and clinical data, we were able to get a deep insight into lung injury and disease. We have studied two lung diseases with a common factor: increased surface tension, due to surfactant dysfunction. In ARDS, surfactant dysfunction leads to alveolar collapse, thus decreasing lung compliance, while in IPF increased surface tension has been related to type II cell injury. We have highlighted the importance of studying surfactant function in ARDS and IPF, in addition to compositional studies, and we have proposed to include surfactant in potential therapies for these pathologies, for counteracting the increased surface tension effect.

In chapter 4 we have concluded that abnormally high surface tension is significantly correlated with clinical parameters indicating lung performance and clinical outcome of ARDS, especially for the cases of direct ARDS, where ARDS is a consequence of lung injury due to pneumonia, bronchiolitis or thoracic trauma. These patients showed at first very low surfactant phospholipid content, therefore the biophysical study of the samples was very limited with possibility of analysing only three patients. They showed a relatively high surface tension that may contribute to the clinical development and outcome of the pathology. We propose to use biophysical data to divide ARDS groups and therefore, the use of supplementation therapy for those with higher surface tensions. So far, supplementation with surfactant therapy has been disappointed in increasing survival of adult ARDS patients. In the first part of this Thesis we have proposed that failure of surfactant supplementation therapy is mainly due to the inactivation of exogenous surfactant by the same molecular mechanisms as the endogenous one. We proposed the development of inactivation-resistant surfactants for the treatment of pathologies such as ARDS. We could not conclude about the mechanisms undergoing surfactant inactivation in ARDS. It seems to be a multifactorial process that may include the presence of surface active compounds that compete for the interface, as well as the insertion of membrane perturbing molecules and probably also alteration of surfactant composition. As seen in chapter 3, treatment with polymers pre-activates surfactant independently of the molecular mechanism of inactivation. Thus, pre-activation of surfactant with polymers, such as hyaluronic acid, seems to be a promising strategy for the treatment of complex and multifactorial pathologies as ARDS.

In chapter 5 we have conclude that even though our mice model does not show fibrotic tissue yet, although lung injury is already undergoing. Probably older animals may show development of fibrotic tissue and higher surface tension of lung surfactant. In addition we hypothesized that this animal model might be more susceptible to the induction of fibrosis. This process is progressive and in humans it appears in the elderly, therefore it seems that the mice studied here are in early stages of fibrosis development. We can conclude that type II cell injury, concerning the accumulation of proteins inside the cell and the activation of ER stress response, seems to precede dysfunction of surfactant, due to SP-B and SP-C deficiency. However, inactivation of surfactant in latter stages may contribute to type II cell injury and fibrotic tissue development. In this case molecular mechanism of

surfactant inactivation may relay on surfactant protein deficiency, thus introduction of a functional surfactant for the incorporation of surfactant proteins does not need an inactivating-resistant surfactant rather than a preparation enriched in surfactant proteins. Therefore we proposed the use of supplementation therapy for “treatment” of high surface tension and SP-B and SP-C deficiency and its potential contribution to attenuate type II cell injury.

Moreover surfactant could be used as vehicle to introduce other compounds for the treatment of inflammation, in the case of ARDS, or anti-fibrotic agents, in the case of IPF, directly to the lung epithelium.

CONCLUSIONS AND PERSPECTIVES

CONCLUSIONES Y PERSPECTIVAS

CONCLUSIONS AND PERSPECTIVES

The work presented in this Thesis highlights the implication of surfactant dysfunction in lung injury and clinical outcomes of respiratory pathologies. From studies on molecular mechanism of inactivation and reactivation and its biophysical implication in surfactant activity to the biophysical study of clinically relevant samples and its contribution to respiratory pathologies. We can conclude that:

1.- Meconium inactivation of surfactant is mainly due to the insertion of cholesterol into surfactant membranes and contributes to the development of MAS. The fluidifying effect of cholesterol on surfactant is shown by the early collapse of the interfacial film during compression. The addition of 4% of cholesterol seems to be enough to inactivate surfactant, only if a proper agent solubilizes cholesterol in water. Solubilisation of cholesterol by bile salts or M β CD resembles the effect of meconium; therefore the main responsible for surfactant inactivation in meconium should be soluble cholesterol.

2.- Optimization of biophysical methods allowed to study the biophysical implication of surfactant inactivation by serum, meconium and cholesterol. Moreover the development of standard methods allowed the systematic study of surfactant inactivation and also the addition of compounds to surfactant preparations, looking for improved resistance to inactivation. We have confirmed that the addition of polymers, such as dextran or hyaluronic acid, restores surfactant activity in the presence of inactivating agents with different molecular mechanisms of action. Therefore it seems that resistance to inactivation provided by polymers is not specific of each inactivating mechanisms but general to surfactant.

3.- Entropic forces, such as osmotic pressure and depletion forces, may act on surfactant resulting in enhancement of interfacial activity. Combination of entropic forces leads to aggregation of surfactant complexes, enhancement of the interfacial activity and refining of the composition. Enrichment on saturated phospholipid species may contribute to the resistance against inactivation imposed by a steric barrier of surface active proteins, and decreased amount of unsaturated species and cholesterol may be beneficial in the presence of an excess of membrane perturbing molecules. Moreover, structural and compositional changes induced by hyaluronic acid are non-reversible, therefore pre-treatment and further elimination of the polymer results in a pre-activated state with a higher resistance to inactivation.

4.- Biophysical characterization of samples from ARDS patients shows significant correlation of abnormally high surface tension with clinical parameters, especially in the case of direct ARDS. Low values of PaO₂/FiO₂ and CRS are correlated with higher values of surface tension, indicating that poor lung performance is related with surfactant dysfunction. Moreover, higher values of PRIMS and Murray's score with higher surface tension indicate poorer clinical outcomes when surfactant function is impaired, especially in direct ARDS cases. This highlights the implication of surfactant dysfunction on the development and outcome of ARDS. Even though we cannot conclude about the exact molecular mechanism of inactivation, it seems that a multifactorial process, including surface active proteins competing for the interface and membrane-perturbing molecules inserting into surfactant membranes, is the main responsible of higher surface tension. Therefore developing surfactant

Conclusions and Perspectives

preparation resistant to a variety of inactivating agents seems to be a promising strategy for the treatment of respiratory pathologies such as ARDS.

5.- Combination of molecular, cellular and biophysical data allow to deeply characterized a Napsin A KO model. Results suggest that in the absence of Napsin A, there is still processing of SP-B, that allowed us to propose an alternative processing pathway that relays on the activation of Cathepsin D and E. Moreover, accumulation of proteins inside type II cells have been demonstrated to activate ER stress response and its consequent cell injury, resembling IPF conditions. Even though animals studied here did not show fibrotic tissue, they showed type II cell injury indicating early stages of IPF development. We hypothesized that these animals may develop IPF at older ages or be more susceptible to induction of IPF.

Combination of molecular, biophysical and clinical data opens the possibility to integrate a number of relevant data that may help in the understanding of respiratory pathologies and development of new therapeutic strategies. We propose here the pre-incubation of surfactant preparations with HA as a step in the production process of clinical surfactants. Whether the available clinical surfactants may show structural and compositional changes in the same direction as the native surfactant, has still to be determined. Current clinical surfactants undergo organic extraction, losing SP-A and its native structure; therefore, effect of HA may not be exactly the same in this case. However developing surfactants with increased resistance to different inactivating agents is a promising strategy for the treatment of respiratory pathologies where external agents reach the alveolar spaces. Moreover, if high surface tension contributes to lung injury, preventing surfactant inactivation may be essential in the therapy of respiratory pathologies. In addition, surfactant could also be used as vehicle for other compounds directed to the lung epithelium. For example, combination of anti-inflammatory agents, for treatment of ARDS, or anti-fibrotic agents, for IPF, with surfactant would be a new therapeutic strategy to explore.

CONCLUSIONES Y PERSPECTIVAS

El trabajo presentado en esta Tesis destaca la implicación de la disfunción del surfactante en el daño pulmonar y los resultados clínicos de patologías respiratorias. Desde estudios moleculares sobre los mecanismos de inactivación y sus implicaciones biofísicas en la actividad de surfactante, hasta el estudio biofísico de muestras con relevancia clínica y la contribución de la inactivación de surfactante en patologías respiratorias. Se puede concluir que:

1.- La inactivación de surfactante pulmonar por meconio se debe principalmente a la inserción de colesterol en las membranas de surfactante y contribuye al desarrollo del MAS. El efecto fluidificante del colesterol en el surfactante se manifiesta como el colapso temprano de la película interfacial durante la compresión. La adición de un 4% de colesterol parece ser suficiente para inactivar el surfactante, siempre que el colesterol esté solubilizado en agua mediante algún agente. La solubilización de colesterol por sales biliares o M β CD simula el efecto del colesterol, así se puede concluir que el principal responsable de la inactivación por meconio debe ser el colesterol soluble en agua.

2.- Optimización de métodos biofísicos permite el estudio de la implicación de la inactivación por suero, meconio y colesterol. Además, el desarrollo de métodos estandarizados que permitan el estudio sistemático de la inactivación del surfactante pulmonar y la adición de compuestos en busca de mejorar la resistencia de las preparaciones de surfactante a la inactivación. Se confirmó que la adición de polímeros, como el dextrano o el ácido hialurónico, restaura la actividad del surfactante pulmonar en presencia de agentes con diferentes mecanismos de inactivación. Por ello, parece que la resistencia a la inactivación adquirida por la presencia de polímeros no es específica para cada mecanismo de inactivación, sino general para el surfactante pulmonar.

3.- Las fuerzas entrópicas, como la presión osmótica o las fuerzas de exclusión (o *depletion*), actúan sobre el surfactante resultando en un incremento de la actividad interfacial del surfactante. Combinación de estas fuerzas entrópicas conlleva la agregación de los complejos de surfactante, incremento de la actividad interfacial y el refinamiento de la composición lipídica. El enriquecimiento en especie saturadas de los fosfolípidos de surfactante contribuye a la resistencia a la inactivación impuesta por una barrera estérica de proteínas tensio-activas, junto con la pérdida de especies insaturadas de fosfolípidos y colesterol que puede resultar beneficiosa en el caso de la presencia de un exceso de moléculas que perturban la estructura y propiedades de las membranas. Además, los cambios en estructura y composición inducidos por el ácido hialurónico son irreversibles, por ello el pre-tratamiento y consiguiente eliminación del polímero resulta en una preparación de surfactante pre-activada con una elevada resistencia a inactivación.

4.- Caracterización biofísica de muestras de pacientes de ARDS nos muestra una correlación significativa entre elevada tensión superficial del surfactante de pacientes con parámetros clínicos, especialmente en el caso de ARDS directo. Valores reducidos de PaO₂/FiO₂ y CRS correlacionan con alta tensión superficial, indicando que una reducida función pulmonar está relacionada con la disfunción del surfactante pulmonar. Además altos valores de PRISM y Murray'score correlacionan

Conclusions and Perspectives

con elevada tensión superficial, indicando peor pronóstico clínico para los pacientes con un surfactante inactivado, especialmente en casos de ARDS directo. Esto destaca la implicación de la inactivación de surfactante en el desarrollo y pronóstico del ARDS. Aunque no se puede concluir sobre el mecanismo molecular exacto de inactivación, parece ser un proceso multifactorial que incluye proteínas tensio-activas que compiten por la interfase, así como la inserción de moléculas que afecta a las propiedades de las membranas de surfactante, el responsable de la inactivación de surfactante y la elevada tensión superficial. Por lo tanto, el desarrollo de surfactantes resistentes a diferentes agentes inactivadores parece una estrategia terapéutica prometedora para el tratamiento de patologías respiratorias como el ARDS.

5.- Combinación de datos moleculares, celulares y biofísicos permiten el estudio detallado de un modelo animal deficiente en Napsina A. Los resultados sugieren que en ausencia de Napsina A la SP-B se sigue procesando, lo que permite proponer una ruta de procesamiento alternativo que se basa en la activación de las Catepsinas D y E. Además, la acumulación de proteínas dentro de los pneumocitos tipo II resulta en la activación de respuestas de estrés en el retículo endoplásmico con su consecuente daño celular, simulando las condiciones de fibrosis pulmonar. Aunque los animales estudiados no muestran desarrollo de tejido fibrótico, muestran principios de daño en los pneumocitos tipo II indicando una etapa temprana de IPF. Se plantea la hipótesis de que probablemente animales más mayores desarrollen IPF o son más susceptibles a la inducción de IPF.

Combinación de datos moleculares, biofísicos y clínicos abre la posibilidad de integrar numerosos datos relevantes que ayudan a entender las patologías respiratorias y desarrollar nuevas estrategias terapéuticas para su tratamiento. Se propone la pre-incubación de preparaciones de surfactante con HA como paso en el proceso de producción de surfactante clínicos. Si los surfactantes clínicos disponibles muestran cambios estructurales y composicionales en la misma dirección que el surfactante nativo todavía está por determinar. Actualmente, los surfactantes clínicos se someten a extracción orgánica, con la consecuente eliminación de la SP-A y la pérdida de la estructura nativa, por lo tanto, el HA no tiene por qué tener el mismo efecto en este caso. Sin embargo, el desarrollo de surfactantes con una elevada resistencia a diferentes agentes inactivadores parece ser una estrategia prometedora para el tratamiento de patologías respiratorias en las que agentes externos llegan a los espacios alveolares. Además, si la tensión superficial elevada contribuye al daño pulmonar, la prevención de la inactivación del surfactante será esencial en el tratamiento de patologías respiratorias. Además, el surfactante aplicado de manera exógena podría ser utilizado como vehículo de transporte de otros compuestos dirigidos al epitelio pulmonar. Por ejemplo, la combinación de agentes anti-inflamatorios, para el tratamiento de ARDS, o de agentes anti-fibróticos, para IPF, con surfactante podría suponer una nueva estrategia terapéutica a explorar.

MATERIALS AND METHODS

MATERIALS

Native porcine lung surfactant

Native porcine lung surfactant was purified from bronchoalveolar lavage (BAL) by NaBr density-gradient centrifugation as previously described (Taeusch et al. 2005). Briefly, bronchoalveolar lavage was performed in porcine lungs with a NaCl 0.9% solution and centrifuged at 1.000g for 5 min to remove cells and cell debris. BALs are stored at -20°C until its use. To obtain surfactant complexes, we first performed a centrifugation at 100.000xg, 4°C 1h to pellet the full membrane fraction, latter these pellets are centrifuged in a discontinuous density gradient for 2h, 120.000g 4°C. Solutions used to prepare the density gradient include NaBr 16%, NaCl 0.9% for the higher density, NaBr 13% NaCl 0.9% for the medium density and NaCl 0.9% for the less dense solution. At the end of the density gradient centrifugation, surfactant complexes, comprising phospholipids and all the proteins that interact with them, including SP-B, SP-C, SP-A and others such as haemoglobin or some immunoglobulins, are concentrated in between the last two density solutions forming a compact layer.

Isolated surfactant was used without further organic extraction, in aqueous solution, and contains the full complement of proteins SP-A, SP-B and SP-C. It also maintains most of its original structure, including a fair amount of lamellar bodies and tubular myelin, as checked by electron microscopy (Ravasio et al. 2010). Surfactant concentration was measured by analysis of lipid phosphorous as it will be described below.

Dilutions of the material to the required phospholipid concentration were made with 5mM Tris buffer, pH 7, containing 150mM NaCl.

Surfactant treatment:

In different experiments, native surfactant was subjected to different treatments, including transient exposure to inactivating and activating agents and fluorescence label.

- Native surfactant was incubated with meconium at the desired concentration before testing the effect on structure and surface activity. First-passed meconium from term infants was collected by Prof William Taeusch at the neonatal service of San Francisco General Hospital and lyophilized as a pool. Dry weight of meconium was used as a basis to dosage in mixtures with surfactant. The organic extract of meconium was obtained following the standard Bligh & Dyer method.
- Taurocholic acid (TA) (Sigma, St Louis, MO) and cholesterol (Avanti Polar Lipids, Birmingham, AL) were pre-mixed with native surfactant at a final concentration of 1mM TA with 4% cholesterol (w/w cholesterol/phospholipid) to surfactant preparation.
- Complexes of cholesterol and methyl- β -cyclodextrine (M β CD) were purchased as Cholesterol Water Soluble from Sigma (St Louis, MO) and added to surfactant at a final proportion of 4% cholesterol (w/w cholesterol/phospholipid).
- Porcine serum was used without further dilution as a final concentration of 100mg/ml protein to test inhibition of surfactant at the CBS.
- To test their properties to prevent or reduce inactivation of surfactant, dextrane (148kDa, Sigma) and hyaluronic acid (HA) were prepared as a concentrated stock solution of 10mg/ml and diluted to the desired

Materials and Methods

concentration with buffer 5mM Tris, 150mM NaCl, pH 7. Two different hyaluronic acids were used in the experiments a 120kDa hyaluronic acid from *Streptococcus zooepidemicus* (H9390, Sigma) and a 150kDa extra pure hyaluronic acid from umbilical cord (HYA-150k, Hyalose), to test variability of effects between HA preparations.

- To label native surfactant with fluorescence probes, BODIPY-PC or Laurdan (Invitrogen) were incorporated at 1% (dye/phospholipid) molar ratio as described in Ravasio et al. 2008. Rhodamine-DPPE or Rhodamine-DOPE and TopFluor-Cholesterol (Avanti, St Louis, MO) were also used to label surfactant at a final concentration of 1% mol/mol (dye/phospholipid)
- Pre-activated surfactant was obtained by incubating surfactant with the desired HA concentration for 30min. For eliminating HA, the mixture was centrifuged at 15.000 rpm for 30min, recovering surfactant within the pellet while HA was eliminated in the supernatant.

Organic extracts of surfactant: organic extracts of the less polar components of surfactant or meconium were obtained following the protocol developed by Bligh and Dyer (Bligh and Dyer 1959). Briefly, 1 volume of the sample was mixed with 2 volumes of methanol and 1 volume of chloroform and vigorously mixed for 30sec. After 30 min of incubation at 37°C of the mixture, soluble proteins appear aggregated. Addition of 1 volume of chloroform and 1 volume of water gives rise to the formation of two phases that can be separated by centrifugation (2500rpm, 5min, 4°C). The organic phase is kept and the aqueous phase is subjected to a second extraction step for maximum efficiency of the lipid extraction. Further addition of 1 volume of chloroform to the aqueous phase, with mixing and centrifugation in the same conditions leads to the maximum yield of phospholipid extraction. Organic phases collected were then stored at -20°C.

Native surfactant from patients

Native surfactant from patients was also isolated from samples of BAL provided by Dr. Daniele de Luca from Hospital A. Gemelli in the context of a clinical study approved by the Ethical Committee of the hospital. Non-bronchoscopic bronchoalveolar lavage was performed within 6h from the fulfilling of ARDS criteria or from the intubation (in controls). Lavage was performed following recommendations of the European Respiratory Society Pediatric Task Force (de Blic et al. 2000) by instillation of two sequential aliquots of 1 mL/kg (up to a maximum of 5 mL) 0.9% NaCl warmed at 37°C, into the endotracheal tube, followed by three respiratory cycles. A straight, snub-nosed, end-hole suction catheter was gently advanced into the endotracheal tube, while continuing ventilation through a Y-connector. When resistance was met, suctioning with 50 mmHg of negative pressure was applied. The procedure was repeated with the infant's head turned 90° to the left and then to the right in order to virtually ensure sampling from the right and the left lung, respectively. An average of 1.8±0.5 mL (about 40% of the instilled volume) was obtained and was diluted with 0.9% saline up to 2 mL and centrifuged (3000 rpm, 4°C, 10min). Cell-free supernatants were separated, immediately frozen at -80°C and thawed only once for the experiments. All BAL samples were later centrifuged at

100.000xg, 1h, 4°C to recover pellets which were used to determine phospholipid concentration by phosphorous assay (see bellow) before diluting them to 10mg/ml with Tris 5mM, NaCl 150mM, pH 7, previous to their testing.

Native surfactant from mice

Native surfactant was isolated from mice BAL. Lavage was performed with an intratracheal catheter by instillation of 300ul of saline solution (0.9% NaCl) 3 times. Murine BAL was centrifuged at 3000rpm (4°C, 10 min) for pelleting cells and cell debris and immediately frozen and stored at -80°C.

Lung tissue from mice

- Homogenate tissue: lungs were stored at -80 °C in saline solution until further homogenization. Homogenization was carried out by adding ceramic pearls to the tissue and shaking the mixture (600g) for 30sec (Precellys® 24, Bertin Technologies, France)
- Tissue for histology: lungs were fixed in situ with 4.5% formaldehyde in phosphate-buffered saline (pH 7.0) at a pressure of 20 cmH₂O (1.96 kPa). After overnight fixation in 4.5% formaldehyde, the lungs were embedded in paraffin, cut into 4-µm slices and stained (see immunohistochemistry procedure bellow)

METHODS

Biochemical assays:

- *Phospholipid quantitation by phosphorous analysis* (Rouser et al. 1966): Briefly, samples and standards are dried in a sand bath, and mineralization of the organic phosphorous from phospholipids was carried by adding perchloric acid (37%) to the samples and incubating for 30min at 260°C. The quantitation of mineralized phosphorous was achieved through a colorimetric reaction upon addition of ammonium molybdate 2.5% that in an acid solution forms phosphomolybdic acid by reacting with phosphorous. Adding a reducing agent such as ascorbic acid 10% turns phosphomolybdic acid into phosphomolybdate with a blue colour. The colorimetric reaction was carried out during 7 min at 100°C, and stopped by keeping the samples in ice until measurement. Then quantitated colour at 820 nm was directly related to phosphorous concentration by interpolation into a calibration curve built with known concentrations of phosphate. The values were transformed to phospholipid concentration using 734Da as the average molecular size of surfactant phospholipids.
- *Quantitation of protein content* (Lowry et al. 1951): this chemical method is based on the reactivity of the peptide bonds (nitrogen) with copper ions under alkaline conditions. Therefore samples and standards (albumin) were mixed with SDS 10%, NaK Tartrate 2%, CuSO₄ 0.01% and

Materials and Methods

Na_2CO_3 0.02% and incubated for 15 min at room temperature. Further incubation during 30 min with Folin reagent (phosphotungstic acid and phosphomolybdic acid) turns the yellow colour of Folin reagent into blue colour of the reduced reagent. The reduction of the Folin reagent is a consequence of the copper-catalyzed oxidation of the Tyrosine residues of the proteins. Therefore the absorbance at 700nm can be directly related to the protein concentration.

- *Quantitation of cholesterol assay:* carried out with a commercial kit (Spinreact, Girona, Spain) based on the activity of the enzyme cholesterol oxydase in a set of coupled reactions that ends with the formation of a coloured compound. A first reaction is carried out by a cholesterol esterase and which breaks down cholesterol esters in cholesterol and fatty acids. Total free cholesterol in the sample is then oxidized by the cholesterol oxidase into 4-cholestenona and H_2O_2 . The colorimetric reaction takes place between H_2O_2 , phenol and 4-aminophenazone to produce quinonimine, a substance with a pinkish colour. Enzymes, substrates and standard are provided in the commercial kit, and the incubation of samples and standards with the enzyme mixture during 15 min at room temperature and followed by measurement of the absorbance at 505nm gives the cholesterol concentration of the samples.
- *Quantitation of bile:* carried out by a commercial kit (Materlab, Madrid, Spain) in which bile acids are converted by 3- α -HSDH (3- α -hydroxysteroid dehydrogenase) into the corresponding ketons, in the presence of NAD. The NADH so formed reacts with NBT (NitroBlue Tetrazolium) yielding formazan (blue coloured). The reaction is catalysed by diaphorase. Therefore, intensity of the colour is directly proportional to bile acid concentration in the sample. Incubation of the sample and standards with the working reagents provided by the commercial kit during 15 min at 37°C produces the colour measured at 540nm.

Surface balance measurements: for evaluating surface activity of surfactant complexes three different methodologies were used in this Thesis. In the surface balances we can evaluate how surface pressure changes during adsorption of surfactant, during the spreading of the film and upon compression-expansion cycling. Every balance has a pressure sensor with a Wilhelmy plate that monitors changes in surface pressure (π). Surface pressure is the difference between surface tension of water in absence and in presence of a surface active material such as lung surfactant ($\pi = \gamma_{\text{water}} - \gamma_{\text{surfactant}}$).

- *Wilhelmy balance:*

- π -t isotherms: surfactant adsorption was measured over time in a thermostated Teflon trough (Nima Technology, Coventry, UK) with

1.5ml of stirred subphase at 25°C, as described (Cruz et al. 2000). 150µg of surfactant were injected into the subphase, that in some experiments contained meconium, and pressure-time kinetics were followed over 5 minutes (as seen in figure 13).

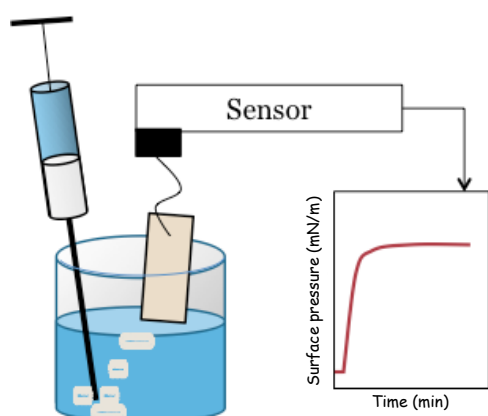


Figure 13: schematic representation of a Wilhelmy balance for interfacial adsorption measurements. The Wilhelmy plate is connected to a pressure sensor; allowing changes in surface pressure to be monitored with time. The sample is injected in the subphase and as soon as surfactant reaches the interface, changes in surface pressure can be observed.

- π -t spreading kinetics: interfacial adsorption of native or meconium-pre-treated surfactant was also assessed after direct spreading of the samples at the interface of a 22.5 cm² Teflon trough (Nima Technology, Coventry, UK) containing 14ml of subphase.

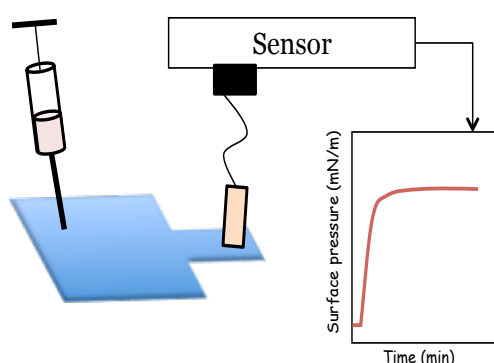


Figure 14: schematic representation of a Wilhelmy balance used for spreading measurements. Samples are applied directly at the interface in the opposite side of the trough to the point where the pressure sensor is located; then changes in surface pressure can be monitored as material spreads from the application point to the Wilhelmy plate.

- *Langmuir-Wilhelmy balance*: it consists of a Teflon thermostated trough that contains an aqueous subphase and a pressure sensor, similar to the setup used for the first time by Clements in 1957 for evaluating surfactant activity under compression-expansion dynamics (Clements 1957). Surfactant is applied at the interface and the amphipathic molecules form an interfacial monolayer or Langmuir film. With a mobile barrier the phospholipid film is confined to a defined changing area (A). Closing the barrier the interfacial film is compressed, modifying the lateral pressure asserted on and by the phospholipids, so that lipid packing can be studied. Opening the barrier, reorganization of the material in an expanded surface can be analyzed. Thus, full π -Area isotherms were obtained. Similar to the one shown in figure 15.

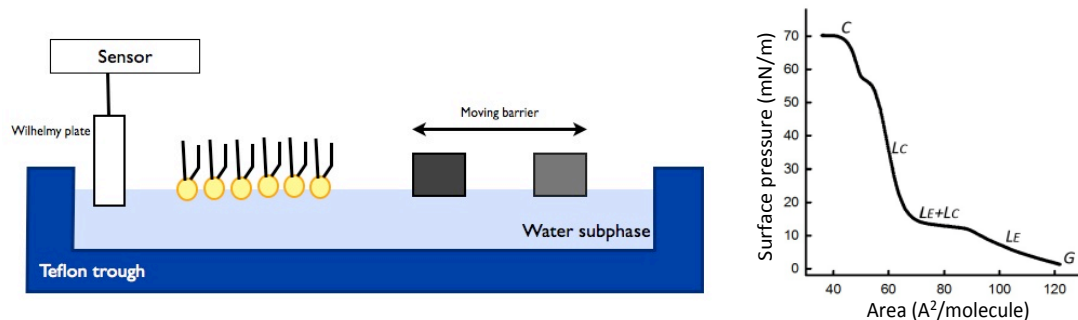


Figure 15: Schematic representation of a Langmuir-Wilhelmy balance (left) and a typical isotherm obtained from a pure DPPC film (left). Labels in the different segments of the isotherm identify lateral phases with different defined packing properties.

During compression of the interfacial film, changes in surface pressure reflect changes in lipid packing and the occurrence of two-dimensional transition phases. In a typical isotherm of DPPC, 5 different packing states can be elucidated. At low surface pressure the interfacial film shows properties of a bi-dimensional gas (G), where the phospholipids are dispersed in the interface with a high degree of motion freedom. Further compression allows intermolecular interactions so that surface pressure starts raising in a phase called liquid-expanded (LE), where the phospholipids still have considerable lateral mobility and numerous trans-gauche isomerizations. Progressive compression leads to the orientation of the acyl chains of the phospholipids perpendicular to the interface plane into a liquid-condensed (LC) state, where the molecules are tightly compressed. A plateau between LE and LC segments of the isotherm indicates a coexistence of both phases, so that the work of compression is used to complete the lateral packing of the phospholipids. If compression is still increased further, it may end in the rupture of the interfacial film or collapse (C) from bi-dimensional to tri-dimensional planes (Takamoto et al. 2001; Takamoto et al. 2001b; Wüstneck et al. 2005). Shifting of the isotherms to larger or smaller areas indicate insertion or desorption of material into or from the interfacial film which may lead to changes in the compressibility properties (lateral compression) of the phospholipids. Therefore, the detailed analysis of compression isotherms allows studying the insertion of material into surfactant interfacial films or its interaction with different substances at the interface.

To study the interfacial properties of native surfactant in a Langmuir-Wilhelmy balance we spread native surfactant as aqueous suspension onto a buffered (5mM Tris pH 7, 150mM NaCl,) subphase in a surface balance equipped with a 200cm² trough and a continuous Teflon ribbon barrier and a (Nima Technology, Coventry, UK). After 10min equilibration, the resulting films were compressed at 60cm²/min from a maximum area of 200 cm² to a minimum area of 20cm². Native surfactant isotherms are different from the pure DPPC films but still allows identification of

liquid-expanded phase, coexistence of LE-LC phases (typically at surface pressure of 45mN/m) and liquid condensed phases (see figure 16).

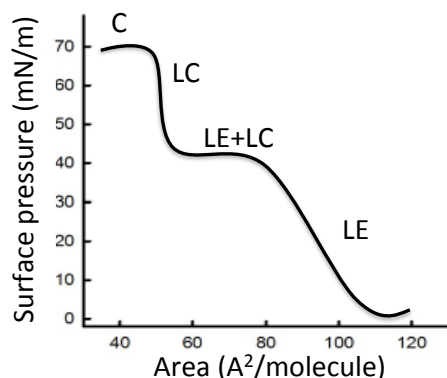


Figure 16: Representation of a complete native surfactant isotherm obtained in a Langmuir-Wilhelmy balance. Native surfactant films can be compressed from liquid expanded to liquid condensed phases with a clear plateau at around 45-50mN/m where both phases co-exist.

In addition to compression isotherms, interfacial films can be also transferred during compression onto solid supports for later structural studies (Blodgett 1935). Following the COVASP (continuously varying surface pressure) method (Wang et al. 2007) films were transferred during compression, so that the structure of the different compression-driven phases could be captured and immobilized. Introduction into the films of a fluorescent label allowed the observation of segregation of different membrane domains as a function of compression. Fluorescence probes such as NBD-PC and BODIPY-PC insert into surfactant membranes, preferentially in disordered phases, thus we can visualize ordered domains as dark spots where the fluorescence probe has been excluded.

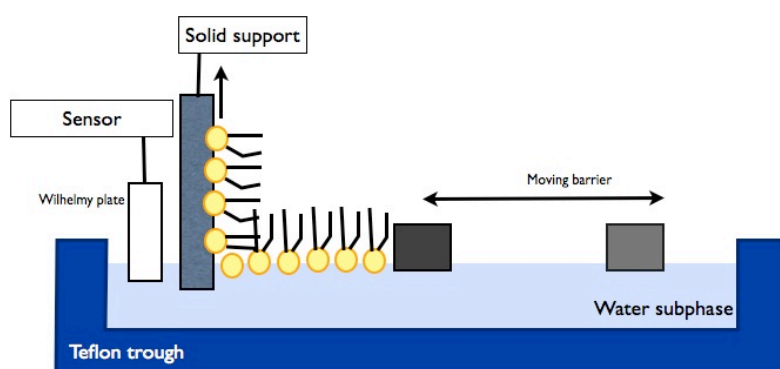


Figure 17: Schematic representation of the method used to obtain supported Langmuir-Blodgett films. Addition to the Langmuir-Wilhelmy balance of a deeper system that holds and moves vertically a solid support, makes COVASP transfer of material possible. In the example shown, the solid support is embedded into the water surface and it is lifted simultaneously to the closing of the barrier.

Materials and Methods

Epifluorescence microscopy images were later obtained from the COVASP films transferred onto a glass coverslide in a Zeiss Axioplan II microscope and analysed with Image J software.

Captive Bubble Surfactometer

The captive bubble surfactometer (CBS) is an experimental setup where surface activity of surfactant can be monitored after adsorption into the air-water interface of an air bubble enclosed in a chamber under controlled environmental conditions. The CBS was firstly design, built and optimized in Dr. Samuel Schurch laboratory at the University of Calgary in the 80's, with the main objective of studying the biophysical behaviour of films formed by surfactants from animal or synthetic sources under physiologically relevant conditions (Schürch et al. 1989). CBS software allows the calculation of the surface tension and the changes in total surface and volume of the bubble, from the diameter and height of the bubble, which is recorded and monitored with a video camera using an axisymmetric model (Schoel et al. 1994).

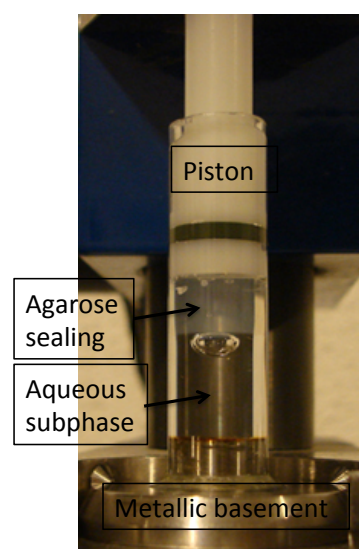
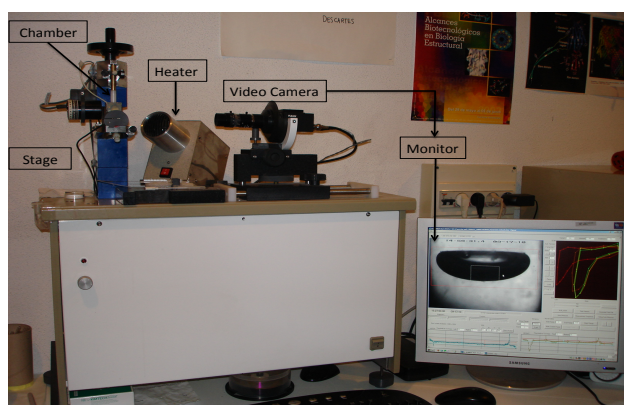


Figure 18: Integration of the different parts of the CBS system used in the current Thesis (left) with a detailed of the bubble chamber (right). The stage includes the chamber containing the air bubble closed by a piston which movement increases or decreases the bubble size. A temperature sensor is introduced into the chamber water bath controlling the heating required for thermostating the system. A digital video camera is constantly recording the change in shape and size of the bubble, which is registered in a computer and analysed with the CBS Post software. At the right image, a zoom of the bubble chamber shows how the bubble is fully enclosed in an aqueous subphase between the metallic basement and the agarose sealing. The piston closes the chamber and its vertical movement increases or decreases the bubble size.

The chamber is basically a glass cylinder with a metallic base perforated by a little hole (2mm) through which the bubble can be created ($0.035\text{-}0.040\text{cm}^3$), by just allowing air to come in, and through which a capillary is inserted to permit the application of the sample. The other side of the chamber is sealed with an agarose

(1% w/v) cap and adjusted to a piston, which will be moved resulting in the compression or expansion of the space between the agarose cap and the metallic base. The chamber is filled with an aqueous solution, typically Tris 5mM, NaCl 150mM containing sucrose 10%. The addition of sucrose to the aqueous subphase increases the density of the solution and therefore when surfactant is applied it floats against the bubble, avoiding dilution of material through the 1.5mL subphase. Prior to the application of the sample, degasification of the subphase is performed by simply expanding a bubble in the sealed chamber and waiting for 10min. The dissolved air in the aqueous subphase is then liberated in form of little bubbles that will join the expanded one, due to the pressure inside the chamber. The chamber is thermostated by a metallic jacket, which constitutes a water bath that distributes heat homogeneously from an external heat source. Temperature is continuously controlled by a feedback system that includes a thermocouple in contact with the water bath, and connected to the computer. Typically, surfactant preparations are applied in CBS experiments at high concentrations, such as 25mg/ml (as in chapter 1), but lower concentrations can also be used for studying surfactant behaviour. In this Thesis we have tested surfactant samples at 10mg/ml (chapter 2-5) and this is also the concentration chosen for studying susceptibility of surfactant to inactivation.

The protocol to characterize the behaviour of surfactant samples at the CBS includes 4 steps, which allows a detailed evaluation of the main biophysical properties of surfactant.

- **Initial adsorption (IA) kinetics:** shows the ability of surfactant to reach the interface and form a film able to reduce surface tension to equilibrium. In the CBS experiments a transparent capillary connected to a syringe is introduced into the chamber. This transparent capillary contains surfactant (150nL) and approaches the bubble surface. In some experiments (such as those carried out chapter 1) the bubble surface is touched with the surfactant-loaded capillary in order to apply the surfactant directly into the interface. In later experiments (those in chapters 2-5) the capillary approaches the bubble but does not touch the bubble surface, so that real adsorption, meaning reaching and transferring material into the interface can be studied. We can visualize the change in surface tension through the changes in bubble shape during 5 min after application of the sample, as the bubble gets flatter at lower surface tension. Typically, surfactant reduces surface tension from around 70mN/m (the surface tension of the aqueous subphase) to 22-23mN/m, the equilibrium surface tension of surfactant, in a few seconds.

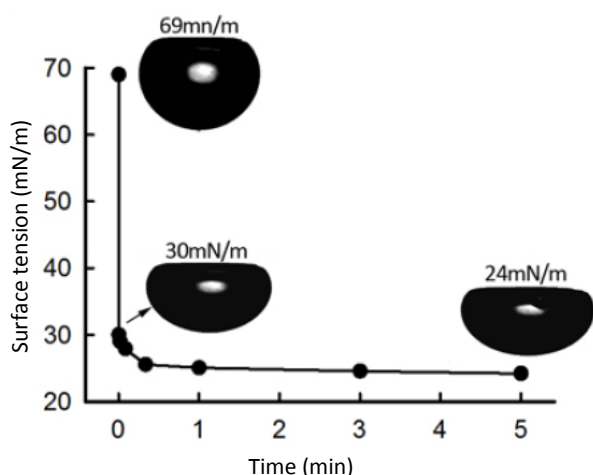


Figure 19: Changes in bubble shape change due to decrease of surface tension during initial adsorption. The bubble gets flatter as the surface tension decreases rapidly within the first seconds after application of the sample down to equilibrium surface tension of around 22-25mN/m.

- **Post-expansion adsorption (PEA) kinetics:** where we can analyse the reorganization, transfer and spreading, of surfactant into an expanding interface. In the CBS experiment, after 5 min of initial adsorption, the chamber is sealed and the bubble is expanded by the movement of the piston controlled by the software to a maximum bubble size of 0.15cm³. Changes in surface tension occurring during 5min after rapid expansion.

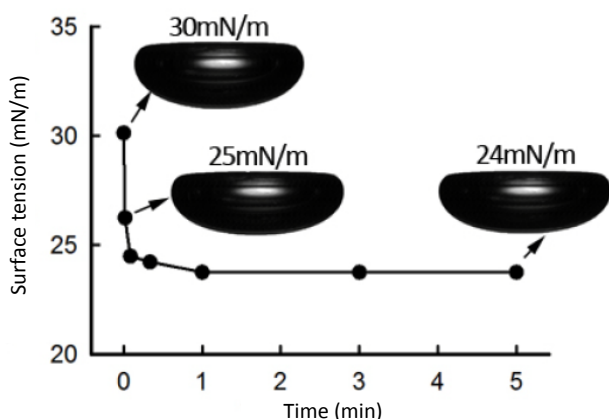


Figure 20: Changes in bubble shape change due to decay of surface tension during post-expansion adsorption. The bubble gets flatter as the surface tension decreases rapidly within the first seconds after expansion of the bubble, down to the equilibrium surface tension of around 22-25mN/m.

- **Quasi-static compression-expansion cycling:** Four slow step-wise compression and expansion cycles are applied to the bubble. Cycles are performed with 1 sec delay between compression steps, each reducing 20% its previous volume. Maximum bubble volume is set during post-expansion, while the operator sets the minimum bubble size just before the interfacial film collapses. Collapse of the bubble can be detected by a decrease of the width of the bubble whilst there is no more flattening. As a consequence, a decrease in the area of the bubble would be produced with no change in surface tension. As the compression-expansion speed in

these experiments is very slow, the film undergoes relaxation and reorganization process that can also be analysed. Thus, first q-static cycles often show a plateau, with a decrease in area and little change in surface tension, during which the energy provided by the compression is used to promote structural transition of material at the interface resulting in a partial depuration of the less active material out from the interface, a process known as “squeeze-out” (Schurch et al. 1994; Wüstneck et al. 2001). In a reversible process, expansion steps may produce similar isotherms to that from compression, but during the first q-static cycle the reorganization of material at the interface gives rise to isotherms with different tilt during compression and expansion, with some hysteresis. The area enclosed by the compression and expansion isotherms represents the ability of material to re-organize during the squeeze-out plateau and the expanding moiety of the cycles. This area represents the hysteresis of the cycle, and thus, the energy spent by the compression-expansion process. The subsequent cycles exhibit progressively reduced hysteresis, indicating that the refinement of material at the interface is irreversible.

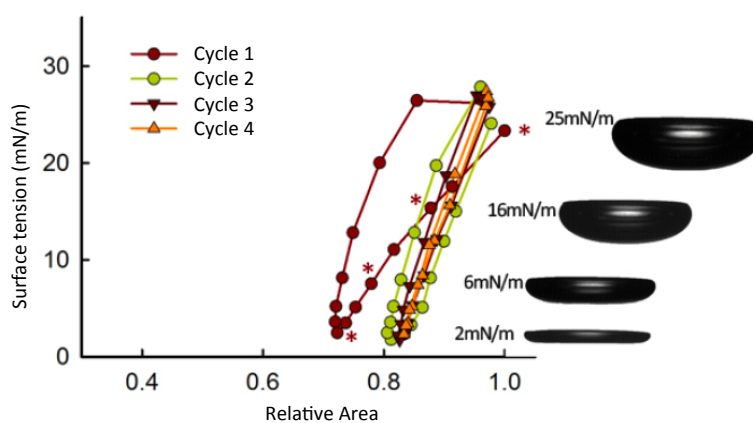


Figure 21: Changes in bubble shape associated with the surface tension/area isotherm during q-static compression-expansion cycles. Compression-expansion q-static isotherms relate the changes in surface tension with decreased and increased area. The change in bubble shape is shown during the first q-static compression.

- **Compression-expansion dynamic cycling:** the bubble is subjected to fast compression-expansion cycles, 20 cycles/min which resembles breathing physiological rates. Maximum and minimum volumes, defining the bubble cycling, are the same used in q-static cycles. With such a quick compression-expansion cycling neither reorganization nor relaxation of the film is permitted. Thus, good operative surfactant films exhibit reduced or no hysteresis and little area compression are needed for them to reach minimum surface tension.

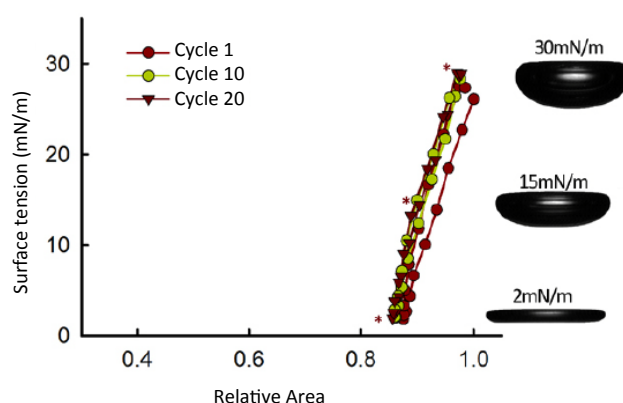


Figure 22: Changes in bubble shape associated with surface tension/area isotherm during dynamic compression-expansion cycles. Compression-expansion isotherms show the changes in surface tension upon reducing and increasing the area. The image illustrates how the shape of the bubble changes during the first dynamic compression.

In Chapter 1, CBS experiments were carried out at a final surfactant phospholipid concentration of 25mg/ml. Premixing with meconium (final concentration of 10mg/ml dry weight) or taurocholic acid (TA) and cholesterol (1mM TA and 4% cholesterol/surfactant phospholipid) were performed prior to injection.

In chapters 2-4, as already described, final concentration of surfactant in the CBS experiments was kept at 10mg/ml phospholipids and the samples were applied near the interface, as explained in detail in chapter 2. In order to study inactivation, we injected serum and surfactant sequentially allowing surfactant to compete with a preformed interfacial layer of serum. To analyze meconium or cholesterol inactivation we used the same method of application. In other experiments, polymers were premixed with surfactant and immediately injected as described above.

Fluorescence microplate assay

Accumulation of surfactant at the interface was evaluated in 96-well microtiter plates as described by Ravasio et al. (Ravasio et al. 2008), in a FLUORSTAR Optima Microplate Reader (BMG Labtech, GmbH). Briefly, this method is based on the addition of a fluorescence probe (i.e., BODIPY-PC) to surfactant membranes and the use of a quenching agent in the subphase (Brilliant black, Sigma Aldrich). Therefore, fluorescence is only detected when surfactant reaches the interface, bringing the probe to the interface out of the quenching subphase. This method allows quantitating not only the material right at the interface but also that accumulated up to 100nm depth into the subphase.

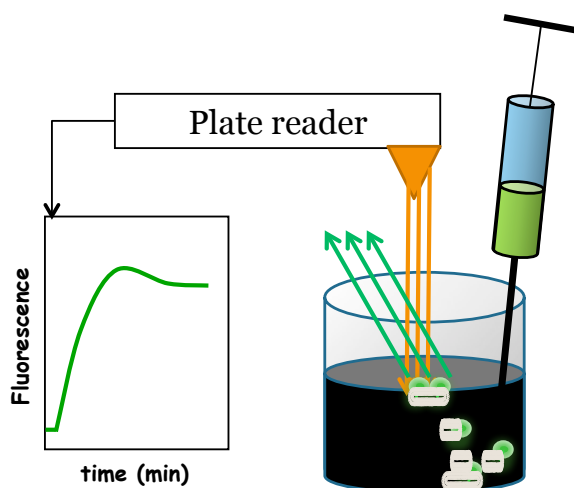


Figure 23: Schematic representation of the basis of the fluorescence microplate assay. A well from a microtiter plate with an aqueous subphase containing a quenching agent is represented. After injection of an aliquot of fluorescently-labelled surfactant, fluorescence intensity is monitored with a plate reader. Only the surfactant reaching the interface would be responsible for the emission of fluorescence.

In these experiments, meconium or meconium organic extract was mixed in 100ml subphase. Three μg of native surfactant was applied at the bottom of each well, and the fluorescence intensity reaching the surface was followed for 2 hours at 25°C. Data in these experiments are presented as the average of three replicates with their standard deviation, in relative fluorescence units (RFU-bg) corrected by subtraction of the measured background.

Laurdan Thermotropic profiles

Laurdan (6-lauroyl naphthalene) is a naphthalene derivative first designed to study dipolar relaxation. The fluorescent naphthalene moiety of this probe possesses a dipole moment that increases upon excitation and may cause reorientation of the solvent dipoles.

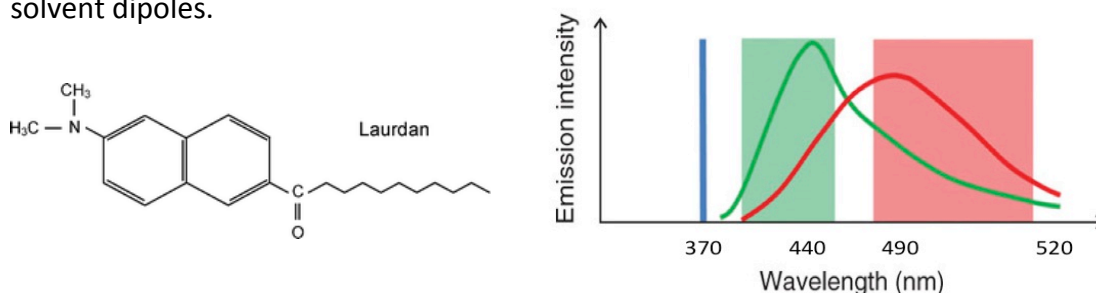


Figure 24: Structure (left) and emission spectra (right) of Laurdan. Emission spectra is shifted from blue (green spectra) to red emission (red spectra) in more polar environments (Owen et al. 2012). Blue line represents the excitation wavelength.

The energy required for solvent reorientation decreases the probe's excited state energy, which is reflected in a continuous red shifting of the probe's emission spectrum with respect to the excitation wavelength. A bluer emission is observed in apolar solvents, while redder emission occurs in polar solvents.

The emission maxima of Laurdan in phospholipids bilayers depend upon its hydration state, which is influenced by the phase state of the phospholipid, being

Materials and Methods

blue in gel phase ($\lambda_{\max} = 440\text{nm}$) and green in the liquid-crystalline phase ($\lambda_{\max} = 490\text{nm}$). At temperatures above the phospholipid phase transition, a continuous red shifting of the emission is observed, to a limiting green emission, with a maximum about 490 nm. This shift of the emission spectrum has been attributed to dipolar relaxation processes occurring in the phospholipid liquid-crystalline phase but not in the gel phase (Parasassi et al. 1998). The generalized polarization function (GP) is a quantitative measurement the extent at which Laurdan molecules are surrounded by liquid crystalline or by gel-phase phospholipids. GP function is defined as $GP = (I_B - I_R) / (I_B + I_R)$, being I_B and I_R the intensities at the blue and red edges of the emission spectrum of Laurdan, respectively (Parasassi et al. 1990; Parasassi et al. 1991).

The fluorescence emission spectra of Laurdan in surfactant suspensions and in surfactant mixed with meconium were obtained at different temperatures in a spectrofluorimeter SLM-Aminco AB2 (Urbana, IL). Emission spectra were recorded at 400-540nm upon excitation at 370nm.

Differential Scanning Calorimetry (DSC)

DSC is a thermoanalytical technique in which the difference in the amount of heat required to increase the temperature of a sample and a reference is measured as a function of temperature. Both the sample and reference are maintained at nearly the same temperature throughout the experiment. The basic principle underlying this technique is that when a sample undergoes a physical transformation such a phase transition, more or less heat will need to flow to it than to the reference to maintain both at the same temperature. Whether less or more heat must flow to the sample depends on whether the process in question is exothermic or endothermic. In a typical adiabatic calorimetry experiment, a chemical or physical transformation may be carried out in a sealed container insulated from heat losses to the outside. Measuring the heat (C_p) excess need to increase the temperature in the sample compared to the reference, at different temperatures, the energy content of the chemical or physical transformation (ΔH) can be calculated as $\Delta H = \Delta T \cdot C_p$.

Typically, lipid molecules forming bilayer structures are characterized by tightly packed all-trans hydrocarbon chains, partially dehydrated head groups and specific interaction between moieties on the polar head groups ($L\beta$). On heating, these structures may convert to the liquid-crystalline phase ($L\alpha$) through fairly energetic processes. Information about the physical properties of this transition can be read out of the thermograms. Firstly, when the peak is positive, the transition is endothermic, indicating the uptake of energy by the sample for the physical transformation. The temperature reached at the maximum heat is the T_m (melting temperature or transition midpoint) where half of the molecules have already changed the lipid phase, being this parameter characteristic of each lipid and lipid mixture depending on its composition. Finally $\Delta T_{1/2}$ is the temperature at half height of the transition peak that indicates the width of the peak and the cooperativity of the transition process (Lewis et al. 2007).

DSC thermograms of native surfactant or surfactant suspensions pre-exposed to meconium or taurocholic acid (TA) and cholesterol (Chol/TA), were obtained in a

Microcal MC-2 microcalorimeter (Amherst, MA, USA). Surfactant concentration in these experiments was 3mg/ml, with or without the addition of 10mg/ml meconium, or TA (10 μ M) + 1.6 % Cholesterol (w/w, Chol/phospholipid) and was analysed against 5mM Tris buffer 150mM NaCl as a reference. Scans were obtained from 15 to 55°C, at 30°C/h. Data were analysed with Origin Software (Northampton, MA).

Quarz crystal microbalance with dissipation (QCM-D)

A QCM consists of a thin quartz disc sandwiched between a pair of electrodes. Due to the piezoelectric properties of quartz, it is possible to excite the crystal to oscillation applying an AC voltage across its electrodes. Normally the electrodes are made in gold.

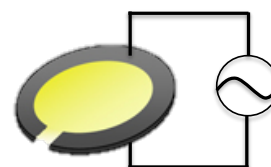


Figure 25: scheme of a gold QCM-D sensor. The gold sensor is connected to an AC voltage power that makes the sensor to oscillate.

The resonance frequency (f) of the sensor depends on the oscillating mass, including the water coupled to the oscillation. When a thin film is attached to the surface of the sensor, the frequency decreases. If the film is thin and rigid the decrease in

frequency is proportional to the mass of the film. In this way, QCM operate as a very sensitive balance. Structural properties are measured as changes in dissipation (damping) of the oscillating crystal. Dissipation is determined from the time it takes for the oscillation to stop when the power is disconnected.

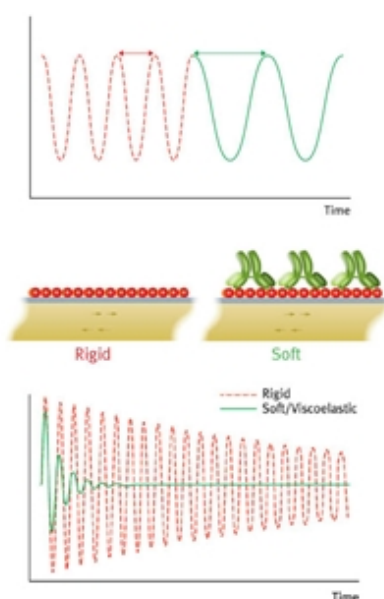


Figure 26: Changes in frequency and dissipation due to the attached mass in the sensor surface. Presence of a rigid material would decrease frequency with a little change in dissipation (red) while a soft material would change the frequency increasing the dissipation (green). Taken from Q-sense (Gothenburg, Sweden).

Hyaluronan-grafted membranes were prepared in the surface of a QCM crystal as described by Wolny et al. 2010. Briefly, a lipid film was first formed by applying a mixture of DOPC and biotinylated PE (Avanti Polar Lipids) followed by the application of neutravidin (NAv), finally biotinylated HA 150kDa (Hyalose, Oklahoma) was applied on top of the film. This allows the exposure of hyaluronan chains for studying specific binding. Finally we applied native surfactant complexes at a concentration of 0.1 mg/ml, to study potential HA/surfactant interactions.

Materials and Methods

Giant unilamellar vesicle (GUV) formation

The electroformation method was developed by Angelova and others and has been widely used for preparing GUVs (Puff and Angelova 2006). Applying a low voltage electric field can promote the formation of unilamellar vesicles. For GUV electroformation, a solution of lipids is dried onto an ITO (Indium Tin Oxide)-coated glass surface connected to electrodes. The hydration is then performed in the presence of an electric (alternating) field. The alternating field induces the formation of unilamellar vesicles upon swelling of the lipid layers in an aqueous environment.

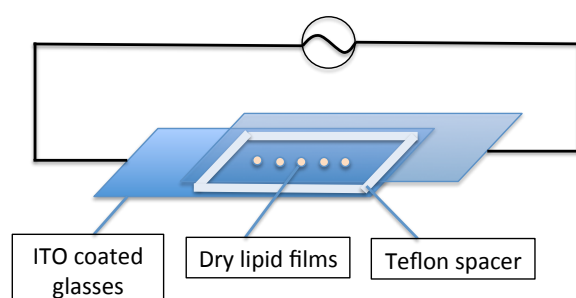


Figure 27: scheme of the disposition of the ITO-coated glass chamber connected to an alternating power supply.

The sample is dried on the surface of the ITO-coated plates prior to chamber assembling. ITO-coated sides of the plates are placed facing each other and the chamber is sealed with Teflon spacers and vacuum grease. The chamber is filled with buffer before complete sealing.

Native surfactant labelled with Rhodamine DOPE and BODIPY-cholesterol at a phospholipid concentration of 2mg/ml was applied as little drops in both ITO-coated glasses and dried at 37°C. Two ITO-coated glasses are then assembled into a capacitor type configuration. The chamber is filled with buffer and sealed with Teflon spacers and vacuum grease. ITO-coated glasses are then connected to a pulse generator and an alternating voltage is applied. We applied 500Hz of frequency and 250mV and increase the voltage every 5 min until 1.5V. Then, frequency and voltage is kept at 500Hz and 1.5V for 1h. Latter we decrease the frequency 100Hz every 10 min (Pott et al. 2008).

Fluorescence spectroscopy

Fluorescence occurs when the electron in the excited state (S_1) has a spin opposite to that of the second electron in the ground state (S_0) orbital (singlet state), consequently the return to the ground state is spin-allowed and occurs rapidly by the emission of a photon with a fluorescence lifetime in the nanosecond scale.

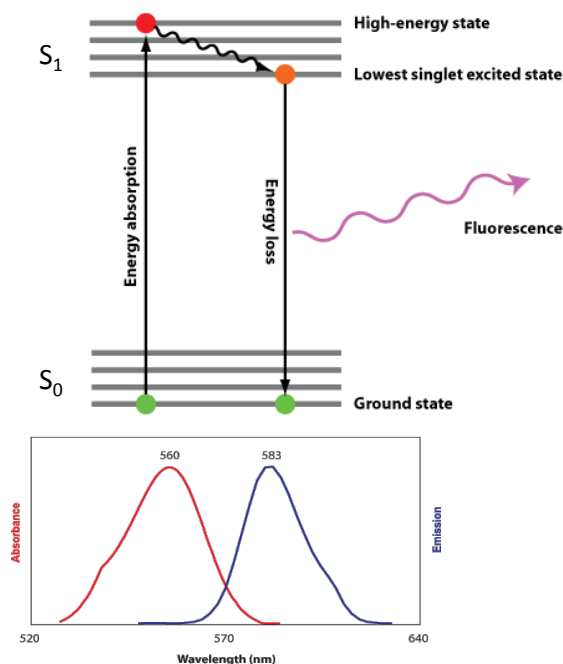


Figure 28: Jablonski diagram showing the energy diagram of the excited states of an electron upon excitation. Returning to the ground state occurs with the emission of fluorescence light. The graph below presents the absorption and emission spectra of a Rhodamine dye. Spectra do not overlap as the difference represents the small loss of energy due to the interactions of the absorbing molecule with surrounding solvent molecules. This shift of the emission wavelength relative to the adsorption wavelength is the so-called Stoke's shift.

Emission spectra of Rhodamine-DOPE or Rhodamine-DPPE labelled surfactant were taken in a spectrofluorimeter SLM-Aminco AB2 (Urbana, IL). Emission spectra were recorded in the 570-640nm range upon excitation at 560nm.

Formation and aggregation of LUVs

Large unilamellar vesicles (LUVs) were formed using a mini extruder (Avanti Polar Lipids) with a membrane of a fixed porous size of 0.1 μ m. Flow of multilamellar vesicles, formed by rehydration of dried lipid films or native surfactant suspensions, through the extruder membranes several times lead to the extrusion of unilamellar vesicles of approximately the same size of the porous size.

Aggregation of LUVs was monitored by the apparent increase in the absorbance at 400nm due to turbidity. Suspended particles in an aqueous suspension may scatter light of wavelength comparable to the particle size, resulting in an apparent light absorption or decrease in light transmittance. Bigger or aggregated particles may scatter more light than small ones.

Absorbance at 400nm was followed in surfactant LUVs upon addition of different concentrations of hyaluronic acid.

Immunohistochemistry

For the immunohistochemistry study of lung tissue from mice models we have used a protocol in which the retrieval of the antigens are carried out by boiling the

Materials and Methods

samples with a citrate buffer. Formalin or other aldehyde fixation forms protein cross-links that mask the antigenic sites in tissue specimens, thereby giving weak or false negative staining for immunohistochemical detection of certain proteins. The citrate-based solution is designed to break the protein cross-links, therefore unmask the antigens and epitopes in formalin-fixed and paraffin embedded tissue sections, thus enhancing staining intensity of antibodies. Firstly, sections are incubated during 2h at 60°C to fix it to the slide and latter sections are immersed in xylol and different ethanol baths to eliminate the paraffin and rehydrate the tissue. Following we proceed to retrieve antigens by boiling the sample with citrate buffer 2mM. After washing the samples with PBS, incubation with antibodies starts. Primary antibodies used are: anti-SP-C (WRAB-76694), anti SP-B (WRAB-48604), anti-proSP-C (WRAB-55522), anti-proSP-B (WRAB-9337) all from Seven Hills (Cincinnati, OH), anti-TTF-1 (sc13040) and anti-XBP-1 (sc7160) were from Santa Cruz Biotechnology (Santa Cruz, CA). Incubation with the primary in 2% BSA-solution (bovine serum albumin in PBS buffer) was performed for 2h at room temperature. Thereafter slides are washed again with PBS for eliminating the excess of primary antibody. For secondary antibody we used ZytoChem-Plus AP Kit (Zytomed Systems, Berlin, Germany), which is based on a polyvalent biotinylated secondary antibody, a solution of streptavidin-alkaline phosphatase conjugate that will accomplish the reaction that will result in pinkish colour of the Fast-Red reagent. Counterstaining of the nuclei was performed with haemalunan. Slides were scanned with Mirax Scan (CarlZeiss, Germany) and evaluated with Miramax Viewer (CarlZeiss, Germany).

SDS-PAGE and Western-Blot

The analysis of the protein content in BAL and LH from Napsin A KO mice was performed by SDS-PAGE and Western-Blot. Briefly, polyacrylamide gels were made at 15% acrylamide for small proteins (mSP-B and mSP-C) and 12% for large proteins (proSP-B and proSP-C) under denaturing conditions. Samples were prepared in the presence of the reducing agent β -mercaptoethanol and boiled for 10 min. Samples from LH had 30 μ g of protein, whereas 20 μ l of each BAL sample were applied onto the gels. Proteins were transferred to PVDF membranes with a semi-dry system for 1.5h at 2.3mA/cm² membrane. Blocking of the membrane was performed by incubating in TBS-T 5% milk for 2h. Over night incubation of the primary antibody in TBS-T (Tris 50mM, Tween 1%), 5% milk was followed by 2h incubation with the secondary antibody. Washing of the membrane was performed between antibodies and before developing with TBS-T. Developing of the bands was done using a commercial ECL (Amersham ECL Prime, GE Healthcare). Densitometry of the western-blot was carried out with Image J software.

Primary antibodies used were: anti-SP-C (WRAB-76694), anti SP-B (WRAB-48604), anti-proSP-C (WRAB-55522), and anti-proSP-B (WRAB-9337) from Seven Hills (Cincinnati, OH). Secondary antibody used was a swain anti rabbit (P0217) from Dako (Germany).

RNA extraction and RT-PCR

RNA extraction was performed after homogenization of lung tissue with the commercial kit RNeasy Plus Mini (Qiagen). Briefly, biological samples were first lysed and homogenized in a highly denaturing guanidine-isothiocyanate-containing buffer, which immediately inactivates RNases to ensure isolation of intact RNA. The lysate is then passed through a gDNA Eliminator spin column. This column, in combination with the optimized high-salt buffer, allows efficient removal of genomic DNA. Ethanol was added to the flow through to provide appropriate binding conditions for RNA, and the sample was then applied to an RNeasy spin column. RNA binds to the membrane and contaminants are efficiently washed away. High-quality RNA was then eluted in water. Once isolated and quantified by the absorbance at 260nm with a NanoDrop (ThermoScientific) RNA could be used for reverse transcription. Reverse transcription was performed using the commercial kit Omniscript® Reverse Transcription from Qiagen. Briefly, reverse transcriptase is a multifunctional enzyme with 3 different enzymatic activities: an RNA-dependent DNA polymerase, a hybrid-dependent exoribonuclease (RNase H), and a DNA-dependent DNA polymerase. In vivo, the combination of these 3 activities allows transcription of single-stranded RNA genome into double-stranded DNA for retroviral infection. For reverse transcription in vitro, the first two activities are utilized to produce single-stranded cDNA. Thus, Omniscript RT (4 units) was mixed with dNTP Mix (0.5mM each), Oligo-dT primer (1uM), RNase inhibitor (10 units) and the appropriate buffer, provided by the commercial kit, and lastly template RNA (2ug) was added to the mixture. Incubation of the reaction mixture at 37°C during 1h resulted in the production of the desired cDNA. Finally polymerase chain reaction (PCR) of the desired genes was performed using the commercial kit Phire® Hot Start II DNA Polymerase (Finnzymes) and the primers designed with the on-line software GeneFisher (<http://bibiserv.techfak.uni-bielefeld.de/genefisher2/>) and synthesized by MetaBion (Germany). Briefly, PCR with Hot Start II DNA polymerase is based on the fact that this enzyme is not active at room temperature, thus avoiding unspecific amplification. The cycling protocol includes 30sec at 98°C for activating the enzyme, followed by 5 sec at 98°C for denaturation of the DNA molecule, another 5sec at the annealing primer temperature, and 20 sec at 72°C where the extension of the nascent DNA chain happens. This protocol was repeated 25-35 cycles, depending on the original level of expression of each gene. A further 1 min at 72°C allowed the final extension of the chains, and the resulting DNA was kept at 4°C till use. PCR mixtures contained dNTPs (200uM each), Phire® Hot Start II DNA polymerase (2.5 units) and Phire® Reaction Buffer, containing Mg²⁺ (1.5mM), all provided in the commercial kit. Finally, addition of forward and reverse primers (0.5µM each) (MetaBion, Germany) and the template DNA (200ng) completed the mixture for the reaction. For visualizing and quantifying the results of the amplified genes, 2% agarose gels were performed with 0.2% etidium bromide. Images of the gels were analysed with the software ImageLab (BioRad).

Primers used (from Metabion), cycling and annealing temperature conditions:

Materials and Methods

| Protein | Forward primer | Reverse primer | Cycles | T(°C) |
|----------------|------------------------|-----------------------|--------|-------|
| β -Actin | CTACAGCTTCACCACCACAG | CTCGTTGCCAATAGTGATGAC | 28 | 62 |
| Napsin A | AGGTCCACATGGAGAGTGTG | CTTGGGGATATCCAAGGCTG | 25 | 63 |
| Pepsinogen C | TGTACACTGGAGAGCTCA | TCCTCCTGGATGGAGGAAG | 30 | 62 |
| Cathepsin D | GGTAACTGAGCCAGGACAC | CCGTGGTAGTACTTGGAGTC | 28 | 60 |
| Cathepsin E | GGAATCATTGGAGCTGATCAAG | CTCCGAAAGTCAGCTCACTG | 28 | 63 |
| Cathepsin H | GAGTCAGCTAATGCTATTGC | CAGTCACCTCAAAGGCGAAG | 28 | 62.4 |
| mSP-B | GGAAGATGCTTTCCAGGAAGC | TGCTCAGAGAAGTCCTGAGTG | 28 | 62.8 |
| mSP-C | TCATGAGATGGTCCTTGAGATG | GGAAGAGTCGGACTCGGAAG | 28 | 61.4 |
| ABCA3 | GCAAGCTCTCCATTGGCATC | CACCAGCTGAGAGATTCCTTC | 25 | 62.4 |
| XBP-1 | GAACCAGGAGTTAAGAACACG | AGGCAACAGTGTGAGAGTCC | 30 | 62 |
| CHOP | CCTAGCTTGGCTGACAGAG | GTCAGGCGCTCGATTTC | 28 | 61 |
| EDEM | GCAATGTTGTGAACATCCAGA | CATCTCCACATCCCCTATCAG | 28 | 63 |

Data reproducibility and statistics

Data are in general terms expressed as average and standard deviation of at least three replicates within independent experiments. For clinical data, averages of three experiments are represented with the 5th and 95th percentiles of each group. When possible, comparison between two groups was carried out by a T-Test; if variance test failed then a Rank Sum test or Saphiro Wilk Test was performed. For clinical data, Spearman correlation coefficient was calculated with its p-value for statistically significance for a confidence interval of 95%.

LIST OF PUBLICATIONS

List of Publications

Lopez-Rodriguez E., Echaide M., Cruz A., Taeusch H.W., and Perez-Gil J. (2011) Meconium impairs pulmonary surfactant by a combined action of cholesterol and bile acids. *Biophysical Journal* 100 (3): 646-655

Lopez-Rodriguez E., Ospina O.L., Echaide M., Taeusch H.W. and Perez-Gil J. (2012) Exposure to polymers reverses inhibition of pulmonary surfactant by serum, meconium or cholesterol in the Captive Bubble Surfactometer. *Biophysical Journal* 103: 1451-1459

Lopez-Rodriguez E., Cruz A., Richter R., Taeusch H.W. and Perez-Gil J (2012) Structural and functional modification of pulmonary surfactant pre-activated by hyaluronic acid. Article in preparation.

Blanco O., Cruz A., Ospina O.L., **Lopez-Rodriguez E.**, Vazquez L and Perez-Gil J (2012) Interfacial behaviour and structural properties of a clinical lung surfactant from porcine source. *Biochimica et Biophysica Acta (BBA)-Biomembranes* 1818 (11): 2756-2766

Lashkmi S., **Lopez-Rodriguez E.**, Ospina O.L., Cruz A., Orgeig S., and Perez-Gil J (2012) Palmitoyl palmitoleoyl phosphatidylcholine and cholesterol form highly packed phases in lung surfactant layers. *Journal of Lipid Research* (submitted)

De Luca D., **Lopez-Rodriguez E.**, Minucci A., Vendittelli F., Leonarda G., Stival E., Conti G, Piastra M., Antonelli M., Echaide M., Perez-Gil J., and Capoluongo E.D. (2012) Clinical and biological role of secretory phospholipase A2 in infants with acute respiratory distress syndrome. *American Journal of Respiratory Critical Care Medicine* (submitted)

List of Publications

REFERENCES

References

- Anzueto, A., R. P. Baughman, K. K. Guntupalli, J. G. Weg, H. P. Wiedemann, A. A. Raventós, F. Lemaire, W. Long, D. S. Zaccardelli and E. N. Pattishall (1996). "Aerosolized Surfactant in Adults with Sepsis-Induced Acute Respiratory Distress Syndrome." New England Journal of Medicine **334**(22): 1417-1422.
- Bae, C.-W., A. Takahashi, S. Chida and M. Sasaki (1998). "Morphology and Function of Pulmonary Surfactant Inhibited by Meconium." Pediatric Research **44**(2): 187-191.
- Ban, N., Y. Matsumura, H. Sakai, Y. Takanezawa, M. Sasaki, H. Arai and N. Inagaki (2007). "ABCA3 as a Lipid Transporter in Pulmonary Surfactant Biogenesis." Journal of Biological Chemistry **282**(13): 9628-9634.
- Baoukina, S. and D. P. Tieleman (2011). "Lung Surfactant Protein SP-B Promotes Formation of Bilayer Reservoirs from Monolayer and Lipid Transfer between the Interface and Subphase." Biophysical Journal **100**(7): 1678-1687.
- Barrett, A. J. (1970). "Cathepsin D. Purification of isoenzymes from human and chicken liver." The Biochemical journal **117**(3): 601-607.
- Baumgart, F., O. L. Ospina, I. Mingarro, I. Rodríguez-Crespo and J. Pérez-Gil (2010). "Palmitoylation of Pulmonary Surfactant Protein SP-C Is Critical for Its Functional Cooperation with SP-B to Sustain Compression/Expansion Dynamics in Cholesterol-Containing Surfactant Films." Biophysical Journal **99**(10): 3234-3243.
- Been, J. V. and L. J. Zimmermann (2007). "What's new in surfactant? A clinical view on recent developments in neonatology and paediatrics." Eur J Pediatr **166**(9): 889-899.
- Bernardino de la Serna, J., G. Orädd, L. A. Bagatolli, A. C. Simonsen, D. Marsh, G. Lindblom and J. Perez-Gil (2009). "Segregated Phases in Pulmonary Surfactant Membranes Do Not Show Coexistence of Lipid Populations with Differentiated Dynamic Properties." Biophysical Journal **97**(5): 1381-1389.
- Bernardino de la Serna, J., J. Perez-Gil, A. C. Simonsen and L. A. Bagatolli (2004). "Cholesterol Rules." Journal of Biological Chemistry **279**(39): 40715-40722.
- Bernardino de la Serna, J., R. Vargas, V. Picardi, A. Cruz, R. Arranz, J. M. Valpuesta, L. Mateu and J. Perez-Gil (2012). "Segregated ordered lipid phases and protein-promoted membran cohesivity are required for pulmonary surfactant films to stabilize and protect the respiratory surface." Faraday Discussions **in press**.
- Bhattacharya, J., T. Cruz, S. Bhattacharya and B. A. Bray (1989). "Hyaluronan affects extravascular water in lungs of unanesthetized rabbits." Journal of Applied Physiology **66**(6): 2595-2599.
- Bi, X., C. R. Flach, J. Pérez-Gil, I. Plasencia, D. Andreu, E. Oliveira and R. Mendelsohn (2002). "Secondary Structure and Lipid Interactions of the N-Terminal Segment of Pulmonary Surfactant SP-C in Langmuir Films: IR Reflection–Absorption Spectroscopy and Surface Pressure Studies†." Biochemistry **41**(26): 8385-8395.
- Blanco, O., A. Cruz, O. L. Ospina, E. López-Rodríguez, L. Vázquez and J. Pérez-Gil (2012). "Interfacial behavior and structural properties of a clinical lung surfactant from porcine source." Biochimica et Biophysica Acta (BBA) - Biomembranes **1818**(11): 2756-2766.

References

- Blanco, O. and J. Pérez-Gil (2007). "Biochemical and pharmacological differences between preparations of exogenous natural surfactant used to treat Respiratory Distress Syndrome: Role of the different components in an efficient pulmonary surfactant." European Journal of Pharmacology **568**(1-3): 1-15.
- Bligh, E. G. and W. J. Dyer (1959). "A rapid method of total lipid extraction and purification." Canadian Journal of Biochemistry and Physiology **37**(8): 911-917.
- Blodgett, K. B. (1935). "Films Built by Depositing Successive Monomolecular Layers on a Solid Surface." Journal of the American Chemical Society **57**(6): 1007-1022.
- Brasch, F. (2004). "Surfactant protein B in type II pneumocytes and intra-alveolar surfactant forms of human lungs." Am J Respir Cell Mol Biol **30**: 449-458.
- Brasch, F., A. t. Brinke, G. Johnen, M. Ochs, N. Kapp, K. M. Muller, M. F. Beers, H. Fehrenbach, J. Richter, J. J. Batenburg and F. Buhling (2002). Involvement of cathepsin H in the processing of the hydrophobic surfactant-associated protein C in type II pneumocytes.
- Brasch, F., M. Ochs, T. Kähne, S. Guttentag, V. Schauer-Vukasinovic, M. Derrick, G. Johnen, N. Kapp, K.-M. Müller, J. Richter, T. Giller, S. Hawgood and F. Böhling (2003). "Involvement of Napsin A in the C- and N-terminal Processing of Surfactant Protein B in Type-II Pneumocytes of the Human Lung." Journal of Biological Chemistry **278**(49): 49006-49014.
- Bray, B. A. (2001). "The Role of Hyaluronan in the Pulmonary Alveolus." Journal of Theoretical Biology **210**(1): 121-130.
- Calkovska, A., D. Mokra, A. Drgova, I. Zila and K. Javorka (2008). "Bronchoalveolar lavage with pulmonary surfactant/dextran mixture improves meconium clearance and lung functions in experimental meconium aspiration syndrome." Eur J Pediatr **167**(8): 851-857.
- Campbell, H., K. Bosma, A. Brackenbury, L. McCaig, L. J. Yao, R. Veldhuizen and J. Lewis (2002). "Polyethylene glycol (PEG) attenuates exogenous surfactant in lung-injured adult rabbits." Am J Respir Crit Care Med **165**(4): 475-480.
- Casals, C. and O. Cañadas (2012). "Role of lipid ordered/disordered phase coexistence in pulmonary surfactant function." Biochimica et Biophysica Acta (BBA) - Biomembranes **1818**(11): 2550-2562.
- Casals, C., A. Varela, M. L. F. Ruano, F. Valiño, J. Perez-Gil, N. Torre, E. Jorge, F. Tendillo and J. L. Castillo-Olivares (1998). "Increase of C-Reactive Protein and Decrease of Surfactant Protein A in Surfactant after Lung Transplantation." American Journal of Respiratory and Critical Care Medicine **157**(1): 43-49.
- Chavarha, M., H. Khoojinian, L. E. Schulwitz Jr, S. C. Biswas, S. B. Rananavare and S. B. Hall (2010). "Hydrophobic Surfactant Proteins Induce a Phosphatidylethanolamine to Form Cubic Phases." Biophysical Journal **98**(8): 1549-1557.
- Clark, J. C., S. E. Wert, C. J. Bachurski, M. T. Stahlman, B. R. Stripp, T. E. Weaver and J. A. Whitsett (1995). "Targeted disruption of the surfactant protein B gene disrupts surfactant homeostasis, causing respiratory failure in newborn mice." Proceedings of the National Academy of Sciences **92**(17): 7794-7798.

- Clements, J. A. (1957). "Surface Tension of Lung Extracts." Proceedings of the Society for Experimental Biology and Medicine. Society for Experimental Biology and Medicine (New York, N.Y.) **95**(1): 170-172.
- Comper, W. D. and T. C. Laurent (1978). "Physiological function of connective tissue polysaccharides." Physiological Reviews **58**(1): 255-315.
- Cook, M., R. C. Caswell, R. J. Richards, J. Kay and P. J. Tatnell (2001). "Regulation of human and mouse procathepsin E gene expression." European Journal of Biochemistry **268**(9): 2658-2668.
- Coultas, D. B., R. E. Zumwalt, W. C. Black and R. E. Sobonya (1994). "The epidemiology of interstitial lung diseases." American Journal of Respiratory and Critical Care Medicine **150**(4): 967-972.
- Creuwels, L. A. J. M., L. M. G. van Golde and H. P. Haagsman (1997). "The Pulmonary Surfactant System: Biochemical and Clinical Aspects." Lung **175**(1): 1-39.
- Cruz, A. and J. Perez-Gil (2007). Langmuir films to determine lateral surface pressure on lipid segregation. Methods in membrane lipids. New Jersey, Humana Press. **400**: 439-457.
- Cruz, A., L. A. D. Worthman, A. G. Serrano, C. Casals, K. M. W. Keough and J. Perez-Gil (2000). "Microstructure and dynamic surface properties of surfactant protein SP-B/dipalmitoylphosphatidylcholine interfacial films spread from lipid-protein bilayers." European Biophysics Journal **29**: 204-213.
- Daniels, C. B. and S. Orgeig (2003). "Pulmonary Surfactant: The Key to the Evolution of Air Breathing." Physiology **18**(4): 151-157.
- de Blic, J., F. Midulla, A. Barbato, A. Clement, I. Dab, E. Eber, C. Green, J. Grigg, S. Kotecha, G. Kurland, P. Pohunek, F. Ratjen and G. Rossi (2000). "Bronchoalveolar lavage in children. ERS Task Force on bronchoalveolar lavage in children. European Respiratory Society." European Respiratory Journal **15**(1): 217-231.
- De Luca, D., S. Baroni, G. Vento, M. Piastra, D. Pietrini, F. Romitelli, E. Capoluongo, C. Romagnoli, G. Conti and E. Zecca (2008). "Secretory phospholipase A2 and neonatal respiratory distress: pilot study on broncho-alveolar lavage." Intensive Care Medicine **34**(10): 1858-1864.
- De Luca, D., A. Minucci, E. Zecca, M. Piastra, D. Pietrini, V. Carnielli, C. Zuppi, A. Tridente, G. Conti and E. Capoluongo (2009). "Bile acids cause secretory phospholipase A2 activity enhancement, revertible by exogenous surfactant administration." Intensive Care Medicine **35**(2): 321-326.
- deFelice, M., D. Silberschmidt, R. DiLauro, Y. Xu, S. E. Wert, T. E. Weaver, C. J. Bachurski, J. C. Clark and J. A. Whitsett (2003). "TTF-1 Phosphorylation Is Required for Peripheral Lung Morphogenesis, Perinatal Survival, and Tissue-specific Gene Expression." Journal of Biological Chemistry **278**(37): 35574-35583.
- Dehority, W., K. W. Lu, J. Clements, J. Goerke, J. F. Pittet, L. Allen and H. W. Taeusch (2005). "Polyethylene glycol-surfactant for lavage lung injury in rats." Pediatr Res **58**(5): 913-918.
- Dejmek, A., P. Naucler, A. Smedjeback, H. Kato, M. Maeda, K. Yashima, J. Maeda and T. Hirano (2007). "Napsin A (TA02) is a useful alternative to thyroid transcription factor-1 (TTF-1) for the identification of pulmonary adenocarcinoma cells in pleural effusions." Diagnostic Cytopathology **35**(8): 493-497.

References

- Dempsey, O. J., K. M. Kerr, L. Gomersall, H. Remmen and G. P. Currie (2006). "Idiopathic pulmonary fibrosis: an update." *QJM* **99**(10): 643-654.
- Desmedt, S. C., P. Dekeyser, V. Ribitsch, A. Lauwers and J. Demeester (1993). "Viscoelastic and Transient Network Properties of Hyaluronic-Acid as a Function of the Concentration." *Biorheology* **30**(1): 31-41.
- Discher, B. M., K. M. Maloney, W. R. Schief Jr, D. W. Grainger, V. Vogel and S. B. Hall (1996). "Lateral phase separation in interfacial films of pulmonary surfactant." *Biophysical Journal* **71**(5): 2583-2590.
- Dushianthan, A., M. P. W. Grocott, A. D. Postle and R. Cusack (2011). "Acute respiratory distress syndrome and acute lung injury." *Postgraduate Medical Journal* **87**(1031): 612-622.
- El Shahed, A., P. A. Dargaville, A. Ohlsson and R. Soll (2007). "Surfactant for meconium aspiration syndrome in full term/near term infants." *Cochrane Database of Systematic Reviews* **3**.
- Fam, H., J. T. Bryant and M. Kontopoulou (2007). "Rheological properties of synovial fluids." *Biorheology* **44**(2): 59-74.
- Fam, H., M. Kontopoulou and J. T. Bryant (2009). "Effect of concentration and molecular weight on the rheology of hyaluronic acid/bovine calf serum solutions." *Biorheology* **46**(1): 31-43.
- Fernsler, J. G. and J. A. Zasadzinski (2009). "Competitive Adsorption: A Physical Model for Lung Surfactant Inactivation." *Langmuir* **25**(14): 8131-8143.
- Fernsler, J. G. and J. A. Zasadzinski (2009). "Competitive adsorption: a physical model for lung surfactant inactivation." *Langmuir* **25**(14): 8131-8143.
- Foster, C., A. Aktar, D. Kopf, P. Zhang and S. Guttentag (2004). "Pepsinogen C: a type 2 cell-specific protease." *American Journal of Physiology - Lung Cellular and Molecular Physiology* **286**(2): L382-L387.
- Fraser, J., T. J. Brown, T. N. P. Cahill, T. C. Laurent and U. B. G. Laurent (1996). "The turnover of hyaluronan in synovial joints." *Immunol Cell Biol* **74**(2): A10-A10.
- Fraser, J. R. E., T. C. Laurent and U. B. G. Laurent (1997). "Hyaluronan: its nature, distribution, functions and turnover." *Journal of Internal Medicine* **242**(1): 27-33.
- Gattinoni, L., M. Bombino and P. Pelosi (1994). "Lung structure and function in different stages of severe adult respiratory distress syndrome." *JAMA: The Journal of the American Medical Association* **271**(22): 1772-1779.
- Gaver, D. P., D. Halpern and O. Jensen (2005). Surfactant and airway liquid flows. *Molecular Mechanisms in Lung Surfactant (Dys)function*. K.Nag. New York, Marcel Dekker: 178-223.
- Gerson, K. D., C. D. Foster, P. Zhang, Z. Zhang, M. M. Rosenblatt and S. H. Guttentag (2008). "Pepsinogen C Proteolytic Processing of Surfactant Protein B." *Journal of Biological Chemistry* **283**(16): 10330-10338.
- Goerke, J. (1998). "Pulmonary surfactant: functions and molecular composition." *Biochimica et Biophysica Acta (BBA)/Molecular Basis of Disease* **1408**: 79-89.
- Gómez-Gil, L., D. Schürch, E. Goormaghtigh and J. Pérez-Gil (2009). "Pulmonary Surfactant Protein SP-C Counteracts the Deleterious Effects of Cholesterol on the Activity of Surfactant Films under Physiologically Relevant Compression-Expansion Dynamics." *Biophysical Journal* **97**(10): 2736-2745.

- Greene, K. E., J. R. Wright, K. P. Steinberg, J. T. Ruzinski, E. Caldwell, W. B. Wong, W. Hull, J. A. Whitsett, T. Akino, Y. Kuroki, H. Nagae, L. D. Hudson and T. Martin, R (1999). "Serial Changes in Surfactant-associated Proteins in Lung and Serum before and after Onset of ARDS." American Journal of Respiratory and Critical Care Medicine **160**(6): 1843-1850.
- Gregory, T. J., W. J. Longmore, M. A. Moxley, J. A. Whitsett, C. R. Reed, A. A. Fowler, L. D. Hudson, R. J. Maunder, C. Crim and T. M. Hyers (1991). "Surfactant chemical composition and biophysical activity in acute respiratory distress syndrome." J. Clin Invest **88**: 1976-1981.
- Gregory, T. J., K. P. Steinberg, R. Spragg, J. E. Gadek, T. M. Hyers, W. J. Longmore, M. A. Moxley, G. Z. Cai, R. D. Hite, R. M. Smith, L. D. Hudson, C. Crim, P. Newton, B. R. Mitchell and A. J. Gold (1997). "Bovine surfactant therapy for patients with acute respiratory distress syndrome." American Journal of Respiratory and Critical Care Medicine **155**(4): 1309-1315.
- Gross, T., E. Zmora, Y. Levi-Kalishman, O. Regev and A. Berman (2006). "Lung-Surfactant-Meconium Interaction: In Vitro Study in Bulk and at the Air-Solution Interface." Langmuir **22**(7): 3243-3250.
- Gunasekara, L., W. M. Schoel, S. Schurch and M. W. Amrein (2008). "A comparative study of mechanisms of surfactant inhibition." Biochim Biophys Acta **1778**(2): 433-444.
- Gunasekara, L., W. M. Schoel, S. Schürch and M. W. Amrein (2008). "A comparative study of mechanisms of surfactant inhibition." Biochimica et Biophysica Acta (BBA) - Biomembranes **1778**(2): 433-444.
- Gunasekara, L., S. Schürch, W. M. Schoel, K. Nag, Z. Leonenko, M. Haufs and M. Amrein (2005). "Pulmonary surfactant function is abolished by an elevated proportion of cholesterol." Biochimica et Biophysica Acta (BBA) - Molecular and Cell Biology of Lipids **1737**(1): 27-35.
- Gunasekara, L. C., R. M. Pratt, W. M. Schoel, S. Gosche, E. J. Prenner and M. W. Amrein (2010). "Methyl-beta-cyclodextrin restores the structure and function of pulmonary surfactant films impaired by cholesterol." Biochim Biophys Acta **1798**(5): 986-994.
- Gunasekara, L. C., R. M. Pratt, W. M. Schoel, S. Gosche, E. J. Prenner and M. W. Amrein (2010). "Methyl- β -cyclodextrin restores the structure and function of pulmonary surfactant films impaired by cholesterol." Biochimica et Biophysica Acta (BBA) - Biomembranes **1798**(5): 986-994.
- Günther, A., M. Kalinowski, S. Rosseau and W. Seeger (1995). "Surfactant incorporation markedly alters mechanical properties of a fibrin clot." American Journal of Respiratory Cell and Molecular Biology **13**(6): 712-718.
- Günther, A., M. Korfei, P. Mahavadi, D. von der Beck, C. Ruppert and P. Markart (2012). "Unravelling the progressive pathophysiology of idiopathic pulmonary fibrosis." European Respiratory Review **21**(124): 152-160.
- Günther, A., P. Markart, M. Kalinowski, C. Ruppert, F. Grimminger and W. Seeger (1999c). "Cleavage of surfactant-incorporating fibrin by different fibrinolytic agents. Kinetics of lysis and rescue of surface activity." Am J Respir Cell Mol Biol **21**: 738-745.
- Günther, A., C. Ruppert, R. Schmidt, P. Markart, F. Grimminger, D. Walmrath and W. Seeger (2001). "Surfactant alteration and replacement in acute respiratory distress syndrome." Respiratory Research **2**(6): 353 - 364.

References

- Günther, A., R. Schmidt, A. Feustel, U. Meier, C. Pucker, M. Ermet and W. Seeger (1999b). "Surfactant Subtype Conversion Is Related to Loss of Surfactant Apoprotein B and Surface Activity in Large Surfactant Aggregates." American Journal of Respiratory and Critical Care Medicine **159**(1): 244-251.
- Günther, A., R. Schmidt, F. Nix, M. Yabut-Perez, C. Guth, S. Rosseau, C. Siebert, F. Grimminger, H. Morr, H. g. Velcovsky and W. Seeger (1999). "Surfactant abnormalities in idiopathic pulmonary fibrosis, hypersensitivity pneumonitis and sarcoidosis." European Respiratory Journal **14**(3): 565-573.
- Günther, A., C. Siebert, R. Schmidt, S. Ziegler, F. Grimminger, M. Yabut, B. Temmesfeld, D. Walmrath, H. Morr and W. Seeger (1996). "Surfactant alterations in severe pneumonia, acute respiratory distress syndrome, and cardiogenic lung edema." American Journal of Respiratory and Critical Care Medicine **153**(1): 176-184.
- Guttentag, S., L. Robinson, P. Zhang, F. Bracsch, F. Hling and M. Beers (2003). "Cysteine protease activity is required for surfactant protein b processing and lamellar body genesis." American Thoracic Society **28**(1): 11.
- Hall, S. B., R. Z. Lu, A. R. Venkitaraman, R. W. Hyde and R. H. Notter (1992). "Inhibition of pulmonary surfactant by oleic acid: mechanisms and characteristics." J Appl Physiol **72**(5): 1708-1716.
- Hallman, M., R. Spragg, J. H. Harrell, K. M. Moser and L. Gluck (1982). "Evidence of lung surfactant abnormality in respiratory failure. Study of bronchoalveolar lavage phospholipids, surface activity, phospholipase activity, and plasma myoinositol." The Journal of Clinical Investigation **70**(3): 673-683.
- Herting, E., P. Rauprich, G. Stichtenoth, G. Walter, J. A. N. Johansson and B. Robertson (2001). "Resistance of Different Surfactant Preparations to Inactivation by Meconium." Pediatric Research **50**(1): 44-49.
- Herzog, E. L., A. R. Brody, T. V. Colby, R. Mason and M. C. Williams (2008). "Knowns and Unknowns of the Alveolus." Proceedings of the American Thoracic Society **5**(7): 778-782.
- Hills, B. A. (1999). "An alternative view of the role(s) of surfactant and the alveolar model." Journal of Applied Physiology **87**(5): 1567-1583.
- Hirano, T., G. Auer, M. Maeda, Y. Hagiwara, S. Okada, T. Ohira, K. Okuzawa, K. Fujioka, B. Franzén, N. Hibi, T. Seito, Y. Ebihara and H. Kato (2000). "Human Tissue Distribution of TA02, Which is Homologous with a New Type of Aspartic Proteinase, Napsin A." Cancer Science **91**(10): 1015-1021.
- Holm, B. A., Z. Wang and R. H. Notter (1999). "Multiple Mechanisms of Lung Surfactant Inhibition." Pediatric Research **46**(1): 85-93.
- Holmes, M. W., M. T. Bayliss and H. Muir (1988). "Hyaluronic acid in human articular cartilage. Age-related changes in content and size." Biochemical Journal **250**: 434-441.
- Ikegami, M., J. A. Whitsett, P. C. Martis and T. E. Weaver (2005). "Reversibility of lung inflammation caused by SP-B deficiency." American Journal of Physiology - Lung Cellular and Molecular Physiology **289**(6): L962-L970.
- Iwanicki, J. L., K. W. Lu and H. W. Tausch (2010). "Reductions of phospholipase A2 inhibition of pulmonary surfactant with hyaluronan." Experimental Lung Research **36**(3): 167-174.

- Johansson, J. and T. Curstedt (1997). "Molecular structures and interactions of pulmonary surfactant components." *Eur J Biochem* **244**(3): 675-693.
- Johansson, J., T. Szyperski, T. Curstedt and K. Wuethrich (1994). "The NMR Structure of the Pulmonary Surfactant-Associated Polypeptide SP-C in an Apolar Solvent Contains a Valyl-Rich .alpha.-Helix." *Biochemistry* **33**(19): 6015-6023.
- Keating, E., Y. Y. Zuo, S. M. Tadayyon, N. O. Petersen, F. Possmayer and R. A. W. Veldhuizen (2012). "A modified squeeze-out mechanism for generating high surface pressures with pulmonary surfactant." *Biochimica et Biophysica Acta (BBA) - Biomembranes* **1818**(5): 1225-1234.
- Kingma, P. S. and J. A. Whitsett (2006). "In defense of the lung: surfactant protein A and surfactant protein D." *Current Opinion in Pharmacology* **6**(3): 277-283.
- Korfei, M., C. Ruppert, P. Mahavadi, I. Henneke, P. Markart, M. Koch, G. Lang, L. Fink, R.-M. Bohle, W. Seeger, T. E. Weaver and A. Guenther (2008). "Epithelial Endoplasmic Reticulum Stress and Apoptosis in Sporadic Idiopathic Pulmonary Fibrosis." *American Journal of Respiratory and Critical Care Medicine* **178**(8): 838-846.
- Korfei, M., C. Ruppert, P. Mahavadi, M. Koch, P. Markart, H. Witt, G. Lang, W. Seeger, T. E. Weaver and A. Günther (2007). "Abnormal accumulation of unprocessed surfactant protein (SP)-B and activation of the ER stress pathway in patients with idiopathic pulmonary fibrosis (IPF) and nonspecific interstitial pneumonia (NSIP)." *Am J Respir Crit Care Med* **175**: A735.
- Lang, C. J., A. D. Postle, S. Orgeig, F. Possmayer, W. Bernhard, A. K. Panda, K. D. Jürgens, W. K. Milsom, K. Nag and C. B. Daniels (2005). "Dipalmitoylphosphatidylcholine is not the major surfactant phospholipid species in all mammals." *American Journal of Physiology - Regulatory, Integrative and Comparative Physiology* **289**(5): R1426-R1439.
- Laurent, T. C., U. B. G. Laurent and J. R. E. Fraser (1996). "The structure and function of hyaluronan: An overview." *Immunol Cell Biol* **74**(2): A1-A7.
- Lawson, W. E., P. F. Crossno, V. V. Polosukhin, J. Roldan, D.-S. Cheng, K. B. Lane, T. R. Blackwell, C. Xu, C. Markin, L. B. Ware, G. G. Miller, J. E. Loyd and T. S. Blackwell (2008). "Endoplasmic reticulum stress in alveolar epithelial cells is prominent in IPF: association with altered surfactant protein processing and herpesvirus infection." *American Journal of Physiology - Lung Cellular and Molecular Physiology* **294**(6): L1119-L1126.
- Leaver, S. K. and T. W. Evans (2007). "Acute respiratory distress syndrome." *BMJ* **335**(7616): 389-394.
- Leonenko, Z., S. Gill, S. Baoukina, L. Monticelli, J. Doehner, L. Gunasekara, F. Felderer, M. Rodenstein, L. M. Eng and M. Amrein (2007). "An Elevated Level of Cholesterol Impairs Self-Assembly of Pulmonary Surfactant into a Functional Film." *Biophysical Journal* **93**(2): 674-683.
- Leonenko, Z., S. Gill, S. Baoukina, L. Monticelli, J. Doehner, L. Gunasekara, F. Felderer, M. Rodenstein, L. M. Eng and M. Amrein (2007). "An elevated level of cholesterol impairs self-assembly of pulmonary surfactant into a functional film." *Biophys J* **93**(2): 674-683.
- Lewis, J. F., M. Ikegami and A. H. Jobe (1990). "Altered surfactant function and metabolism in rabbits with acute lung injury." *Journal of Applied Physiology* **69**(6): 2303-2310.

References

- Lewis, R. N., D. A. Mannoock and R. D. McElhaney (2007). Differential scanning calorimetry in the study of lipid phase transition in model and biological membranes: practical considerations. Methods in membrane lipids. New Jersey, Humana Press. **400**: 171-195.
- Li, J. J., R. L. Sanders, K. P. McAdam, C. A. Hales, B. T. Thompson, J. A. Gelfand and J. F. Burke (1989). "Impact of C-reactive protein (CRP) on surfactant function." The Journal of trauma **29**(12): 1690-1697.
- Lim, J. Y. and S. Arulkumaran (2008). "Meconium aspiration syndrome." Obstetrics, Gynaecology & Reproductive Medicine **18**(4): 106-109.
- Lindenskov, P. H., A. Castellheim, G. Aamodt and O. D. Saugstad (2005). "Meconium induced IL-8 production and intratracheal albumin alleviated lung injury in newborn pigs." Pediatr Res **57**(3): 371-377.
- Lopez-Rodriguez, E., M. Echaide, A. Cruz, H. W. Taeusch and J. Perez-Gil (2011). "Meconium Impairs Pulmonary Surfactant by a Combined Action of Cholesterol and Bile Acids." Biophysical Journal **100**(3): 646-655.
- Lowry, O. H., N. J. Rosebrough, A. L. Farr and R. J. Randall (1951). "Protein measurement with the Folin phenol reagent." J Biol Chem **193**(1): 265-275.
- Lu, J. R., T. J. Su and J. Penfold (1999). "Adsorption of Serum Albumins at the Air/Water Interface." Langmuir **15**(20): 6975-6983.
- Lu, K. W., J. Goerke, J. A. Clemens and H. W. Taeusch (2005). "Hyaluronan Reduces Surfactant Inhibition and Improves Rat Lung Function after Meconium Injury." Pediatric Research **58**(2): 206-210. 210.1203/1201.PDR.0000169981.0000106266.0000169983E.
- Lu, K. W., J. GOERKE, J. A. CLEMENTS and H. W. TAEUSCH (2005). "Hyaluronan Reduces Surfactant Inhibition and Improves Rat Lung Function after Meconium Injury." Pediatric Research **58**(2): 206-210.
- Lu, K. W., J. Goerke, J. A. Clements and H. W. Taeusch (2005b). "Hyaluronan decreases surfactant inactivation in vitro." Pediatr Res **57**(2): 237-241.
- Lu, K. W., J. s. P√@rez-Gil, M. Echaide and H. W. Taeusch (2011). "Pulmonary surfactant proteins and polymer combinations reduce surfactant inhibition by serum." Biochimica et Biophysica Acta (BBA) - Biomembranes **1808**(10): 2366-2373.
- Lu, K. W., J. s. P√@rez-Gil and H. W. Taeusch (2009). "Kinematic viscosity of therapeutic pulmonary surfactants with added polymers." Biochimica et Biophysica Acta (BBA) - Biomembranes **1788**(3): 632-637.
- Lu, K. W., J. Perez-Gil, M. Echaide and H. W. Taeusch (2011). "Pulmonary surfactant proteins and polymer combinations reduce surfactant inhibition by serum." Biochim Biophys Acta **1808**(10): 2366-2373.
- Lu, K. W., J. Perez-Gil and H. W. Taeusch (2009). "Kinematic viscosity of therapeutic pulmonary surfactants with added polymers." Biochim Biophys Acta **1788**(3): 632-637.
- Luhr, O. R., K. Antonsen, M. Karlsson, S. Aardel, A. Thorsteinsson, F. C. G., J. Bonde and t. A. S. Group (1999). "Incidence and Mortality after Acute Respiratory Failure and Acute Respiratory Distress Syndrome in Sweden, Denmark, and Iceland." American Journal of Respiratory and Critical Care Medicine **159**(6): 1849-1861.
- Lukovic, D., A. Cruz, A. Gonzalez-Horta, A. Almlen, T. Curstedt, I. Mingarro and J. Pérez-Gil (2012). "Interfacial Behavior of Recombinant Forms of Human Pulmonary Surfactant Protein SP-C." Langmuir **28**(20): 7811-7825.

- Mahavadi, P., M. Korfei, I. Henneke, G. Liebisch, G. Schmitz, B. R. Gochuico, P. Markart, S. Bellusci, W. Seeger, C. Ruppert and A. Guenther (2010). "Epithelial Stress and Apoptosis Underlie Hermansky-Pudlak Syndrome-associated Interstitial Pneumonia." American Journal of Respiratory and Critical Care Medicine **182**(2): 207-219.
- Markart, P., C. Ruppert, M. Wygrecka, T. Colaris, B. Dahal, D. Walmrath, H. Harbach, J. Wilhelm, W. Seeger, R. Schmidt and A. Guenther (2007). "Patients with ARDS show improvement but not normalisation of alveolar surface activity with surfactant treatment: putative role of neutral lipids." Thorax **62**(7): 588-594.
- Matar, O. K., R. V. Craster and M. R. E. Warner (2002). "Surfactant transport on highly viscous surface films." Journal of Fluid Mechanics **466**: 85-111.
- McEachren, T. M. and K. M. Keough (1995). "Phosphocholine reverses inhibition of pulmonary surfactant adsorption caused by C-reactive protein." American Journal of Physiology - Lung Cellular and Molecular Physiology **269**(4): L492-L497.
- Meyer, K. C. and J. J. Zimmerman (2002). "Inflammation and surfactant." Paediatric Respiratory Reviews **3**(4): 308-314.
- Montgomery, A., M. Stager, C. Carrico and L. Hudson (1985). "Causes of mortality in patients with the adult respiratory distress syndrome." American Journal of Respiratory and Critical Care Medicine **132**(3): 485-489.
- Mulugeta, S. and M. F. Beers (2006). "Surfactant protein C: Its unique properties and emerging immunomodulatory role in the lung." Microbes and Infection **8**(8): 2317-2323.
- Mulugeta, S., J. A. Maguire, J. L. Newitt, S. J. Russo, A. Kotorashvili and M. F. Beers (2007). "Misfolded BRICHOS SP-C mutant proteins induce apoptosis via caspase-4- and cytochrome c-related mechanisms." American Journal of Physiology - Lung Cellular and Molecular Physiology **293**(3): L720-L729.
- Nag, K., J. G. Munro, S. A. Hearn, J. Rasmusson, N. O. Petersen and F. Possmayer (1999). "Correlated Atomic Force and Transmission Electron Microscopy of Nanotubular Structures in Pulmonary Surfactant." Journal of Structural Biology **126**(1): 1-15.
- Nag, K., J. Perez-Gil, M. L. F. Ruano, L. A. D. Worthman, J. Stewart, C. Casals and K. M. W. Keough (1998). "Phase Transitions in Films of Lung Surfactant at the Air-Water Interface." Biophysical Journal **74**(6): 2983-2995.
- Nag, K., S. Vidyashankar, R. Devraj, M. Fritzen Garcia and A. K. Panda (2010). "Physicochemical studies on the interaction of serum albumin with pulmonary surfactant extract in films and bulk bilayer phase." J Colloid Interface Sci **352**(2): 456-464.
- Nesslein, L. L., K. R. Melton, M. Ikegami, C.-L. Na, S. E. Wert, W. R. Rice, J. A. Whitsett and T. E. Weaver (2005). "Partial SP-B deficiency perturbs lung function and causes air space abnormalities." American Journal of Physiology - Lung Cellular and Molecular Physiology **288**(6): L1154-L1161.
- Nettelblatt, O., A. Tengblad and R. Hallgren (1989). "Lung accumulation of hyaluronan parallels pulmonary edema in experimental alveolitis." American Journal of Physiology - Lung Cellular and Molecular Physiology **257**(6): L379-L384.

References

- Nkadi, P. O., T. A. Merritt and D.-A. M. Pillers (2009). "An overview of pulmonary surfactant in the neonate: Genetics, metabolism, and the role of surfactant in health and disease." Molecular Genetics and Metabolism **97**(2): 95-101.
- Noble, P. W. and R. J. Homer (2005). "Back to the future : Historical perspective on the pathogenesis of idiopathic pulmonary fibrosis." American Thoracic Society **33**(2): 113-120.
- Nogee, L. M. (1998). "Genetics of the hydrophobic surfactant proteins." Biochimica et Biophysica Acta (BBA) - Molecular Basis of Disease **1408**(2-3): 323-333.
- Nogee, L. M. (2004). "Alterations in SP-B and SP-C expression in neonatal lung disease." Annual review of physiology **66**: 601-623.
- Nogee, L. M., G. Garnier, H. C. Dietz, L. Singer, A. M. Murphy, D. E. deMello and H. R. Colten (1994). "A mutation in the surfactant protein B gene responsible for fatal neonatal respiratory disease in multiple kindreds." J Clin Invest **93**(4): 1860-1863.
- Notter, R. H. (2000). Lung surfactants: basic science and clinical applications. New York, Marcel Decker.
- Ochs, M., J. R. Nyengaard, A. Jung, L. Knudsen, M. Voigt, T. Wahlers, J. Richter and H. J. G. Gundersen (2004). "The Number of Alveoli in the Human Lung." American Journal of Respiratory and Critical Care Medicine **169**(1): 120-124.
- Oh, M. H. and C. W. Bae (2000). "Inhibitory effect of meconium on pulmonary surfactant function tested in vitro using the stable microbubble test." European Journal of Pediatrics **159**: 770-774.
- Olmeda, B. (2011). Relaciones estructura-función del sistema de surfactante pulmonar: detección de complejos multiproteicos nativos y participación del surfactante en la difusión interfacial de oxígeno. Madrid, Universidad Complutense de Madrid, Bioquímica y Biología Molecular I.
- Olmeda, B., B. García-Álvarez and J. Pérez-Gil "Structure–function correlations of pulmonary surfactant protein SP-B and the saposin-like family of proteins." European Biophysics Journal: 1-14.
- Olmeda, B., L. Villén, A. Cruz, G. Orellana and J. Perez-Gil (2010). "Pulmonary surfactant layers accelerate O₂ diffusion through the air-water interface." Biochimica et Biophysica Acta (BBA) - Biomembranes **1798**(6): 1281-1284.
- Orgeig, S. and C. B. Daniels (2001). "The roles of cholesterol in pulmonary surfactant: insights from comparative and evolutionary studies." Comparative Biochemistry and Physiology - Part A: Molecular & Integrative Physiology **129**(1): 75-89.
- Orgeig, S., P. S. Hiemstra, E. J. A. Veldhuizen, C. Casals, H. W. Clark, A. Haczku, L. Knudsen and F. Possmayer (2010). "Recent advances in alveolar biology: Evolution and function of alveolar proteins." Respiratory Physiology & Neurobiology **173**: S43-S54.
- Owen, D. M., C. Rentero, A. Magenau, A. Abu-Siniyeh and K. Gaus (2012). "Quantitative imaging of membrane lipid order in cells and organisms." Nat. Protocols **7**(1): 24-35.
- Palaniyar, N., J. Nadesalingam and K. B. M. Reid (2002). "Pulmonary Innate Immune Proteins and Receptors that Interact with Gram-positive Bacterial Ligands." Immunobiology **205**(4-5): 575-594.

- Parasassi, T., G. De Stasio, A. d'Ubaldo and E. Gratton (1990). "Phase fluctuation in phospholipid membranes revealed by Laurdan fluorescence." *Biophys J* **57**(6): 1179-1186.
- Parasassi, T., G. De Stasio, G. Ravagnan, R. M. Rusch and E. Gratton (1991). "Quantitation of lipid phases in phospholipid vesicles by the generalized polarization of Laurdan fluorescence." *Biophys J* **60**(1): 179-189.
- Parasassi, T., M. Di Stefano, M. Loiero, G. Ravagnan and E. Gratton (1994). "Influence of cholesterol on phospholipid bilayers phase domains as detected by Laurdan fluorescence." *Biophysical Journal* **66**(1): 120-132.
- Parasassi, T., E. K. Krasnowska, L. Bagatolli and E. Gratton (1998). "Laurdan and Prodan as Polarity-Sensitive Fluorescent Membrane Probes." *Journal of Fluorescence* **8**(4): 365-373.
- Park, K.-H., C.-W. Bae and S.-J. Chung (1996). "In vitro effect of meconium on the physical surface properties and morphology of exogeneous pulmonary surfactant." *Journal of Korean Medical Science* **11**(5): 429-436.
- Parmigiani, S. and E. Solari (2003). "The era of pulmonary surfactant from Laplace to nowadays." *Acta Biomedica* **74**(2): 69-75.
- Parra, E., L. H. Moleiro, I. López-Montero, A. Cruz, F. Monroy and J. Pérez-Gil (2011). "A combined action of pulmonary surfactant proteins SP-B and SP-C modulates permeability and dynamics of phospholipid membranes." *Biochemical Journal* **438**(3): 555-564.
- Pérez-Gil, J. (2001). "Lipid-protein interactions of hydrophobic proteins SP-B and SP-V in lung surfactant assembly and dynamics." *Fetal & Pediatric Pathology* **20**(6): 445-469.
- Pérez-Gil, J. (2008). "Structure of pulmonary surfactant membranes and films: The role of proteins and lipid-protein interactions." *Biochimica et Biophysica Acta (BBA) - Biomembranes* **1778**(7-8): 1676-1695.
- Pérez-Gil, J., C. Casals and D. Marsh (1995). "Interactions of Hydrophobic Lung Surfactant Proteins SP-B and SP-C with Dipalmitoylphosphatidylcholine and Dipalmitoylphosphatidylglycerol Bilayers Studied by Electron Spin Resonance Spectroscopy." *Biochemistry* **34**(12): 3964-3971.
- Pérez-Gil, J. and K. M. W. Keough (1998). "Interfacial properties of surfactant proteins." *Biochimica et Biophysica Acta (BBA) - Molecular Basis of Disease* **1408**(2-3): 203-217.
- Pérez-Gil, J. and T. E. Weaver (2010). "Pulmonary Surfactant Pathophysiology: Current Models and Open Questions." *Physiology* **25**(3): 132-141.
- Perkins, W. R., R. B. Dause, R. A. Parente, S. R. Minchey, K. C. Neuman, S. M. Gruner, T. F. Taraschi and A. S. Janoff (1996). "Role of Lipid Polymorphism in Pulmonary Surfactant." *Science* **273**(5273): 330-332.
- Phelps, D., T. Umstead, O. Quintero, C. Yengo and J. Floros (2011). "In vivo rescue of alveolar macrophages from SP-A knockout mice with exogenous SP-A nearly restores a wild type intracellular proteome; actin involvement." *Proteome Science* **9**(1): 67.
- Phua, J., J. R. Badia, N. K. J. Adhikari, J. O. Friedrich, R. A. Fowler, J. M. Singh, D. C. Scales, D. R. Stather, A. Li, A. Jones, D. J. Gattas, D. Hallett, G. Tomlinson, T. E. Stewart and N. D. Ferguson (2009). "Has Mortality from Acute Respiratory Distress Syndrome Decreased over Time?" *American Journal of Respiratory and Critical Care Medicine* **179**(3): 220-227.
- Pison, U., W. Seeger, R. Buchhorn, T. Joka, M. Brand, U. Obertacke, H. Neuhofer and K.-P. Schmit-Neuerburg (1989). "Surfactant Abnormalities in Patients

References

- with Respiratory Failure after Multiple Trauma." American Journal of Respiratory and Critical Care Medicine **140**(4): 1033-1039.
- Possmayer, F., S. B. Hall, T. Haller, N. O. Petersen, Y. Y. Zuo, J. Bernardino de la Serna, A. D. Postle, R. A. W. Veldhuizen and S. Orgeig (2010). "Recent advances in alveolar biology: Some new looks at the alveolar interface." Respiratory Physiology & Neurobiology **173**: 55-64.
- Pott, T., H. Bouvrais and P. Méléard (2008). "Giant unilamellar vesicle formation under physiologically relevant conditions." Chemistry and Physics of Lipids **154**(2): 115-119.
- Pryhuber, G. S. (1998). "Regulation and Function of Pulmonary Surfactant Protein B." Molecular Genetics and Metabolism **64**(4): 217-228.
- Puff, N. and M. I. Angelova (2006). Chapter 7 Lipid Vesicles—Development and Applications for Studying Membrane Heterogeneity and Interactions. Advances in Planar Lipid Bilayers and Liposomes. A. L. Liu, Academic Press. **Volume 5**: 173-228.
- Raghu, G., W. Craig Johnson, D. Lockhart and Y. Mageto (1999). "Treatment of Idiopathic Pulmonary Fibrosis with a New Antifibrotic Agent, Pirfenidone." American Journal of Respiratory and Critical Care Medicine **159**(4): 1061-1069.
- Ravasio, A., A. Cruz, J. Perez-Gil and T. Haller (2008). "High-throughput evaluation of pulmonary surfactant adsorption and surface film formation." J. Lipid Res. **49**(11): 2479-2488.
- Ravasio, A., B. Olmeda, C. Bertocchi, T. Haller and J. Perez-Gil (2010). "Lamellar bodies form solid three-dimensional films at the respiratory air-liquid interface." J Biol Chem **285**(36): 28174-28182.
- Ravasio, A., B. Olmeda, C. Bertocchi, T. Haller and J. Pérez-Gil (2010). "Lamellar Bodies Form Solid Three-dimensional Films at the Respiratory Air-Liquid Interface." Journal of Biological Chemistry **285**(36): 28174-28182.
- Righetti, C., D. G. Peroni, A. Pietrobelli and C. Zancanaro (2003). "Proton Nuclear Magnetic Resonance Analysis of Meconium Composition in Newborns." Journal of Pediatric Gastroenterology and Nutrition **36**(4): 498-501.
- Rouser, G., A. N. Siakotos and S. Fleischer (1966). "Quantitative analysis of phospholipids by thin-layer chromatography and phosphorus analysis of spots." Lipids **1**(1): 85-86.
- Ruano, M. L. F., I. García-Verdugo, E. Miguel, J. Pérez-Gil and C. Casals (2000). "Self-Aggregation of Surfactant Protein A." Biochemistry **39**(21): 6529-6537.
- Rubinfeld, G. D., E. Caldwell, E. Peabody, J. Weaver, D. P. Martin, M. Neff, E. J. Stern and L. D. Hudson (2005). "Incidence and Outcomes of Acute Lung Injury." New England Journal of Medicine **353**(16): 1685-1693.
- Rubin, B. K., R. P. Tomkiewicz, M. E. Patrinos and D. Easa (1996). "The surface and transport properties of meconium and reconstituted meconium solutions." Pediatr Res **40**(6): 834-838.
- Rubinstein, M. and R. H. Colby (2008). Polymer physics. New York, Oxford University Press.
- Rushing, S. and L. R. Ment (2004). "Preterm birth: A cost benefit analysis." Seminars in Perinatology **28**(6): 444-450.
- Saad, S. M., Z. Policova, A. Dang, E. J. Acosta, M. L. Hair and A. W. Neumann (2009). "A double injection ADSA-CSD methodology for lung surfactant inhibition and reversal studies." Colloids Surf B Biointerfaces **73**(2): 365-375.

- Sáenz, A., A. López-Sánchez, J. Mojica-Lázaro, L. Martínez-Caro, N. Nin, L. A. Bagatolli and C. Casals (2010). "Fluidizing effects of C-reactive protein on lung surfactant membranes: protective role of surfactant protein A." The FASEB Journal **24**(10): 3662-3673.
- Saftig, P., M. Hetman, W. Schmahl, K. Weber, L. Heine, H. Mossmann, A. Köster, B. Hess, M. Evers and K. von Figura (1995). "Mice deficient for the lysosomal proteinase cathepsin D exhibit progressive atrophy of the intestinal mucosa and profound destruction of lymphoid cells." EMBO J. **14**(15): 3599-3608.
- Sahu, S. C. (1980). "Hyaluronic acid." Inflammation **4**(1): 107-112.
- Sano, H. and Y. Kuroki (2005). "The lung collectins, SP-A and SP-D, modulate pulmonary innate immunity." Molecular Immunology **42**(3): 279-287.
- Schauer-Vukasinovic, V., D. Bur, E. Kitas, D. Schlatter, G. Rossé, H.-W. Lahm and T. Giller (2000). "Purification and characterization of active recombinant human napsin A." European Journal of Biochemistry **267**(9): 2573-2580.
- Schmidt, R., U. Meier, M. Yabut-Perez, D. Walmrath, F. Grimminger, W. Seeger and A. Günther (2001). "Alteration of Fatty Acid Profiles in Different Pulmonary Surfactant Phospholipids in Acute Respiratory Distress Syndrome and Severe Pneumonia." American Journal of Respiratory and Critical Care Medicine **163**(1): 95-100.
- Schoel, W. M., S. Schürch and J. Goerke (1994). "The captive bubble method for the evaluation of pulmonary surfactant: surface tension, area, and volume calculations." Biochimica et Biophysica Acta (BBA) - General Subjects **1200**(3): 281-290.
- Schürch, D., O. L. Ospina, A. Cruz and J. Pérez-Gil (2010). "Combined and Independent Action of Proteins SP-B and SP-C in the Surface Behavior and Mechanical Stability of Pulmonary Surfactant Films." Biophysical Journal **99**(10): 3290-3299.
- Schürch, S., H. Bachofen, J. Goerke and F. Possmayer (1989). "A captive bubble method reproduces the in situ behavior of lung surfactant monolayers." J Appl Physiol **67**(6): 2389-2396.
- Schürch, S., F. H. Y. Green and H. Bachofen (1998). "Formation and structure of surface films: captive bubble surfactometry." Biochimica et Biophysica Acta (BBA) - Molecular Basis of Disease **1408**(2-3): 180-202.
- Schurch, S., D. Schurch, T. Curstedt and B. Robertson (1994). "Surface activity of lipid extract surfactant in relation to film area compression and collapse." Journal of Applied Physiology **77**(2): 974-986.
- Selman, M., T. King and P. A (2001). "Idiopathic pulmonary fibrosis: prevailing and evolving hypotheses about its pathogenesis and implications for therapy. ." Ann Intern Med **134**: 136-151.
- Selman, M., V. J. Thannickal, A. Pardo, D. A. Zisman, F. J. Martinez and I. J. P. Lynch (2004). "Idiopathic Pulmonary Fibrosis: Pathogenesis and Therapeutic Approaches." Drugs **64**(4): 405-430.
- Serrano, A. G. and J. Pérez-Gil (2006). "Protein-lipid interactions and surface activity in the pulmonary surfactant system." Chemistry and Physics of Lipids **141**(1-2): 105-118.
- Souza-Fernandes, A. B., P. Pelosi and P. R. M. Rocco (2006). "Bench-to-bedside review: The role of glycosaminoglycans in respiratory disease." Critical Care **10**.

References

- Spragg, R., J. Lewis, W. Seeger, W. Wurst and F. Rathgeb (1999). "Treatment of ARDS with rSP-C surfactant." Shock **12**: 7-8.
- Spragg, R. G. (2002). "The Future of Surfactant Therapy for Patients with Acute Lung Injury – New Requirements and New Surfactants." Neonatology **81**(Suppl. 1): 20-24.
- Spragg, R. G., F. J. H. Taut, J. F. Lewis, P. Schenk, C. Ruppert, N. Dean, K. Krell, A. Karabinis and A. Günther (2011). "Recombinant Surfactant Protein C-based Surfactant for Patients with Severe Direct Lung Injury." American Journal of Respiratory and Critical Care Medicine **183**(8): 1055-1061.
- Stenger, P. C., S. G. Isbell, D. St. Hillaire and J. A. Zasadzinski (2009). "Rediscovering the Schulze-Hardy Rule in Competitive Adsorption to an Air-Water Interface." Langmuir **25**(17): 10045-10050.
- Stenger, P. C., O. A. Palazoglu and J. A. Zasadzinski (2009b). "Mechanisms of polyelectrolyte enhanced surfactant adsorption at the air-water interface." Biochimica et Biophysica Acta (BBA) - Biomembranes **1788**(5): 1033-1043.
- Stenger, P. C. and J. A. Zasadzinski (2007). "Enhanced surfactant adsorption via polymer depletion forces: a simple model for reversing surfactant inhibition in acute respiratory distress syndrome." Biophys J **92**(1): 3-9.
- Suri, L. N. M., L. McCaig, M. V. Picardi, O. L. Ospina, R. A. W. Veldhuizen, J. F. Staples, F. Possmayer, L.-J. Yao, J. Perez-Gil and S. Orgeig (2012). "Adaptation to low body temperature influences pulmonary surfactant composition thereby increasing fluidity while maintaining appropriately ordered membrane structure and surface activity." Biochimica et Biophysica Acta (BBA) - Biomembranes **1818**(7): 1581-1589.
- Szecs, P. B. (1992). "The aspartic proteases." Scandinavian Journal of Clinical & Laboratory Investigation **52**(s210): 5-22.
- Taeusch, H. W. (2000). "Treatment of Acute (Adult) Respiratory Distress Syndrome." Neonatology **77**(Suppl. 1): 2-8.
- Taeusch, H. W., J. Bernardino de la Serna, J. Perez-Gil, C. Alonso and J. A. Zasadzinski (2005). "Inactivation of pulmonary surfactant due to serum-inhibited adsorption and reversal by hydrophilic polymers: experimental." Biophys J **89**(3): 1769-1779.
- Taeusch, H. W., J. B. de la Serna, J. Perez-Gil, C. Alonso and J. A. Zasadzinski (2005). "Inactivation of Pulmonary Surfactant Due to Serum-Inhibited Adsorption and Reversal by Hydrophilic Polymers: Experimental." Biophysical Journal **89**(3): 1769-1779.
- Taeusch, H. W., E. Dybbro and K. W. Lu (2008). "Pulmonary surfactant adsorption is increased by hyaluronan or polyethylene glycol." Colloids Surf B Biointerfaces **62**(2): 243-249.
- Taeusch, H. W., K. W. LU, J. GOERKE and J. A. CLEMENTS (1999). "Nonionic Polymers Reverse Inactivation of Surfactant by Meconium and Other Substances." Am. J. Respir. Crit. Care Med. **159**(5): 1391-1395.
- Taeusch, H. W., K. W. Lu, J. Goerke and J. A. Clements (1999). "Nonionic polymers reverse inactivation of surfactant by meconium and other substances." Am J Respir Crit Care Med **159**(5 Pt 1): 1391-1395.
- Takahashi, K., Y. Kimura, K. Nagata, A. Yamamoto, M. Matsuo and K. Ueda (2005). "ABC proteins: key molecules for lipid homeostasis." Medical Molecular Morphology **38**(1): 2-12.

- Takamoto, D. Y., E. Aydil, J. A. Zasadzinski, A. T. Ivanova, D. K. Schwartz, T. Yang and P. S. Cremer (2001). "Stable Ordering in Langmuir-Blodgett Films." Science **293**(5533): 1292-1295.
- Takamoto, D. Y., M. M. Lipp, A. von Nahmen, K. Y. C. Lee, A. J. Waring and J. A. Zasadzinski (2001b). "Interaction of Lung Surfactant Proteins with Anionic Phospholipids." Biophysical Journal **81**(1): 153-169.
- Tashiro, K., T. Kobayashi and B. Robertson (2000). "Dextran reduces surfactant inhibition by meconium." Acta Paediatr **89**(12): 1439-1445.
- ten Brinke, A., L. M. G. van Golde and J. J. Batenburg (2002). "Palmitoylation and processing of the lipopeptide surfactant protein C." Biochimica et Biophysica Acta (BBA) - Molecular and Cell Biology of Lipids **1583**(3): 253-265.
- Tokieda, K., J. A. Whitsett, J. C. Clark, T. E. Weaver, K. Ikeda, K. B. McConnell, A. H. Jobe, M. Ikegami and H. S. Iwamoto (1997). "Pulmonary dysfunction in neonatal SP-B-deficient mice." American Journal of Physiology - Lung Cellular and Molecular Physiology **273**(4): L875-L882.
- Tollofsrud, P. A., S. Medbo, A. B. Solas, C. A. Drevon and O. D. Saugstad (2002). "Albumin mixed with meconium attenuates pulmonary dysfunction in a newborn piglet model with meconium aspiration." Pediatr Res **52**(4): 545-553.
- Turino, G. M. and J. O. Cantor (2003). "Hyaluronan in Respiratory Injury and Repair." American Journal of Respiratory and Critical Care Medicine **167**(9): 1169-1175.
- Ueno, T., S. Linder, C.-L. Na, W. R. Rice, J. Johansson and T. E. Weaver (2004). "Processing of Pulmonary Surfactant Protein B by Napsin and Cathepsin H." Journal of Biological Chemistry **279**(16): 16178-16184.
- van Ierland, Y. and A. J. de Beaufort (2009). "Why does meconium cause meconium aspiration syndrome? Current concepts of MAS pathophysiology." Early Human Development **85**(10): 617-620.
- Vandenbussche, G., A. Clercx, M. Clercx, T. Curstedt, J. Johansson, H. Jornvall and J. M. Ruysschaert (1992). "Secondary structure and orientation of the surfactant protein SP-B in a lipid environment. A Fourier transform infrared spectroscopy study." Biochemistry **31**(38): 9169-9176.
- Vandenbussche, G., A. Clercx, T. Curstedt, J. Johansson, H. JÖRnvall and J.-M. Ruysschaert (1992b). "Structure and orientation of the surfactant-associated protein C in a lipid bilayer." European Journal of Biochemistry **203**(1-2): 201-209.
- Veldhuizen, R., K. Nag, S. Orgeig and F. Possmayer (1998). "The role of lipids in pulmonary surfactant." Biochimica et Biophysica Acta (BBA) - Molecular Basis of Disease **1408**(2-3): 90-108.
- Veldhuizen, R. A., L. A. McCaig, T. Akino and J. F. Lewis (1995). "Pulmonary surfactant subfractions in patients with the acute respiratory distress syndrome." American Journal of Respiratory and Critical Care Medicine **152**(6): 1867-1871.
- Vockeroth, D., L. Gunasekara, M. Amrein, F. Possmayer, J. F. Lewis and R. A. W. Veldhuizen (2010). "Role of cholesterol in the biophysical dysfunction of surfactant in ventilator-induced lung injury." American Journal of Physiology - Lung Cellular and Molecular Physiology **298**(1): 117-125.
- Vorbroker, D. K., S. A. Profitt, L. M. Noguee and J. A. Whitsett (1995). "Aberrant processing of surfactant protein C in hereditary SP-B deficiency."

References

- American Journal of Physiology - Lung Cellular and Molecular Physiology **268**(4): L647-L656.
- Walmrath, D., A. Günther, H. A. Ghofrani, R. Schermuly, T. Schneider, F. Grimminger and W. Seeger (1996). "Bronchoscopic surfactant administration in patients with severe adult respiratory distress syndrome and sepsis." American Journal of Respiratory and Critical Care Medicine **154**(1): 57-62.
- Wang, L., A. Cruz, C. R. Flach, J. Perez-Gil and R. Mendelsohn (2007). "Langmuir-Blodgett Films Formed by Continuously Varying Surface Pressure. Characterization by IR Spectroscopy and Epifluorescence Microscopy." Langmuir **23**(9): 4950-4958.
- Ware, L. B. and M. A. Matthay (2000). "The Acute Respiratory Distress Syndrome." New England Journal of Medicine **342**(18): 1334-1349.
- Weaver, T. E. (1998). "Synthesis, processing and secretion of surfactant proteins B and C." Biochimica et Biophysica Acta (BBA) - Molecular Basis of Disease **1408**(2-3): 173-179.
- Weaver, T. E. and D. C. Beck (1999). "Use of Knockout Mice to Study Surfactant Protein Structure and Function." Neonatology **76**(Suppl. 1): 15-18.
- Webster, N. R., A. T. Cohen and J. F. Nunn (1988). "Adult respiratory distress syndrome—how many cases in the UK?" Anaesthesia **43**(11): 923-926.
- Wert, S. E., M. Yoshida, A. M. LeVine, M. Ikegami, T. Jones, G. F. Ross, J. H. Fisher, T. R. Korfhagen and J. A. Whitsett (2000). "Increased metalloproteinase activity, oxidant production, and emphysema in surfactant protein D gene-inactivated mice." Proceedings of the National Academy of Sciences **97**(11): 5972-5977.
- Whitsett, J. A. and T. E. Weaver (2002). "Hydrophobic Surfactant Proteins in Lung Function and Disease." New England Journal of Medicine **347**(26): 2141-2148.
- Williams, G. D., J. Christodoulou, J. Stack, P. Symons, S. E. Wert, M. J. Murrell, Noguee and Lm (1999). "Surfactant protein B deficiency: Clinical, histological and molecular evaluation." Journal of Paediatrics and Child Health **35**(2): 214-220.
- Willson, D., T. N. J. and M. B. P. (2005). "Effect of exogenous surfactant (calfactant) in pediatric acute lung injury: A randomized controlled trial." JAMA: The Journal of the American Medical Association **293**(4): 470-476.
- Wiswell, T. E., R. M. Smith, L. B. Katz, L. Mastroianni, D. Y. Wong, D. Willms, S. Heard, M. Wilson, R. D. Hite, A. Anzueto, S. D. Revak and C. G. Cochrane (1999). "Bronchopulmonary Segmental Lavage with Surfaxin (KL4-Surfactant) for Acute Respiratory Distress Syndrome." American Journal of Respiratory and Critical Care Medicine **160**(4): 1188-1195.
- Woischnik, M., A. Bauer, R. Aboutaam, A. Pamir, F. Stanzel, J. de Blic and M. Griese (2008). "Cathepsin H and napsin A are active in the alveoli and increased in alveolar proteinosis." European Respiratory Journal **31**(6): 1197-1204.
- Wolny, P. M., S. Banerji, C. Gounou, A. R. Brisson, A. J. Day, D. G. Jackson and R. P. Richter (2010). "Analysis of CD44-Hyaluronan Interactions in an Artificial Membrane System." Journal of Biological Chemistry **285**(39): 30170-30180.
- Wright, J. R. (2003). "Pulmonary surfactant: a front line of lung host defense." American Society for Clinical Investigation **111**(10): 1453-1455.

- Wu, H., A. Kuzmenko, S. Wan, L. Schaffer, A. Weiss, J. H. Fisher, K. S. Kim and F. X. McCormack (2003). "Surfactant proteins A and D inhibit the growth of Gram-negative bacteria by increasing membrane permeability." American Society for Clinical Investigation **111**(10): 1589-1602.
- Wüstneck, N., R. Wüstneck, V. B. Fainerman, R. Miller and U. Pison (2001). "Interfacial behaviour and mechanical properties of spread lung surfactant protein/lipid layers." Colloids and Surfaces B: Biointerfaces **21**(1-3): 191-205.
- Wüstneck, N., R. Wüstneck, J. Perez-Gil and U. Pison (2003). "Effects of Oligomerization and Secondary Structure on the Surface Behavior of Pulmonary Surfactant Proteins SP-B and SP-C." Biophysical Journal **84**(3): 1940-1949.
- Wüstneck, R., J. Perez-Gil, N. Wüstneck, A. Cruz, V. B. Fainerman and U. Pison (2005). "Interfacial properties of pulmonary surfactant layers." Advances in Colloid and Interface Science **117**(1-3): 33-58.
- Yamano, G., H. Funahashi, O. Kawanami, L.-X. Zhao, N. Ban, Y. Uchida, T. Morohoshi, J. Ogawa, S. Shioda and N. Inagaki (2001). "ABCA3 is a lamellar body membrane protein in human lung alveolar type II cells." FEBS Letters **508**(2): 221-225.
- Yang, L., J. Johansson, R. Ridsdale, H. Willander, M. Fitzen, H. T. Akinbi and T. E. Weaver (2010). "Surfactant Protein B Propeptide Contains a Saposin-Like Protein Domain with Antimicrobial Activity at Low pH." The Journal of Immunology **184**(2): 975-983.
- Yasuda, Y., T. Kageyama, A. Akamine, M. Shibata, E. Kominami, Y. Uchiyama and K. Yamamoto (1999). "Characterization of New Fluorogenic Substrates for the Rapid and Sensitive Assay of Cathepsin E and Cathepsin D." Journal of Biochemistry **125**(6): 1137-1143.
- Yoshida, I., N. Ban and N. Inagaki (2004). "Expression of ABCA3, a causative gene for fatal surfactant deficiency, is up-regulated by glucocorticoids in lung alveolar type II cells." Biochemical and Biophysical Research Communications **323**(2): 547-555.
- Zasadzinski, J. A., T. F. Alig, C. Alonso, J. Bernardino de la Serna, J. Perez-Gil and H. W. Tausch (2005). "Inhibition of pulmonary surfactant adsorption by serum and the mechanisms of reversal by hydrophilic polymers: theory." Biophys J **89**(3): 1621-1629.
- Zasadzinski, J. A., T. F. Alig, C. Alonso, J. B. de la Serna, J. Perez-Gil and H. W. Tausch (2005). "Inhibition of Pulmonary Surfactant Adsorption by Serum and the Mechanisms of Reversal by Hydrophilic Polymers: Theory." Biophysical Journal **89**(3): 1621-1629.
- Zasadzinski, J. A., P. C. Stenger, I. Shieh and P. Dhar (2010). "Overcoming rapid inactivation of lung surfactant: analogies between competitive adsorption and colloid stability." Biochim Biophys Acta **1798**(4): 801-828.
- Zasadzinski, J. A., P. C. Stenger, I. Shieh and P. Dhar (2010). "Overcoming rapid inactivation of lung surfactant: Analogies between competitive adsorption and colloid stability." Biochimica et Biophysica Acta (BBA) - Biomembranes **1798**(4): 801-828.
- Zhou, L., L. Lim, R. H. Costa and J. A. Whitsett (1996). "Thyroid transcription factor-1, hepatocyte nuclear factor-3beta, surfactant protein B, C, and Clara cell secretory protein in developing mouse lung." Journal of Histochemistry & Cytochemistry **44**(10): 1183-1193.

References

- Zhou, Y., R. Doyen and L. M. Lichtenberger (2009). "The role of membrane cholesterol in determining bile acid cytotoxicity and cytoprotection of ursodeoxycholic acid." Biochim Biophys Acta **1788**(2): 507-513.
- Zuo, Y. Y., R. A. Veldhuizen, A. W. Neumann, N. O. Petersen and F. Possmayer (2008). "Current perspectives in pulmonary surfactant--inhibition, enhancement and evaluation." Biochim Biophys Acta **1778**(10): 1947-1977.
- Zuo, Y. Y., R. A. W. Veldhuizen, A. W. Neumann, N. O. Petersen and F. Possmayer (2008). "Current perspectives in pulmonary surfactant -- Inhibition, enhancement and evaluation." Biochimica et Biophysica Acta (BBA) - Biomembranes **1778**(10): 1947-1977.